



Faculty of Sciences
Department of Analytical Chemistry

Fast detection of counterfeit drugs with Raman spectroscopy

Marleen de Veij

Thesis submitted in fulfilment of the requirements for the degree of
Doctor (PhD) of Science: Chemistry

Promoter: Prof. Dr. L. Moens
Prof. Dr. P. Vandenabeele

Table of contents

Chapter 1: Introduction

1.1 The history of drugs	1
1.2 Counterfeiting of drugs	2
1.3 Legislation against counterfeiting	3
1.4 Identification of counterfeit drugs	4
1.5 Outline of this thesis	6
1.6 References	7

Chapter 2: Theory of the Raman effect

2.1 Discovery of the Raman effect	11
2.2 Theoretical approach of the Raman effect	11
2.3 The Raman spectrum	12
2.4 Raman spectrometer	13
2.5 References	13

Chapter 3: Dispersive and Fourier transform (FT) Raman spectroscopy

3.1. Introduction	17
3.2 Dispersive versus Fourier transform Raman spectroscopy	17
3.3 The advantages and disadvantages of both of the techniques	18
3.4 Applications in the pharmaceutical research	20
3.4.1 Drug identification of the active agent and excipients in tablets	20
3.4.2 Polymorphism	20
3.4.3 Imaging / Mapping	20
3.4.4 Industrial applications	22
3.4.5 Quantitative analysis	22

3.5 Conclusion	23
3.6 Notes on this publication	23
3.7 References	24

Chapter 4: Counterfeit drugs

4.1 What are counterfeit drugs?	29
4.2 How big is the problem of counterfeit drugs?	30
4.3 Actions against counterfeiters	34
4.4 Analytical techniques used to detect counterfeit drugs	37
4.5 History of Raman spectroscopy as a detection method of counterfeit drugs	39
4.6 Conclusion	40
4.7 References	40

Chapter 5: Qualitative analyses of counterfeit drugs

5.1 Experimental	46
5.2 Analysis of erectile dysfunction drugs	47
5.2.1 Functioning of erectile dysfunction drugs	47
5.2.2 Content of the three erectile dysfunction drugs	47
5.2.3 Viagra [®] tablets	51
5.2.4 Viagra [®] gel	53
5.2.5 Tablets containing the active ingredient of Cialis [®]	54
5.3 Analysis of Noromectin [®]	56
5.3.1 Introduction of Noromectin [®]	56
5.3.2 Analysis of packaging	57
5.3.3 Analysis of the content of the syringes	60
5.4 Analysis of Amoxil [®]	61
5.5 Conclusion	65
5.6 References	65

Chapter 6: Analysis of counterfeit antimalarial tablets

6.1 Introduction	70
6.2 Experimental	73
6.3 Results and Discussion	75
6.3.1 Spectral Interpretation	75
6.3.2 Chemometrical classification of counterfeit drug samples	79
6.4 Conclusion	82
6.5 Notes on this publication	83
6.6 References	84

Chapter 7: Analysis of counterfeit Viagra[®] tablets

7.1 Introduction	90
7.2 Experimental	92
7.3 Results and discussion	93
7.3.1 Visual inspection of the tablets	93
7.3.2 Visual inspection of the Raman spectra	94
7.3.3 Chemometrical analyses	99
7.4 Conclusion	101
7.5 Notes on this publication	102
7.6 References	102

Chapter 8: Database of Raman spectra of commonly used excipients

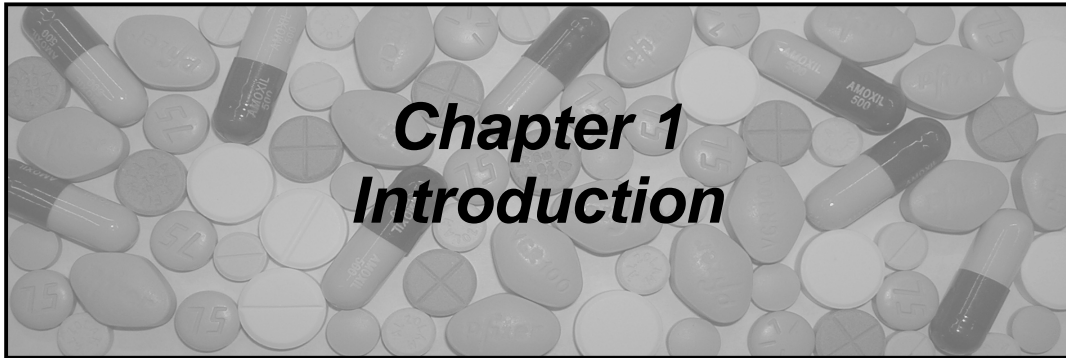
8.1 Introduction	108
8.2 Experimental	109
8.3 Results and Discussion	110
8.3.1 Mono- and disaccharides	112
8.3.2 Polysaccharides	113

8.3.3 Polyalcohols	116
8.3.4 Carboxylic acids and salts	117
8.3.5 Esters	119
8.3.6 Inorganic substances	121
8.3.7 Others	123
8.4 Table with Raman bands of the 43 excipients	125
8.5 Chemical structures of the 43 excipients	128
8.6 Conclusion	130
8.7 Notes on publication	131
8.8 References	131

Chapter 9: Quantitative analysis of drugs with Raman spectroscopy

9.1 Introduction	137
9.2 Experimental	138
9.3 Preparation of the calibration tablets and analysis conditions	140
9.3.1 Homogeneity of the calibration tablets	140
9.3.2 Influence of the rotation of tablets during analysis	143
9.4 Quantitative analysis based on specific Raman bands	145
9.4.1 Analysis based on the intensity of three Raman bands	145
9.4.1.1 Antimalarial tablets	145
9.4.1.2 Viagra [®] tablets	148
9.4.2 Analysis based on the area of three Raman bands	153
9.5 Quantitative analysis based on PCR	155
9.6 Analysis with Fourier transform (FT) Raman Spectroscopy	159
9.6.1 Analysis based on the intensity of three Raman bands	159
9.6.2 Analysis based on PCR	161
9.7 Influence of grinding and repressing of tablets	165
9.7.1 Analysis based on the intensity of three Raman bands	166
9.7.2 Analysis based on PCR	168

9.8 Conclusion	171
9.9 References	172
<i>Conclusion and summary</i>	175
<i>Samenvatting en besluit</i>	183
<i>Appendix: Chemometrics</i>	191
<i>Dankwoord</i>	207



Chapter 1
Introduction

1 Introduction

1.1 The history of drugs

In the beginning, people attributed sickness to various modes of evil spirits or divine intervention¹. One of the first to separate drugs from religion and applying reasoning and observation to medical practice was Hippocrates (ca. 460 - 375 BC), who is now referred to as the “father of medicine” (fig. 1.1)². He was the founder of the Hippocratic School of Medicine, and due to Hippocrates, medicine was now recognized as a science². But even in Greek times, opinions about this new science “medicine” were mixed, since the word *pharmakos* meant both remedy and poison as well².



Figure 1.1 Hippocrates²

The earliest form of drugs consisted of the use of plants and animal parts as part of remedies. The majority of these “recipes” of plants and animal parts were passed on from one generation to the next⁴. The first to write about the use of herbs against illnesses was a Greek physician, Pedanius Dioscorides (ca. 40 - 90 AD), who was a surgeon in Nero’s army². He wrote the *Materia Medica* (fig. 1.2), which is the basis of modern pharmacy, and has been used for almost 1600 years².



Figure 1.2 *De medicinali materia libri sex*. (1549)³.

The *Materia medica* consisted of five volumes: the first book deals with aromatics, while the second book covers animals, cereals and herbs, the third and fourth book describe the use of roots, juices, herbs and seeds, while the last book describes the uses of wines and minerals².

About 40 years later, another Greek physician, Galen (ca. 129 - ca. 200 AD), wrote about 350 authentic titles on drugs, which was about as much as all other Greek medical writings together at that time. Galen described 473 recipes where he used plants and animal parts, but also components from mineral origin. The descriptions were supplemented by drawings of the herbs used².

The collapse of the Roman Empire stopped the further development of drugs. However, the original medical manuscripts were preserved throughout Mediaeval times. The revival of formal drugs took place in the 12th century in Italy. Around 1200, hospital building started in Europe and coincided with the flourishing of universities in Italy, Spain, France, and England².

The modern pharmaceutical industry began around 1860, with the discovery of the transmission of diseases by bacteria, by Louis Pasteur (1822 – 1896) in France and Robert Koch (1843 – 1910) in Germany². Shortly after, antibiotics were discovered in the early 19th century, and from then onwards, science made enormous leaps forward in the understanding of diseases².

1.2 Counterfeiting of drugs

Counterfeiting of pharmaceutical products is an age-old practice, which flourishes in many countries, and is motivated mainly by the huge profits which can be made⁴. First concerns about the quality of drugs date back as far as the 4th century BC. The first one to mention counterfeit drugs was Pedanius Dioscorides⁵. The caricature in figure 1.3, from the early 19th century, shows the feelings of the public towards the pharmacists and counterfeiting².



Figure 1.3 caricature by A.Park².

Since then, the problem has increased, and currently, it is estimated that about 10% of the drugs sold worldwide are counterfeited⁶. The production of these counterfeit drugs is usually done in ordinary households, in their kitchen or just in a shed in the backyard⁶. Sophisticated equipment for the manufacture and packaging of these drugs has increased the difficulty of detecting the counterfeit products⁴. Since, there is a high demand for drugs, which are often quite expensive, the counterfeiting business has become extremely lucrative. The absence of any deterrent legislation in many countries encourages these counterfeiters, since there is only a small change of being apprehended and prosecuted⁶.

1.3 Legislation against counterfeiting

It was not until the middle of the 19th century, before the first regulation on the trade of drugs was implemented⁵. This regulation only involved the trade of drugs and did not mention the production of counterfeit drugs. The first time that resolutions against counterfeit drugs were adopted, was not until 1988⁵.

The trade of counterfeit drugs affects people worldwide, irrespective on whether they live in the developing or developed countries⁴. There are certain factors enabling the spread of these counterfeit drugs. The main reason for counterfeiting drugs is, evidently, the huge profit that can be made. The pharmaceutical industry is immensely capital-intensive, and spends billions to develop a single drug. The average total research and development cost for new drugs in the late 1990s was \$897 million, according to a report by the Tufts Centre for the Study of Drug Development⁷. These investments have to be recovered afterwards, by adding a significant premium over the production costs; costs which counterfeiters of course lack.

Moreover, there is also a lack of legislation. Penal sanctions are usually very weak or absent at all⁴. In some countries, counterfeiters have to pay a penalty that is usually just a fraction of the profit that they make with their trade in counterfeit drugs⁵.

These counterfeit drugs have a tremendous effect on people's health, causing morbidity, mortality, and reducing the effectiveness of the health care system. They are also difficult to detect, since the existing analytical methods have a long analysis time or are just too expensive, especially for developing countries. One of the possibilities to stop or to reduce this problem, is a fast, easy, and cheap detection system.

1.4 Identification of counterfeit drugs

The first step in the identification of possible counterfeit drugs, is the visual inspection. Based on packaging, labelling, and physical appearance of the dosage form, e.g. shape, colour, etc., counterfeit drugs could be detected⁵. But lately, counterfeiters have become so sophisticated, that simple visual inspection is not sufficient anymore, and a more advanced analytical approach is needed.

In the middle of the 19th century, counterfeit drugs were often made from clay. A fast and easy method to identify the counterfeits, was to place the tablets in an oven. When, after incineration, only 2% dry matter was left, it was a genuine tablet, where as the counterfeit tablets left 29% dry matter². Nowadays, the detection of counterfeit drugs is much more complicated.

However, there are some cheap and easy methods available for this purpose. For example, test-tube colour reactions, melting-point determination or thin-layer chromatography (TLC) can be used to easily identify the active ingredient in drugs⁴. The disadvantage of these methods is that they are only qualitative. Moreover, other additives, which may be harmful, are not detected. These methods can only be used as a fast screening procedure, and could identify the products that require further investigation⁴. Techniques that could be used for quantitative detection are high performance liquid chromatography (HPLC), mass spectrometry (MS) or nuclear magnetic resonance (NMR)^{4,5}. The disadvantage of these methods is their extended sample preparation: samples have to be grinded and often diluted in organic solvents, and additionally, highly trained analysts are necessary to interpret the results.

The use of Raman spectroscopy can avoid these problems. Its non-destructive character and high speed of analysis make Raman spectroscopy well suited for the detection of counterfeit drugs. This spectroscopic method can be used on samples without any preparation, it can measure through blister packages, and small particles can as well be analysed. Within a few seconds, the Raman spectrum can tell if the drug is counterfeit, based on the absence of the declared active ingredient.

In cases where the active ingredient is present, the focus is moved to the excipients that are used in the drugs. If declared excipients are lacking, or if additional excipients are present which are not used in the genuine drug, the drug is considered a counterfeit. For this qualitative analysis, a highly trained analyst is required to analyse the Raman spectrum, but if the spectrometer is equipped with an elaborate database and a spectral searching algorithm is implemented, a semi-trained professional could use this technique. This way, Raman spectroscopy could not only be useful for rich countries, but could also provide a method to reduce the amount of counterfeit drugs in developing countries.

Until now, Raman spectroscopy has been used mainly for the qualitative identification of ecstasy tablets and cocaine^{8,9,10,11}. Since the production of these drugs is highly illegal, research was focussed on identifying the producers. Based on excipients used in these ecstasy tablets, it was possible to trace the producer^{8,9}. The same is valid for cocaine.

Cocaine is frequently adulterated or “cut” in order to increase the profit. The most common used cutting agents are baking soda, starch, lactose, dextrose, or anaesthetics^{10,11}. These cutting agents in cocaine could also be used to trace the producer. So far, Raman spectroscopy has mainly been used the detection of illicit drugs, and is not known as a common technique to identify counterfeit pharmaceuticals.

The purpose of this research is to develop Raman spectroscopy as a fast and easy method to detect counterfeit drugs. The first part of this research is focussed on the qualitative analysis. Since lately, counterfeit drugs appear on the international market with the correct active ingredient, quantitative analysis becomes necessary as well.

This is the base of the second part of this research. Finally, we hope that this project can ease the qualitative as well as quantitative detection of counterfeit drugs by using Raman spectroscopy.

1.5 Outline of this thesis

As mentioned before, this thesis is focussed on qualitative and quantitative analysis of counterfeit drugs with Raman spectroscopy. The first part of this thesis covers the general background of this project. In chapter 2, the theoretical background of Raman spectroscopy is discussed. During this project, we had the opportunity to work with different Raman spectrometers, dispersive as well as Fourier transform (FT). The difference between these two Raman spectrometers is discussed in chapter 3, together with several pharmaceutical applications of dispersive and FT-Raman spectroscopy. In chapter 4, the problem of counterfeit drugs is described, not only the magnitude of the problem is mentioned, but also different analytical techniques that have been used so far.

The next three chapters cover the qualitative investigation of counterfeit drugs with Raman spectroscopy. Chapter 5 describes the analyses of single cases of counterfeit drugs, that were seized in Belgium. Chapter 6 focuses on the qualitative detection of counterfeit antimalarial drugs seized in Southeast Asia while chapter 7 focuses on Viagra[®] tablets from different origins. Since many of these counterfeits could be detected based on excipients that were present and/or lacking in the drugs, a database of the most commonly used excipients was made which is described in chapter 8.

Counterfeiters are becoming more and more sophisticated, so quantitative analysis is necessary as well. Chapter 9 elaborates on the quantitative analysis of different drugs. For the quantitative calculations, different methods were used, including chemometrics (PCA and PCR) which are summarised in the appendix. Finally, a conclusion and summary of this entire project is given in the final chapter.

1.6 References

1. Lock S, Last JM, Dunea G, *The Oxford Illustrated Companion to Medicine*, Oxford University Press, 3rd edition, Oxford, 2001.
2. Porter R, *The greatest benefit to mankind, A medical history of humanity from antiquity to the present*, Fontana Press, London, 1997.
3. www.abdijbibliotheken.be
4. World Health Organization (WHO), *Counterfeit Drugs, guidelines for the development of measures of combat counterfeit drugs*, 1999.
5. Newton PN, Green MD, Fernandez FM, Day NPJ, White NJ, *Lancet Infect. Dis.* 2006, 6: 602-613.
6. World Health Organization (WHO), Fact sheet N°275 Revised 14 November 2006.
7. Maron M, *Psychiatric News*, 2003, 38(15), 25.
8. Bell SEJ, Burns DT, Dennis AD, Speers JS, *Analyst* 2000; 125: 541-544.
9. Bell SEJ, Burns DT, Dennis AD, Matchett LJ, Speers JS, *Analyst* 2000; 125: 1811-1816.
10. Ryder AG, O'connor GM, Glynn TJ, *J. Forensic. Sci.* 1999; 44(5): 1013-1019.
11. Hodges CM, Akhavan J, *Spectroc. Acta Pt. A-Molec. Biomolec. Spectr.*, 1990; 46A(2): 303-308.



Chapter 2
Theory of the Raman effect

2 Theory of the Raman effect

2.1 Discovery of the Raman effect

The Raman effect was first predicted by Adolf Smekal (1895 - 1959)¹ in 1923. But it was for the first time observed in 1928 by sir Chandrasekhara Venkata Raman (1888 - 1970) along with Kariamanikam Srinivasa Krishnan (1898 – 1961)^{1,2}. In 1922 his work on the “Molecular diffraction of light” was published which was the start of a series of investigations which led to the discovery of the Raman effect. Six years later, in 1928, his work was published in Nature where he described the changes in wavelength of scattered light³. He was awarded the Nobel Prize of Physics for his work on the scattering of light and for the discovery of the effect that was named after him in 1930¹.

2.2 Theoretical approach of the Raman effect

When monochromatic light is aimed at a sample, the light is transmitted, reflected or even scattered⁴. The easiest way to describe this effect is via an energy level diagram, which is shown in figure 2.1⁴.

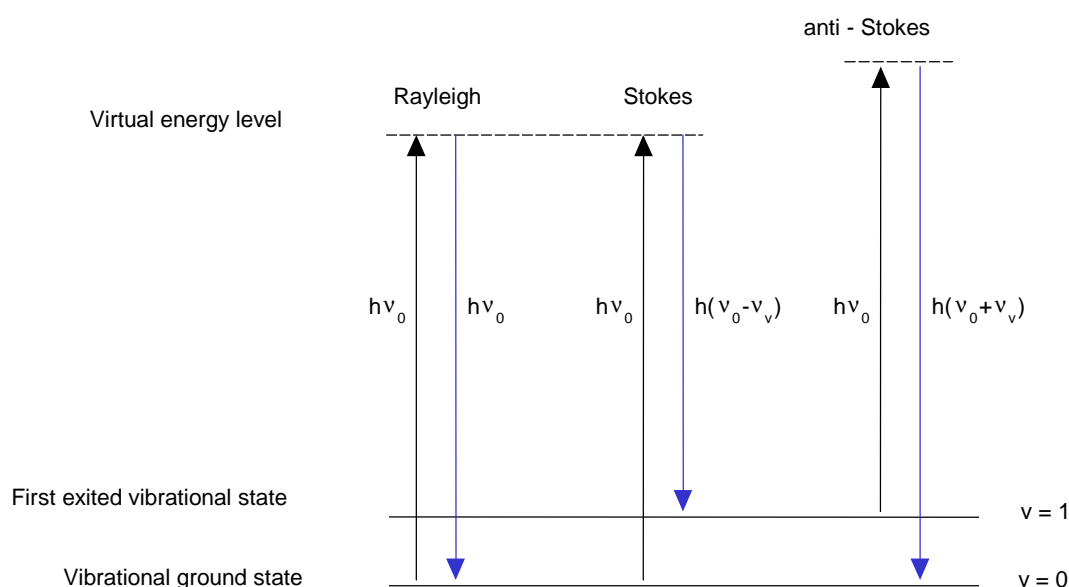


Figure 2.1 Overview of the different energy states involved in Raman spectroscopy.

The majority of the scattered light has the same energy as the incident light. In this case (fig. 2.1), a molecule is excited from the vibrational ground state to a virtual energy level. Since this virtual energy level is not a stable energy state of the molecule, the molecule relaxes back to the original vibrational ground state while emitting light. The energy of the incident light is similar to the energy of the scattered light: this situation is called Rayleigh scattering^{4,5}.

The origin of Raman spectroscopy is the inelastic scattering effect, which is caused by a very small portion of the molecules in the sample (approximately 10^{-6} to 10^{-8})⁵. This results in a difference in energy between the incident light and the scattered light⁵. In the second example (fig. 2.1), the molecule is excited from the vibrational ground state to a virtual energy level. Instead of relaxing to the original vibrational ground state, it relaxes to the 1st excited vibrational state. The energy of the incident light ($E = h\nu_0$) is therefore larger than the emitted light ($E = h(\nu_0 - \nu_v)$): this is called Stokes scattering, which is the basis of Raman spectroscopy⁵. The third option, the anti-Stokes scattering, consists of molecules leaving from the first excited state and relaxing to the vibrational ground state. In this case (fig. 2.1), the energy of the incident light ($E = h\nu_0$) is smaller than the emitted light ($E = h(\nu_0 + \nu_v)$). The number of molecules in any excited vibrational state is always far less than that of the vibrational ground state. That is the reason why Stokes scattering is normally used for molecular characterization⁵.

2.3 The Raman spectrum

For Raman spectroscopy, a vibrational mode is only Raman-active when there is a change in polarizability during the vibration⁵. As vibrational energy levels are product specific, the different position(s) of the Raman band(s) can give us information about the product analysed. These Raman band(s) are characteristic for functional groups. So, different regions in a Raman spectrum correspond with different types of functional groups. The position of the Raman band in the Raman spectrum, is determined by the energy difference between the vibrational ground state and the first excited vibrational state and expressed as a Raman shift (cm^{-1}). The intensity of the Raman Stokes scattered light is proportional to the number of molecules, which is the basis for the use of Raman spectroscopy as a quantitative method of analysis.

At thermal equilibrium, the fraction of molecules in one vibrational energy level, relative to another, can be given by the Boltzmann distribution (Eq. 2.1)²:

$$\frac{N_1}{N_0} = \left(\frac{g_1}{g_0} \right) \cdot e^{[-(\Delta E)/kT]} \quad (\text{Eq. 2.1})$$

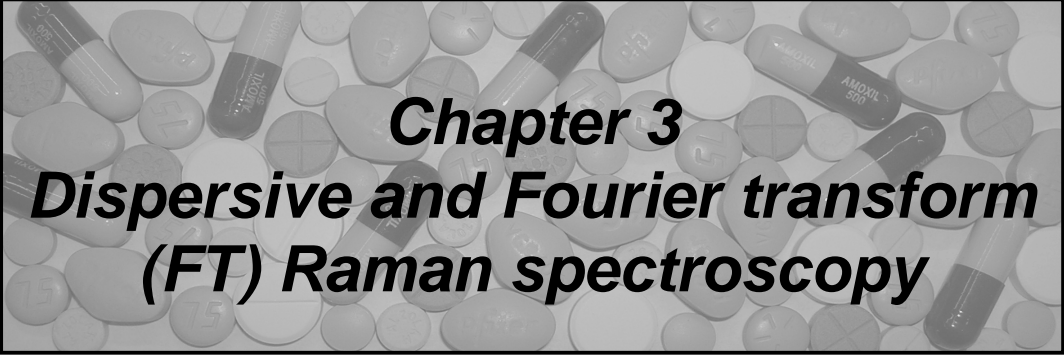
where N_1 = number of molecules in a higher vibrational energy level
 N_0 = number of molecules in a lower vibrational energy level
 g_0 = degeneracy of the higher vibrational level
 g_1 = degeneracy of the lower vibrational level
 ΔE = energy difference between the higher and lower vibrational energy levels
 k = Boltzmann constant ($1,3807 \times 10^{-23} \text{ J K}^{-1}$)
 T = temperature, K

2.4 Raman spectrometer

During this research project, the majority of the analyses were performed with dispersive Raman spectrometers. For the quantitative analysis, a Fourier Transform (FT) Raman spectrometer is also used. The differences between these two types of Raman spectrometers are described in Chapter 3, which is based on a review article published in *European Pharmaceutical Review*. This article also describes various pharmaceutical applications of dispersive and FT Raman spectroscopy.

2.5 References

1. Singh R, *Phys. Perspect.*, 2002; 4: 399-420.
2. Gardiner DJ, Graves PR, *Practical Raman Spectroscopy*, Springer-Verlag, Berlin, 1989.
3. Raman CV, Krishnan KS, *Nature*, 1928; 121: 501-502.
4. Grassell JG, Bulkin BJ, *Analytical Raman spectroscopy*, Wiley, New York (N.Y.), 1991.
5. Lin-Vien D, Colthup NB, Fateley WG. *The handbook of infrared and Raman characteristic frequencies of organic molecules*, Academic press, San Diego (Calif.), 1991.



Chapter 3
***Dispersive and Fourier transform
(FT) Raman spectroscopy***

3 Dispersive and Fourier transform (FT) Raman spectroscopy

Based on the paper: de Veij M, Vandenabeele P, Moens L, The rise of Raman, European Pharmaceutical Review, Issue 3, 2005, 86 – 89.

The benefits and downsides of dispersive and FT-Raman spectroscopy in the field of pharmaceutical applications are described in this chapter. Traditionally, analyses in pharmaceutical research and industry are often performed using Nuclear Magnetic Resonance (NMR) or Mass Spectrometry (MS). However, researchers nowadays are aware that Raman Spectroscopy possesses certain advantages in pharmaceutical research.

3.1 Introduction

The Raman effect was first observed in 1928 by Sir C.V. Raman. These early experiments were carried out using focussed sunlight and filters and relied on visual observations of colour changes in the scattered light¹. A few years later, with the use of a mercury lamp and a spectrograph, Sir C.V. Raman recorded spectra of several liquids, including benzene and CCl₄¹. The first commercial Raman instrument was introduced in 1953, making Raman spectroscopy available to a wider audience². The interest in Raman spectroscopy flourished even more in the mid-1960's with the introduction of the first commercial reliable continuous wave gas lasers. The introduction of high-quality holographic filters (1970's), diode array detection (1980's), fibre optics (1980's) and the coupling of microscopes to Raman spectrometers (1980's) expanded the range of the applications³.

3.2 Dispersive versus Fourier Transform Raman spectroscopy

A Raman spectrometer, as shown in figure 3.1, basically consists of a light source (A), collection optics (B), a dispersing optical element (C) and a detection system (D). Two major technologies are used to collect the Raman spectra: dispersive and Fourier Transform (FT) Raman spectroscopy.

The major difference between the two techniques is the way Raman scattering is detected and analysed⁴.

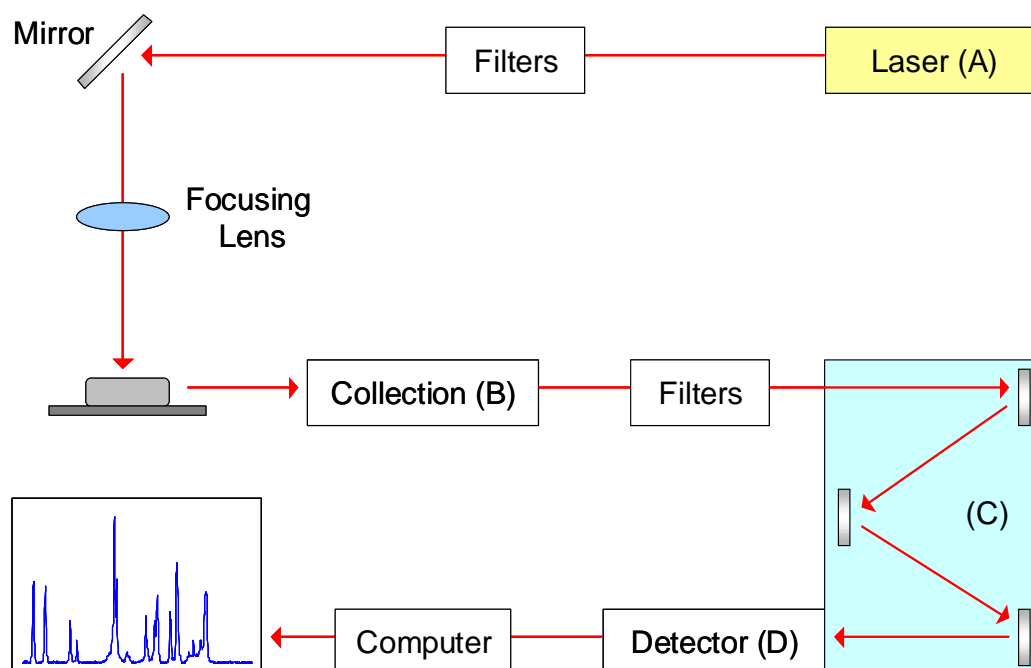


Figure 3.1 Schematic layout of Raman instrument^{1,2,3}.

Typically, the lasers used in dispersive Raman spectroscopy are in the visible region and have wavelengths of for instance 785 nm (diode laser), 633 nm (He-Ne) or 532 nm (frequency doubled Nd:YAG). In general the lasers used in FT-Raman spectroscopy have a wavelength of 1064nm (Nd:YAG)^{4,5}.

The spectral analysis in dispersive Raman spectrometers is done by using a grating⁴. The spectrum is produced by rotating the grating so that the desired spectral window is presented to a multi-channel detector (e.g. charge-coupled-device, CCD)¹. FT-Raman spectrometers use interferometric optics to collect the light from the sample, allowing to collect all the wavelengths simultaneously^{2,3}.

3.3 The advantages and disadvantages of both techniques

The advantages and disadvantages of dispersive and FT-Raman spectroscopy are shown in table 3.1.

Topic	dispersive Raman spectroscopy	FT-Raman spectroscopy
Low wavenumbers	+	
Spectral window	(+)	+
Spectral precision	(+)	+
Sensitivity	+	
Small spot size	+	
Thermal degradation minimal	+	
Operating costs	+	
Speed of analysis		+
Fluorescence suppression		+

Table 3.1 Advantages / disadvantages of dispersive and FT-Raman spectroscopy³.

One of the disadvantages of dispersive Raman spectroscopy is that there is a low spectral precision caused by motion of the grating (or thermal drift) which can degrade precision; when extreme stability is requested an extensive calibration may be needed⁶. The interferometer used with FT-Raman ensures high wavelength precision, which allows easy spectral subtraction in order to remove background or solvent features³. Another disadvantage of dispersive Raman spectroscopy is that the influence from fluorescence is generally larger with dispersive Raman than with FT-Raman since the latter uses a longer laser wavelength.

A disadvantage of FT-Raman spectroscopy is that the low-frequency region of the spectrum is often not available, as well as the cost of running an experiment with FT-Raman spectroscopy which is higher than dispersive Raman spectroscopy due to the use of liquid nitrogen for the detector. It is clear that the choice between dispersive and FT-Raman spectroscopy depends on the samples needed to be analysed, since both techniques have specific advantages and disadvantages.

3.4 Applications in the pharmaceutical research

3.4.1 Drug identification of the active agent and excipients in tablets

A study by Bell et al.⁷ showed that dispersive Raman spectroscopy (810 nm laser wavelength) can be used to distinguish between ecstasy and various other phenethylamine ecstasy analogues, commonly seized in the UK. The spectra could be used to distinguish between the chemically-similar substances such as isomers and polymorphic/hydrated forms. Within an hour 20 samples could be analysed, showing that Raman spectroscopy could be used as a fast and non-destructive method for drug identification. Further research on this subject⁸ showed that the variation in composition of the tablets could be identified, which is useful for tracing drug distribution networks.

3.4.2 Polymorphism

Polymorphism is important for the pharmaceutical industry since it can affect the chemical stability, the behaviour in pharmaceutical formulations, such as the tendency to absorb water, the solubility and thus the bioavailability⁹. The majority of the polymorphism experiments are performed by FT-Raman spectroscopy. For instance, the quantitative analysis of mannitol polymorphs by Roberts et al.¹⁰, in which they studied binary mixtures of beta and delta mannitol. Different mixtures were studied and the results indicate that levels till 2% of beta mannitol could be quantified.

3.4.3 Imaging / Mapping

Raman spectroscopy can be used to analyse and evaluate the content of pharmaceutical products as well as the homogeneity of the tablets. There are two different methods. Imaging is accomplished by illuminating the sample and imaging the scattered light (the so-called wide field illumination)¹¹ onto an imaging two-dimensional array detector¹². Mapping involves recording a spectrum at each point of a grid, for well-defined spatial locations of a

sample¹². A chemical image is the spatial distribution of a compound of interest, based on its intensity at a uniquely assignable Raman shift¹¹. Before starting imaging this Raman shift should be known in advance. One of the main advantages of imaging is the fast productions of images.

In a study by Šašić et al.¹¹ a comparison is made between different data processing ways for the chemical images of pharmaceuticals. Raman spectroscopy with a laser at 782 nm was used to create an image of pharmaceutical beads, which consisted of four different layers. Within 60 seconds, acceptable images were created¹¹, showing the speed of recording images of pharmaceuticals.

Mapping can be used to determine the homogeneity of an ingredient in, for example, a tablet. Spectra are taken, from the entire surface of the tablet, for instance a 10 x 10 map or higher. Specific software allows mapping of the chemical composition of the tablet by rationing characteristic band intensities.

An example of the mapping is the distribution of vitamin B₁₂ trough tablets (own research) by Raman spectroscopy with a diode laser (785 nm). In this case a 8 x 8 map (steps of 1 mm) was created of both sides of the tablets (fig. 3.2) and the colour of the map corresponds with the band intensity, corresponding with the concentration.

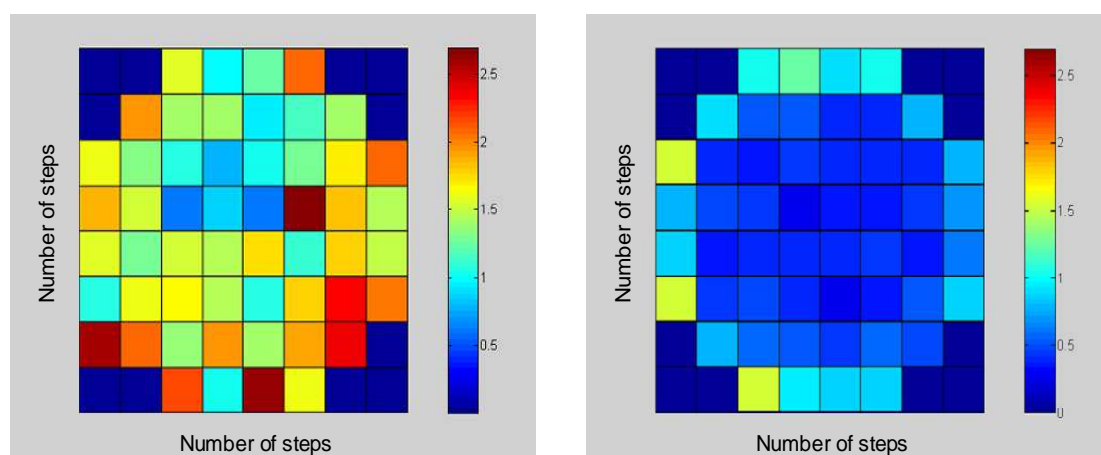


Figure 3.2 Mapping of Vitamin B₁₂ tablets, side a (left) and side b (right).

3.4.4 Industrial applications

One of the advantages of Raman spectroscopy is that measurements can take place through, for instance, blister packages or drug vials. This is a major benefit for the use of Raman spectroscopy in industry. A dispersive Raman spectrometer (laser wavelength 488 nm) was used for a study by Powell on sealed drug vials, for a quick headspace analysis¹⁴. Drug vials with pharmaceuticals that decompose when in contact with oxygen are packaged under nitrogen atmosphere. Raman spectroscopy was able to detect the presence of oxygen in the headspace of the vial.

Raman spectroscopy has been used to measure the concentration of bucindolol in gel capsules¹⁵ inside the blister packages with dispersive (micro) Raman spectroscopy (785 nm laser wavelength). FT-Raman spectroscopy has also been used for the in-line monitoring of a pharmaceutical blending process¹⁶. The blending process of diltiazem hydrochloride pellets and paraffin wax beads was monitored and the results of these experiments were confirmed by HPLC¹⁶. These three experiments demonstrate the potential of Raman spectroscopy in the pharmaceutical industry.

3.4.5 Quantitative analysis

In the last few years, increasingly more papers are published on quantitative analysis of the active ingredient in tablets. For example, a study performed by Izolani et al.¹⁷, describes the quantitative determination by using FT-Raman of Dipyrone (an antipyretic drug) in different tablets. A drawback of this study was that the tablets had to be grinded, homogenized and pressed again to make tablets of 250 mg, disregarding the absence of sample preparation that Raman spectroscopy usually requires. A similar approach was also used for the determination of Ciprofloxacin in pharmaceuticals¹⁸ in which different concentrations of Ciprofloxacin were mixed with maize starch and pressed into tablets to be used as standards. The commercial tablets were grinded as well and pressed into 300 mg discs.

Many more articles²⁰⁻²³ are available about the quantitative measurements of pharmaceuticals with the use of FT-Raman spectroscopy. The majority of the quantitative analysis has been established by FT-Raman spectroscopy. However, some quantitative studies have been performed by dispersive Raman spectrometry. For instance in the study by Fauilloux et al.²⁴ a laser with a wavelength of 514 nm was used for the quantitative measurement of the degradation of retinol (vitamin A). These results were compared with HPLC results and differed only 8 %. Quantification with dispersive Raman spectroscopy generally needs more time than FT-Raman spectroscopy, since the spectra have to be calibrated against standards, which for this research was done with the 992 cm⁻¹ Raman band of benzene²⁴.

3.5 Conclusion

This review gives an overview on pharmaceutical applications of Raman spectroscopy. It shows that Raman spectroscopy is a well established method for quantitative as well as qualitative measurements. Gradually, Raman spectroscopy becomes a more commonly used research method in pharmaceutical studies. In this review, the use of dispersive and FT-Raman spectroscopy is described for different pharmaceutical applications. Both techniques have their advantages and disadvantages: the choice between the two techniques mainly depends on the specific research question.

3.6 Notes on this publication

This article illustrates the differences between dispersive and FT-Raman spectroscopy, and their specific pharmaceutical applications. In this research project, dispersive Raman spectroscopy is used for the qualitative analysis of the counterfeit drugs. For the quantitative analysis of counterfeit Viagra[®] drugs, dispersive Raman spectroscopy is compared with FT-Raman, which is described in chapter 9.

3.7 References

1. Gardiner DJ, Graves PR, *Practical Raman Spectroscopy*, Springer-Verlag, Berlin, 1989.
2. Pelletier MJ, *Analytical Applications of Raman Spectroscopy*, Blackwell Science, England, 1999.
3. Grasselli JG, Bulkin BJ, *Analytical Raman Spectroscopy*, John Wiley & Sons, New York, 1991.
4. Vankeirsbilck T, Vercauteren A, Baeyens W, Van der Weken G, Verpoort F, Vergote G, Remon JP, *Trends. Anal. Chem.*, 2002; 21(12): 869-877.
5. Laserna JJ, *Modern Techniques in Raman Spectroscopy*, John Wiley & Sons, England, 1996.
6. Hutsebaut D, Vandenabeele P, Moens L, *Analyst*, 2005; 130: 1204-1214.
7. Bell SEJ, Burns DT, Dennis AC, Speers JS, *Analyst*, 2000; 125: 541-544.
8. Bell SEJ, Burns DT, Dennis AC, Matchett LJ, Speers JS, *Analyst*, 2000; 125: 1811-1815.
9. Langkilde FW, Sjöblom J, Tekenbergs-Hjelte L, Mrak J, *J. Pharm. Biomed. Anal.*, 1997; 15: 687-696.
10. Campbell Roberts SN, Williams AC, Grimsey IM, Booth SW, *J. Pharm. Biomed. Anal.*, 2002; 28: 1135-1147.
11. Šašić S, Clark DA, Mitchell JC, Snowden MJ, *Analyst*, 2004; 129: 1001-1007.
12. Schoonover JR, Havrilla GJ, Treado PJ, *The internet journal of vibrational spectroscopy*, 2004; 3: 3.
13. Breitenbach J, Schrof W, Neumann J, *Pharm. Res.*, 1999; 16(7): 1109-1113.
14. Powell LP, Champion A, *Anal. Chem.*, 1986; 8(11): 2350-2352.
15. Niemczyk TM, Delgado-Lopez MM, Allen FS, *Anal. Chem.*, 1998; 70(13): 2762-2765.
16. Vergote GJ, De Beer TRM, Vervaet C, Remon JP, Baeyens WRG, Diericx N, Verpoort F, *Eur. J. Pharm. Sci.*, 2004; 21: 479-485.
17. Izolani AO, de Moraes MT, Téllez SCA, *J. Raman Spec.*, 2003; 34: 837-843.

18. Skoulika SG, Georgiou CA, *Appl. Spectrosc.*, 2001; 55(9): 1259-1265.
19. Szostak R, Mazurek S, *Analyst*, 2002; 127: 144-148.
20. Pelletier MJ, *Appl. Spectrosc.*, 2003; 57(1): 20A-42A.
21. De Beer TRM, Vergote GJ, Baeyens WRG, Remon JP, Vervaet C, Verpoort F, *Eur. J. Pharm. Sci.*, 2004; 23: 355-362.
22. Szostak R, Mazurek S, *J. Mol. Struct.*, 2004; 704: 229-233.
23. Strachan CJ, Pratiwi D, Gordon KC, Rades T, *J. Raman Spectrosc.*, 2004; 35: 347-352.
24. Failloux N, Bonnet I, Baron M, Perrier E, *Appl. Spectrosc.*, 2003; 57(9): 1117-1122.



Chapter 4
Counterfeit drugs

4 Counterfeit drugs

The previous two chapters discussed the theory of Raman spectroscopy and the pharmaceutical applications of this technique. This research project is focussed on the detection of counterfeit drugs with Raman spectroscopy. Chapter 4 elaborates on the definition of counterfeit drugs, the magnitude of the problem and the benefits of Raman spectroscopy as a fast and easy method to detect these counterfeit drugs.

The production of counterfeit drugs is a significant problem that contributes to morbidity, mortality, drug resistance and lost of confidence in the health-care systems¹. During the last decade the amount of counterfeit drugs on the worldwide market has rapidly increased. It is difficult to determine the exact scale of this problem, since not all counterfeit drugs are reported or even detected. The International Federation of Pharmaceutical Manufacturers Associations (IFPMA) has estimated that 10% of the drugs sold worldwide are counterfeits². The value of this trade is more than 30 billion US\$ and it is expected to reach 75 billion US\$ in 2010³.

4.1 What are counterfeit drugs?

Counterfeit drugs are part of substandard pharmaceuticals, which are drugs that are manufactured below established standards of quality³. Definitions of substandard and counterfeit drugs according to the World Health Organization (WHO) are³:

A substandard drug is a genuine drug product that does not meet the quality specifications set for the specific drug.

A counterfeit drug is one which is deliberately and fraudulently mislabelled with respect to identity and/or source. Counterfeiting can apply to both branded and generic products and counterfeit products may include products with the correct ingredients or with the wrong ingredients, without active ingredients, with insufficient active ingredient or fake packaging.

At the Conference of Experts on the Rational Use of Drugs in Nairobi (Kenya) in 1985, the problem of counterfeit drugs was first addressed⁴. Three years later, in 1988, the World Health Assembly adopted a resolution which requested for the prevention and detection of export, import and smuggling of counterfeit pharmaceutical products⁴. The first international meeting on counterfeit drugs was organised by the WHO and the IFPMA in 1992. Since then the awareness on the harmful effects of counterfeit drugs has grown slowly at international level⁴.

In order to create more awareness to this increasing problem of counterfeit drugs, the IMPACT (International Medicinal Products Anti-Counterfeiting Taskforce) was created in February 2006. The IMPACT is comprised of all 193 WHO member states and consists of international organizations, national drug regulatory authorities, enforcement agencies, customs, policy organizations, associations representing pharmaceutical manufactures, non-governmental organizations, wholesalers, health professionals, and patient groups³.

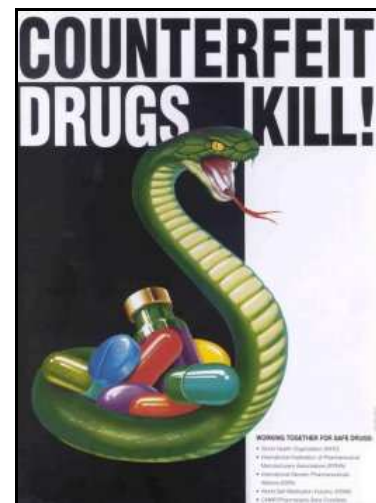


Figure 4.1 poster from WHO to increase public awareness

Figure 4.1 represents a poster used by the WHO to warn the public against the harmful effects of counterfeit drugs. Since IMPACT has only started less than two years ago, it is too early to indicate the effect of this program.

4.2 How big is the problem of counterfeit drugs?

Any kind of drugs ranging from expensive lifestyle drugs up to drugs to treat life-threatening illnesses like HIV/Aids are counterfeited. The drugs that are often counterfeited can be divided into two groups, depending on the region where they are brought on the market: developing or developed countries.

- In wealthier countries, expensive lifestyle drugs are frequently counterfeited, such as Lipitor[®] (a cholesterol lowering drug), Viagra[®] and Cialis[®] (drugs to treat erectile dysfunctions) and steroids^{3,5}.
- In developing countries drugs for treatment of life-threatening diseases such as malaria, tuberculosis and HIV/AIDS are frequently counterfeited^{3,5}.

The number of counterfeit drugs has been increasing rapidly during the last decade. Since it is difficult to show this in statistical proven research, it will be demonstrated by the number of counterfeit drug cases annually opened by the U.S.A. Food and Drug Administration (FDA) which is presented in figure 4.2.

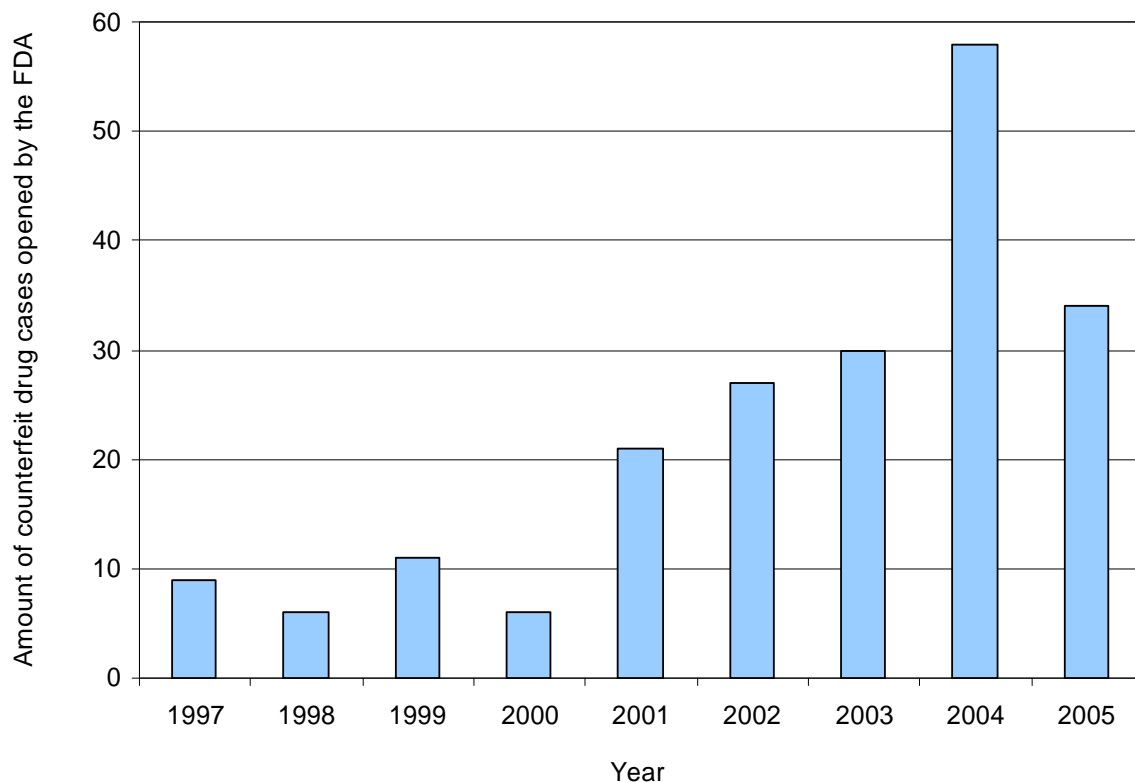


Figure 4.2 Number of counterfeit drug cases opened by the FDA per year⁶.

In figure 4.2 the number of drug cases from 1997 until 2005 is presented. This is an estimation from the FDA which are preliminary data depending on ongoing investigation⁷. A decline in counterfeited drug cases investigated by the FDA can be seen in 2005, with only 32 cases. This decline covers only the number of counterfeit cases investigated by the FDA and does not indicate the amount of drugs involved.

It could be possible that the number of cases decreased but that the total amount of counterfeit drugs seized increased. In order to get a clear idea of this problem, the quantity of counterfeit drugs found in each counterfeit drug case is necessary.

The regular use of counterfeit drugs can lead to therapeutic failure or drug resistance. In some cases, it can even lead to death as can be seen in these examples of incidents with counterfeit drugs, showing the scope of this problem^{2,3,8,9,10}:

- The consumption of paracetamol cough syrup prepared with diethylene glycol (a toxic chemical used in antifreeze), instead of propylene glycol, led to the death of 109 children in Nigeria in 1990, 59 children in Haiti in 1996 and 30 children in India in 1998.
- In Niger, between 1995 and 1996 over 50.000 people were inoculated with fake vaccines against meningitis (the vaccines consisted only of water). These were donated by a country which thought it was safe but it resulted in the death of at least 2.500 people.
- In 2000, 6 million ampoules of counterfeit Voltaren[®] (painkiller) were seized in Colombia.
- 240.000 packs of counterfeit drugs and 2 ton of raw materials, worth 1 million US\$, were seized in 2000 in Italy.
- In a single counterfeiting factory in India, 660 kg of counterfeit drugs, 1000 kg of raw materials and boxes bearing the logo of another company were found in 2001.
- In 2003, 200.000 bottles of Lipitor[®] were recalled in the USA. Lipitor[®] is used together with lifestyle changes (diet, weight-loss, exercise) to reduce the amount of cholesterol and other fatty substances in the blood.

- In December 2003, approximately 5 million capsules of assorted counterfeit drugs including amoxicillin, ampicillin, cloxacillin, ampiclox and other products were seized in Myanmar.

As shown by these examples, the problem does not only exist in developing countries, but has reached the western world as well. The production of these counterfeit drugs does not necessarily need to happen in large infrastructures or facilities. The majority of these drugs are produced in ordinary households, small cottage industries or just in peoples backyard³.

An additional problem that has contributed to the increase of counterfeit drugs on the market, is the sale of drugs through the internet¹¹. For instance in the U.S.A., it is very common to order prescription drugs online. Recently, the FDA released a warning about the risk involved in buying drugs online, and issued a warning against 24 websites, which sold counterfeit drugs¹¹.

The National Association of Boards of Pharmacy released a specified list of susceptible products in 2004. This list includes 32 prescription drugs which are to be susceptible to adulteration, counterfeiting or diversion and posing therefore the potential for a greater public health risk¹². From these 32 drugs, 16 are used of the treat HIV/ AIDS: Combivir[®], Crixivan[®], Epivir[®], Gamimune[®], Gammagard[®], Immune globulin, Panglobulin[®], Retrovir[®], Sustiva[®], Trizivir[®], Venoglobulin[®], Videx[®], Viracept[®], Viramune[®], Zerit[®] and Ziagen[®].

On this list are also drugs to treat infections (Diflucan[®], Lamisil[®], Rocephin[®]), to treat anaemia (Epogen[®] and Procrit[®]), to lower cholesterol levels (Lipitor[®] and Zocor[®]), to treat different symptoms of cancer (Lupron[®], Zofran[®] and Zoladex[®]), and to help against schizophrenia (Risperdal[®] and Zyprexa[®]). Also on the list are Neupogen[®], to increase the level of white blood cells, Viagra[®], to treat erectile dysfunction, Nutropin AQ[®] and Serostim[®], which are both hormones to enhance growth^{12,13,14}.

4.3 Actions taken against counterfeiters

Countries need appropriate legislation in order to combat manufacturing and distribution of counterfeit drugs. So far, there is no specific legislation on international level and strangely enough, there is apparently, no emphasis by the industry to enforce legislation. Pharmaceutical companies have spent a large amount of money to develop a single new drug (approximately 500-800 million dollar per drug). If this drug is counterfeited the pharmaceutical companies are, on one hand afraid for loss in revenues and, on the other hand, anxious to face damage of brand integrity, which can destroy a companies reputation².

Counterfeit drugs can also damage the confidence that people have in their national health care system; additionally, the government has less tax revenues, while there is an increase in the cost of monitoring the efficacy and safety of pharmaceuticals². Particularly in the U.S.A., the emphasis is not only focussed on the improvement of technology to protect the drug supply but also to improve the nation's prescription drug distribution system². So far, it seems that the priority of the governments and the pharmaceutical industry is to avoid that customers suspect their drugs to be counterfeited. This could explain why emphasis on legislation in the western world is limited.

Currently in the U.S.A., the penalty for counterfeiting a drug label is 10 years imprisonment, while the penalty for counterfeiting the actual drug is only 3 years⁶. However, this might change since in the U.S.A., in the beginning of 2007, a new bill has been introduced in the House of Representatives to increase the penalties for drug counterfeiting (the counterfeit drug prevention act of 2007, HR 780). It is suggested that the penalties for counterfeiting drugs should be increased to an imprisonment for at least 20 years. If the counterfeit drug is the proximate cause of a consumers death, the penalty can be increased to life imprisonment¹⁵.

On the contrary, in the developing world, emphasis is on legislation and the penalties are therefore much higher. In the Philippines offenders can face penalties from 6 months to life imprisonment along with a hefty fine of 1 million peso (circa \$ 25,000)¹.

While in India, under the Indian Drugs Act, a counterfeit drugs manufacturer can face an imprisonment of at least 3 years and 5000 Rupees (circa \$ 1,000) fine. Recently the government of India discussed the death penalty as a sentence for counterfeiters¹. In May 2007, the former head of China's Food and Drug safety agency was sentenced to death, after pleading guilty to corruption and accepting bribes (\$ 850.000) for approving drug-production licenses¹⁶. Over the last few years, the governments have become aware of the fact that the penalties for counterfeiters have to be increased in order to tackle the problem of counterfeit drugs.

Besides increasing the penalties for counterfeiters, steps have been taken to make it more difficult for the counterfeiters to sell the drugs on the market or to add the drugs to the legal supply chain. One of these steps is the use of tracking or trace detection systems by legal pharmaceutical manufactures. There are two authentication features that can be used: optical variable coatings and holograms. These security features are apparent and visible and, therefore do not require any instruments to detect them².

The use of holograms has grown rapidly over the last decade: these are generated from the interference patterns obtained through the interaction of laser beams². Advantages of these holograms are that they are recognizable to the customer and relatively cheap.

Newton et al.¹⁷ started a large project on the distribution of counterfeit antimalarial tablets in Southeast Asia. Based on the hologram used by Guilin Pharma, the counterfeit tablets could be easily detected (100% accurate) in the first survey (1999/2000)¹⁷. However, experience is required to identify the counterfeits and due to increased counterfeiter sophistication, this method was less accurate in a second survey (2002/2003)¹⁸. In figure 4.3 the genuine hologram attached to the blisterpack of Guilin Pharma is shown (A) with two kinds of fake holograms (B and C): it is difficult to distinguish the fake holograms from the genuine one.

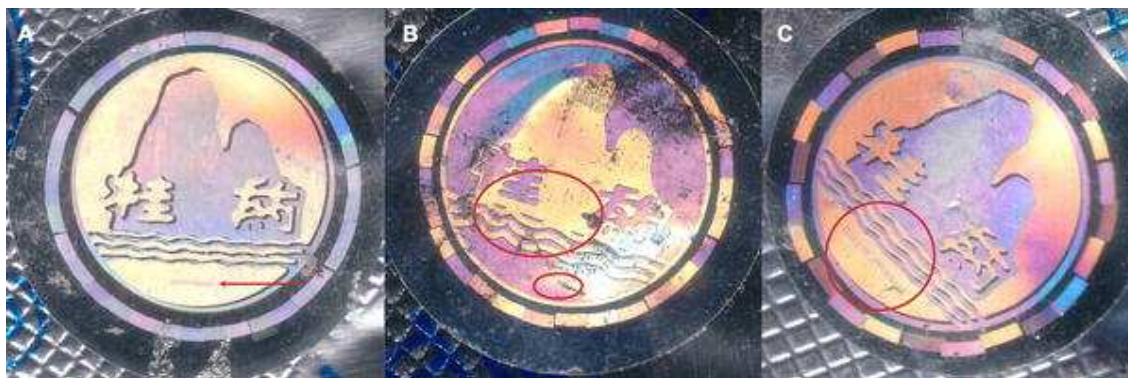


Figure 4.3 Genuine (A) and fake (B and C) Guilin Pharma artesunate blister pack holograms found in mainland Southeast Asia¹⁹. The red circles highlight the differences of the fake holograms (B and C) compared to the genuine one (A).

Apparently, the counterfeiters have no trouble in duplicating the holograms. Holograms that are being used by at least two pharmaceutical companies in Asia, were conventional holograms and are known to be duplicated by counterfeiters within a month after product launch²⁰.

Another measure taken against counterfeiting is adding features that are hidden and not immediately apparent. These features can be easily identified with the use of a simple instrument, like for instance a UV lamp or a microscope¹. These chemical or physical markers (taggants) can be added on the product and/or packaging. Four different types of taggants are available, namely spectroscopic, biological, chemical and physical. For spectroscopic taggants, inks are used that are UV absorbers while biological taggants may include ink with strands of a specific DNA. This DNA-embedded ink is very difficult to replicate. Chemical taggants can include materials that can only be detected with IR spectroscopy or X-ray fluorescence. The last group are physical taggants, which are for instance microscopic plastic particles and are only visible with the use of a microscope¹. These four different taggants allows rapid identification of the counterfeits.

The manufactures and distributors are forced to improve technologies against counterfeiters, since the criminals, that introduce counterfeit drugs, are becoming increasingly more sophisticated. One of these new developed methods is the track-and-trace technology which, with the use of radio frequency chips, can track the

products from the point of manufacturing to the point of dispensing^{2,21}. The key to this track-and-trace technology is the use of a unique serial number for each and every prescription drug. By using radio frequency identification (RFID), these serial numbers can be automatically read by sensors over short distances²¹. RFID varies in cost, ranging from a few cents to several dollars per package, depending on data capacity, range and read/write capability². The downside of this method, at this moment, is that it is affordable for developed countries but too expensive to use to combat the problem of counterfeit drugs in developing countries.

4.4 Analytical techniques used to detect counterfeit drugs

The first step in detecting counterfeit drugs, is the careful visual inspection of the package and label, since even the smallest modifications may indicate a potential counterfeit. But since the counterfeiters become more sophisticated, additional analytical techniques are necessary to detect the counterfeits from the genuine drugs. So far, several analytical techniques have been used to detect counterfeit drugs.

Chromatography is one of the most commonly used techniques, for instance, high performance chromatography (HPLC) to detect counterfeit antimalarial drugs. Green et al²² investigated drugs containing artesunate, chloroquine phosphate (tablets and injectables), quinine sulfate capsules and sulfadoxine / pyrimethamine tablets from Laos. The samples were dissolved in organic solvents and diluted before analysis with the HPLC. The accuracy of the method is $\pm 8\%$ ²². A second example of the use of HPLC to detect counterfeit is the research performed by Atemnkeng et al. which focused on the detection of artemisinin-derivatives (including artesunate) from Kenya and DR Congo²³. The tablets for this research were weighed, crushed and dissolved in the appropriate solvents. The correct active ingredient was present in each case, the dosage however was in some cases substandard²³. Additional to these two investigations, HPLC has proven to be an accurate analytical technique for the detection of counterfeit homeopathic medicinal products²⁴, determination of oseltamivir phosphate in tamiflu²⁵ and detection of counterfeit anti-diabetic drugs²⁶ as well.

For the detection of counterfeit antimalarial medicines, reversed-phase liquid chromatography (LC) can also be used. Gaudiano et al. demonstrated the use of this technique on antimalarial drugs (chloroquine, quinine and mefloquine) purchased from markets in Congo, Burundi and Angola²⁷. The drugs analysed in this study, contained less than 90% of required active ingredient. Additionally, the level of impurities in these drugs, was much higher than tablets sold on the Italian market²⁷.

Another method is the use of thin layer chromatography (TLC) for the detection of counterfeit drugs. TLC is much cheaper than HPLC or LC. Laserson et al. demonstrated the use of TLC for tuberculosis drugs²⁸. With this method, 10 % of the samples analysed, contained less than 85% of the required active ingredient²⁸. The downside of all these chromatographic methods is the extended sample preparation, since the tablets have to be grinded, dissolved, diluted and analysed.

Some methods require hardly any sample preparation. The first one is X-ray powder diffraction (XRD), where the only sample preparation is the removal of the coating (ca. 2mm x 14mm) before analysis²⁹. In case of analyzing Viagra[®], the diffraction pattern of a genuine tablet, containing 100 mg active ingredient, is compared to the diffraction patterns of the six counterfeit ones. By using this method, the presence of the active ingredient sildenafil citrate could be determined as well as some excipients used in the tablet, for instance the cellulose and anhydrous calcium hydrogen phosphate. This method could easily distinguish the counterfeit from the genuine based on the visual examination of the diffraction patterns. The conclusion of this investigation has to be used very carefully since the results are based on the analysis of six Viagra tablets[®].

Counterfeit Viagra[®] tablets have also been analysed by using near-infrared spectroscopy (NIRS), another method which requires no sample treatment³⁰. Since NIRS spectrum reflects both chemical and physical properties, the spectrum could be used to detect counterfeit drugs. In total 103 samples were analysed, and with the use of wavelength correlation and principal component analysis (PCA), the counterfeits could be distinguished from the genuine samples. From the 103 samples screened, 99 were correctly analysed with the use of NIRS. Additionally, other

substances present in the Viagra[®] tablets were detected, for instance quinine and amphetamine³⁰. A downside of these analytical techniques is, that they require trained analysts for analysis and data interpretation. Moreover, the cost of the equipment can be quite high.

Colorimetry is a cheap and easy to use method, where the intensity of the positive colour reaction is proportional to the concentration of the active ingredient². This method was proven to be effective for the detection of counterfeit antimalarial tablets by Green et al²². By simply adding diazonium fast red TR salt (C₇H₉Cl₂N) to a small amount of powder from the tablet, it could be demonstrated whether the antimalarial tablet contained the active ingredient artesunate²². A downside of this method is that for each drug a new colorimetric agent has to be developed. Moreover, no information about excipients present in the drugs is presented with this method.

4.5 History of Raman spectroscopy as a detection method of counterfeit drugs

The use of Raman spectroscopy in the pharmaceutical field has been increasing for the last few years. Raman spectroscopy has some specific benefits, which are very useful for the detection of counterfeit drugs: a Raman spectrum can be recorded rapidly without any sample preparation. Moreover, this technique provides not only information about the active ingredient present in the drug, but a Raman spectrum contains also information on the concentration of the active ingredient, identification of excipients present in the drug².

This technique has been used for the detection of different kinds of illicit drugs, such as cocaine, heroin and ecstasy^{31,32}. Bell et al. used Raman spectroscopy for the analysis of ecstasy tablets and other phenethylamine ecstasy analogues. By determining the excipients used, links between the seized tablets could also be established^{33,34}.

4.6 Conclusion

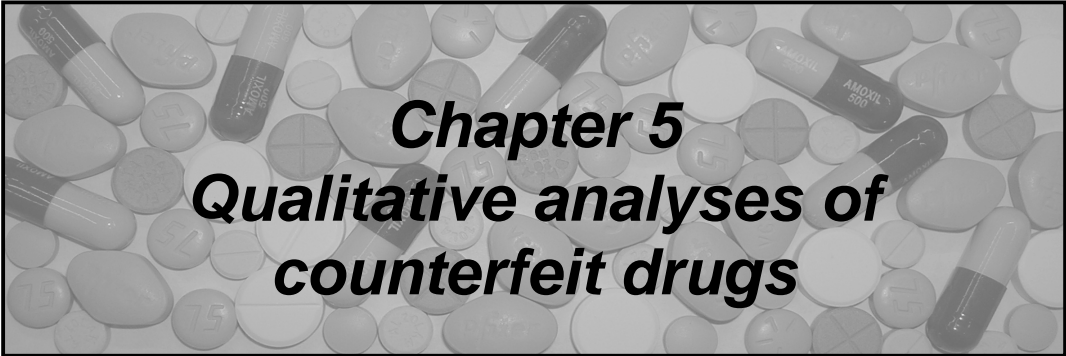
So far, Raman spectroscopy has been used for the detection of illicit drugs but not for counterfeit drugs. This PhD thesis will demonstrate the use of Raman spectroscopy as a fast and easy detection method of counterfeit drugs. In this thesis the focus is not only on the analysis of the active ingredient in the drugs (qualitative and quantitative), but also on the excipients used. To ease the detection of excipients in counterfeit drugs, an elaborate database is presented in chapter 8 with the most frequently used excipients in the pharmaceutical field. Chapter 5, 6, and 7 will cover the qualitative analysis of counterfeit drugs while in chapter 9 the quantitative determination of these counterfeit drugs will be discussed.

4.7 References

1. Newton PN, Green MD, Fernandez FM, Day NPJ, White NJ, *Lancet Infect. Dis.*, 2006; 6: 602-613.
2. Deisingh AK, *Analyst*, 2005; 130: 271-279.
3. World Health Organization (WHO), *Fact Sheet N°275*, Revised 14 November 2006.
4. Counterfeit drugs, *Guidelines for the development of measures to combat counterfeit drugs*, Department of Essential Drugs and Other Medicines, World Health Organization (WHO), Geneva, Switzerland, 1999.
5. World Health Organization (WHO) Drug Information, 2004, 18, 2.
6. Food and Drug Administration (FDA), *Combating Counterfeit Drugs*, A report of the Food and Drug administration, update 2005.
7. Lutter R, Remarks by Lutter R presented at: RFID World Conference, March 1st 2006, Dallas, Texas.
8. Akunyuli DN and Nnani IPC, *International Journal of Risk & Safety in medicine*, 2004; 16(3): 181-190.
9. www.nlm.nih.gov
10. Shakoor O, Taylor RB, *Analyst*, 1996; 121: 1473-1477.
11. Food and Drug Administration (FDA) News, *FDA warns consumers about counterfeit drugs from multiple internet sellers*, P07-76, may 1, 2007.

12. National Association of Boards of Pharmacy (NABP), *National Specified List of Susceptible Products*, December 28, 2004.
13. Kemp SF, Kuntze J, Attie KM, Maneatis T, Butler S, Frane J, Lippe B, *J. Clin. Endocrinol. Metab.*, 2005; 90(9): 5247-5253.
14. Goldsmith DR, Wagstaff AJ, *Drugs*, 2006; 66: 387-401.
15. House of Representatives of the United States of America, Counterfeit Drug Prevention Act of 2007, HR 780 IH (www.govtrack.us)
16. International Herald Tribune, May 29 2007.
17. Newton P, Proux S, Green M, Smithuis FM, Rozendaal J, Prakongpan S, Chotivanich K, Mayxay M, Looareesuwan S, Farrar JJ, Nosten F, White NJ, *Lancet*, 2001; 357: 1948–1950.
18. Dondorp AM, Newton PN, Mayxay M, Van Damme W, Smithuis FM, Yeung S, Petit A, Lynam AJ, Johnson A, Hien TT, McGready R, Farrar JJ, Looareesuwan S, Day NPJ, Green MD, White NJ, *Tropical Medicine and International Health*, 2004; 9(12): 1241-1246.
19. Cockburn R, Newton PN, Kyeremateng Agyarko E, Akunyili D, White NJ, *PLOS Medicine*, 2005; 2(4): 302-308.
20. Forcinio H, *Pharmaceutical Technology*, 2002; 6: 26-34.
21. Ducca AT, *Journal of Pharmacy Practice*, 2006; 19(4): 230-235.
22. Green MD, Nettey H, Vollaiva Rojas O, Pamanivong C, Khounsaknalath, Grande Ortiz M, Newton PN, Fernandez FM, Vongsack L, Manolin O. *Journal of Pharmaceutical and Biomedical Analysis*, 2007; 43: 105-110.
23. Atemnkeng MA, De Cock K, Plaizie-Vercammen J, *Trop. Med. Int. Health*, 2007; 12(1): 68-74.
24. Panus A, Multai G, Incarnato G, Gagliari L, *J. Pharm. Biomed. Anal.*, 2007; 43: 1221-1227.
25. Joseph-Charles J, Geneste C, Laborde-Kummer E, Gheyouche R, Boudis H, Dubost JP, *J. Pharm. Biomed. Anal.*, 2007; 44: 1008-1013.
26. Yao J, Shi YQ, Li ZR, Jin SH, *J. Chromatogr. B*, 2007; 853: 254-259.
27. Gaudiano MC, Antoniella E, Bertocchi P, Valvo L, *J. Pharm. Biomed. Anal.*, 2006; 42:132-135.
28. Laserson KF, Kenyon AS, Kenyon TA, Layloff T, Binkin NJ, *Int. J. Tuberc. lung dis.*, 2001; 5(5): 448-454.

-
29. Maurin JK, Pluciński, Mazurek AK, Fijałek Z, *J. Pharm. Biomed. Anal.*, 2007; 43: 1514-1518.
 30. Vredenbregt MJ, Blok-Tip L, Hoogerbrugge R, Barends DM, de Kaste D, *J. Pharm. Biomed. Anal.*, 2006; 40: 840-849.
 31. Ryder AG, O'connor GM, Glynn TJ, *J. Forensic Sci.*, 1999; 44(5): 1013-1019.
 32. Hodges CM, Akhavan J, *Spectroc. Acta Pt. A-Molec. Biomolec. Spectr.*, 1990; 46A(2): 303-307.
 33. Bell SEJ, Burns DT, Dennis AD, Speers JS, *Analyst*, 2000; 125: 541-544.
 34. Bell SEJ, Burns DT, Dennis AC, Matchett LJ, Speers JS, *Analyst*, 2000; 125: 1811-1815.



Chapter 5
Qualitative analyses of
counterfeit drugs

5 Qualitative analysis of counterfeit drugs

As mentioned in the previous chapter, numerous techniques can, and have been used, to detect counterfeit drugs. Raman spectroscopy has certain benefits that the other techniques lack. There is no sample preparation necessary, the sample can be measured through glass or the blister package, and above all, this technique is non-destructive.

In order to verify if Raman spectroscopy can be useful for qualitative detection of counterfeit drugs, different kinds of possible counterfeit drugs are analysed. This chapter describes the qualitative analysis of tablets, gels, syringes and capsules. These drugs are, either seized at customs at Brussels airport, at raids in different houses, buildings or companies in Belgium by the FAGG (Federal Agency for Medicines and Health Products), or received anonymously.

This chapter describes the analyses of different possible counterfeit drugs. Firstly, erectile dysfunction drugs are analysed. Three different genuine erectile dysfunction drugs are available, namely Viagra[®], Cialis[®] and Levitra[®]. Viagra is still the most commonly counterfeited erectile dysfunction drug, but the amount of counterfeit Cialis has rapidly increased over the last few years¹. The Raman spectra of these genuine drugs are compared with the Raman spectra of possible counterfeits. The group of possible counterfeits consists of two Viagra[®] tablets, a gel containing the same active ingredient as Viagra[®] and two tablets claiming to contain the same active ingredient as Cialis[®].

Secondly, possible counterfeit Noromectin[®], which is an oral paste used to cure horses from different kinds of parasites, is analysed. Noromectin[®] is sold in a blue and white plastic syringe, which was sold illegally on the Belgium market in 2005. With Raman spectroscopy, not only the content is analysed, but the plastics of the syringe and the inks used on the label are analysed as well. These Raman spectra are compared to the corresponding Raman spectra of the genuine Noromectin[®] sample.

Finally, two examples of possible counterfeited Amoxil[®] are analysed and compared to a genuine sample. Amoxil[®] contains the active ingredient amoxicillin and is an antibiotic (penicillin). It is used for treating numerous infections of the chest, tonsils, ears, sinuses and the urinary tract. Amoxil[®] can also be used to treat gonorrhoea. These examples will demonstrate the use of Raman spectroscopy as a fast and easy qualitative method of detection².

5.1 Experimental

Two dispersive Raman spectrometers (MArtA and Renishaw System-1000 instrument) are used for the qualitative analysis and are described below:

MArtA^{3,4}:

The core of the mobile art analyser (MartA) is a modified portable Raman imaging microscope (PRIM) (Spectracode, West Lafayette, Ind. USA), which is based on a SpectraPro-150i 150-mm spectrometer and a thermo-electrically cooled, charge-coupled device detector (Roper Scientific / Prince Instruments). The system is equipped with a 785 nm diode laser (Process Instruments, Salt Lake City, Ut., USA) for excitation, with a power of ca. 70 mW at the sample. A 6x objective lens is used which creates a spot size of ca. 25 μm . All spectra are recorded in the spectral window of 0 to 2500 cm^{-1} . The analysis time and number of accumulations differ between the samples analysed. The standard deviation on the position of a Raman band ranges from 4 – 8 cm^{-1} .

Renishaw⁵:

The Renishaw System-1000 spectrometer (Wotton-under-Edge, UK) is connected to a Olympus BH-2 microscope. The diode laser has a power of 50 mW at the source and a wavelength of 785 nm (DL 100, TuiOptics GmbH, Martinsried/Munich, Germany). A 5x objective lens (Olympus MDPlan5, 0.10 NA, Omnilabo, Aartselaar, Belgium) is used and the collected Raman radiation is dispersed with a 1200 lines mm^{-1} grating (focal length 250 mm) and focussed on a Peltier-cooled CCD

detector, allowing to obtain a spectral resolution of ca. 1 cm^{-1} . All spectra are recorded in the spectral window of 200 to 1800 cm^{-1} . The analysis time and number of accumulations differ between the samples analysed. The standard deviation on the position of a Raman band is circa 1 cm^{-1} . The recorded spectra are averaged (three per sample) and baseline-corrected with ACD/Specmanager (version 9.13, Advanced Chemistry Development, inc. Toronto, Canada) to eliminate the influence of broadband fluorescence.

5.2 Analysis of erectile dysfunction drugs

5.2.1 Functioning of erectile dysfunction drugs

During sexual stimulation, nitric oxide (NO) is released from the nerve endings and endothelial cells in the corpus cavernosum. NO activates the enzyme guanylate cyclase, which results in an increased level of cyclic guanosine monophosphate (cGMP), allowing inflow of blood which causes the erection. Phosphodiesterase type 5 (PDE5) is responsible for the degradation of the cGMP level in the corpus cavernosum^{6,7,8}. The three most common drugs against erectile dysfunction are Viagra[®], Cialis[®], and Levitra[®]. These oral drugs inhibit PDE5, therefore increasing the amount of cGMP, which is responsible for the erection^{6,7,8}. Since the introduction of these drugs, the amount that is available through Internet, legally as well as illegally, has increased.

5.2.2 Content of the three erectile dysfunction drugs

The active ingredients of these three oral drugs, and excipients present in the tablets, are described below:

Viagra^{®6}:

The active ingredient of Viagra[®] is sildenafil citrate. Sildenafil citrate is designated chemically as 1-[[3-(6,7-dihydro-1-methyl-7-oxo-3-propyl-1*H*-pyrazolo[4,3-*d*]pyrimidin-5-yl)-4-ethoxyphenyl]sulfonyl]-4-methylpiperazine citrate. The structural formula and picture of a genuine Viagra[®] tablet are shown in figure 5.1⁶.

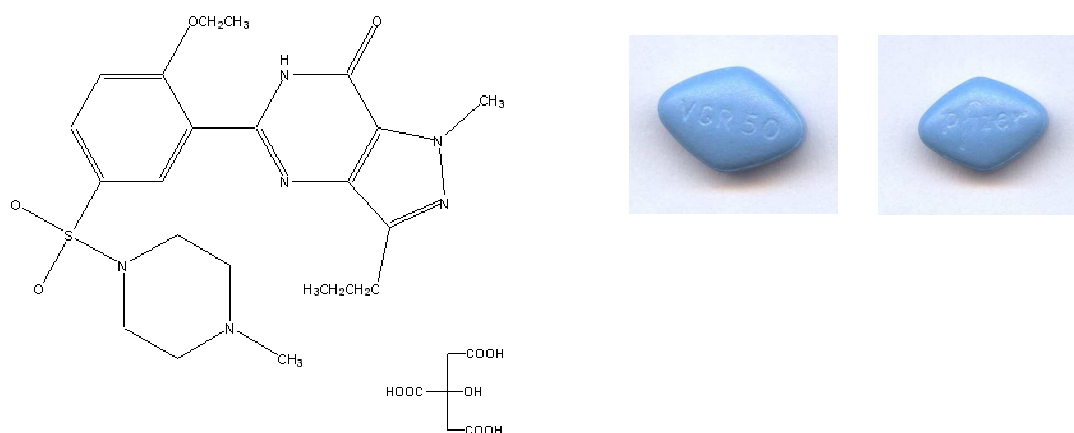


Figure 5.1 Left: structural formula of sildenafil citrate; right: both sides of a genuine Viagra[®] tablet⁶.

The tablets made for oral administration are blue, diamond shaped and are sold in three different doses of respectively 25, 50 and 100 mg sildenafil citrate. Viagra[®] also consists of the following excipients: microcrystalline cellulose, anhydrous dibasic calcium phosphate, croscarmellose sodium, magnesium stearate, hypromellose, titanium dioxide, lactose, triacetin and FD&C Blue 2 aluminum lake⁶.

Cialis[®]⁷:

The active ingredient of Cialis[®] is tadalafil. Tadalafil is designated chemically as pyrazino[1',2':1,6] pyrido[3,4-b] indole-1,4-dione,6-(1,3-benzodioxol-5-yl) -2,3,6,7,12,12a -hexahydro-2-methyl-,(6R,12aR)-. The structural formula and a picture of a genuine Cialis[®] tablet are presented in figure 5.2⁷.

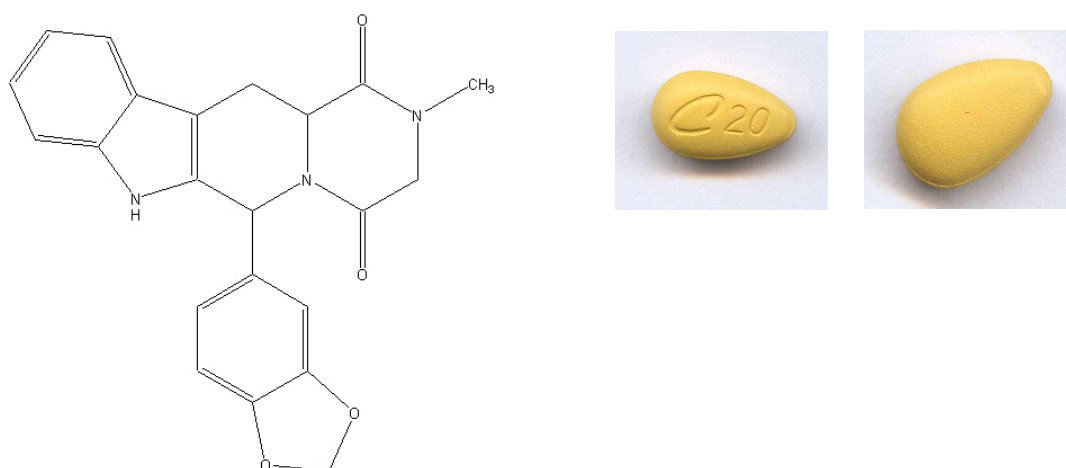


Figure 5.2 Left: structural formula of tadalafil; right: both sides of a genuine Cialis[®] tablet⁷.

The tablets, made for oral administration, are yellow, almond shaped and sold in three different dosages of 5, 10 and 20 mg active ingredient. Cialis[®] also consists, besides the active ingredient, of the following excipients: croscarmellose sodium, hydroxypropyl cellulose, hypromellose, iron oxide, lactose monohydrate, magnesium stearate, microcrystalline cellulose, sodium lauryl sulfate, talc, titanium dioxide and triacetin⁷.

Levitra^{®8}:

The active ingredient of Levitra[®] is vardenafil HCl. Vardenafil HCl is designated chemically as piperazine,1-[[3-(1,4-dihydro-5-methyl-4-oxo-7-propylimidazo[5,1-f][1,2,4]triazin-2-yl)-4-ethoxyphenyl]sulfonyl]-4-ethyl-,monohydrochloride. The formula and figure of a genuine Levitra[®] tablet are presented in figure 5.3⁸.

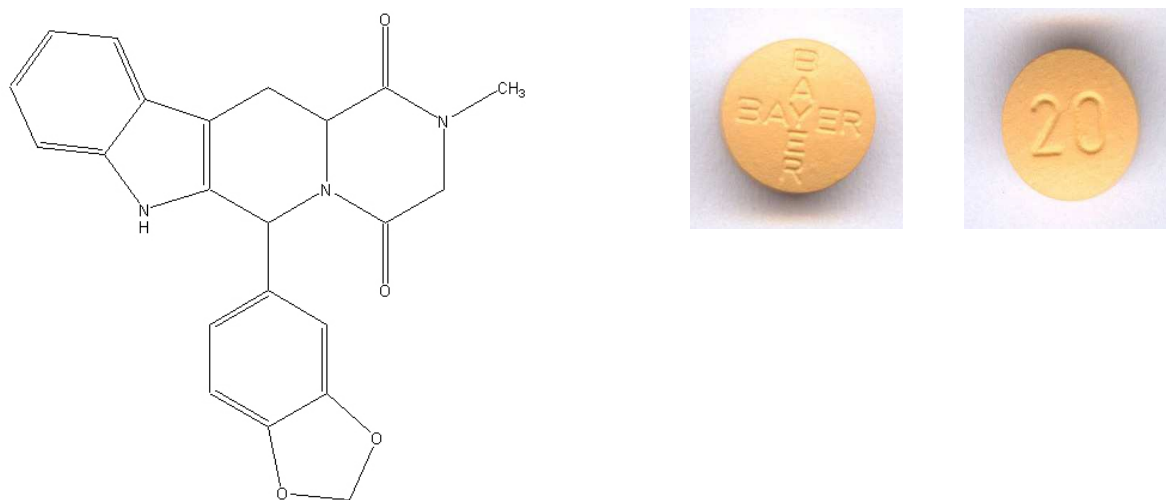


Figure 5.3 Left: the structural formula of vardenafil; right: a genuine Levitra[®] tablet⁸.

The tablets, made for oral administration, are orange, round shaped tablets and have 2.5, 5, 10 or 20 mg active ingredient. Levitra[®] also consists, besides the active ingredient, of the following excipients: microcrystalline cellulose, crospovidone, colloidal silicon dioxide, magnesium stearate, hypromellose, polyethylene glycol, titanium dioxide, yellow ferric oxide, and red ferric oxide⁸.

The first step of the analysis of counterfeit drugs is recording of the Raman spectra of the genuine drugs, which can be used as a reference. Figure 5.4 shows the Raman spectra of genuine Viagra[®], Cialis[®] and Levitra[®] tablets.

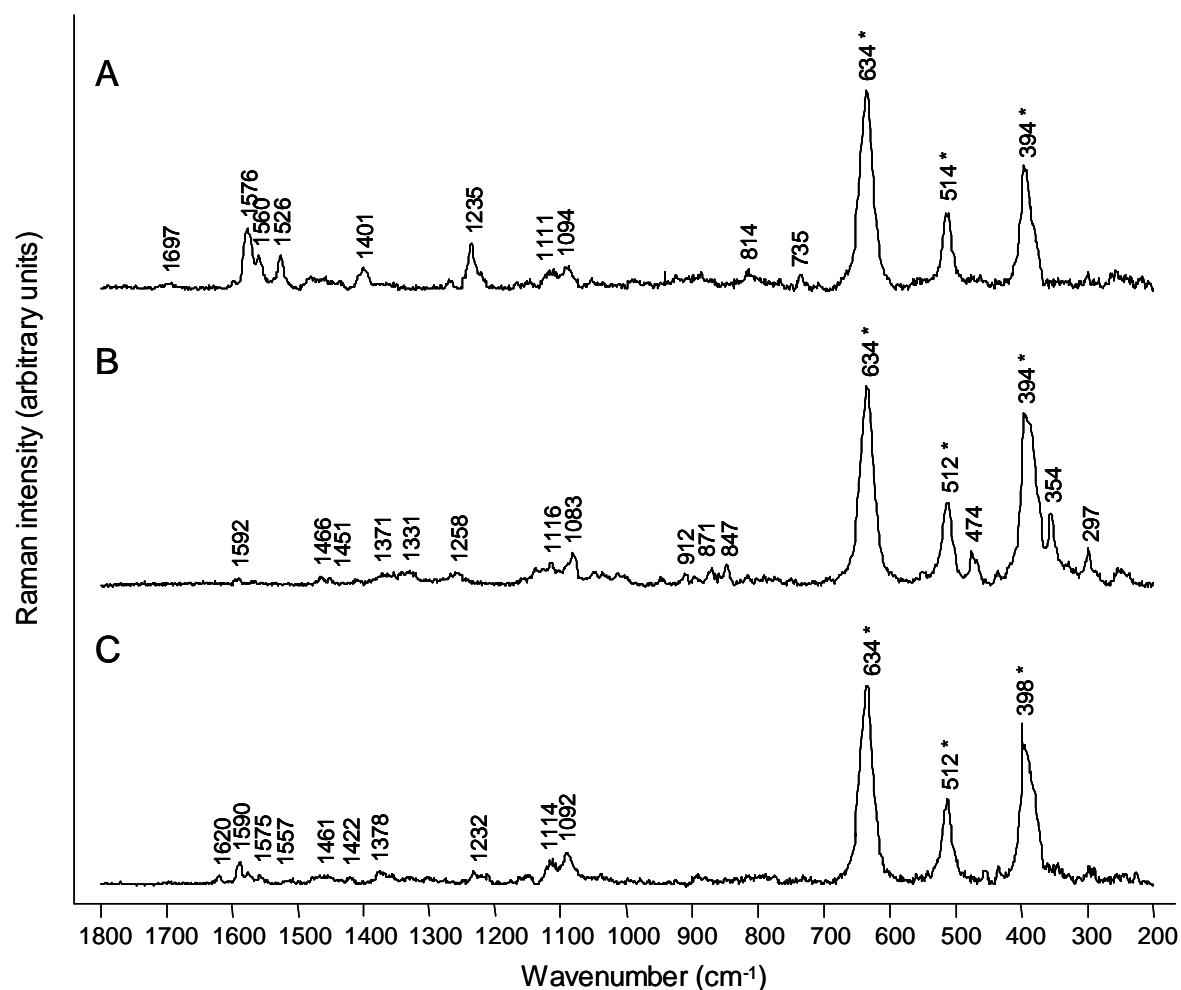


Figure 5.4 Raman spectra of erectile dysfunction drugs, all analysed with the Renishaw System-1000 instrument with a 5x objective (25 acc. x 30 s): (A) genuine Viagra[®] tablet (50 mg), (B) genuine Cialis[®] tablet (20 mg) and (C) genuine Levitra[®] tablet (20 mg). Raman bands marked with * can be assigned to anatase titanium dioxide.

All three tablets against erectile dysfunctions show strong Raman bands at ca. 395, 513 and 636 cm^{-1} , which can be assigned to anatase TiO_2 (chapter 8, figure 7C). To avoid these strong Raman bands, the spectral window, presented in figure 5.5 is reduced to the range of 700 to 1800 cm^{-1} . This emphasizes the Raman bands of the active ingredients.

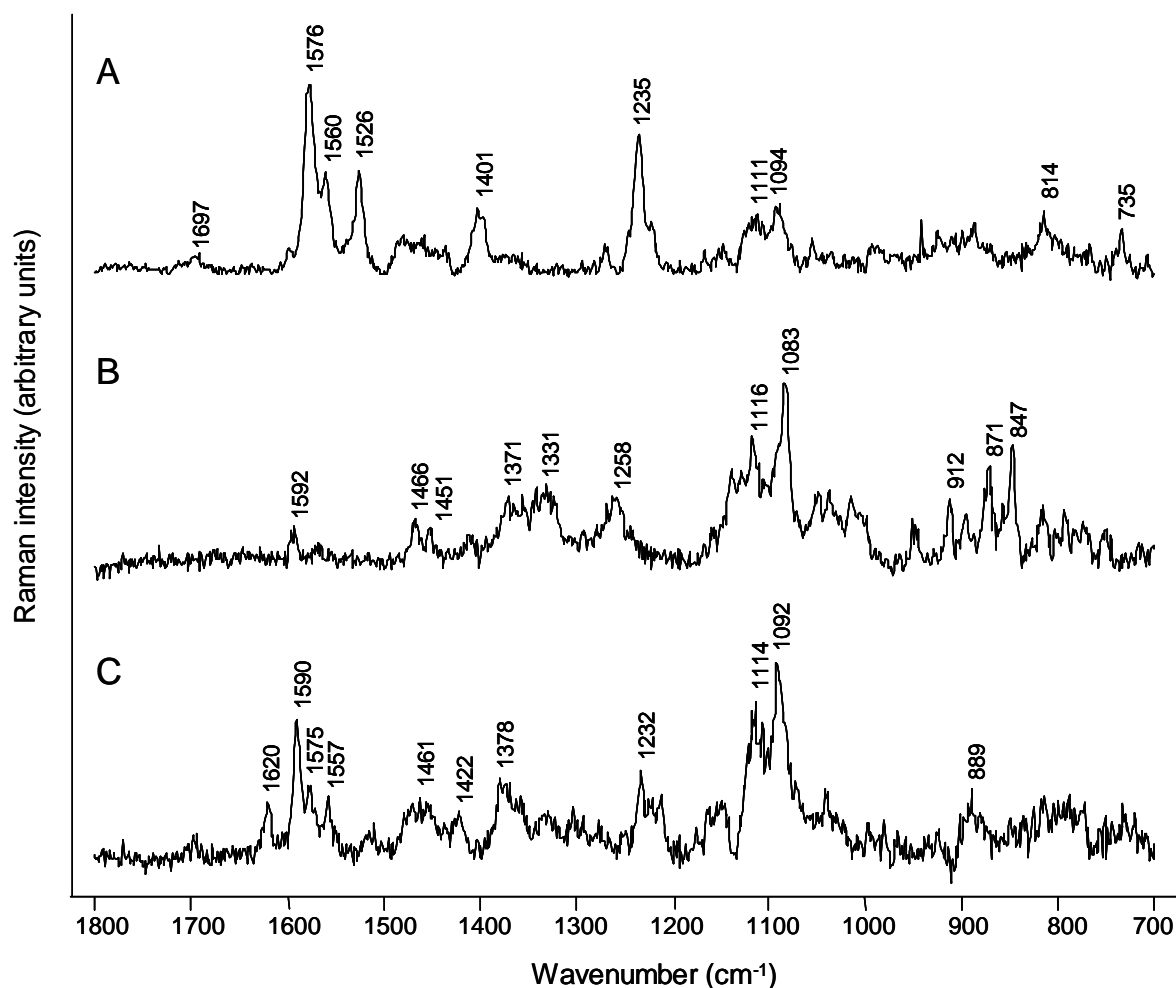


Figure 5.5 Raman spectra of erectile dysfunction drugs (range 700 till 1800 cm^{-1}) all analysed with the Renishaw System-1000 instrument with a 5x objective (25 acc. x 30 s): (A) genuine Viagra[®] tablet, (B) genuine Cialis[®] tablet and (C) genuine Levitra[®] tablet.

The Raman bands in the spectra of the genuine erectile dysfunction drugs are used as reference to detect the counterfeit drugs discussed in the following paragraphs (5.2.3 - 5.2.5).

5.2.3 Viagra[®] tablets

Two anonymously received tablets, possible Viagra[®] counterfeits, are analysed with the use of the Renishaw System-1000 spectrometer, and compared to a genuine Viagra[®] tablet. Figure 5.6 shows the tablets analysed, while figure 5.7 shows the Raman spectrum of the two possible counterfeits (B and C) in a range of 200 - 1800 cm^{-1} compared with genuine Viagra[®] (A).



Figure 5.6 Genuine Viagra[®] (A) and two possible counterfeit Viagra[®] tablets (B and C).

Visual inspection shows that the first possible counterfeit tablet (B) is not significantly different from the genuine Viagra[®] (A). However, the second possible counterfeit tablet (C) shows clear differences with the genuine one: the Pfizer logo is lacking and the amount of active ingredient is mentioned as “50 mg” in stead of “VGR 50”. Figure 5.7 shows the Raman spectrum of these two possible counterfeits and the spectrum of the genuine Viagra[®] as a reference.

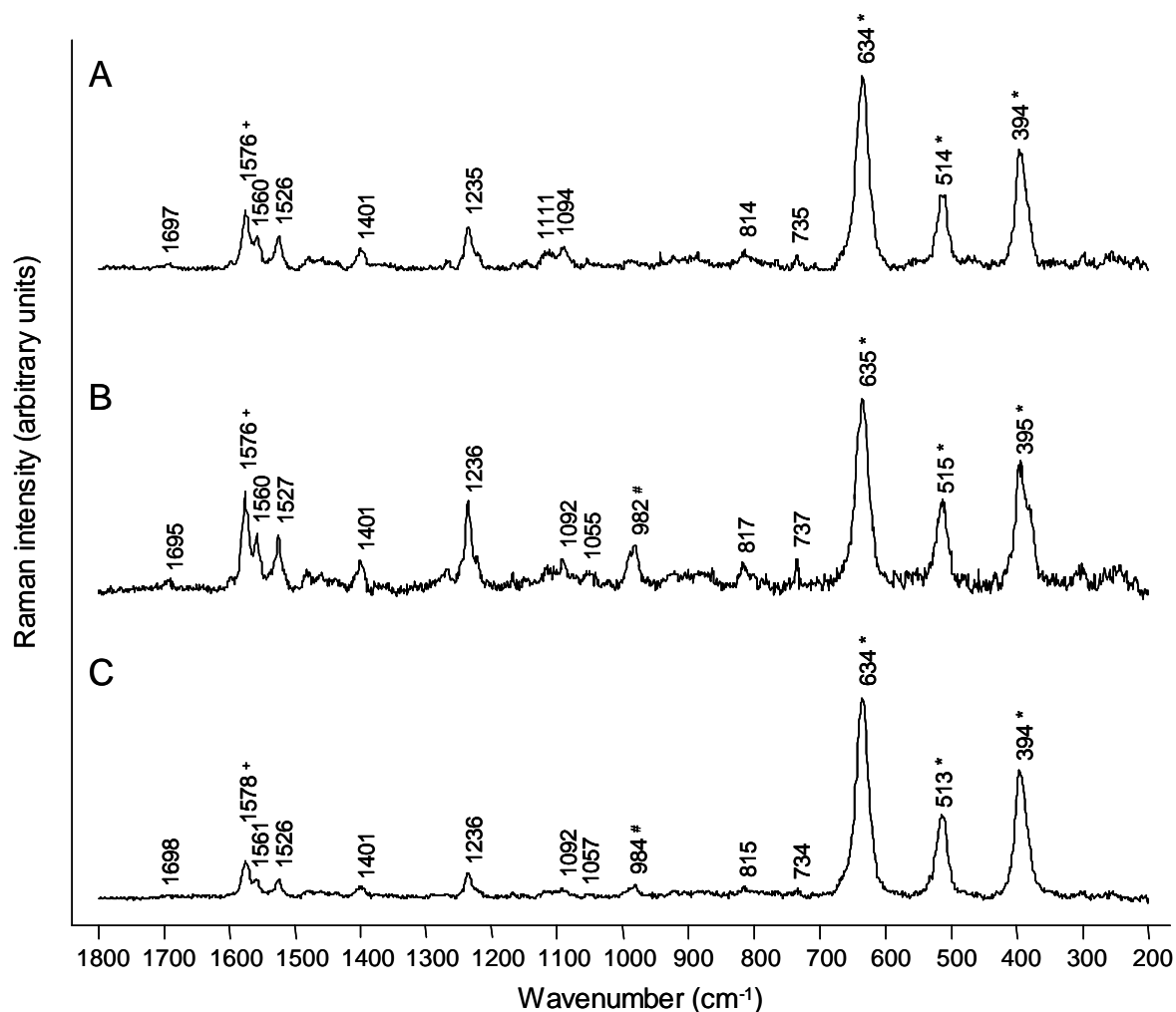


Figure 5.7 Raman spectra of genuine Viagra[®] tablet (A) and two possible counterfeit Viagra[®] tablets (B and C), all analysed with the Renishaw System-1000 instrument (5 acc. x 30 s). Raman bands marked with *, # and + can be assigned to respectively anatase TiO₂, barium sulfate and sildenafil citrate.

Figure 5.7 shows the spectral range of 200 till 1800 cm^{-1} . In all the spectra the three Raman bands of anatase titanium dioxide (TiO_2), at ca. 394, 513 and 634 cm^{-1} are present (chapter 8, fig. 8.7C). When the spectrum of the genuine Viagra[®] (fig. 5.7A) is compared to the two spectra of the possible counterfeits (fig. 5.7B and C), differences can be noted.

- Firstly, when looking at the intensities of the Raman band of TiO_2 at ca. 634 cm^{-1} and of the active ingredient at ca. 1576 cm^{-1} in the genuine Viagra[®] (fig. 5.7A), the ratio of these two intensities is approximately 3:1. However, for tablet B this ratio is circa 2:1, and for tablet C this ratio is circa 5:1, this could be an indication that these two tablets are possibly counterfeited.
- Secondly, both possible counterfeit tablets show an additional Raman band around 982 cm^{-1} , which can be assigned to barium sulfate (BaSO_4 , chapter 7, fig. 7.6A).

Based on these differences, the two tablets can be considered as counterfeited.

5.2.4 Gel containing the active ingredient of Viagra[®]

At Brussels airport, Seyagra gel sachets (fig. 5.8) containing the active ingredient of Viagra[®], namely sildenafil citrate, were seized. According to the manufacturer, it is a gel which is not only “fast acting” but also “great tasting”. In figure 5.9, the Raman spectrum of this gel is shown (B), next to the Raman spectrum of the active ingredient of genuine Viagra[®]: sildenafil citrate (A).



Figure 5.8 Seyagra gel

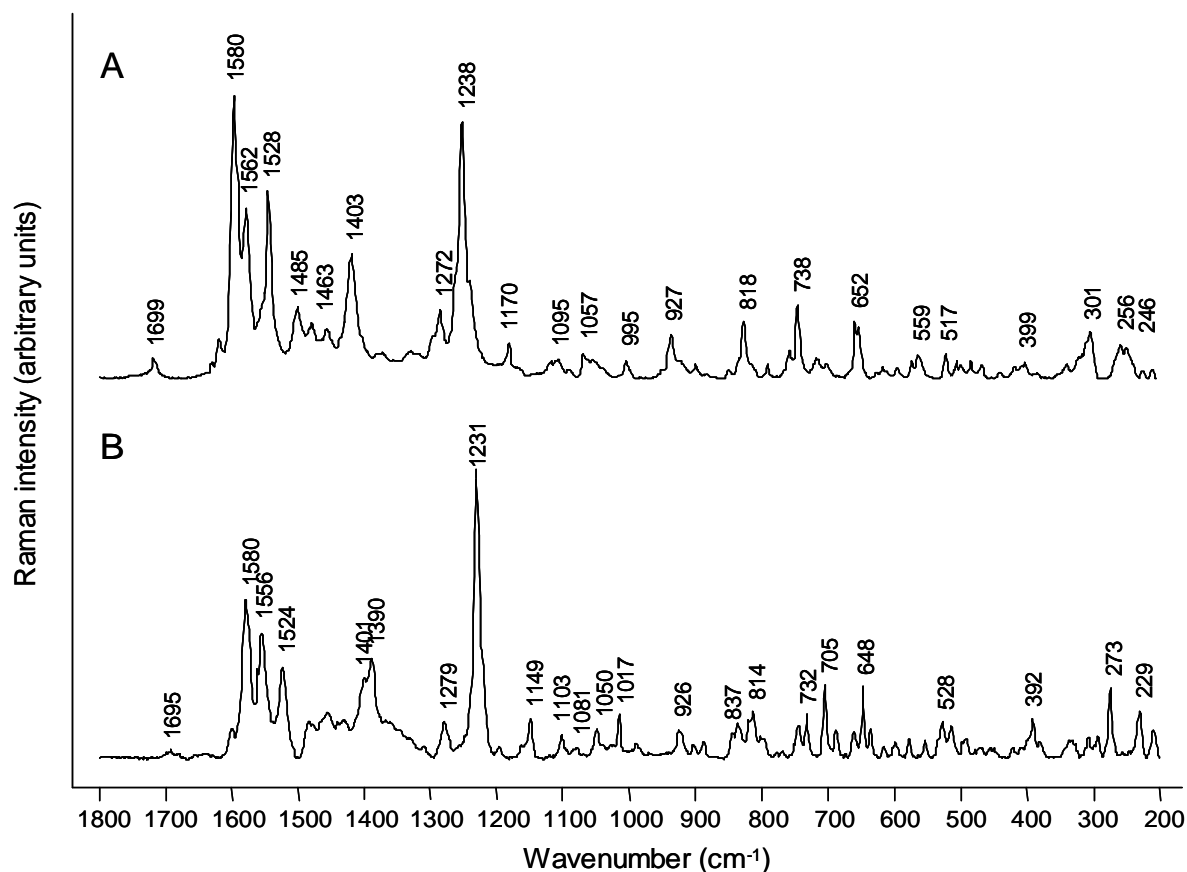


Figure 5.9 Raman spectrum of sildenafil citrate (A: 10 acc. x 30 s) and Seyagra gel (B: 20 acc. x 30 s) both analysed with the Renishaw System-1000 instrument.

The Raman bands of sildenafil citrate could be easily recognized, but some additional bands, not caused by the active ingredient, are present as well. These Raman bands, at 1390, 1017, 837, 705, three bands around 660 cm^{-1} , and several bands between 500 and 200 cm^{-1} have so far been unidentified.

5.2.5 Tablets containing the active ingredient of Cialis®

At Brussels airport, on two different occasions, tablets were seized, claiming to contain the active ingredient of Cialis® (fig. 5. 10).



Figure 5.10 Genuine Cialis® (A) and two tablets claiming to contain tadalafil (B and C).

Visual inspection of the tablets shows a clear difference in appearance compared to genuine Cialis[®]. The appearance of the tablets show more similarity with the Levitra[®] tablet, shown in figure 5.3. In figure 5.11 the Raman spectrum of genuine Cialis[®] is compared to the Raman spectra of the seized tadalafil tablets.

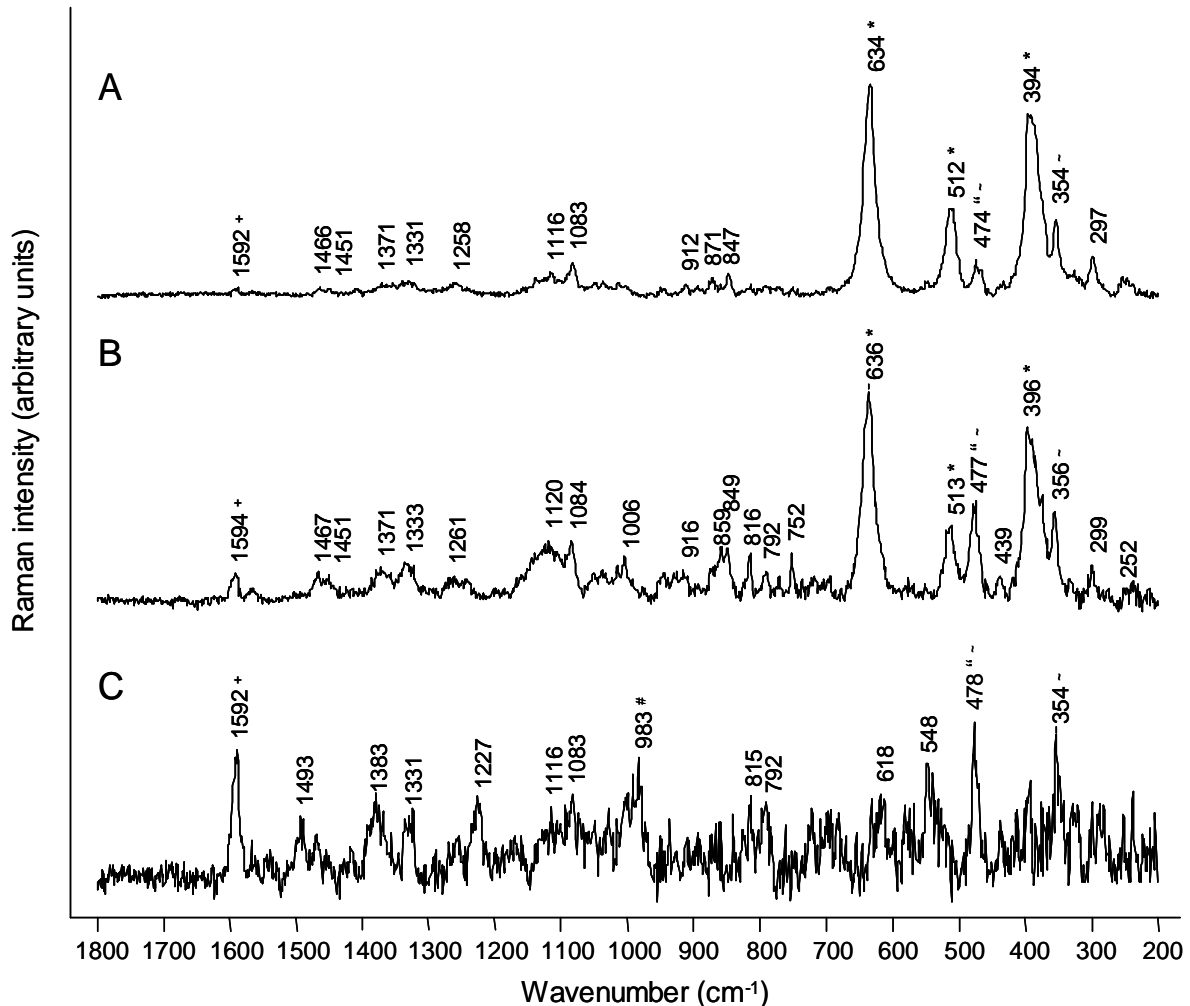


Figure 5.11 Raman Spectra of genuine Cialis[®] (A) and the two seized tablets (B and C) analysed with the Renishaw System-1000 instrument (25 acc. x 30 s). Raman bands marked with *, #, "-", and + can be assigned to respectively anatase TiO₂, barium sulfate, starch, lactose and tadalafil.

When the spectrum of genuine Cialis[®] is compared to the two spectra of the possible counterfeits (fig. 5.11B and C), the following differences can be noticed:

-
- The three Raman bands of titanium dioxide (TiO_2 , ca. 396, 515 and 634 cm^{-1}) are only present in the first two spectra. However, as seen in the analysis of counterfeit Viagra[®] (paragraph 5.2.3), the ratio of the intensities of the active ingredient (ca. 1593 cm^{-1}) and TiO_2 differs significantly. In the genuine Cialis[®] (fig. 5.11A) the ratio is circa 1:25 while in tablet B the ratio is circa 1:7 which is an indication that less TiO_2 is used, compared to the active ingredient.
 - Secondly, all Raman spectra show the Raman bands of lactose at ca. 353 cm^{-1} and ca. 474 cm^{-1} (chapter 8, fig. 8.1D). However, the ratio between these two Raman bands differs significantly in both counterfeits. The ratio in the genuine Cialis[®] is approximately 2:1 while in the counterfeits these ratios are 1:1 (B) or 1:3 (C). The increase of the relative intensity of the Raman band ca. 474 cm^{-1} can be attributed to starch (chapter 8, fig. 3A).
 - In the second counterfeit tablet the Raman band at ca. 985 cm^{-1} , can be assigned to barium sulfate (BaSO_4 , chapter 7, fig. 6A).

Since the active ingredient, tadalafil, was not available for analysis it can not be guaranteed that the active ingredient is present in the tablets. However, based on the detected Raman bands, it can be stated that these tablets contain additional excipients that are not commonly used in genuine Cialis[®] tablets.

5.3 Analysis of Noromectin[®]

5.3.1 Introduction of Noromectin[®]

In January 2005, a Dutchman was arrested for selling 1500 plastic syringes with the brand logo of Noromectin[®]. Noromectin[®] is an oral paste which is used for the treatment of gastrointestinal roundworms, lungworms, grubs, hornflies, sucking and biting lice and sarcoptic mange mites in horses. The active ingredient in the paste is Ivermectin (22,23-dihydroavermectin). Besides 1,87% w/w active ingredient, the paste consists of the following excipients: hydroxypropyl cellulose, hydrogenated castor oil, titanium dioxide and propylene glycol^{9,10}.

5.3.2 Analysis of packaging

First a visual inspection of the syringes is executed and secondly, the content, the packaging, and labeling, are analysed with Raman spectroscopy. Based on their appearance (figure 5.12), small differences between the two syringes can be noted. Both logos show a blue label with a picture of a white horse, but in different formats.



Figure 5.12 Genuine (A) and counterfeit (B) Noromectin[®] syringe.

But whether the syringe is counterfeit or whether it just has a new and improved packaging, it is difficult to say. So, it is necessary to analyze not only the content of both syringes with Raman spectroscopy, but the package as well. The Raman spectrum and chemical structure of the active ingredient Ivermectin, is shown in figure 5.13. Figure 5.14 shows the results of the first step in the investigation, which is the analysis of the white and blue plastics used for the syringes.

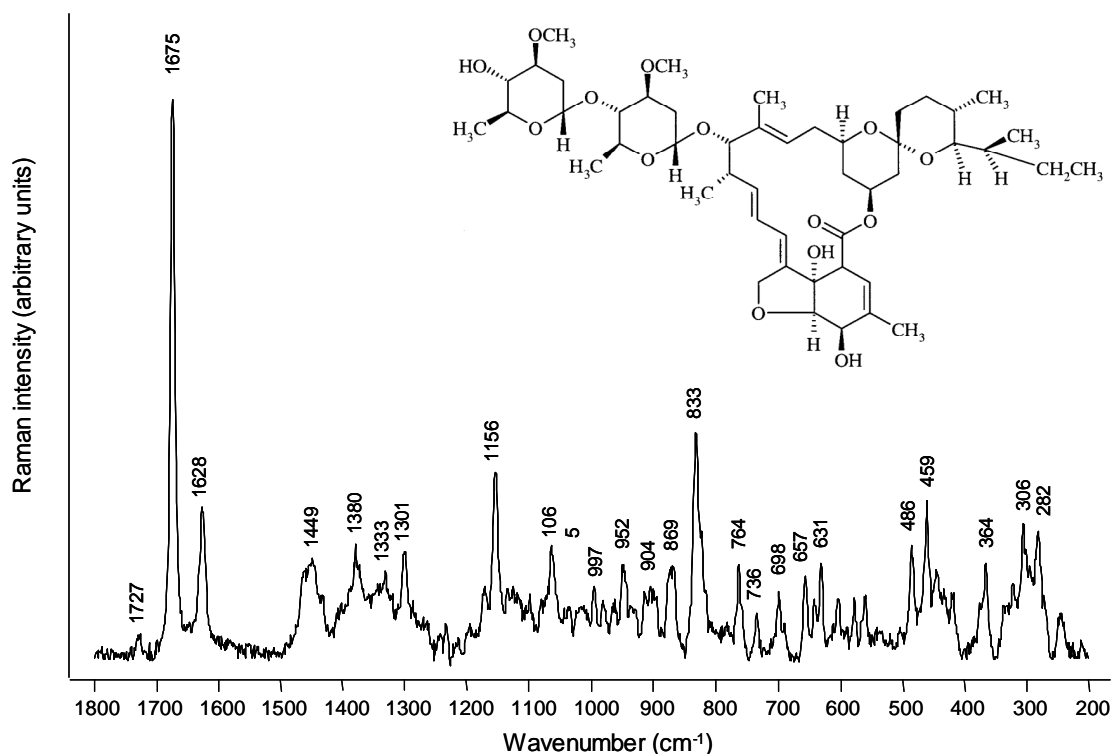


Figure 5.13 Raman spectrum of pure Ivermectin recorded with the Renishaw System-1000 spectrometer (5 acc. x 30 s) and its chemical structure⁹.

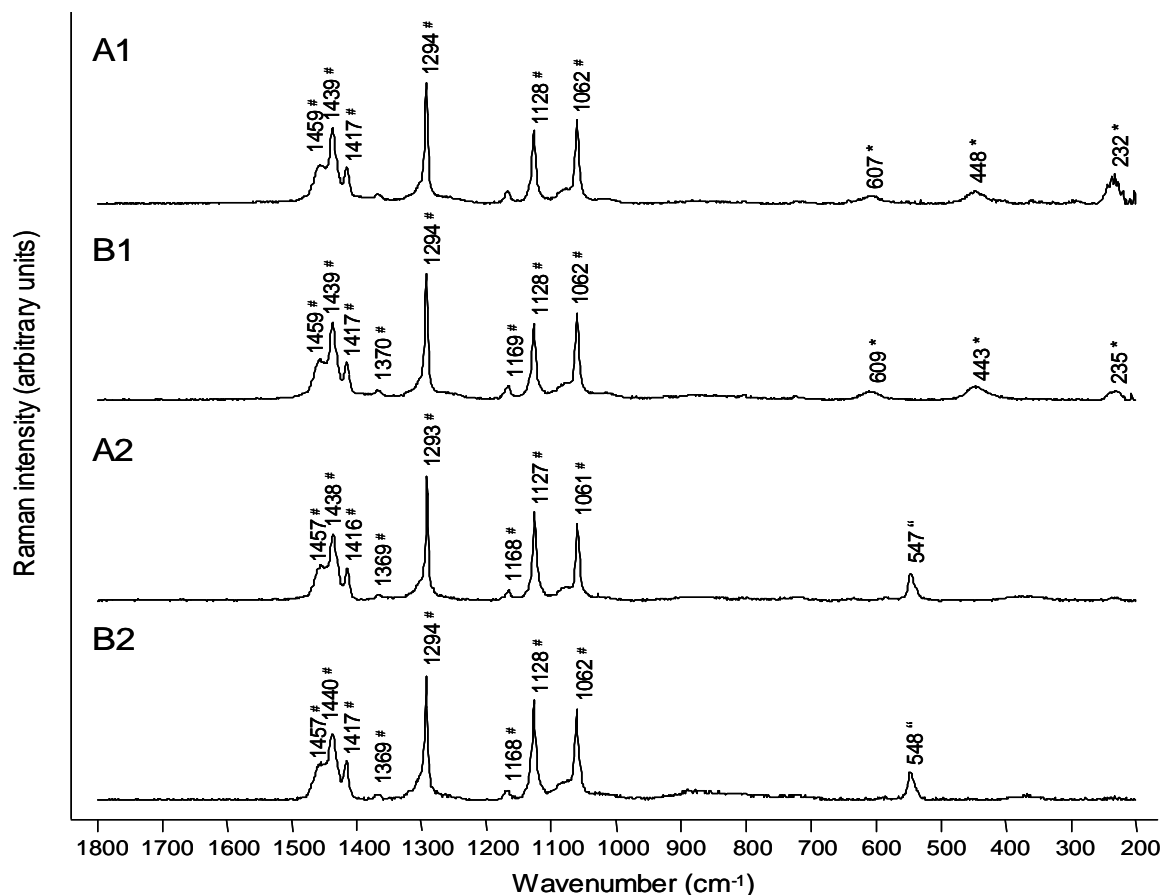


Figure 5.14 Raman spectra of white (A1) and blue (A2) plastic packaging of the genuine Noromectin[®] and white (B1) and blue (B2) plastic of the counterfeit Noromectin[®] analysed with the Renishaw System-1000 spectrometer (10 acc. x 30 s). Raman bands marked with *, # and " can be assigned to respectively rutile TiO₂, polyethylene and ultramarine.

All four spectra shown in figure 5.14 reveal similar Raman bands between 1060 and 1460 cm⁻¹. These Raman bands can be attributed to polyethylene¹¹. The Raman bands at ca. 1062 and 1128 cm⁻¹ are due to $\nu(\text{C-C})$ stretching vibrations, the $\delta(\text{CH})$ twisting vibration is situated at ca. 1294 cm⁻¹, while the Raman bands between 1400 and 1460 cm⁻¹ can be assigned to $\delta(\text{CH})$ bending vibrations¹¹. Figure 5.14 A1 and B1, the white plastics from the syringe, show three Raman bands at ca. 232, 448 and 607 cm⁻¹. These can be assigned to the rutile form of titanium dioxide (chapter 8, fig. 8.7D). The blue caps shown in figure 5.14 A2 and B2 have just one additional band at ca. 547 cm⁻¹ which is caused by the blue color (ultramarine blue, approximately Na₈[Al₆Si₆O₂₄]S_n) added to the polyethylene^{12,13}. This Raman band can be assigned to the symmetric stretching vibration (ν_3) of ultramarine blue¹⁴.

Based on the spectra of the plastic syringes, the counterfeit could not be distinguished from genuine Noromectin[®]. Therefore, the next step is to focus on the colours used in the label of the two syringes (fig. 5.15). The colours showed similar Raman spectra, except the spectra of the two small blue dots on the bottom of each label (fig. 5.16).



Figure 5.15 A represents the label of the genuine Noromectin[®] and B the counterfeit label.

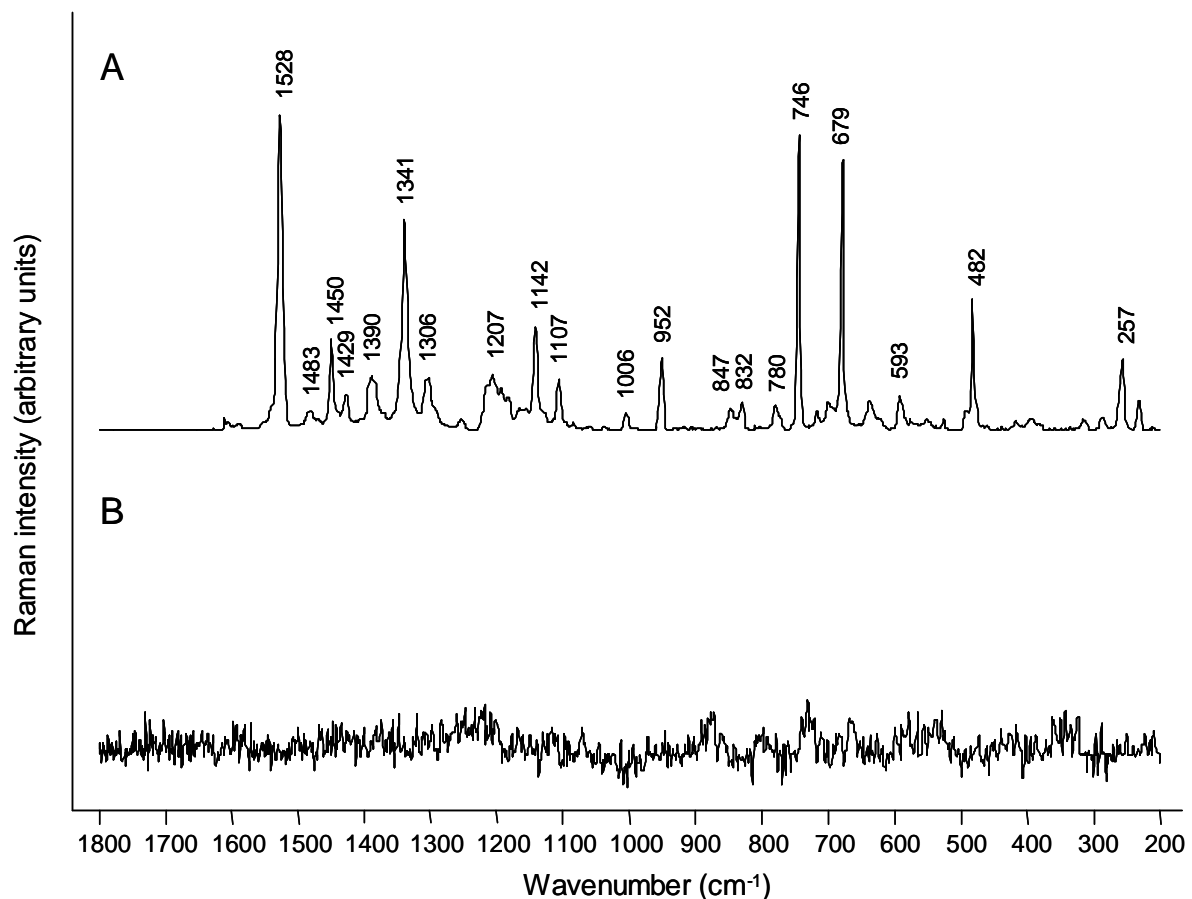


Figure 5.16 Raman spectra of the blue dots on the labels from the (A) genuine Noromectin[®] syringe (Renishaw System-1000, 5x obj., 10 acc. x 30 s) and the (B) counterfeit Noromectin[®] syringe (MArTA, 6x obj., 30 acc. x 30 s).

The Raman spectra of the genuine and counterfeit can be easily distinguished from each other. All Raman bands in the spectrum of the genuine Noromectin[®] syringe, can be assigned to the blue pigment copper phthalocyanine¹⁵, while these Raman bands could not be identified in the Raman spectrum of the counterfeit sample.

5.3.3 Analysis of the content of the syringes

Based on the Raman spectra of these two small blue dots on the labels, the counterfeit Noromectin[®] syringe could be differentiated from the genuine. In order to analyse the content of these syringes, the blue cap was removed and by using the mobile Raman spectrometer (MArtA), the laser beam is aimed in the syringe. These Raman spectra are shown in figure 5.17.

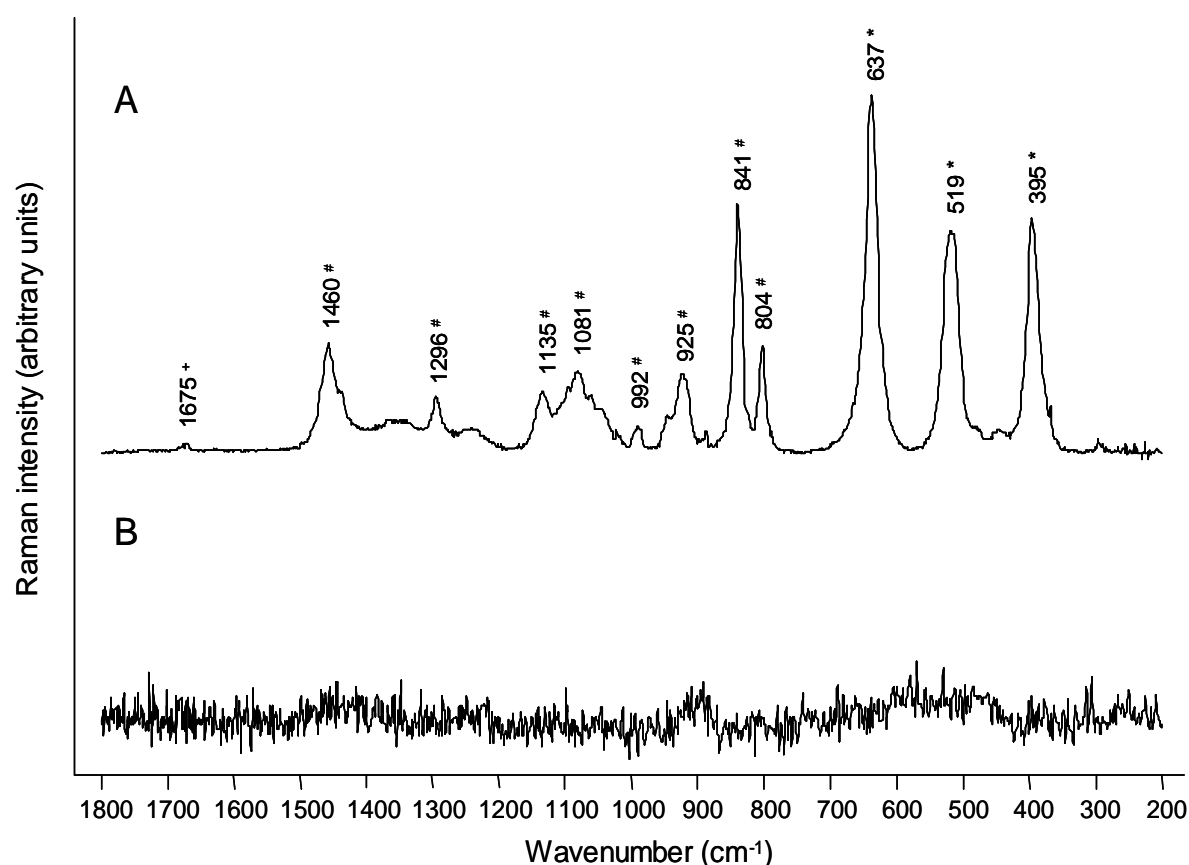


Figure 5.17 Raman spectra of the content of genuine (A) and counterfeit (B) Noromectin[®] syringes (MArtA, genuine sample: 5 acc. x 30 s, counterfeit sample: 30 acc. x 60 s). Raman bands marked with *, # and + can be assigned to respectively anatase TiO₂, propylene glycol and Ivermectin.

As can be seen in figure 5.17 the counterfeit Noromectin[®] (B) is not Raman active. The genuine product (A) shows the three intense bands of anatase titanium dioxide at ca. 395, 519 and 637 cm⁻¹ (chapter 8, fig. 8.7C). The Raman bands between 800 and 1460 cm⁻¹ can be assigned to propylene glycol (chapter 8, fig. 8.4A). The Raman bands at 804 and 841 cm⁻¹ can be assigned to the in-phase $\nu(\text{CCO})$ stretching vibration while Raman bands between 925 and 1137 cm⁻¹ can be attributed to the out-of-phase $\nu(\text{CCO})$ stretching vibration.

Since the active ingredient (fig. 5.13) is only present in a very small amount (1,87% w/w), the Raman band at 1675 cm⁻¹ is small, but distinguishable in figure 5.17. Based on the Raman spectra of the content and the label of the syringe, the counterfeit Noromectin[®] sample could be distinguished from the genuine.

5.4 Analysis of Amoxil[®]

Amoxil[®] is an antibiotic that is used to treat a wide range of infections and is produced by GlaxoSmithKline (GSK). It belongs to a group of antibiotics, called “penicillin”. The capsule contains the active ingredient amoxicillin, in either 250 mg or 500 mg. Amoxicillin is designated chemically as: (2*S*,5*R*,6*R*)-6-[(*R*)-(-)-2-amino-2-(*p*-hydroxyphenyl) acetamido] -3,3- dimethyl -7-oxo-4-thia-1-azabicyclo [3.2.0] heptane-2-carboxylic acid trihydrate².

The medicine, made for oral administration, is a red and yellow capsule, consisting of 250 or 500 mg active ingredient and magnesium stearate as excipient. The capsule is made from gelatin, erythrosine, indigo carmine, iron oxides and titanium dioxide².

The first step in the evaluation is the visual analysis of the capsules. Figure 5.18 shows the pictures of the genuine Amoxil capsule and two possible counterfeits, seized by the FAGG (B) and customs at Brussels airport (C).



Figure 5.18 Genuine Amoxil[®] (A) and two possible counterfeit Amoxil[®] (B and C) capsules.

Based on visual examination, no obvious differences can be noted between the genuine capsule and the two possible counterfeits (B and C). With Raman spectroscopy, the Raman spectrum of the active ingredient amoxicillin (fig. 5.19) is compared to the Raman spectra of the content of these three capsules (fig. 5.20).

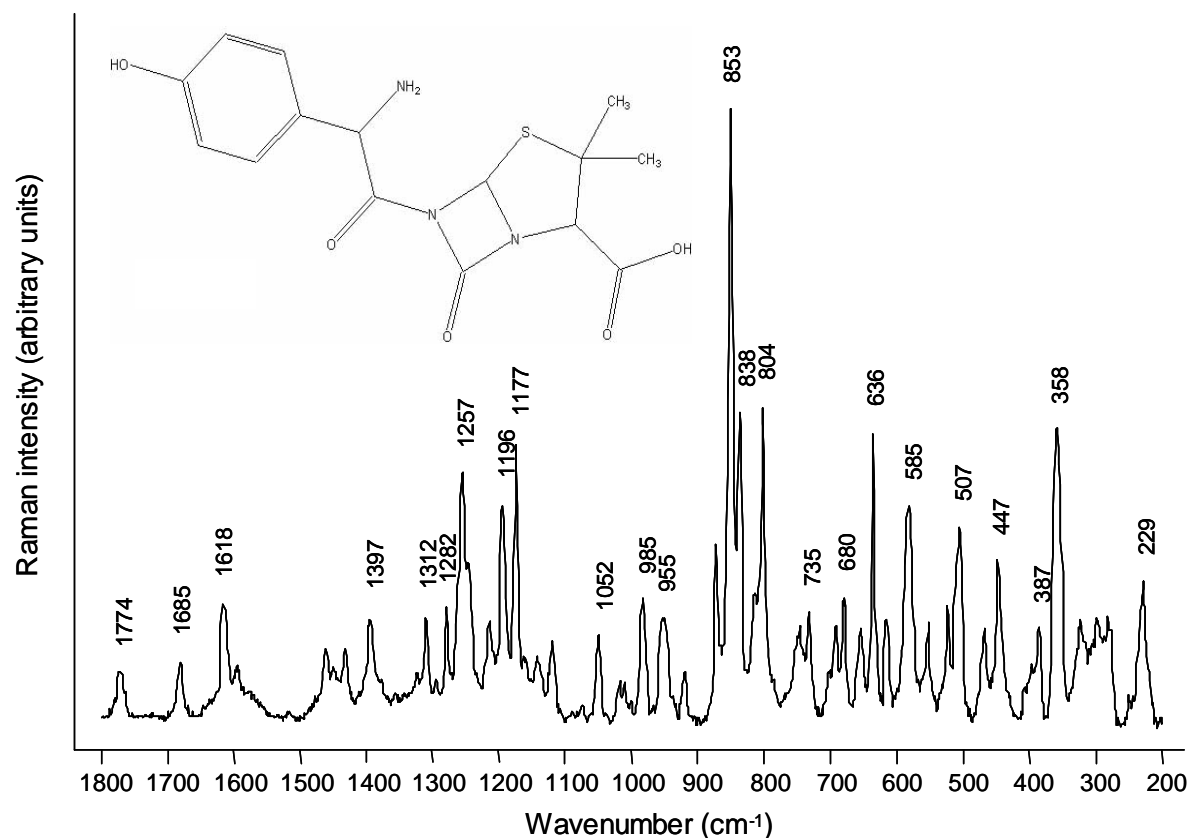


Figure 5.19 Raman spectrum of pure amoxicillin with the Renishaw System-1000 instrument (10 acc. x 30 s) and its chemical structure⁹.

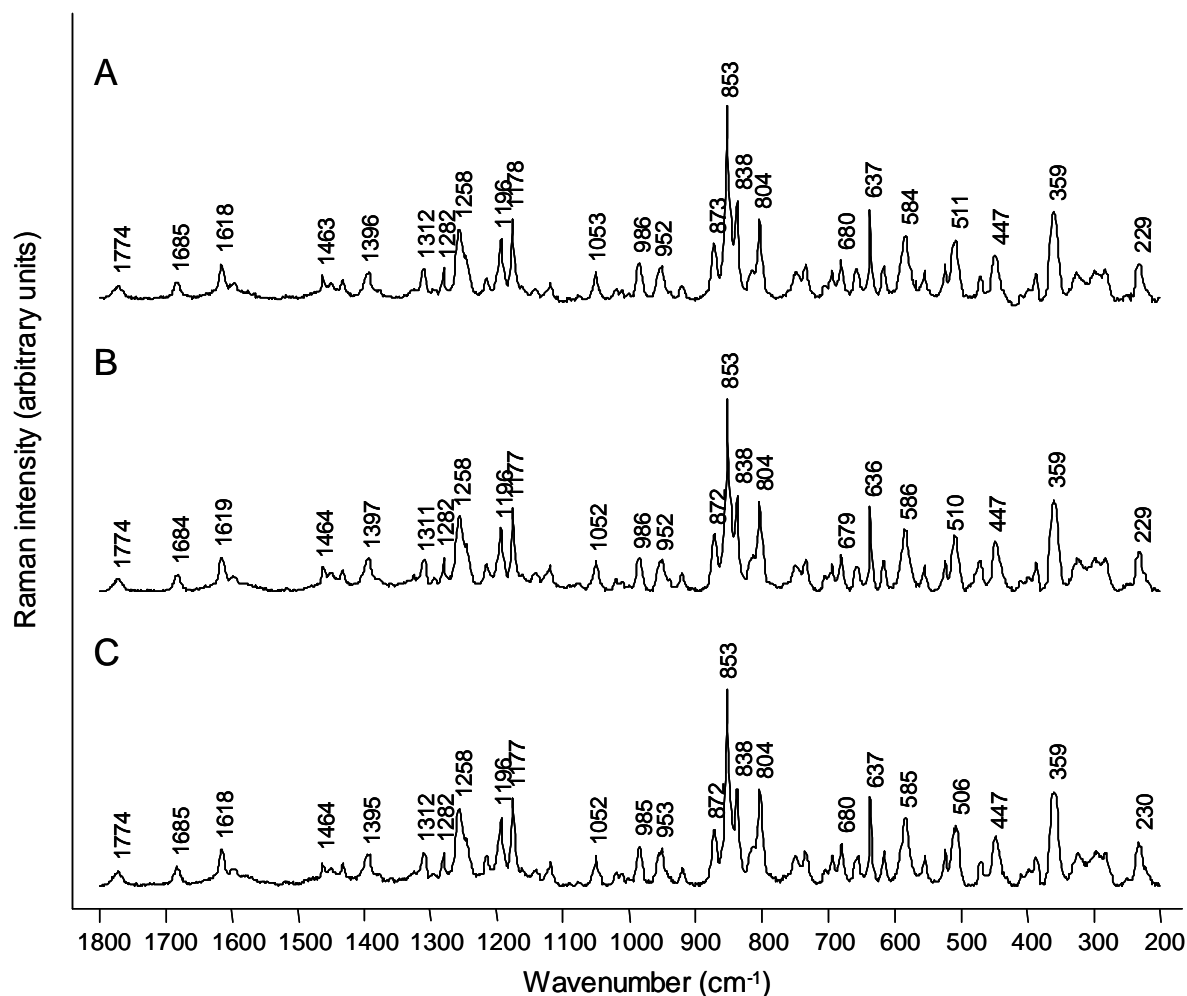


Figure 5.20 Raman spectra of content of genuine (A) and two possible counterfeits Amoxil[®] (B and C) with the Renishaw System-1000 instrument (5 acc. x 30s).

The three spectra of the Amoxil capsules in figure 5.20 show all the distinctive Raman bands of the active ingredient amoxicillin (figure 5.19). The content of a genuine Amoxil capsule consists of the active ingredient and magnesium stearate (chapter 8, fig. 5C). No additional Raman bands in these spectra could be assigned to this excipient.

Based on these Raman bands, no difference can be noted between the genuine sample (A) and two possible counterfeits (B and C). In order to visualize differences between the genuine Amoxil[®] and two possible counterfeits, a difference spectrum is calculated between the active ingredient, amoxicillin, and the content of the three capsules (A, B and C) with the use of ACD Specmanager. The three difference spectra are shown in figure 5.21.

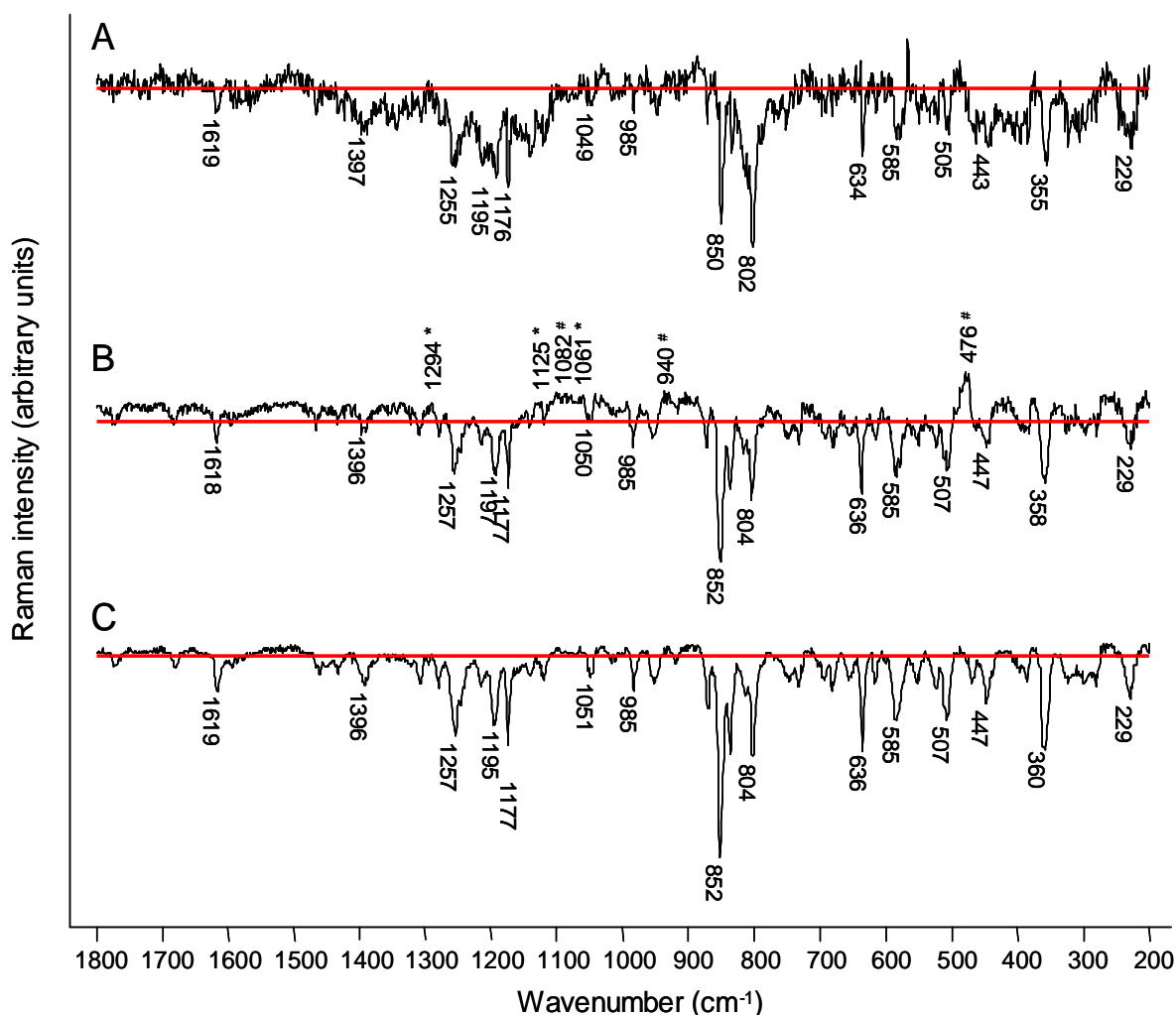


Figure 5.21 Difference spectra between content of Amoxil capsules (genuine (A) and two possible counterfeits (B and C)) and active ingredient amoxicillin. Raman bands marked with * and # can be assigned to respectively magnesium stearate and starch.

The difference can now be noted between the genuine Amoxil capsule (A) and the two possible counterfeits (B and C). The differences spectrum of sample B shows several additional bands due to magnesium stearate (chapter 8, fig. 5C) and starch (chapter 8, fig. 3A). Raman bands at 1061, 1125 and 1294 cm^{-1} can be assigned to magnesium stearate while the Raman bands at 476, 940 and 1082 cm^{-1} are due to starch. Based on the presence of an additional excipient, the Amoxil[®] capsule seized by the FAGG can be considered as counterfeit.

The difference spectrum of sample C in figure 5.21 shows no additional Raman bands compared with the difference spectrum of the genuine sample. However, when using the same subtraction factor, the negative Raman bands of the active ingredient in sample C are more prominent than for the genuine sample, indicating possibly a lower level of active ingredient in the capsule.

5.5 Conclusion

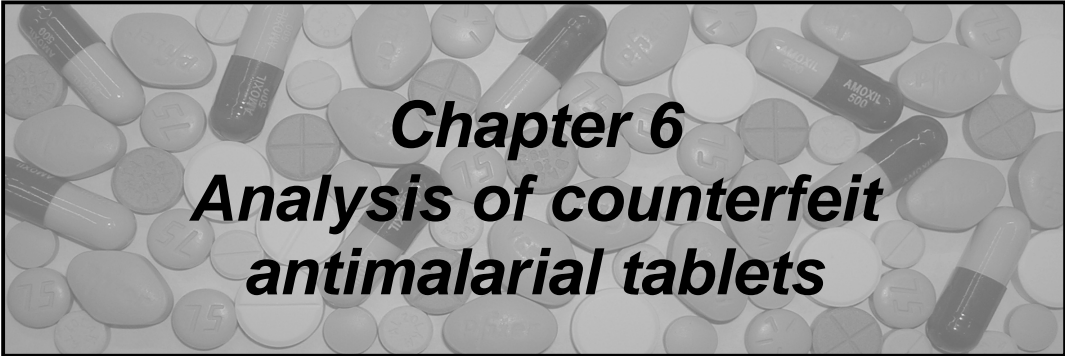
By using Raman spectroscopy, differences between genuine and possible counterfeit samples could be detected. This chapter described the qualitative analysis of tablets, gels, syringes and capsules. Based on a simple visual examination of the drugs, not all counterfeits could be detected, which illustrates that counterfeiters are becoming highly sophisticated. With Raman spectroscopy, based on the presence or absence of Raman bands (active ingredient and/or excipients) the counterfeits could be differentiated from the genuine samples.

This chapter, however, is only based on one or two counterfeits per example. The next two chapters, describe the use of Raman spectroscopy to qualitatively detect larger groups of possible counterfeits. Chapter 6 describes the analysis of 50 anti-malarial tablets while chapter 7 describes the analysis of 18 Viagra® tablets.

5.6 References

1. Venhuis BJ, Barends DM, Zwaagstra ME, de Kaste D, *Recent developments in counterfeits and imitations of Viagra, Cialis and Levitra, A 2005-2006 update*, National Institute for Public Health and the Environment (RIVM), Report 370030001/20007. RIVM 2007.
2. Prescription information Amoxil® by GlaxoSmithKline (2005), www.gsk.com.
3. Vandenameele P, Castro K, Hargreaves M, Moens L, Madariaga JM, Edwards HGM, *Anal. Chim. Acta.*, 2007; 588 (1): 108-116.
4. Vandenameele P, Weis TL, Grant ER, Moens L, *Anal. Bioanal. Chem.*, 2004; 379: 137-142.
5. de Veij M, Vandenameele P, Alter Hall K, Fernandez FM, Green MD, White NJ, Dondorp AM, Newton PN, Moens L, *J. Raman Spectrosc.*, 2007; 38(2):181-187.

-
6. Prescription information Viagra[®], FDA (2007), www.fda.gov.
 7. Prescription information Cialis[®], FDA (2003), www.fda.gov.
 8. Prescription information Levitra[®], FDA (2007), www.fda.gov.
 9. Bilmen JG, Wootton LL, Michelangeli F, *Biochem. J.* 2002; 366: 255-263.
 10. Freedom of information summary, ANADA 200-272, FDA, 2005, www.fda.gov.
 11. Hahn DW, Wolfart DL, Parks NL, *J. Biomed. Mater. Res.*, 1997; 35: 31-37.
 12. Shen AG, Wang XH, Xie W, Shen J, Li HY, Liu ZA, Hu JM, *J. Raman spectrosc.*, 2006; 37: 230-234.
 13. Chaplin TD, Jurado-López A, Clark RJH, Beech DR, *J. Raman spectrosc.*, 2004; 35: 600-604.
 14. Landman AA, de Waal D, *Materials Research Bulletin*, 2004; 39: 655-667.
 15. Basova TV, Kol'tsov EK, Igumenov IK, *Sensors and Actuators B*, 2005: 105; 259-265.
 16. Pais da Silva MI, Nery MP, S Téllez CA, *Materials Letters*, 2000: 45; 197-202.



Chapter 6
***Analysis of counterfeit
antimalarial tablets***

6 Analysis of counterfeit antimalarial tablets

Based on the paper: de Veij M, Vandenabeele P, Alter Hall K, Fernandez FM, Green MD, White NJ, Dondorp AM, Newton PN, Moens L, Fast detection and identification of counterfeit antimalarial tablets by Raman spectroscopy, Journal of Raman Spectroscopy, 38, 2007, 181-187.

Malaria is an infectious disease, affecting people worldwide. There are four principal species of the genus *Plasmodium* which can cause Malaria, namely: *P. falciparum*, *P. vivax*, *P. malariae*, and *P. ovale*. *Plasmodium falciparum* is by far the most common and deadly type of malaria infection^{1,2,3}. According to the World Health Organization, each year more than 500 million people become severely ill with malaria³. The number of different types of antimalarial drugs is small; predominately chloroquine is used, despite its decreasing efficiency². One of the most efficient antimalarial drugs momentarily, is artesunate, which is an artemisinin derivative². These derivatives were discovered in the early 1970s by Chinese scientists and since then this drug is used extensively in Southeast Asia². This chapter is focused on detection of counterfeit antimalarial drugs with the use of Raman spectroscopy.

Abstract

During the last decade there has been an apparent increase in the prevalence of counterfeit medicines in developing as well as developed countries. The pivotal antimalarial artesunate has been counterfeited on a large scale in SE Asia. In this work, the possibilities of Raman spectroscopy are explored as a fast and reliable screening method for the detection of counterfeit artesunate tablets. In this study 50 “artesunate tablets”, purchased in South-east Asia, were examined.

This spectroscopic method was able to distinguish between genuine and counterfeit artesunate and to identify the composition of the counterfeit tablets. These contained no detectable levels of artesunate, but consisted mostly of starch, calcite (CaCO₃), and paracetamol (4-acetamidophenol).

In one particular case an admixture of rutile (TiO₂) and artesunate was detected. The results of the investigation by Raman spectroscopy were in agreement with these of the artesunate colorimetric test and of liquid chromatography mass spectrometry.

Moreover, principal components analysis (PCA) was combined with hierarchical cluster analysis to establish an automated approach for the discrimination between different groups of counterfeits and genuine artesunate tablets.

These results demonstrate that Raman spectroscopy combined with multivariate analysis is a promising and reliable methodology for the fast characterization of genuine and counterfeit artesunate antimalarial tablets.

6.1 Introduction

Counterfeit medicines happen to be a problem, not only for many developing nations but for developed countries as well⁴. The United States Food and Drug Administration (FDA) estimates that counterfeits make up of more than 10% of the global medicines market⁵. In 2004, FDA's Office of Criminal Investigations initiated 58 counterfeit drug cases in the United States compared to 9 cases in 1997, which shows that counterfeit drugs is an increasing problem⁶.

Counterfeit medicines include drugs without sufficient active ingredient, without any active ingredients or with fake packaging^{4,5}. In wealthier countries new and expensive medicines, such as hormones, corticosteroids, and cancer drugs, are frequently counterfeited⁷. Amongst the most well-known counterfeit drugs in wealthier countries are Viagra[®] and Cialis[®] which are used against erectile dysfunction^{4,8}. In developing countries, the most counterfeited medicines are those used to treat widespread infectious diseases, such as tuberculosis and malaria⁷.

Until recently, analytical controls in the drug distribution system were considered to be supplementary⁹ to the Quality Control at the production unit. Counterfeit drug detection is often a complex process. Careful visual inspection of the product's packaging and labelling is the first step of defence, since modifications may indicate a potential counterfeit.

Visual inspection is followed by chemical analysis, often using high performance liquid chromatography (HPLC)¹⁰. HPLC is considered to be the golden standard analytical method in drug analysis, since it allows active components as well as impurities to be determined quantitatively¹⁰. In the last few years more methods^{4,8,11,12,13} have been developed for the quality control of drugs, such as thin layer chromatography (TLC), UV/VIS-spectroscopy, near-infrared (NIR) spectroscopy, and liquid-chromatography mass spectrometry (LC-MS).

This paper describes the fast analysis of genuine and counterfeit 'artesunate tablets' by Raman spectroscopy. Artesunate is a key drug in the treatment of multi-drug resistant *Plasmodium falciparum* malaria in Southeast Asia¹⁴. As counterfeit antimalarials usually contain insufficient or no active ingredient, the unwitting patient is at substantial risk of developing severe malaria and even dying due to lack of treatment¹⁵.

According to the World Health Organisation (WHO), one million deaths per year occur due to malaria and as many as 200.000 deaths could be avoided if the medicines available were of good quality⁵. In two surveys^{14,15} conducted in 2000-2001 and 2002-2003 'artesunate' bought in mainland Southeast Asia (Burma (Myanmar), Lao PDR, Vietnam, Cambodia and on the Thai/Burma border) the prevalence of counterfeit artesunate increased from 38 % in the first study to 53 % in the following years.

Counterfeit artesunate tablets may be detected using several methods, relying on visual inspection, chemical assays and instrumental analysis¹⁵. First counterfeits can be classified qualitatively as genuine or counterfeit, based on the characteristics of the hologram, blisterpack and packaging.

Although this is an inexpensive approach, it has been found to be 100% accurate in recognizing counterfeit tablets in the first survey of counterfeit artesunate tablets in SE Asia¹⁴. However, experience is required to identify the counterfeits and with increased counterfeiter sophistication, this method was not as accurate in the second survey¹⁵.

The simplest chemical assay is a coloured-based dye test, based on the reaction between an alkali decomposition product of artesunate and a diazonium fast red Tr salt¹⁶. This is a simple and inexpensive test, but it does not give information regarding the chemical composition of the counterfeit tablets or regarding substandard amounts of artesunate¹⁶.

Moreover, this approach is limited to the identification of artesunate; the investigation of other counterfeit drugs requires the development of another dye test. The reference method to determine quantitatively the amount of artesunate in tablets is high-performance-liquid-chromatography (HPLC), which has been used to confirm the results of the first two tests during the 2002-2003 surveys¹⁴⁻¹⁶. Although HPLC is very sensitive and provides comprehensive information about the sample, the sample preparation and analysis is time-consuming and requires trained chemists for the analysis as well as for the interpretation of the results.

Therefore, we have investigated the potential use of Raman spectroscopy for the detection of counterfeit artesunate, since the technique does not require any sample preparation and if needed the tablet components can even be analyzed through the blister package. Its non-destructive character and high speed of analysis make Raman spectroscopy well-suited for investigating possible counterfeit drugs. Moreover, since mobile fibre optics spectrometers are becoming increasingly available, small instruments can be deployed for in situ analysis. By using chemometric techniques to compare the recorded spectra with those in a reference library, instrument operation and spectral interpretation can be automated in order to give a pragmatic answer to non-specialist operators in the field.

Pharmaceutical analysis by Raman spectroscopy is becoming a commonly accepted approach, as illustrated by the rising number of research papers that are published in this field. Raman spectroscopy has been used for the identification of active substances in pharmaceuticals^{17,18}, their qualitative¹⁹ and quantitative analysis²⁰, the characterization of different crystalline forms^{21,22} and even for on-line monitoring of pharmaceutical blending process²³.

Moreover, the identification of illicit drugs (cocaine, heroin and MDMA) which are contaminated with one or more cutting agents^{24,25} has been presented. Raman spectroscopy is also used for the identification of seized ecstasy tablets^{18,26}. These results show that Raman spectroscopy can be used to distinguish between ecstasy and various other phenethylamine ecstasy analogues.

So far, no research papers have been published on the use of Raman spectroscopy for the identification of counterfeit pharmaceuticals. The first aim of this study is to evaluate the ability of Raman spectroscopy to rapidly discriminate between genuine and counterfeit artesunate tablets. Second, an attempt is undertaken to classify the different counterfeit tablets, since this could be of help, in combination with other analytical techniques, to pinpoint the relationships (between location of sample sale, sample production source and distribution routes) in different forgery cases.

Finally, possibilities for the application of Raman spectroscopy in counterfeit drug detection are examined, by developing a basic chemometrics algorithm and automated classification procedure.

6.2 Experimental

The analyses were carried out with a Renishaw System-1000 spectrometer (Wotton-under-Edge, UK) connected to a Olympus BH-2 microscope. The diode laser has a power of 50 mW at the source and a wavelength of 785 nm (DL 100, TuiOptics GmbH, Martinsried/Munich, Germany).

By using a 20x objective lens (Olympus MDPlan20, 0.20 NA, Omnilabo, Aartselaar, Belgium) spectra of particles with a diameter down to ca. 5 μm can be recorded. The collected Raman radiation was dispersed with a 1200 lines mm^{-1} grating (focal length 250 mm) and focussed on a Peltier-cooled CCD detector allowing to obtain a spectral resolution of ca. 1 cm^{-1} . All spectra were recorded in the spectral window of 200 to 1800 cm^{-1} , with 5 accumulations of 30s each. Spectra were baseline-corrected before presentation, to eliminate the influence of broadband fluorescence.

The artesunate samples, including both genuine artesunate and counterfeit tablets were collected in Vietnam, Cambodia, Lao PDR (Laos), the Thai Burma border, Burma and Hong Kong¹⁵. Pure artesunate (Apin Chemicals, UK) was used as a reference.

Since Raman analysis of these samples was preceded by colorimetric test¹⁶ and liquid chromatography mass spectrometry (LC-MS) analyses²⁷, tablets had been previously ground with a mortar and pestle. Reference samples of excipients, such as calcite (CaCO_3 , UCB Belgium), starch (starch, soluble reagent, UCB Belgium) and 4-acetamidophenol (Acros, Belgium) were also analyzed by Raman spectroscopy.

Liquid chromatography-mass spectrometry (LC-MS) experiments were performed on an AccuTOF orthogonal time-of-flight mass spectrometer (JEOL, Peabody, MA, USA) coupled to an Agilent 1100 HPLC system (Palo Alto, CA USA) via an electrospray ionization interface. A Zorbax 300Å 300 Extend-C18 column (2.1mm ID and 150mm long, Agilent, Palo Alto, CA USA) was used in all of the experiments.

The LC was operated at a flow rate of 200 $\mu\text{L min}^{-1}$, with an injection volume of 20 μL . The binary pump used HPLC grade water with 0.01% acetonitrile as mobile phase A and mobile phase B was acetonitrile. The gradient started at 5% B and ramped to 45% B until 7 minutes, it increased to 100% B from 7 to 8 minutes and it was held at 100% B until 12 minutes.

Data processing was done with Matlab 6.5 (The MathWorks Inc. Natick, MA, U.S.A.) and the PLS toolbox, version 3.0 (Eigenvector Research Inc., Manson, Washington). For display, a manual baseline correction was performed by using Grams/AI(7.01) (Thermo Galactic, Waltham, MA, U.S.A.).

6.3 Results and Discussion

6.3.1 Spectral Interpretation

In order to classify the samples into genuine artesunate and counterfeit tablets, a spectrum of pure artesunate was recorded (fig. 6.1).

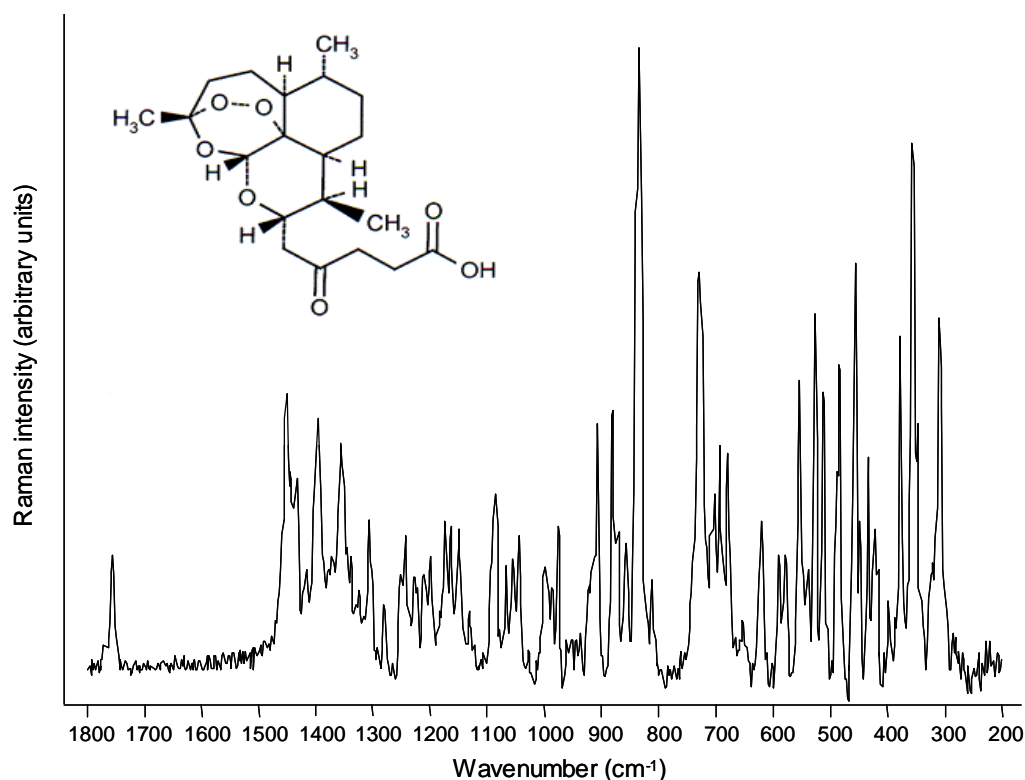


Figure 6.1 Raman spectrum of artesunate analysed with the Renishaw System-1000 spectrometer (5 acc. x 30 s) and its molecular structure.

The Raman bands in the spectrum could be assigned to the corresponding functional groups, including the endoperoxide function, the epoxy rings and the carboxylic groups, which are reflected in the Raman bands at 833, 728 and 1757 cm⁻¹, respectively²⁸. Raman bands assignments for the spectrum of artesunate are summarized in table 6.1.

Wavelength	Assignments
1757 cm ⁻¹	v(C=O)
1452 cm ⁻¹	δ(CH ₃), δ(CH ₂) scissoring
1438 cm ⁻¹	δ(CH ₂) Cyclo-alkane
1397 cm ⁻¹	v(CO ₂)
1356 cm ⁻¹	δ(CH), δ(CH ₃) symmetric
1309 cm ⁻¹	CH ₂ in phase twist
1174 – 1309 cm ⁻¹	CH ₂ twist and rock, CH ₂ in-phase
1045 cm ⁻¹	Anti-symmetric v(COCOC)
977 – 1164 cm ⁻¹	v(CC)
908 cm ⁻¹	Symmetric v(COC)
881 cm ⁻¹	v(CC) skeletal stretch
858 – 881 cm ⁻¹	vs(COC)
833 cm ⁻¹	v(O-O)
728 cm ⁻¹	Ring vibration (epoxy rings)
526 cm ⁻¹	δ(OOCOC)
422 – 483 cm ⁻¹	δ(COC)
308 – 434 cm ⁻¹	Chain expansion n-alkanes
347 cm ⁻¹	δ(COCOC)

Table 6.1 Raman band assignments for artesunate²⁸.

In our first approach, the presence or absence of these Raman bands was used to distinguish between genuine and counterfeit artesunate samples. A total of fifty samples were analysed under identical conditions (5 accumulations of 30 s). According to their spectra, the fifty samples could be divided into four different groups.

Figure 6.2 shows representative spectra of these four types of samples which were labelled group A - D.

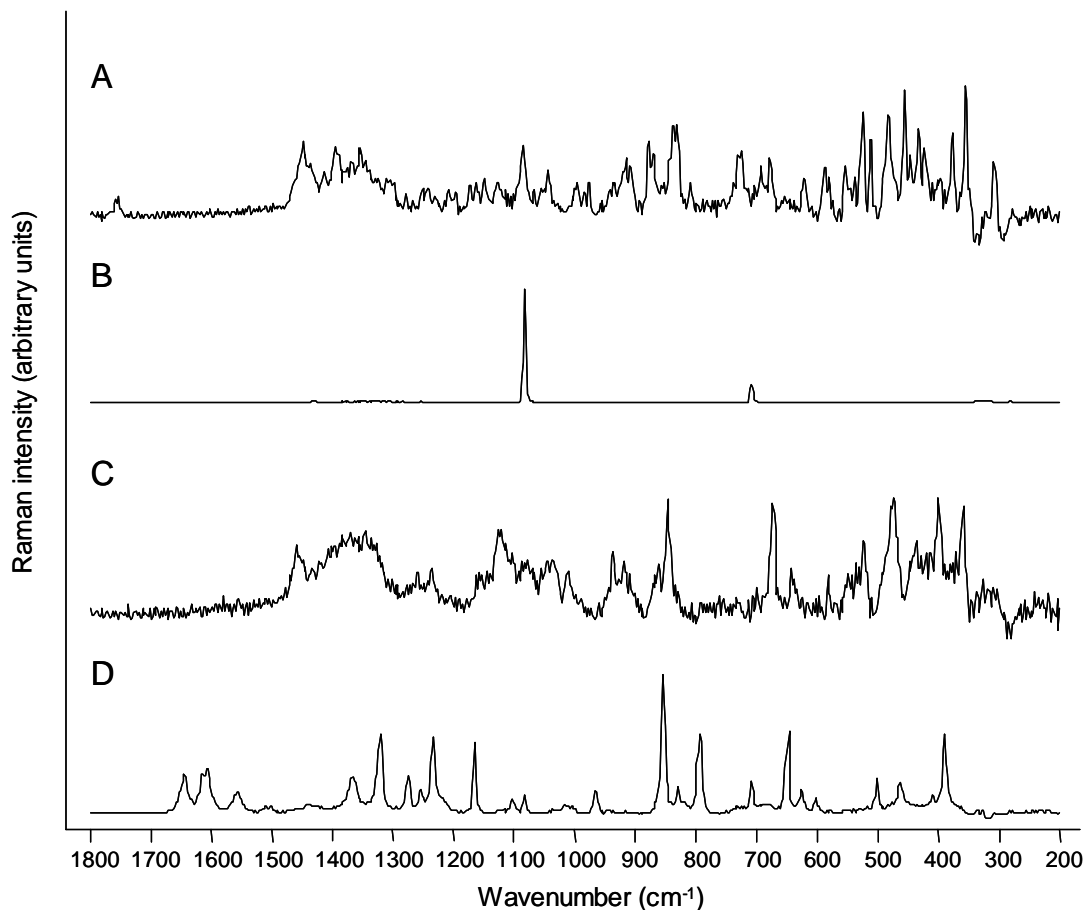


Figure 6.2 Overview of the four classes of antimalarial samples analysed with the Renishaw system-1000 spectrometer: A: Genuine samples; B: Calcite-containing; C: Starch-containing; D: Paracetamol-containing. (5 acc. x 30 s).

Group A consists of the genuine artesunate tablets (fig. 6.2, top trace). The spectra of these samples are highly similar to the spectrum of the artesunate standard. For instance the $\nu(\text{C}=\text{O})$ stretching vibration at 1757 cm^{-1} , the Raman band of the $\nu(\text{O}-\text{O})$ stretch at 833 cm^{-1} and the ring vibration at 728 cm^{-1} are present in their spectra.

The other Raman bands of artesunate were also present in the spectrum of these samples, which coincides with positive results from the artesunate colorimetric test and with the detection of the $[\text{M}+\text{Na}]^+$ ($m/z=407$) and $[\text{2M}+\text{Na}]^+$ ($m/z=791$) artesunate ions at a retention time of 18.1 ± 0.4 min by LC-MS. Therefore, Group A can be safely considered as genuine tablets containing artesunate.

Group B (fig. 6.2, second trace) samples showed very simple spectra, with only two prominent Raman bands. The Raman bands at 1086 and 712 cm^{-1} are consistent with the Raman spectrum of calcite (CaCO_3)²⁹ which was confirmed by a spectrum taken of pure CaCO_3 .

Because samples were extracted with acetonitrile before LC-MS analysis, no signals that could be attributed to calcium carbonate-related species were detected in the mass spectra of Group B samples.

Group C samples show spectra which are easily distinguished from the genuine tablets and which are very similar to the spectrum of starch³⁰. For instance the glycoside chain expansion vibration at 475 cm^{-1} , the symmetric $\nu(\text{COC})$ vibration at 940 cm^{-1} and the $\nu(\text{COC})$ vibration at 868 cm^{-1} of starch are present in the spectra of group C samples.

Unmodified starch was as well detected by LC-MS as a series of equally spaced peaks at $m/z=365, 527, 689, 851, 1013, \text{ and } 1175$ with a 162 Da separation consistent with the formula $[(\text{C}_6\text{H}_{10}\text{O}_5)_n + \text{Na}]^+$ for $n = 1$ to 7. Interestingly, one additional Raman band is present in the samples, which is not consistent with the spectrum of starch. This is the Raman band at 675 cm^{-1} indicating the presence of another compound in the sample, which coincides with two intense MS signals at $m/z=438$ and 493. The identity of this compound is yet to be determined.

The fourth group (D), consisted of compounds with spectra different to those of the previous groups; group D spectra show strong Raman bands at 857, 1167, 1235 and 1322 cm^{-1} . These spectra are consistent with the spectrum of 4-acetaminophen (paracetamol)³¹. This was confirmed by a Raman spectrum taken of pure 4-acetaminophen and by the LC-MS results which revealed a peak at $m/z=152$. There are two additional Raman bands present in the spectra, at 1086 and 712 cm^{-1} , which are consistent with the Raman spectrum of calcite (CaCO_3)²⁹.

Of the 50 samples analysed, 26 samples contained artesunate, 10 samples consisted of starch and an unknown compound, 10 samples consisted of calcite and 4 samples consisted of paracetamol mixed with calcite. The results of these groups are consistent with the results obtained by the colorimetric test for artesunate¹⁶ and by (LC-MS)²⁷.

6.3.2 Chemometrical classification of counterfeit drug samples

When designing an automated system, to be used in the field by non-specialist operators, it is necessary to provide an automated spectral interpretation or classification algorithm. In this exploratory chemometrical approach, principal components analysis (PCA), followed by unsupervised hierarchical cluster analysis (HCA) was performed.

Before analysis, a data matrix was constructed, consisting of 50 rows (50 samples) and 1467 columns (1467 data points, between 400 and 1800 cm^{-1}). To take sample inhomogeneity (since the lateral resolution in the current Raman set-up was ca. 5 μm) into account, triplicate spectra for each sample were obtained and averaged.

In order to correct for non-specific fluorescence, which causes a sloping spectral background, the first derivative of the spectra was used (Savitsky-Golay algorithm³², 2nd degree polynomial, 13 data points window). Each first derivative spectrum was scaled to zero mean and unit variance (SNV). Subsequently the PCA algorithm was run on the data matrix, without any further preprocessing.

The resulting Scree plot, loading plots (shifted for better visualization) and score plots are given in figure 6.3.

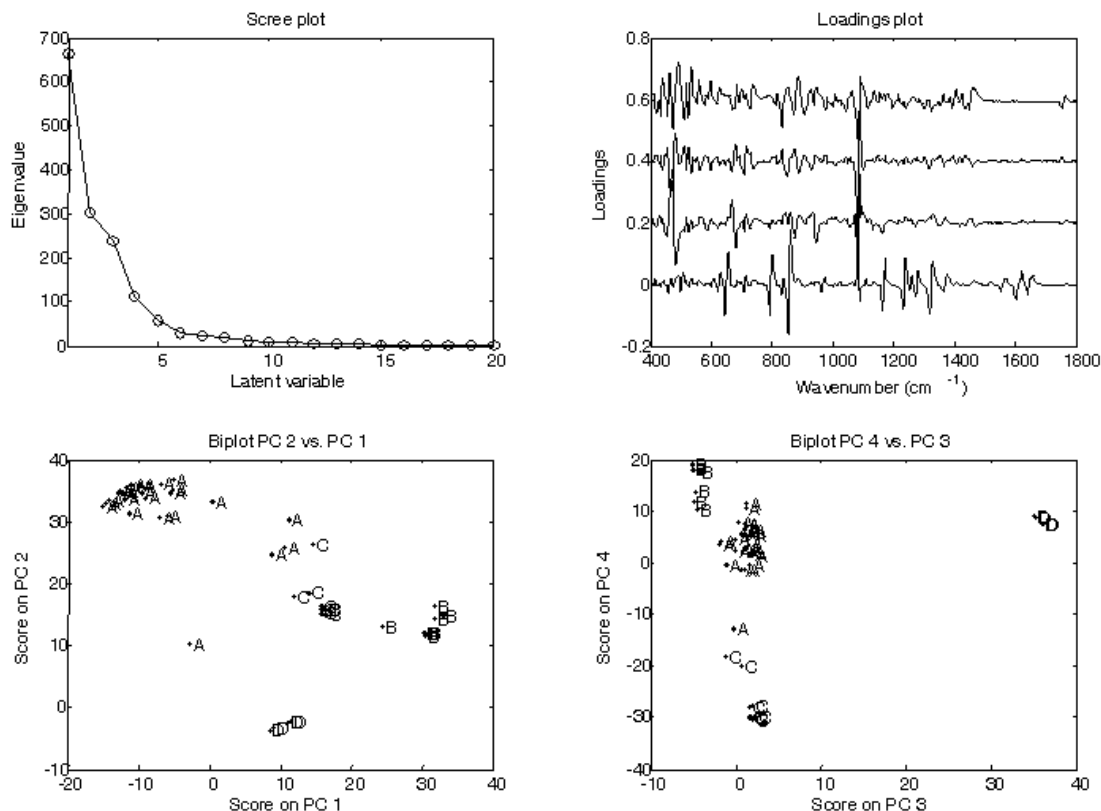


Figure 6.3 Principal components analysis of the Raman spectra of 50 drug samples. Preprocessing performed: Savitsky Golay 1st derivative and SNV. No scaling was used. Scree plot is given, along with the loadings plot for the first 4 principal components (loadings are shifted for visualisation). Labels in the biplots correspond with the groupings as observed after visual inspection (fig. 6.2). Each case is the average spectrum of 3 spectra (5 acc. x 30 s) with no baseline correction.

Scores on PC 2 and PC 3 seem to be highly discriminative for the spectra of group D, while the score on PC 4 accounts for the differentiation of group C. By using the scores of the first 4 principal components as the input for a simple K means clustering algorithm, HCA was performed on the data set. Clustering was thus based on the Euclidean distances (fig. 6.4). Although the Scree plot seems to suggest including more than five principal components, there were no improvements in the sample clustering. Therefore, to avoid over fitting, the number of principal components included, was limited to four (99,57 % variance captured in total). In figure 6.4, four different groups can be clearly distinguished from each other.

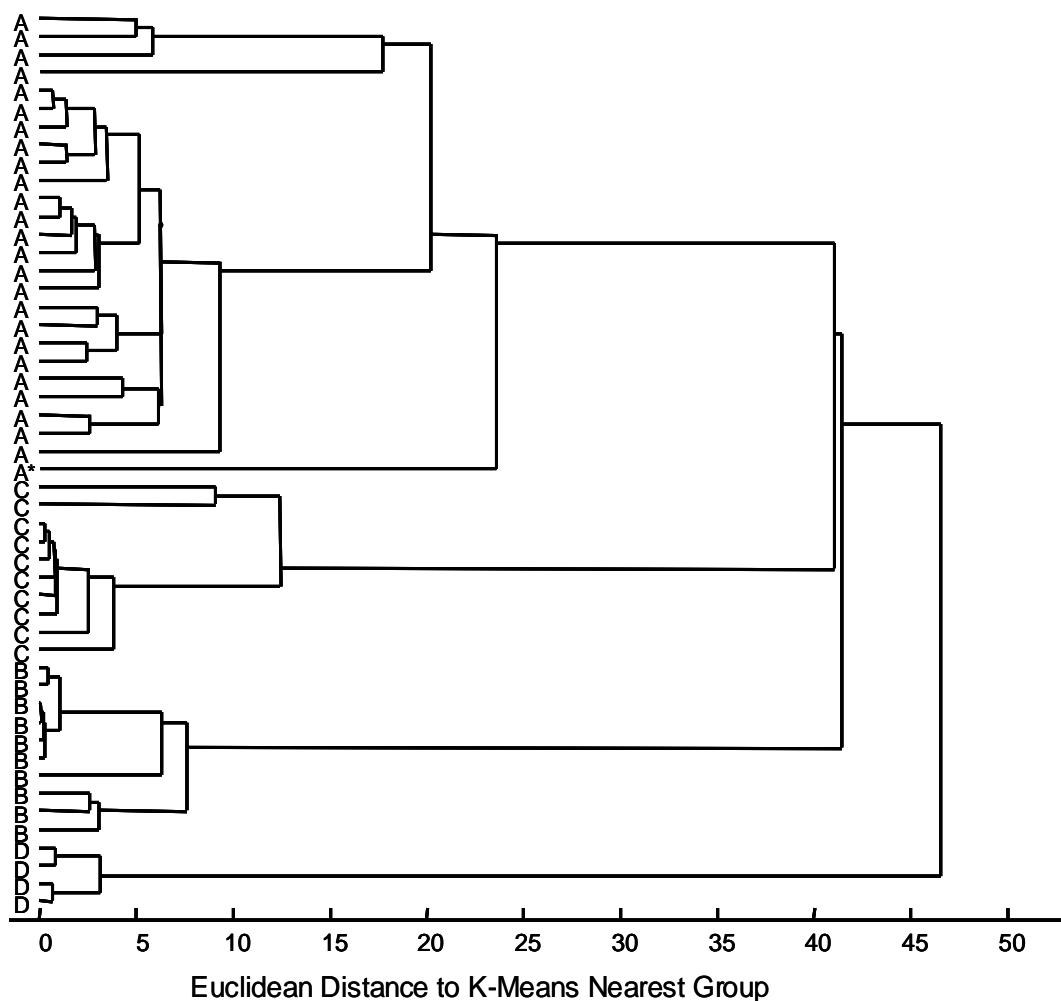


Figure 6.4 Dendrogram as obtained by hierarchical cluster analysis of the first 4 principal components of 50 drug samples. Labels are according to the groups obtained after visual inspection (fig. 6.2). The asterisk (*) refers to a specific case, as explained in the text. Each case is the average spectrum of 3 spectra, recorded under the same conditions as in figure 6.2 (no baseline correction).

These groups are in agreement with the visual inspection of the Raman spectra. In the group of genuine artesunate samples, one spectrum seems to be significantly different from the others (marked with an asterisk (*) in the dendrogram shown in fig. 6.4). The spectrum of this artesunate sample had some prominent Raman bands in the low wavenumbers region (fig. 6.5) which distinguished this sample from the other genuine tablets. These bands are caused by the presence of rutile³³, one of the polymorphs of TiO_2 , a product that is used as a whitener. Despite this interference, this simple classification algorithm still classifies this sample in the proper group.

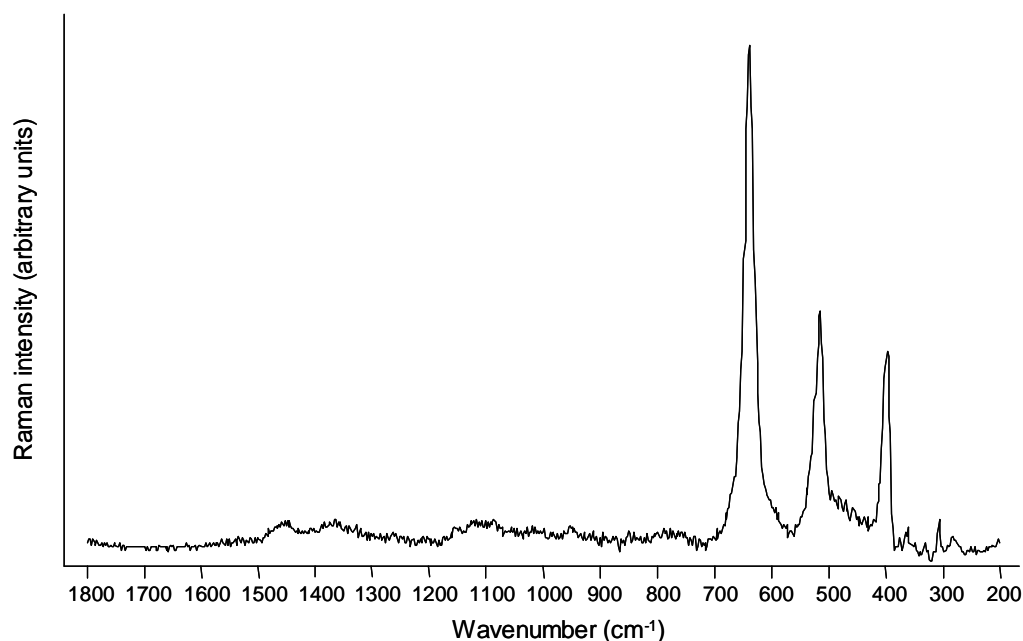


Figure 6.5 Raman spectrum of an artesunate sample, analysed with the Renishaw System-1000 spectrometer (5 acc. x 30 s), that shows intense Raman bands of rutile (TiO₂) (case marked with an * in fig. 6.4).

Within the A-branch of the dendrogram, a small group of 4 artesunate samples is separated from the rest of the group: these spectra showed Raman bands that were slightly broader than the Raman bands of the other artesunate samples. This may indicate a lower degree of crystallinity.

It has to be considered that, when the database of reference products and possible counterfeits becomes more complex (i.e. more entries as well as an increasing number of classes to distinguish), more advanced chemometric techniques, such as linear discriminant analysis (LDA) or artificial neural networks (ANNs) may be required. Until now the spectral analysis was focused towards the qualitative composition of these tablets, but in future work, quantitative aspects will also be investigated.

6.4 Conclusion

This research shows that Raman spectroscopy has a great potential for the fast detection of counterfeit artesunate tablets, one of the most widely counterfeited antimalarial drugs. Spectra of genuine artesunate and three

different groups of counterfeits could be differentiated by careful spectroscopic interpretation, as well as by an automatic approach (principal components and hierarchical clustering algorithms). These results suggest that Raman spectroscopy, in combination with chemometry, is not only able to discriminate between genuine and counterfeit tablets, but also to produce a “chemical fingerprint” of different types of counterfeits, which is helpful in determining the relationships between different samples. The combination of Raman spectroscopy and multivariate clustering can thus assist in the forensic investigation of the sources and trade routes of these drugs. These protocols may also be implemented in mobile Raman spectrometers, which could potentially allow customs officers, law-enforcement personnel and drug regulatory authorities to conveniently and rapidly analyse suspect tablets in the field.

6.5 Notes on this publication

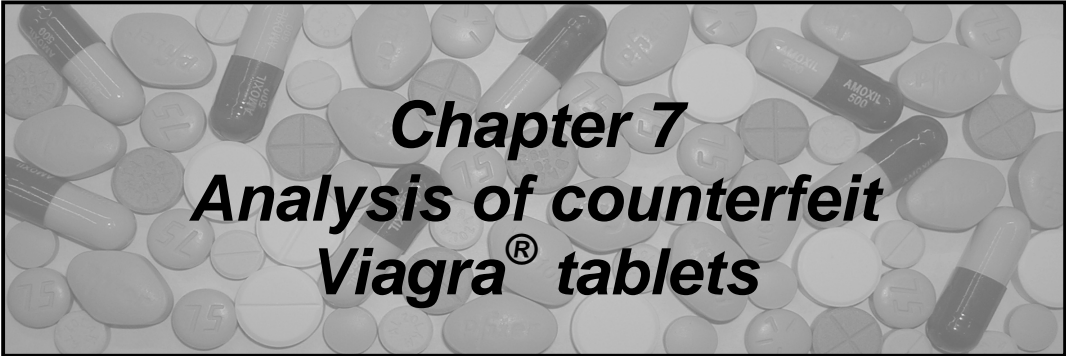
The work presented in this publication has also been used by KA Hall et al. for comparing the analysis of these 50 artesunate tablets with Liquid Chromatography – Mass Spectrometry (LC-MS)²⁷, which not only focuses on qualitative but as well on quantitative analysis. The qualitative results of that investigation were compared with results of the Fast Red TR colorimetric method and Raman spectroscopy. Additionally, counterfeits were detected by focusing on the holograms on the blisterpack¹⁴. All methods confirmed our results with Raman spectroscopy, and could also detect the counterfeits from the genuine artesunate samples.

However, since the counterfeiters are becoming increasingly sophisticated, quantitative analysis becomes increasingly important. Group A are considered genuine artesunate tablets, but so far, it is not proven that the amount of active ingredient is identical to the amount stated on the package. Therefore, quantitative analysis has to be performed on the tablets as well. Results of the quantitative analysis of antimalarial tablets will be described in Chapter 9. In the next chapter, however, we will focus on the analysis of another type of drug that is often counterfeited in the western world, namely Viagra[®].

6.6 References

1. Dunavan CP, *Scientific American*, 2005; December : 56-63.
2. Taylor WRJ, White NJ, *Drug Safety*, 2004; 27(1): 25-61.
3. WHO, *Fact Sheet N°94*, May 2007.
4. Deisingh AK, *Analyst*. 2005; 130: 271-279.
5. WHO, *Substandard and counterfeit medicines*, fact sheet N°275, November 2003.
6. FDA, *Combating counterfeit drugs: a report of the food and drug administration*, 2004.
7. WHO, *Drug Information*, 2004; vol. 18 No.2.
8. Blok-Tip L, Vogelpoel H, Vredenburg MJ, Barends DM, de Kaste D *Counterfeits and imitations of Viagra and Cialis tablets: trends and risks to public health*, RIVM report 267041001/2005.
9. WHO, *Counterfeit Drugs, guidelines for the development of measures of combat counterfeit drugs*, 1999.
10. Shakoor O, Taylor RB, Behrens RH, *Trop. Med. Int. Health*, 1997; 2(9): 839-845.
11. Scafi SHF, Pasquini C, *Analyst*, 2001; 126: 2218-2224.
12. Rodionova OY, Houmøller LP, Pomerantsev AL, Geladi P, Burger J, Dorofeyev VL, Arzamastsev AP, *Anal. Chim. Acta*, 2005; 549: 151-158.
13. Ermer J, Vogel M, *Biomed. Chromatogr.* 2000; 14: 373-383.
14. Newton P, Proux S, Green M, Smithuis FM, Rozendaal J, Prakongpan S, Chotivanich K, Mayxay M, Looareesuwan S, Farrar JJ, Nosten F, White NJ, *Lancet*, 2001; 357: 1948–1950.
15. Dondorp AM, Newton PN, Mayxay M, Van Damme W, Smithuis FM, Yeung S, Petit A, Lynam AJ, Johnson A, Hien TT, McGready R, Farrar JJ, Looareesuwan S, Day NPJ, Green MD, White NJ, *Trop. Med. Int. Health*, 2004; 9(12): 1241-1246.
16. Green MD, Dwight LM, Wirtz RA, White NJ, *J. Pharm. Biomed. Anal.* 2000; 24: 65-70.
17. Taylor LS, Langkilde FW, *J. Pharm. Sci.* 2004; 89(10): 1342–1353.

18. Bell SEJ, Burns DT, Dennis AD, Speers JS, *Analyst*, 2000; 125: 541-544.
19. Lombardi DR, Wang C, Sun B, Fountain III AW, Vickers TJ, Mann CK, Reich FR, Douglas JG, Crawford BA, Kohlasch FL, *Appl. Spectrosc.* 1994; 48(7): 875–883.
20. Pelletier MJ, *Appl. Spectrosc.* 2003; 57(1): 20A-37A.
21. Langkilde FW, Sjöblom J, Tekenbergse-Hjelte L, Mrak J, *J. Pharm. Biomed. Anal.* 1997; 15: 687–696.
22. Findlay WP, Bugay DE, *J. Pharm. Biomed. Anal.* 1998; 16: 921–930.
23. Vergote GJ, De Beer TRM, Vervaet C, Remon JP, Baeyens WRG, Diericx N, Verpoort F, *Eur. J. Pharm. Sci.* 2004; 21: 479–485.
24. Ryder AG, O'connor GM, Glynn TJ, *J. Forensic Sci.* 1999; 44(5): 1013-1019.
25. Hodges CM, Akhavan J, *Spectroc. Acta Pt. A-Molec. Biomolec. Spectr.* 1990; 46A(2): 303-307.
26. Bell SEJ, Burns DT, Dennis AC, Matchett LJ, Speers JS, *Analyst*, 2000; 125: 1811-1815.
27. Hall KA, Newton PN, Green MD, Pizzanelli D, Mayxay M, Dondorp A, White NJ, Fernandez FM, *Am. J. Trop. Med. Hyg.* 2006; 75(5): 804-811.
28. Lin-Vein D, Colthup NB, Fateley WG, Grasselli JG, *The handbook of Infrared and Raman Characteristic Frequencies of Organic Molecules*, Academic Press, London, UK , 1991.
29. Lee I, Han SW, Choi HJ, Kim K, *Adv. Mater.* 2001; 13(31): 1617-1620.
30. Vandenabeele P, Grimaldi DM, Edwards GM, Moens L, *Spectroc. Acta Pt. A-Molec. Biomolec. Spectr.* 2003; 59: 2221–2229.
31. Szostak R, Mazurek S, *Analyst*, 2002; 127: 144-148.
32. Savitzky A, Golay MJE, *Anal. Chem.* 1964; 36; 8: 1627-1639.
33. Edwards HGM, Hassan NFN, Middleton PS, *Anal. Bioanal. Chem.* 2006; 384(6): 1356-1365.



Chapter 7
Analysis of counterfeit
Viagra® tablets

7 Analysis of counterfeit Viagra® tablets

Based on the paper: de Veij M, Deneckere A, Vandenabeele P, de Kaste D, Moens L, Detection of counterfeit Viagra® with Raman spectroscopy, Journal of Pharmaceutical and Biomedical analysis, 2008; 46: 303-309.

In the previous chapter, it is demonstrated that Raman spectroscopy can be used to qualitatively detect counterfeit antimalarial drugs in developing countries. This chapter focuses on one of the most counterfeited drugs in developed countries, namely is Viagra®. Initially, Pfizer developed Viagra® as



Fig.7.1 Chinese advert for Viagra®

a treatment against angina and high blood pressure. During the clinical trials, some positive side effects were found. Since 1996, the FDA has approved Viagra as the first drug to treat erectile dysfunction. Pfizer earns approximately 1 billion US\$ each year with the production of Viagra¹. At this moment, it is the most used drug against erectile dysfunction worldwide, even in China (fig. 7.1), and the most counterfeited as well.

Abstract

During the last few years, counterfeiters have become increasingly sophisticated by falsifying drugs and making them look identical to genuine tablets. In this paper, Raman spectroscopy is proposed as a fast and reliable method for the detection of counterfeit Viagra® tablets. This technique can easily detect genuine from counterfeit tablets without the need of sample preparation. In total 18 tablets were analysed which all contained the active ingredient sildenafil, but different excipients were used, as could be observed in the Raman spectra between 1150 and 700 cm⁻¹. So, the spectra could be divided into genuine or counterfeit.

Additionally, principal component analysis (PCA), combined with hierarchical cluster analysis (HCA), was used to establish an automated approach for the discrimination of counterfeit from genuine Viagra[®] tablets. Raman spectroscopy, combined with principal components analysis, could be used in the future by customs or in the field to identify counterfeit tablets on the spot without involvement of trained chemists.

7.1 Introduction

Since the introduction of Viagra[®] for erectile dysfunction by Pfizer in 1998¹, numerous websites have been appearing, where people easily and anonymously can purchase Viagra[®] tablets. Viagra[®] has been falsified numerous times² and has been put on the National Specified List of Susceptible Products by the National Association of Boards of Pharmacy³ in the U.S.A. The products on this list are popular among counterfeiters and could therefore pose a potential risk for public health.

According to the World Health Organization (WHO) a counterfeit medicine is one which is deliberately and fraudulently mislabelled, with respect to its identity and/or source⁴. This includes products with correct ingredients or with the wrong ingredients, without active ingredients, with insufficient active ingredient or with fake packaging⁴.

So far, different methods have been used for the analysis of sildenafil in Viagra[®] tablets. These methods include capillary gas chromatography⁵, polymer membrane sensors⁶, NMR (¹H, ¹³C, ¹⁵N)⁷, UV-VIS^{8,9}, infrared spectroscopy^{9,10}, micellar electrokinetic capillary chromatography¹¹, high-performance liquid chromatography with diode-array detection^{9,12,13}, liquid chromatography coupled with mass spectrometry (LC-DAD-MS⁹, LC-ECI-MS/MS¹² and LC-MS/MS¹⁴) and thin-layer chromatography^{9,13}. The disadvantage of many non-spectroscopic methods is their need for sample preparation, e.g. by pulverizing the tablet and dissolving it.

Until now, in literature only two methods have been used, specifically to detect counterfeit Viagra®, namely X-ray powder diffraction analysis¹⁵ and near-infrared spectroscopy (NIRS)⁹. With X-ray diffraction only six Viagra® tablets were investigated and compared with a genuine Viagra® tablet. Based on the information it could predict if the active ingredient and/or particular excipients were present, so the analysis with X-ray diffraction is only qualitative¹⁵. A downside of this method is that the coating of the Viagra® tablet had to be removed before analysis and the technique requires a trained analyst operator as well. For the analysis of the Viagra® with NIRS, a total of 103 samples were analysed. The method can be used to check homogeneity of a batch, distinguish counterfeits and imitations from authentic Viagra® and screen for the presence of sildenafil citrate⁹. NIRS can therefore give an indication if sildenafil citrate is present in the tablet but for definitive confirmation LC-MS analysis are necessary⁹.

Lately, it has become very difficult to distinguish counterfeit from genuine drugs, based on their appearance¹⁶. So it is necessary to develop a fast and easy method, in order to identify these counterfeit drugs in the field. In this paper, we propose a Raman spectroscopic method for the detection of counterfeit Viagra® tablets.

Pharmaceutical analysis by Raman spectroscopy is becoming a commonly accepted approach as illustrated by the rising number of research papers that are published in this field¹⁷. Raman spectroscopy has been used for drug identification of active ingredients as well as excipients¹⁸, polymorphism¹⁹, imaging of tablets²⁰, quality control²¹, industrial applications²². This technique requires no sample preparation; tablets can even be analysed through their coating, while non-destructive character and high speed of analysis make Raman spectroscopy well-suited for investigating possible counterfeit drugs^{23,24}. Moreover, by using chemometric techniques to compare the recorded spectra with those in a reference library, instrument operation and spectral interpretation can be automated, in order to give a pragmatic answer.

7.2 Experimental

The analyses of the Viagra[®] tablets were carried out with a Renishaw System-1000 spectrometer (Wotton-under-Edge, UK) which is connected to an Olympus BH-2 microscope. The laser used is a diode laser with a wavelength of 785 nm and a power of 50 mW (DL 100, TuiOptics GmbH, Martinsried/Munich, Germany). A 5x objective lens (Olympus MDPlan5, 0.10 NA, Omnilabo, Aartselaar, Belgium) was used to focus the laser light on the sample and to collect the scattered light. The collected Raman radiation was dispersed with a 1200 lines mm⁻¹ grating (focal length 250 mm) and focussed on a Peltier-cooled CCD detector, allowing to obtain a spectral resolution of ca. 1 cm⁻¹.

18 tablets were recorded in the spectral window of 700 to 1800 cm⁻¹, with 10 accumulations of 30 s each. Besides the 18 tablets, an genuine Viagra[®] tablet (provided by a pharmacy, Ghent, Belgium), the active ingredient (provided by the National Institute for Public Health and the Environment, RIVM, Bilthoven, the Netherlands) and inactive components of a genuine Viagra[®] tablet were analysed as well. These are: microcrystalline cellulose (Sigma-Aldrich, Belgium), calcium hydrogenphosphate (Sigma-Aldrich, Belgium), croscarmellose (Certa, Belgium), magnesium stearate (Sigma-Aldrich, Belgium), hypromellose (Shin Etsu, Japan), lactose (DMV international, the Netherlands), triacetin (Sigma-Aldrich, Belgium) and indigo carmine (Fluka, Belgium).

Additionally, several reference products were analysed, namely: barium sulphate (UCB, Belgium), calcium sulphate (Fluka, Switzerland), calcium carbonate (Merck, Belgium), mannitol (Cerestar, Belgium) and sucrose (Merck, Belgium).

Three spectra were recorded, averaged and baseline-corrected before presentation, to eliminate the influence of broadband fluorescence.

18 “Viagra” tablets (fig. 7.2) were purchased in local pharmacies in China (tablet 1 & 3 from Shanghai, tablet 2 from Beijing and tablet 4, 5, 6, 17 & 18 from Suzhou) and Mexico (tablet 7 from Cancun). Other “Viagra” tablets were donated by Public Health and Environment in the Netherlands (tablet 8, 9, 10, 11, 12 & 13), customs at Brussels Airport (tablet 14 & 16) and by the Federal Agency for Medicines and Health Products in Belgium (tablet 15).



Figure 7.2 Picture of the 18 tablets used in this research. In some cases, tablets are broken, for reason of differentiation of the coating and the bulk of these tablets.

Data processing was performed with Matlab 6.5 (The MathWorks Inc. Natick, MA, U.S.A.) and the PLS toolbox, version 3.0 (Eigenvector Research Inc., Wenatchee, WA, U.S.A.). The average of the three or five spectra (depending on tablet or pure substance) and a manual baseline correction was performed by using ACD/Specmanager (version 9.13, Advanced Chemistry Development, Inc. Toronto, Canada).

7.3 Results and discussion

7.3.1 Visual inspection of the tablets

The first step in detecting counterfeit drugs is based on the appearance of the tablet. Viagra® is known for its distinct blue diamond shape, with on one side

the Pfizer-logo and on the other side the abbreviation “VGR” plus the amount of sildenafil in mg (25, 50 or 100). Based on this information the tablets 16, 17 and 18 can be eliminated as genuine Viagra[®] tablet, since tablet 16 lacks the blue colour, tablet 17 has different names pressed in the tablet and tablet 18 has a different shape. Tablet 1 till 15, based on their appearance, look similar to genuine Viagra[®] tablet and for these tablets Raman analysis is necessary.

7.3.2 Visual inspection of the Raman spectra

To be able to differ the 18 tablets based on their Raman spectrum, a Raman spectrum of a genuine Viagra[®] tablet is necessary. Figure 7.3 shows the spectrum of pure sildenafil (A), its chemical structure and the spectrum of genuine Viagra[®] (B). The majority of the Raman bands in the genuine Viagra[®] spectrum (fig. 7.3B) can be assigned to the corresponding functional groups²⁵ of the active ingredient (fig. 7.3A).

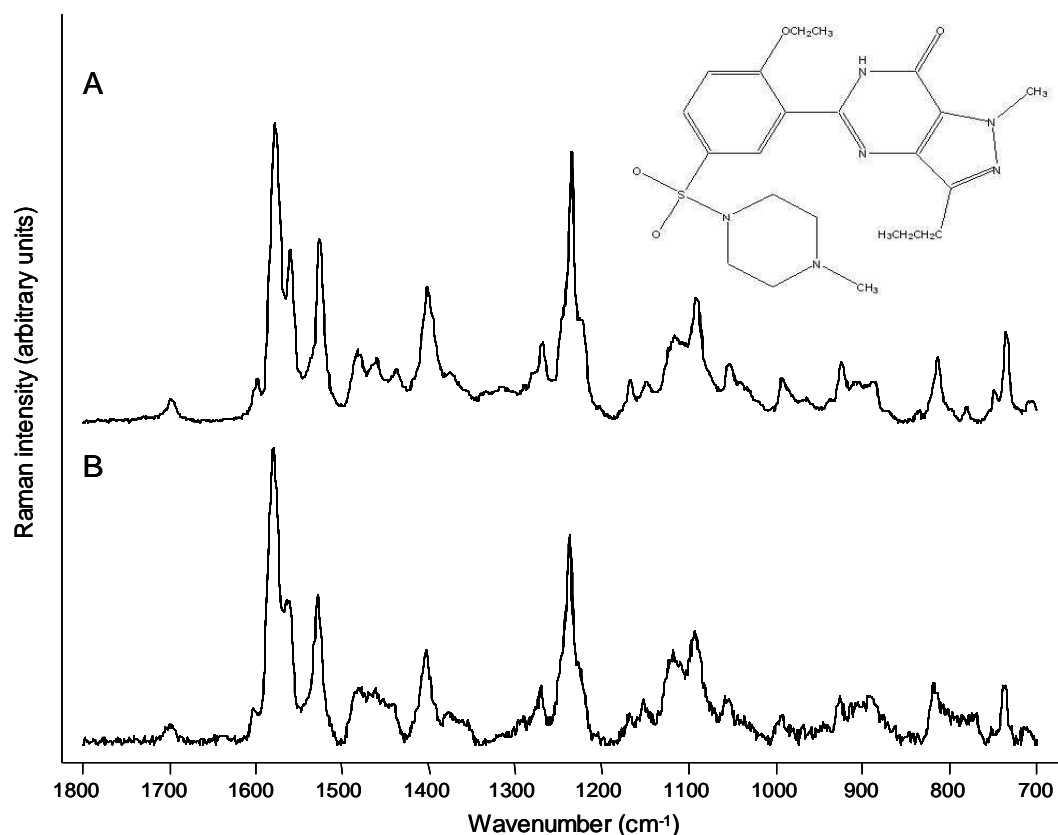


Figure 7.3 Raman spectrum of sildenafil and its molecular structure (A) and the genuine Viagra[®] tablet (B) analysed with the Renishaw System-1000 spectrometer (10 acc. x 30 s).

A Raman band at the far end of the spectrum at 1699 cm^{-1} can be assigned to the stretching vibration of the C=O group, additionally the doublet at $1580 / 1562\text{ cm}^{-1}$ is attributed by the C=C bond. Raman bands at 1528 cm^{-1} ($\nu(\text{N-C=N})$), 1238 and 1272 cm^{-1} ($\nu(\text{C=N})$) and the Raman band at 927 cm^{-1} ($\nu(\text{C-N})$) are attributed to nitrogen containing bonds. The Raman bands at 1170 and 1057 cm^{-1} can be assigned to the symmetric $\nu(\text{SO}_2)$ and the asymmetric $\nu(\text{SO}_2)$ vibrations, respectively.

There are some additional Raman bands present in the spectrum of genuine Viagra® which can not be attributed to the active ingredient, but can be assigned to one of the excipients (769 , 847 , 873 , 1117 , 1294 and 1352 cm^{-1} , weakly, not always visible in fig. 7.3B).

A Viagra® tablet consists of a white core and a blue coating. The core of the tablet consists of sildenafil citrate, microcrystalline cellulose, calcium hydrogen phosphate, croscarmellose and magnesium stearate. The coating of the tablet consists of hypromellose, lactose, triacetin, titanium dioxide and indigo carmine for its distinct blue colour²⁶.

The Raman spectra of these excipients are shown in figure 7.4, the spectrum of titanium dioxide is not presented, since this spectrum only consist of three very strong Raman bands below 700 cm^{-1} (394 , 514 and 635 cm^{-1})²⁷.

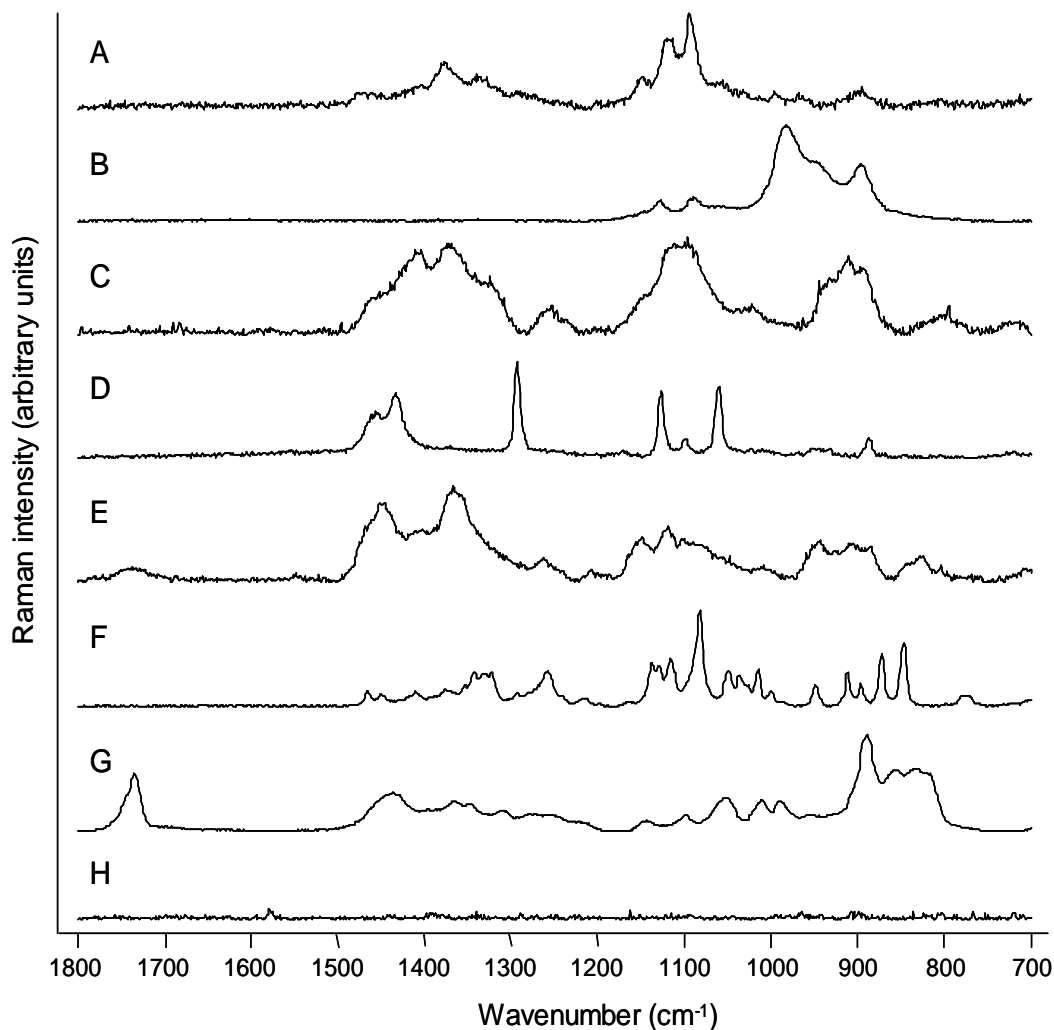


Figure 7.4 Raman spectrum of excipients used in a Viagra[®] tablet analysed with the Renishaw System-1000 spectrometer, A: microcrystalline cellulose (10 acc. x 30 s), B: calcium hydrogen phosphate (5 acc. x 30 s), C: croscarmellose (50 acc. x 60 s), D: magnesium stearaat (5 acc. x 30 s), E: hypromellose (15 acc. x 60 s), F: lactose (5 acc. x 30 s), G: triacetin (5 acc. x 30 s) and H: indigo carmine (40 acc. x 30 s).

Based on these spectra, the additional bands in the spectrum (fig. 7.3B) of the genuine Viagra[®] tablet can be assigned to microcrystalline cellulose (1352 and 1117 cm⁻¹)²⁸, magnesium stearate (1294 and 769 cm⁻¹) and lactose (873 and 847 cm⁻¹)²⁸. The spectrum of genuine Viagra[®] (fig. 7.3B) is compared to the Raman spectra of the 18 tablets in figure 7.5.

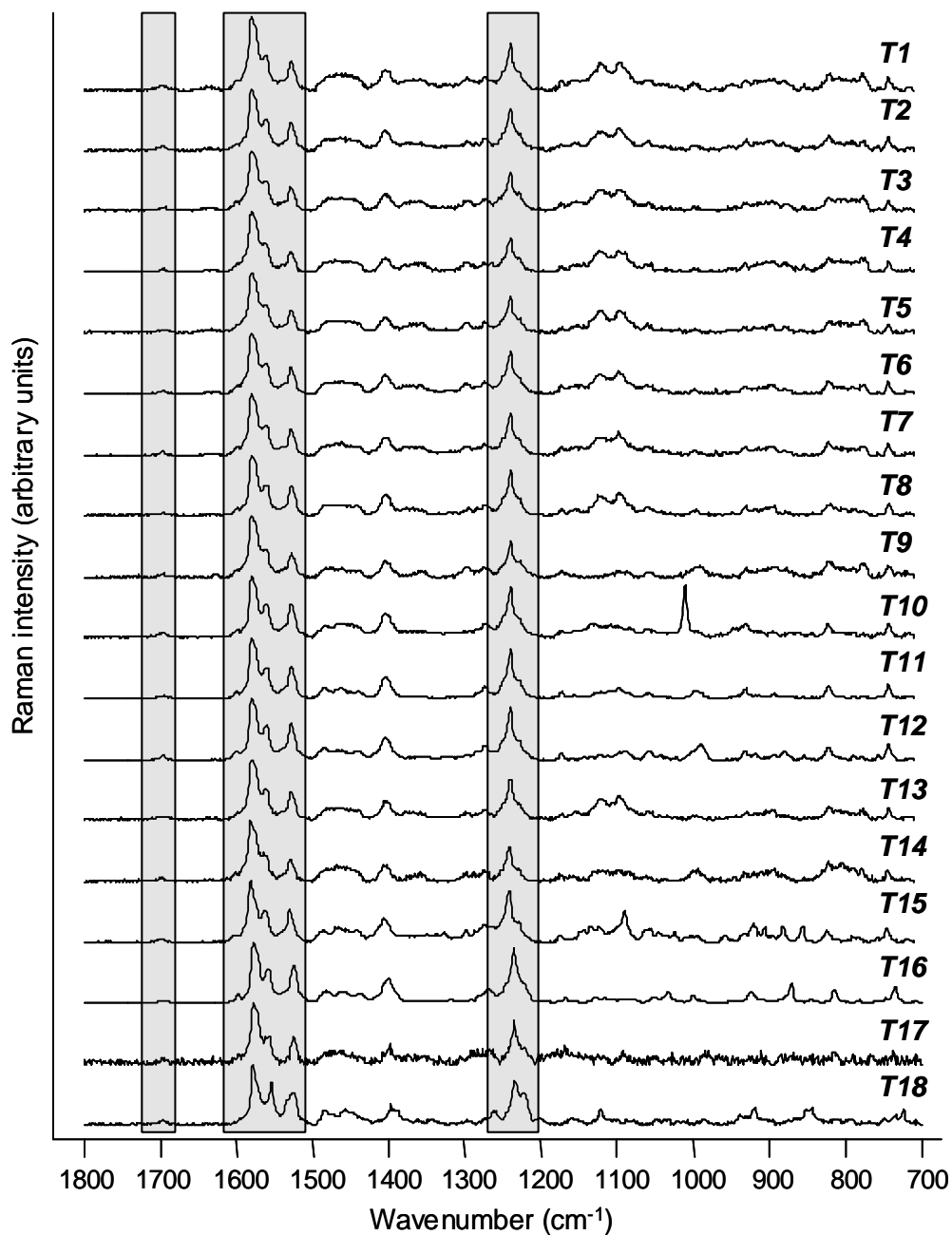


Figure 7.5 Raman spectra of the 18 tablets analysed with the Renishaw System-1000 spectrometer (10 acc. x 30 s).

The Raman bands at 1699 cm^{-1} ($\nu(\text{C}=\text{O})$ stretch vibration), 1580 and 1562 cm^{-1} ($\nu(\text{C}=\text{C})$ doublet), 1528 cm^{-1} ($\nu(\text{C}=\text{N})$ stretch) and at 1238 cm^{-1} ($\nu(\text{C}-\text{N})$ stretch), which are grey highlighted in figure 7.5, were used to check for the presence of the active ingredient. It can be concluded that all 18 tablets contain the active ingredient.

However, when focussing on the Raman bands between 1150 and 700 cm^{-1} , differences between these tablets can be noticed:

- Tablet 1 till 8 and tablet 13 show the same spectrum as the genuine Viagra[®], including the Raman band of microcrystalline cellulose at 1117 cm^{-1} (fig. 7.4A). This Raman band is clearly lacking in the tablets 9 till 12 and 14 till 18, which therefore can be considered as counterfeits. These 9 tablets (9 - 12 and 14 - 18) do not show certain Raman bands which are present in the spectrum of genuine Viagra[®] and/or have additional Raman bands of other excipients.
- Five tablets have extra Raman bands which are attributed by different excipients not present in genuine Viagra[®].
 - Tablet 9 has an additional Raman band at 985 cm^{-1} which can be assigned to barium sulphate (fig 7.6A)²⁹ whereas tablet 10 has an extra Raman band at 1005 cm^{-1} attributed by calcium sulphate (fig. 7.6B)²⁹.
 - Raman bands at 711 and 1084 cm^{-1} which are specific for calcium carbonate (fig. 7.6C)³⁰ can be observed in the spectrum of tablet 15. Mannitol (fig. 7.6D)³¹ is present in tablet 16 according to the three Raman bands at 782, 872 and 1034 cm^{-1} .
 - Tablet 18 shows three additional Raman bands at 846, 921 and 1123 cm^{-1} which can be assigned to sucrose (fig. 7.6E)³¹.
- The three tablets 11, 12 and 14 lack the Raman band at 1117 cm^{-1} , as do all 9 counterfeits, but show no obvious Raman bands of other excipients besides the excipients used in genuine Viagra[®].
- Finally, besides the Raman bands of sildenafil (fig. 7.3A) no other Raman bands can be observed in the Raman spectrum of tablet 17, not even Raman bands from the excipients used in the genuine Viagra[®].

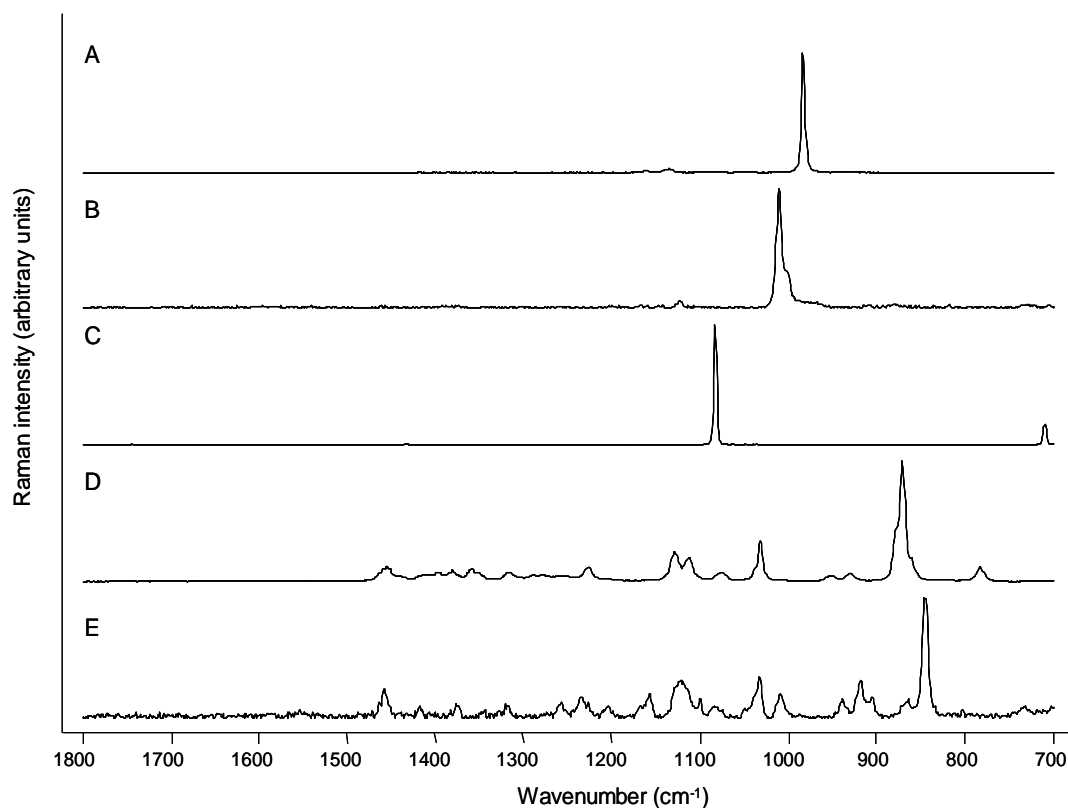


Figure 7.6 Raman spectra excipients found in the analysed “Viagra” tablets with use of the Renishaw System-1000 spectrometer, A: barium sulphate (1 acc. x 30 s), B: calcium sulphate (20 acc. x 30 s), C: calcium carbonate (1 acc. x 30 s), D: mannitol (5 acc. x 120 s) and E: sucrose (20 acc. x 30 s).

In stead of using Raman bands of the active ingredient as distinction between genuine and counterfeit Viagra®, the tablets could be divided into these two categories based on the excipients used.

7.3.3 Chemometrical analyses

When considering an analytical technique for routine or screening investigations, this technique has to fulfil several requirements. These include, amongst others, a high speed of analysis, easiness to operate and the technique should be quite robust. It is clear that the accuracy of the applied method is also critical. Raman spectroscopy seems to meet many of these conditions. However, if this technique has to be operated by non-specialist users (e.g. at customs), there is need for an automated spectral interpretation.

Here a chemometrical approach combined with an elaborated database with Raman spectra of genuine pharmaceutical products has to be considered.

Here, in an exploratory approach, we use a combination of principal components analysis (PCA) and hierarchical cluster analysis (HCA). However, it is not the aim of this work to select the most appropriate chemometrical technique for this discrimination.

The dataset, consisting of the Raman spectra of 19 Viagra[®] tablets is arranged in a 19 by 1205 data matrix (1205 data points, between 700 and 1800 cm⁻¹). In order to avoid contributions from the broad-featured fluorescence background, the 2nd derivative of all spectra was taken by using the Savitsky-Golay algorithm³². A 13 - point window-function and the use of a 3rd order polynomial happened to yield the best results. The mean-centered dataset was reduced, retaining the first 8 principal components. Subsequently, K-means clustering was applied, by using the nearest group clustering algorithm and Euclidean distance in the 8-dimensional principal component space. The resulting Dendrogram is presented in figure 7.7.

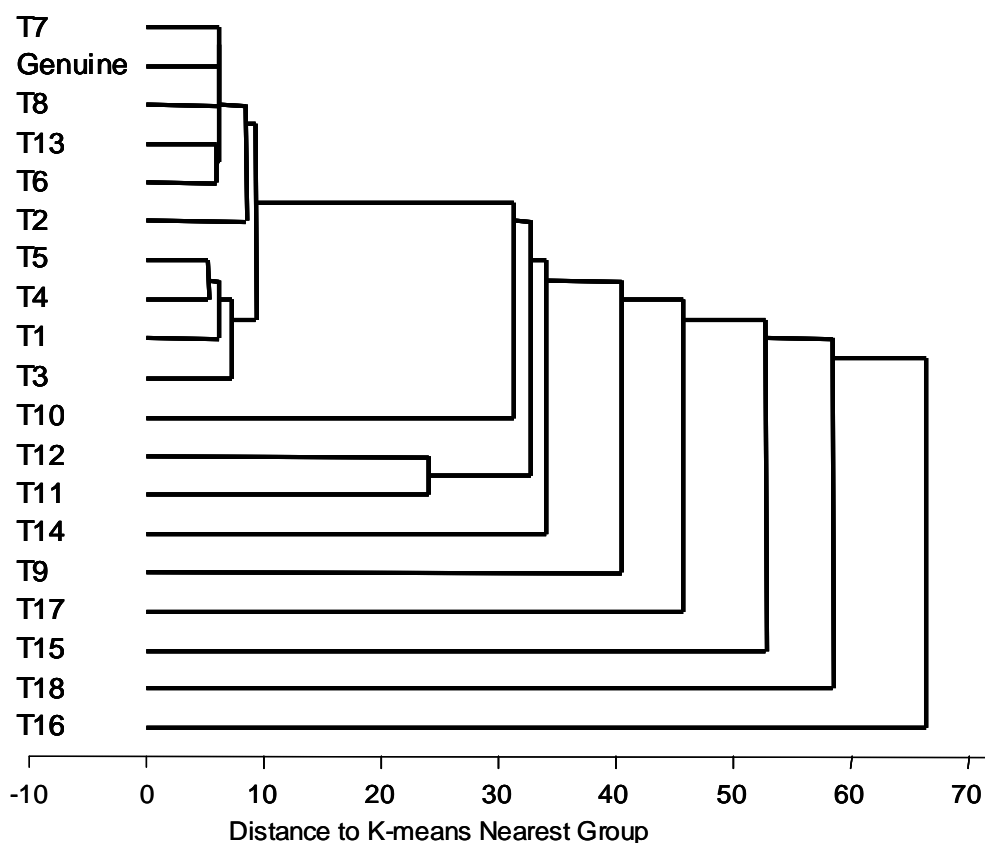


Figure 7.7 Dendrogram of the 18 Viagra[®] tablets and genuine Viagra[®] tablet.

In this dataset, a clear cluster is observed containing the spectra of tablets 1– 8, tablet 13 and the genuine tablet. This group contains Raman spectra of the genuine Viagra® tablets. The other tablets are on a distinct distance from this group, showing that chemometrical methods are able to discriminate genuine from counterfeit Viagra® tablets. Amongst the counterfeit spectra, the dendrogram seems to show some tailing effects which is a consequence from the minute differences that are observed between these falsifications. Most of these counterfeits are different from each other. Only tablets 11, 12 and 14 resemble in the sense that they all lack the cellulose additive, which is present in genuine Viagra®. Apparently, from the cluster diagram tablets 11 and 12 seem to be more closely related than 14. Although, large-scale research is needed before final conclusions can be drawn, indication of relationships between the counterfeit tablets might contain useful information in forensics in order to track down the origin of these products.

7.4 Conclusion

Raman spectroscopy has been proposed as a fast and reliable qualitative technique for the detection of counterfeit Viagra® tablets. In this work, 18 tablets were examined. From visual inspection, 3 tablets (16 - 18) could be assigned as counterfeit, whereas Raman spectroscopy was able to detect an additional 9 counterfeit tablets (9 – 12 and 14 - 15) from our test set. Although these tablets contain the active ingredient sildenafil citrate, they can be considered as counterfeit, since they contain less or other inactive compounds. In the spectra of counterfeit Viagra® tablets, Raman bands of barium sulphate, calcium sulphate, calcium carbonate, mannitol and sucrose could be detected. The other tablets (1 – 8 and 13) show an identical Raman spectrum compared to the Raman spectrum of the genuine Viagra®. By using a combined approach of principal components analysis (PCA) and hierarchical cluster analysis (HCA), with Raman spectroscopy it was possible to design an automated approach to distinguish between genuine and counterfeit tablets. The latter turns out to be useful when considering this technique for screening by non-specialist operators, for instance at customs.

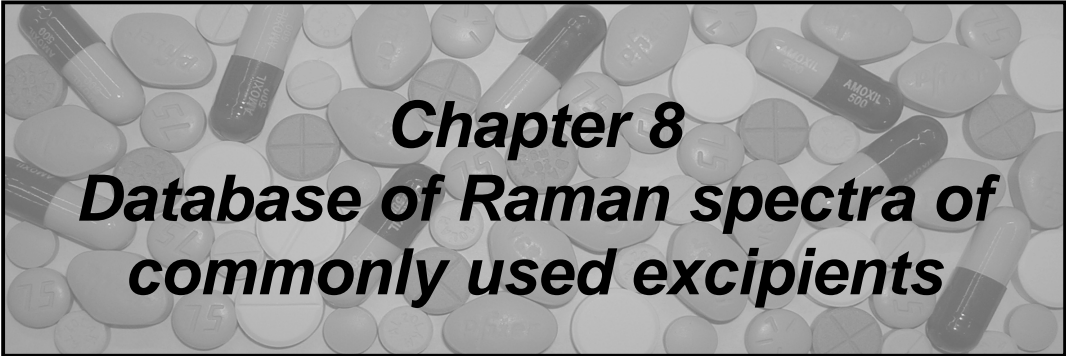
7.5 Notes on this publication

Counterfeit Viagra has, so far, been analysed with different analytical methods such as GC⁵, NMR⁷, UV-VIS^{8,9}, HPLC^{9,12,13} and LC-MS/MS¹⁴. Compared to these techniques, Raman spectroscopy has the advantage for being a fast and easy technique. This project shows that, even if all the tablets have, qualitatively speaking, the correct active ingredient as the genuine Viagra[®], it was possible to distinguish the counterfeits based on the excipients used. This shows the importance of establishing a database with reference spectra of commonly used excipients (chapter 8). Since the counterfeiters are becoming so sophisticated, quantitative analysis is required as well. The possibilities of quantitative analysis with Raman spectroscopy is discussed in Chapter 9.

7.6 References

1. Patient Information Sheet Viagra[®], U.S. Department of Health and Human services, Food and Drug Administration, Rockville MD, U.S.A., June 2005.
2. Blok-Tip L, Vogelpoel H, Vredenburg MJ, Barends DM, de Kaste D, RIVM report 267041001/2005, Bilthoven, The Netherlands.
3. National Specified List of Susceptible Products, National Association of Boards of Pharmacy, Mount Prospect II, U.S.A., December 28th 2004.
4. Counterfeit Drugs, guidelines for the development of measures to combat counterfeit drugs, Department of Essential Drugs and Other Medicines, World Health Organization, Geneva, Switzerland, 1999.
5. Berzas JJ, Rodríguez J, Villaseñor MJ, Contento AM, Cabello MP, *Chromatographia*, 2002; 55: 601-606.
6. Othman AM, Rizk NMH, El-shahawi MS, *Anal. Chim. Acta*, 2004; 515: 303-309.
7. Wawer I, Pisklak M, Chilmonczyk Z, *J. Pharm. Biomed. Anal.* 2005; 38: 865-870.
8. Dinesh ND, Nagaraja P, Made Gowda NM, Rangappa KS, *Talanta* 2002; 57: 757-764.

9. Vredenburg MJ, Blok-Tip L, Hoogerbrugge R, Barends DM, de Kaste D, *J. Pharm. Biomed. Anal.* 2006; 40: 840-849.
10. Wang Y, Chen G, Zhu Z, Zhu J, Lu W, *Int. J. Infrared Millimeter Waves*, 2003; 24(7): 1177-1185.
11. Rodriguez Flores J, Berzas Nevado JJ, Castañeda Peñalvo GC, Mora Diez N, *J. Chromatogr. B*, 2004; 811: 231-236.
12. Zhou P, Oh SSY, Hou PL, Low MY, Koh HL, *J. Chromatogr. A*, 2006; 1104: 113-122.
13. Mikami E, Ohno T, Matsumoto H, *Forensic Sci. Int.* 2002; 130: 140-146.
14. Liang Q, Qu J, Luo G, Wang Y, *J. Pharm. Biomed. Anal.* 2006; 40: 305-311.
15. Maurin JK, Pluciński F, Mazurek AP, Fijalek Z, *J. Pharm. Biomed. Anal.* 2007; 43: 1514-1518.
16. Newton PN, McGready R, Fernandez F, Green MD, Sunjio M, Bruneton C, Phanouvong S, Millet P, Whitty CJM, Talisuna AO, Proux S, Christophel EM, Malenga G, Singhhasivanon P, Bojang K, Kaur H, Palmer K, Day NPJ, Greenwood BM, Nosten F, White NJ, *Plos Med*, 2006; 3(6): 752-755.
17. de Veij M, Vandenabeele P, Moens L, *European Pharmaceutical Review*, 2005; 3: 86-89.
18. Ghebremeskel AN, Vemavarapu C, Lodaya M, *Int. J. Pharm.* 2007; 328: 119-129.
19. Karabas I, Orkoula MG, Kontoyannis CG, *Talanta* 2007; 71: 1382-1386.
20. Sasic S, *Appl. Spectrosc.* 2007; 61(3): 239-250.
21. Kauffman JF, Dellibovi M, Cunningham CR, *J. Pharm. Biomed. Anal.* 2007; 43: 39-48.
22. Vergote GJ, De Beer TRM, Vervaet C, Remon JP, Baeyens WRG, Diericx N, Verpoort F, *Eur. J. Pharm. Sci.* 2004; 21: 479-485.
23. de Veij M, Vandenabeele P, Alter Hall K, Fernandez FM, Green MD, White NJ, Dondorp AM, Newton PN, Moens L, *J. Raman Spectrosc.* 2007; 38(2): 181-187.



Chapter 8
Database of Raman spectra of
commonly used excipients

8 Database of Raman spectra of commonly used excipients

Based on the paper: de Veij M, Vandenaabeele P, De Beer TRM, Remon JP, Moens L, Reference database of Raman spectra of pharmaceutical excipients, to be submitted.

Another way of distinguishing counterfeit drugs is the analysis of excipients used. This requires an extensive database of commonly used excipients. Since access to commercially available databases is quite expensive, a database focusing on only excipients has been established. Based on the research of the most commonly used drugs, a list of excipients has been established. The Raman spectra of these excipients are presented and discussed in this chapter.

Abstract

Raman spectroscopy has evolved to an important technique in pharmaceutical analysis. Usually, the focus in this field concentrates mainly on the numerous active ingredients and not on the excipients used. A collection of Raman spectra of pharmaceutical excipients is presented in this paper, which can serve as a reference for the interpretation of Raman spectra. The 43 analysed excipients can be classified in seven categories, namely: mono- and disaccharides (dextrose, lactitol, maltitol, lactose and sucrose), polysaccharides (microcrystalline cellulose, methylcellulose, carboxymethylcellulose, hydroxypropyl cellulose, hydroxypropyl methylcellulose, wheat starch, maltodextrin, primojel, tragacanth and pectin), polyalcohols (propylene glycol, erythritol, xylitol, mannitol and sorbitol), carboxylic acids and salts (alginic acid, glycine, magnesium stearate, sodium acetate, sodium benzoate), esters (arachis oil, lubritab, dibutyl sebacate, triacetin, eudragit E100 and RL100), inorganic compounds (calcium phosphate, talc, anatase and rutile (TiO₂), calcium carbonate, magnesium carbonate, sodium bicarbonate and calcium sulfate) and some unclassified products (gelatin, macrogol 4000 (PEG), polyvinyl pyrrolidone and sodium laurilsulfas).

8.1 Introduction

The most widely used spectroscopic techniques in pharmaceutical research include nuclear magnetic resonance (NMR) and mass spectrometry (MS)¹. Lately, Raman spectroscopy is becoming increasingly more accepted as a powerful tool in this field, mainly since this approach has some major benefits compared to the well established ones¹. When using Raman spectroscopy, no sample preparation is necessary, the microscope allows us to study very small particles (down to 1 μm) and it is even possible to measure through blister packages².

Raman spectroscopy has been used as an important research tool for different domains in the pharmaceutical world, quantitative as well as qualitative analysis³. In the past, this technique has been used for the identification of active ingredients and their different polymorphic crystalline forms^{4,5,6}.

Another domain is the production of pharmaceuticals where this technique can be used for process monitoring during the manufacturing of pharmaceuticals or as a quality control method^{7, 8}. Raman spectroscopy can also be used for the identification of counterfeit drugs, as has been shown by the identification of counterfeit antimalarial⁹ and Viagra[®] tablets¹⁰.

The majority of the articles in pharmaceutical research focuses on active ingredients but hardly pay any attention to the excipients present in these drugs. Pharmaceutical dosage forms contain both active ingredient(s) and excipients added to aid the formulation and manufacture of the subsequent dosage form¹¹.

In general, different types of application of excipients can be distinguished, such as diluents, binders, lubricants, disintegrants, colours and sweeteners¹¹. Diluents are added to increase the size of the tablet or the amount of powder present in a capsule. Binders are added to improve the cohesiveness of

powders in order for the powder to form granulates which are necessary to form tablets. To reduce the friction between the granulation and the wall during compression and ejection of the tablets, lubricants are added. Disintegrants are added to facilitate the break-up of tablets after administration while colours and sweeteners are added to improve the look appearance and the taste of the drug¹¹.

There are many active ingredients on the market, especially compared to the number of excipients which have hardly changed over the last years¹. Databases of pharmaceutical ingredients are commercially available but the downside of these databases is that they are generally relatively expensive and that they are usually not always available for Raman spectroscopy combined with a diode laser.

Additionally, these databases usually only show the Raman spectrum of the excipient and do not include any interpretation of the Raman bands and/or references for the excipient. In this paper, we study the Raman spectra of the most commonly used excipients in pharmaceutical preparations. These spectra can serve as a reference to simplify the interpretation of Raman spectra of different drug formulations.

8.2 Experimental

Raman analyses were carried out with a Renishaw System-1000 spectrometer (Wotton-under-Edge, UK) connected to an Olympus BH-2 microscope with a 5x objective lens (Olympus MDPlan5, 0.10 NA, Omnilabo, Aartselaar, Belgium). The diode laser of 785 nm has a power of 50 mW at the source (DL 100, TuiOptics GmbH, Martinsried/Munich, Germany). The collected Raman radiation was dispersed with a 1200 lines mm⁻¹ grating (focal length 250 mm) and focussed on a Peltier-cooled CCD detector allowing to obtain a spectral resolution of ca. 1 cm⁻¹. All spectra were recorded in the spectral window of 200 to 1800 cm⁻¹.

The analysis time and number of accumulations to obtain a well-resolved Raman spectrum vary, depending on the excipient. An average of 3 Raman spectra per excipient were used for the database in order to check sample homogeneity.

For display, spikes were removed and a manual baseline correction was performed by using ACD/Specmanager (version 9.13, Advanced Chemistry Development, inc. Toronto, Canada). The Raman bands were assigned with the use of ACD/Specmanager and the Raman intensities are described as weak (w), medium (m), strong (s) and very strong (vs).

The 43 excipients analysed for this database are listed in table I, including the supplier and the function of this excipient in the pharmaceutical process. The figure in which the specific excipient is presented is also mentioned. These 43 excipients were selected based on their presence in articles about pharmaceuticals.

8.3 Results and Discussion

Table 8.1 gives an overview of the excipients that were used in this study, their suppliers and their main use. However, often one excipient can have different uses in drug formulation. For instance, maltodextrin can be added as a coating agent but can also be added as a tablet and capsule diluent.

Therefore, in this paper, we preferred to classify the excipients according to their chemical composition. The following classification was used: 1) mono- and disaccharides, 2) polysaccharides, 3) polyalcohols, 4) carboxylic acids and salts, 5) esters, 6) inorganic substances and 7) others.

Name	Company	Functional category¹	Fig.
Dextrose	Vel	Tablet and capsule diluent, therapeutic agent	1a
Lactitol	Danisco	Sweetening agent, tablet and capsule diluent	1b
Maltitol	Roquette	Coating agent, diluent	1c
Lactose	DMV International	Binding agent, directly compressible tableting excipient	1d
Sucrose	Merck	Coating agent, granulating agent	1e
Microcrystalline cellulose	Sigma-Aldrich	Absorbent, suspending agent	2a
Methylcellulose	Fluka	Coating agent, emulsifying agent	2b
Carboxymethylcellulose	Sigma-Aldrich	Stabilizing agent, suspending agent	2c
Hydroxypropyl cellulose	Klucel	Coating agent, emulsifying agent	2d
Hydroxypropyl methylcellulose	Shin-Etsu	Suspending agent, viscosity-increasing agent	2e
Wheat starch	Alpha Pharma	Glidant, tablet and capsule diluent	3a
Maltodextrin	Roquette	Coating agent, tablet and capsule diluent	3b
Primojel	Avebe	Tablet and capsule disintegrant	3c
Tragacanth	Sigma-Aldrich	Suspending agent, viscosity-increasing agent	3d
Pectin	Federa	Absorbent, emulsifying agent	3e
Propylene glycol	Merck	Antimicrobial preservative, disinfectant	4a
Erythritol	Cerestar	Sweetening agent, tablet and capsule diluent	4b
Xylitol	Roquette	Antimicrobial preservative, coating agent	4c
Mannitol	Cerestar	Diluent, sweetening agent	4d
Sorbitol	Cerestar	Humectant, plasticizer	4e
Alginic acid	Sigma-Aldrich	Stabilizing agent, suspending agent	5a
Glycine	Acros	bulking agent in freeze-dried formulations ²	5b
Magnesium stearate	Sigma-Aldrich	Tablet and capsule lubricant	5c
Sodium acetate	Federa	Antimicrobial preservative, buffering agent	5d
Sodium benzoate	Sigma-Aldrich	Antimicrobial preservative, tablet and capsule lubricant	5e
Arachis oil	Delhaize	Oleaginous vehicle, solvent	6a
Lubritab	Mendell	Tablet and capsule lubricant, tablet binder	6b
Dibutyl sebacate	BASF	Plasticizer	6c
Triacetin	Sigma-Aldrich	Humectant, plasticizer	6d
Eudragit E 100	Rohm Pharma	Film former, tablet binder	6e
Eudragit RL 100	Rohm Pharma	Film former, tablet binder	6f
Calcium phosphate	Sigma-Aldrich	Tablet and capsule diluent	7a
Talc	Pleuger	Anticaking agent, glidant	7b
Anatase (TiO ₂)	Sennlier Paris	Coating agent, pigment	7c
Rutile (TiO ₂)	UCB	Coating agent, pigment	7d
Calcium carbonate	Merck	Buffering agent, coating agent	8a
Magnesium carbonate	Riedel-de-Haen	Absorbent, antacid	8b
Sodium bicarbonate	RPL	Alkalisng agent, therapeutic agent	8c
Calcium sulfate	Fluka	Tablet and capsule diluent	8d
Gelatin	Merck	Coating agent, film-former	9a
Macrogol 4000	Fagron	Ointment base, plasticizer	9b
Polyvinyl pyrrolidone	Sigma-Aldrich	Disintegrants, dissolution aid	9c
Sodium lauryl sulfate	Alpha Pharma	Anionic surfactant, detergent	9d

Table 8.1 Suppliers of the 43 excipients and functional categories of each excipient.

8.3.1 Mono- and disaccharides

The first group of excipients consists of mono- and disaccharides (structures are given in the appendix), namely: dextrose, lactitol, maltitol, lactose, and sucrose. Dextrose is commonly used as a sweetening agent, but is also used as a direct-compression tablet diluent and binder, primarily in chewable tablets¹¹. Another sweetener used in pharmaceutical preparations is lactitol, 4-*O*- β -D-galactopyranosyl-D-glucitol, which can also be used as a diluent in solid dosage forms^{11,12}. Maltitol is a disaccharide consisting of a glucose unit linked with a sorbitol unit¹¹ while lactose consists of galactose and glucose. Lactose is a natural disaccharide which exists as two anomeric forms, α and β , which are normally handled as the monohydrate and the anhydrous material, respectively. In the pharmaceutical industry, lactose is widely used as a filler or diluent in capsules and tablets¹³. Maltitol is made from maltose and it is almost as sweet as sucrose and can therefore be used as its replacement. Sucrose is obtained from sugar cane, sugar beet or other sources and is widely used in oral pharmaceutical formulations.

The spectra of the three monomers (dextrose, lactitol and maltitol) and the two dimers (lactose and sucrose) are highly similar as can be seen in figure 8.1. The Raman spectra can be distinguished^{14,15,16} from each other, based on the $\delta(\text{CC})$ and $\delta(\text{CO})$ bending vibrations in the region, between 800 and 900 cm^{-1} . Differences between the spectra can also be seen in the regions between 730 and 960 cm^{-1} and between 1200 and 1460 cm^{-1} which contain $\delta(\text{CH})$ deformations and in the region between 1430 and 1480 cm^{-1} (plus Raman bands around 830 cm^{-1}) which contain $\delta(\text{CH}_2)$ deformations^{13,15}. Since these monomers and dimers lack any C=O or C=C bonds in their structure (see paragraph 8.5), there are no Raman bands present above 1500 cm^{-1} . When comparing the Raman spectra of the monomers (dextrose (fig. 8.1A), lactitol (fig. 8.1B) and maltitol (fig. 8.1C)) with dimers (lactose (fig. 8.1D) and sucrose (fig. 8.1E)), it can be noted that Raman bands of the dimers are much broader than those of the monomers¹¹.

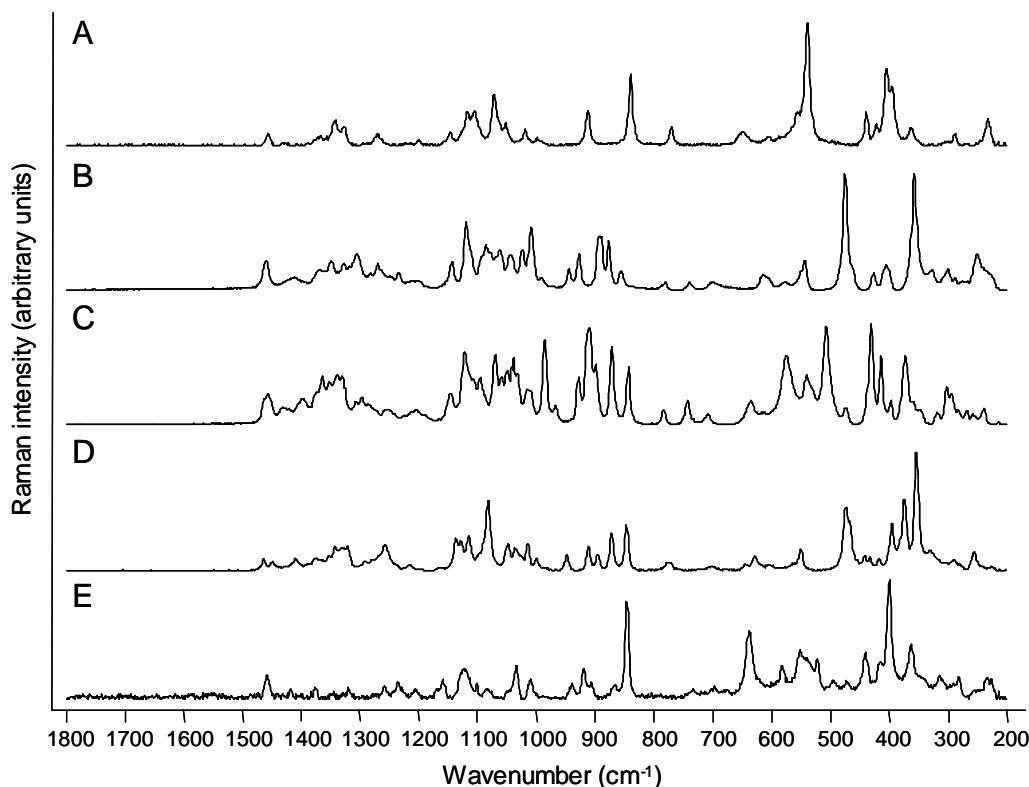


Figure 8.1 Raman spectra of mono- and disaccharides with the Renishaw System-1000 spectrometer, A: dextrose (3 acc. x 30 s), B: lactitol (5 acc. x 120 s), C: maltitol (5 acc. x 60 s), D: lactose (5 acc. x 120 s) and E: sucrose (20 acc. x 30 s).

8.3.2 Polysaccharides

Raman spectra of 10 polysaccharides are presented in figures 8.2 and 8.3. Polysaccharides are mainly used in tablet formulations as a binder (microcrystalline cellulose, methylcellulose (MC), carboxymethylcellulose (CMC), hydroxypropyl cellulose (HPC), hydroxypropyl methylcellulose (HPMC), starch and maltodextrin), diluent (microcrystalline cellulose, carboxymethylcellulose (CMC), starch and maltodextrin) and disintegrant (carboxymethylcellulose (CMC), starch and primojel) in both direct-compression and wet-granulation¹¹. The function of two polysaccharides (tragacanth and pectin) is different from the rest of this group. Pectin is not only used as a binding agent, but predominately as part of controlled-release matrix tablet formulations¹⁷. Finally, tragacanth gum is used as an emulsifying and suspending agent in a variety of pharmaceutical formulations, such as creams, gels and emulsions¹¹.

Figure 8.2 represents the Raman spectra of excipients that consist of cellulose while figure 8.3 contains spectra of the other polysaccharides.

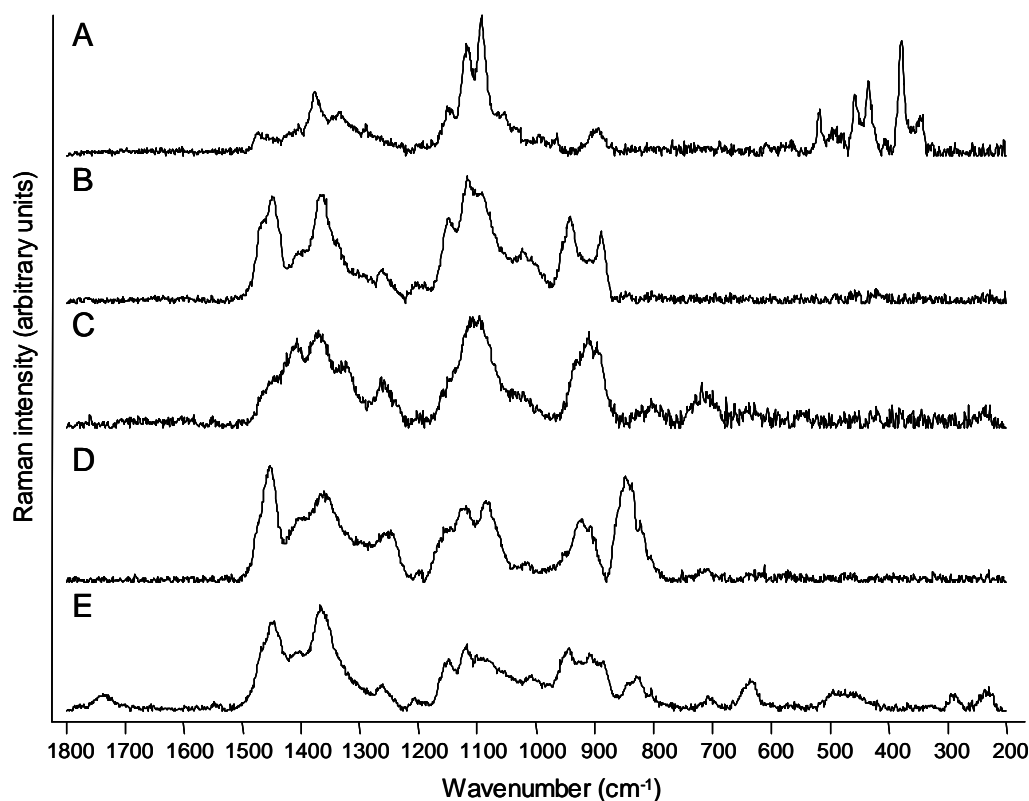


Figure 8.2 Raman spectra of polysaccharides with the Renishaw System-1000 spectrometer, A: microcrystalline cellulose (10 acc. x 30 s), B: methylcellulose (15 acc. x 60 s), C: carboxymethylcellulose (15 acc. x 60 s), D: hydroxypropyl cellulose (15 acc. x 60 s), E: hydroxypropyl methylcellulose (15 acc. x 60 s).

The general appearance of the Raman spectra of the polysaccharides is quite similar in the region between 850 and 1500 cm^{-1} , where $\nu(\text{C-O})$ and $\nu(\text{C-C})$ stretching vibrations and $\delta(\text{CH}_2)$ deformations^{20,21,22,23,24} can be observed. However, in the Raman spectra of microcrystalline cellulose (fig. 8.2A) an additional Raman band at 1093 cm^{-1} is present, which is characteristic of unsubstituted cellulose rings²⁰. In the region between 300 and 700 cm^{-1} , there are clear differences between the Raman spectra of the polysaccharides and based on these Raman bands, the spectra can be distinguished from each other. For instance, microcrystalline cellulose (fig. 8.2A) has additional bands between 380 and 460 cm^{-1} which can be assigned to $\delta(\text{CCC})$, $\delta(\text{CO})$, $\delta(\text{CCO})$ bending vibrations and ring deformations¹⁸.

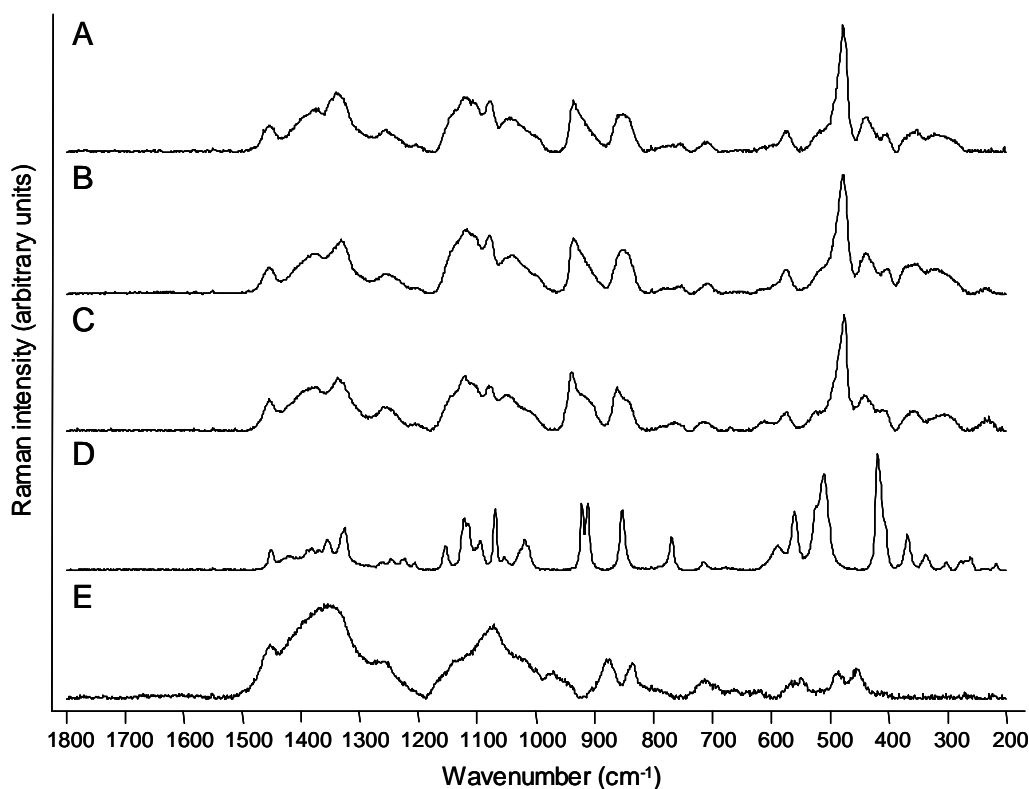


Figure 8.3 Raman spectra of polysaccharides with the Renishaw System-1000 spectrometer, A: wheat starch (15 acc. x 60 s), B: maltodextrin (20 acc. x 60 s), C: primojel (20 acc. x 30 s), D: tragacanth (30 acc. x 30 s), E: pectin (15 acc. x 60 s).

The strong Raman band around 477 cm^{-1} , which can be assigned to the $\nu(\text{CC})$ backbone stretch¹⁹, is characteristic for substances that contain starches (fig. 8.3A, 8.3B and 8.3C). For starch only the Raman spectrum of wheat starch (fig. 8.3a) is presented since this spectrum was similar to that of pure amylose and different starches (rice, corn and potato). Maltodextrin (fig. 8.2B) has two additional bands at 452 and 487 cm^{-1} which probably arise from the $\delta(\text{C-C=O})$ deformations¹⁴.

The Raman spectra of HPC (fig. 8.2D) and HPMC (fig. 8.2E) are highly similar, although there are some differences between the two spectra: mainly the relative intensities of Raman bands are different. For instance, when comparing the intensity of $\delta(\text{CH}_2)$ deformations at ca. 1360 cm^{-1} relative to the band at ca. 1450 cm^{-1} it shows a increase when HPC is compared to HPMC²⁰, which is consistent with the higher number of $-\text{CH}_3$ groups in HPMC.

Tragacanth is a gum which has different characteristics in the Raman spectrum (fig. 8.3D) compared to the other polysaccharides. The bands below 400 cm^{-1} can be assigned to the skeletal breathing modes, bands near 500 cm^{-1} are due to the ring deformations, while the strong features between 800 and 1100 cm^{-1} and at ca. 1400 cm^{-1} are characteristic for sugars²⁵.

8.3.3 Polyalcohols

The spectra of five polyalcohols are shown in figure 8.4. These polyols are commonly added to foods because of their sweet taste and lower caloric content compared to sugar. Erythritol, xylitol, sorbitol and mannitol are mainly used as diluents in for instance, chewable tablets¹¹. Propylene glycol is widely used as solvent and preservative in pharmaceutical formulations. It is also commonly used as plasticizer in aqueous film-coating formulations¹¹.

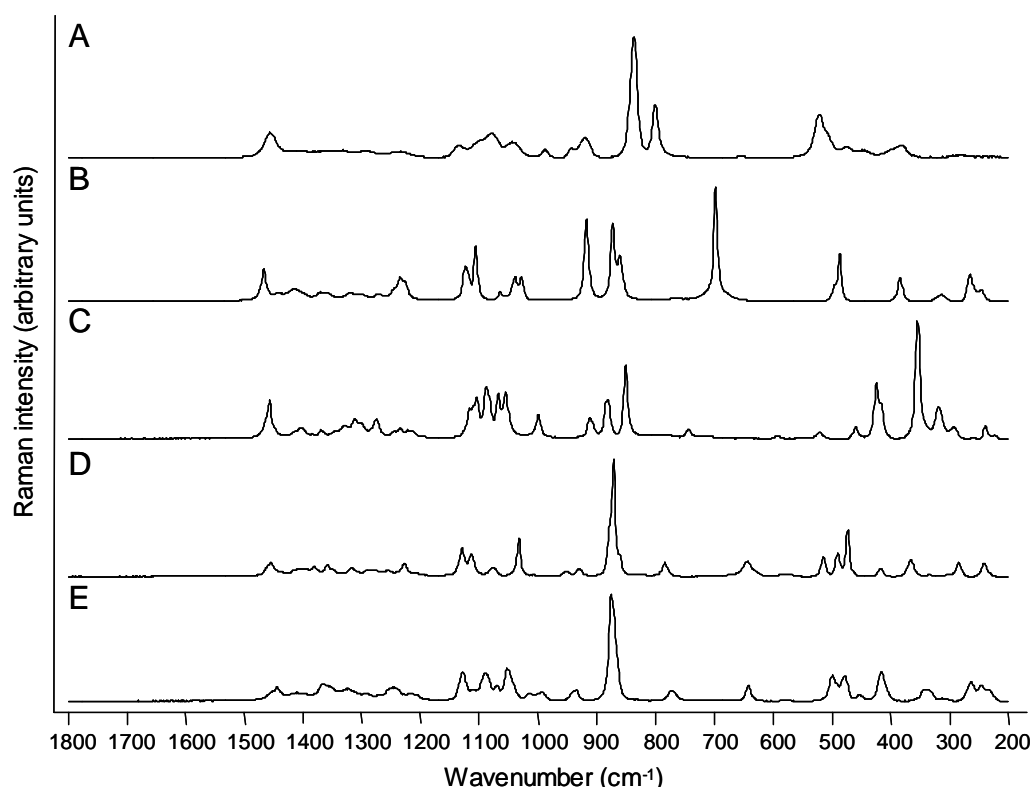


Figure 8.4 Raman spectra of polyalcohols with the Renishaw System-1000 spectrometer, A: propylene glycol (5 acc. x 30 s), B: erythritol (5 acc. x 120 s), C: xylitol (5 acc. x 60 s), D: mannitol (5 acc. x 120 s), E: sorbitol (5 acc. x 60 s).

There is little information available on the Raman spectra of polyalcohols, except for the quantitative analysis of mannitol polymorphs by Roberts et al²⁶ and the mapping of amorphous sorbitol by Ward et al²⁷.

Characteristic for these polyols are the strong Raman band between 430 and 500 cm^{-1} , bands between 800 and 900 cm^{-1} and a group of Raman bands in the region between 1000 and 1150 cm^{-1} , which are due to the $\delta(\text{CCO})$ bending vibration, the in-phase $\nu(\text{CCO})$ stretching vibration and the out-of-phase $\nu(\text{CCO})$ stretching vibration, respectively^{25,28}. The Raman band position of the $\nu(\text{CCO})$ stretching vibration increases with increasing chain length and number of OH groups (paragraph 8.5): the band at 838 cm^{-1} in the spectrum of propylene glycol, shifts to 851 cm^{-1} for xylitol, 872 cm^{-1} for mannitol and 878 cm^{-1} for sorbitol.

Since mannitol is isomeric with sorbitol, their Raman spectra appear to be similar, except for small differences in Raman bandwidth or shifts of Raman bands. For instance, the $\delta(\text{CCO})$ bending vibration for sorbitol consists of a single band (454 cm^{-1}) and a doublet (478 and 499 cm^{-1}) while this vibration consists of a triplet for mannitol (473, 490 and 515 cm^{-1}). Another difference between mannitol and sorbitol is the out-of-phase $\nu(\text{CCO})$ stretching vibration which shifts from 1034 cm^{-1} (mannitol) to 1054 cm^{-1} (sorbitol).

8.3.4 Carboxylic acids and salts

Figure 8.5 shows the Raman spectra of alginic acid, glycine, magnesium stearate, sodium acetate and sodium benzoate. In tablet and capsule formulations, alginic acid is used, both as binder and as a disintegrant agent but is also used as thickening agent in a variety of pastes, creams and gels¹¹. There are three polymorphic forms of anhydrous glycine, namely α -, β - and γ -glycine. When cooling aqueous glycine solutions, it results in the crystallization of β -glycine. Glycine is commonly used as bulking agent in freeze-dried formulations²⁹. Magnesium stearate is a very fine, white powder which is primarily used as a lubricant in capsule and tablet manufacturing.

The last two substances of this group are sodium acetate and sodium benzoate, which are both used as antimicrobial preservative.

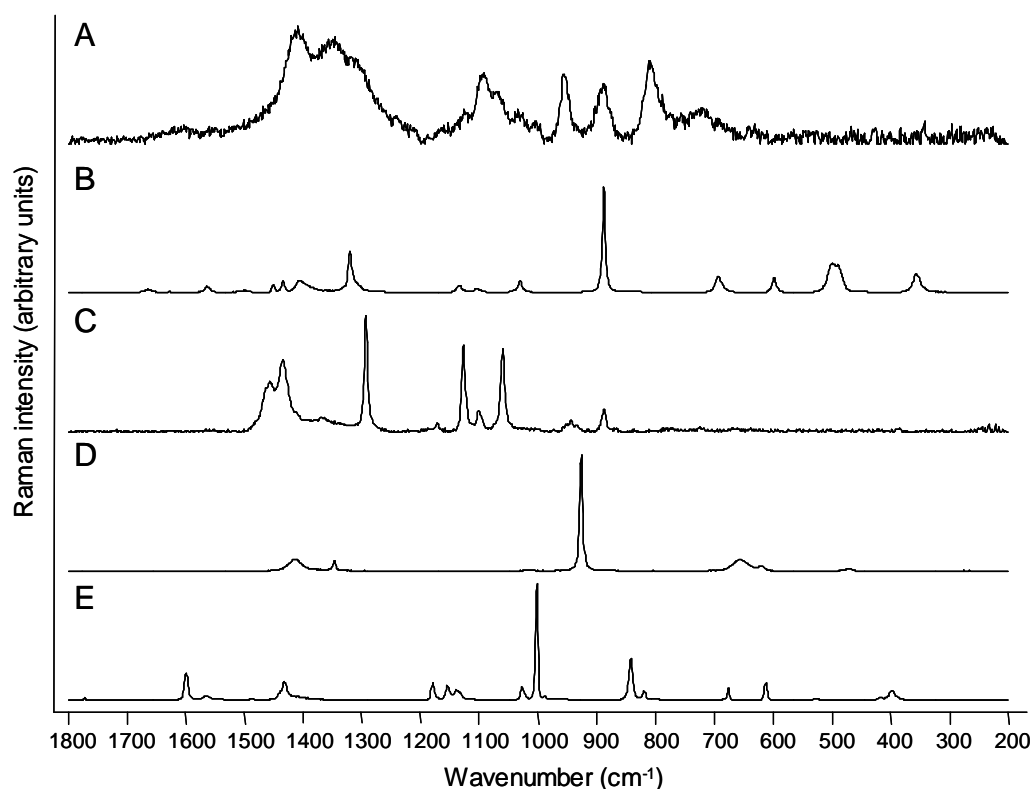


Figure 8.5 Raman spectra of carboxylic acids and salts with the Renishaw System-1000 spectrometer, A: alginic acid (15 acc. x 60 s), B: glycine (15 acc. x 30 s), C: magnesium stearate (5 acc. x 50 s), D: sodium acetate (5 acc. x 30 s), E: sodium benzoate (10 acc. x 30 s).

The first Raman spectrum is of alginic acid (fig. 8.5A) which shows three Raman bands between 810 and 960 cm^{-1} , which can be assigned to a combination of $\nu(\text{CO})$ ring breathing, $\nu(\text{CC})$ stretch and $\nu(\text{COC})$ ring vibrations. Furthermore, the $\delta(\text{CH})$ deformations cause multiple broad bands in the region between 1300 and 1450 cm^{-1} .

The spectra of glycine, magnesium stearate, sodium acetate en sodium benzoate have several strong Raman bands, including $\nu(\text{CC})$ stretching vibrations. These give rise to strong Raman band(s) at 890 cm^{-1} for glycine³⁰, two Raman bands at 1060 and 1128 cm^{-1} for magnesium stearate³¹, at 928 cm^{-1} for sodium acetate³² and finally at 1434 cm^{-1} for sodium benzoate³³.

For glycine, magnesium stearate and sodium acetate the $\delta(\text{CH}_2)$ and respectively $\delta(\text{CH}_3)$, are found between 1400 and 1460 cm^{-1} ^{30,31,32}. The spectrum of sodium benzoate shows an additional strong Raman band at 1003 cm^{-1} which can be assigned to ring breathing of the benzene ring.

8.3.5 Esters

In total, 6 excipients were used for the database with an ester structure. The first excipient is peanut oil (arachis oil), which is mainly used as a solvent for intramuscular injections¹¹. The second oil in this group is lubritab which is a hydrogenated vegetable oil consisting of a mixture of triglycerides of fatty acids and is used as a lubricant in tablet and capsule formulations¹¹. The four other excipients (dibutyl sebacate, triacetin, Eudragit E100 and RL 100) are used in pharmaceutical preparations as film coating agents of capsules, tablets, beads or granules. The applications of these coating agents are different from each other, for instance Eudragit E100 is used as a film former and is soluble in gastric fluid while RL 100 is used to form water-insoluble film coatings for sustained-release products¹¹.

The spectra of these six esters are shown in figure 8.6. In the lower region at ca. 600 cm^{-1} the Raman spectra of triacetin and Eudragit (E100 and RL100) show an intense Raman band. This band in the spectrum of triacetin can be assigned to $\delta(\text{CO})$ deformation^{14,28} while this band in the spectra of Eudragit is due to the $\nu(\text{CN})$ stretching vibration^{14,28}.

The spectra all show Raman bands assigned to the $\nu(\text{CC})$ stretching vibration between 800 and 900 cm^{-1} . Triacetin also has an additional band at 890 cm^{-1} due to the $\nu(\text{COC})$ symmetric stretch^{14,28}. The $\nu(\text{C-CO-C})$ vibration can be seen in the spectrum of dibutyl sebacate in between 800 and 900 cm^{-1} and between 1000 and 1150 cm^{-1} : symmetric and asymmetric stretching vibrations, respectively^{14,28}.

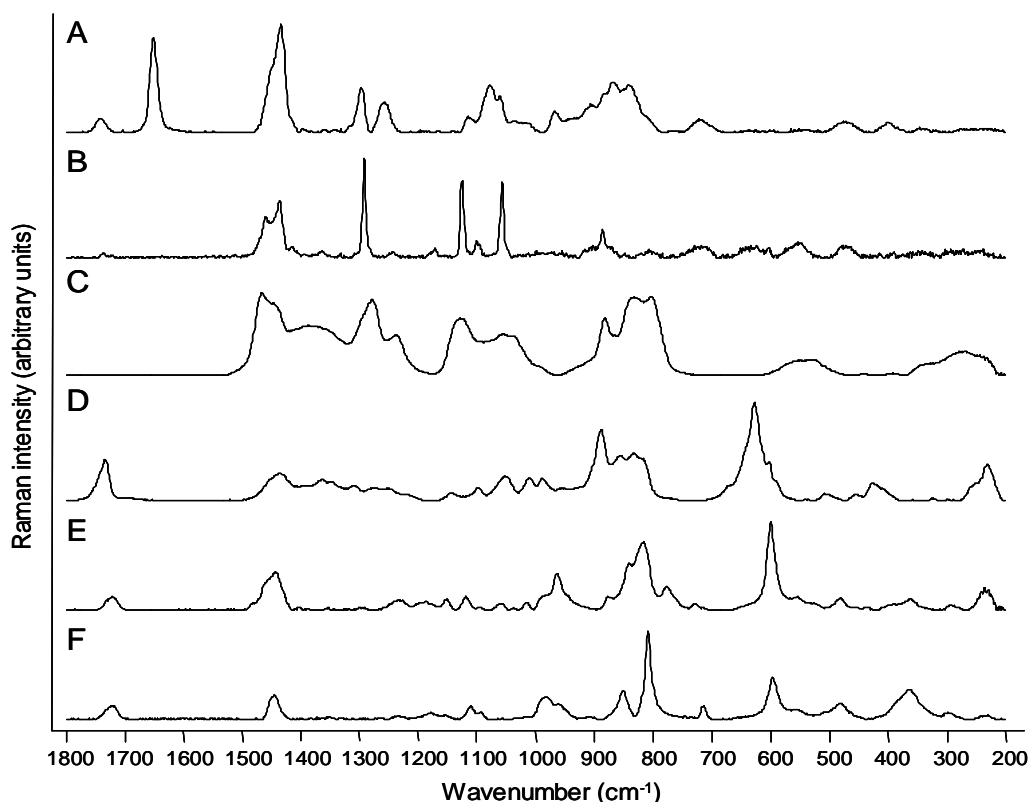


Figure 8.6 Raman spectra of esters with the Renishaw System-1000 spectrometer, A: arachis oil (20 acc. x 60 s), B: lubritab (15 acc. x 60 s), C: dibutyl sebacate (20 acc. x 30 s), D: triacetin (5 acc. x 30 s), E: eudragit E100 (20 acc. x 30 s) and F: eudragit RL100 (20 acc. x 30 s).

Since Eudragit E100 and Eudragit RL100 have a predominately similar chemical structure, the spectra will differ only slightly. Comparing the intensity of the $\nu(\text{CN})$ stretching vibration at ca. 600 cm^{-1} to the $\nu(\text{CC})$ stretching vibration at ca. 810 cm^{-1} , it shows that for Eudragit E100 the relative intensities are very similar, while Eudragit RL 100 shows a large difference between the intensity of these two Raman bands^{14,28}. In the Raman spectra of all 6 excipients, $\delta(\text{CH}_2)$ and $\delta(\text{CH}_3)$ deformations are observed in the region between 1400 and 1500 cm^{-1} ^{14,34,35}. Some differences can be noted between the spectra of these excipients in the region between 1600 and 1800 cm^{-1} . Arachis oil (fig. 8.6A), for instance, has a distinct intense Raman band at 1653 cm^{-1} , which can be assigned to the $\nu(\text{C}=\text{C})$ stretching vibration due to the oleic acid present in the oil²⁸. Arachis oil, triacetin and eudragit E100 and RL100 also contains a Raman band at ca. 1730 cm^{-1} that can be assigned to the $\nu(\text{C}=\text{O})$ stretching vibration which is typical for esters^{14,24}.

8.3.6 Inorganic substances

In figures 8.7 and 8.8 the Raman spectra of 8 inorganic substances are shown. Half of these organic substances (calcium phosphate, calcium- and magnesium carbonate and calcium sulfate) are used as diluents in pharmaceutical preparations, mainly in solid-dosage forms¹¹. Sodium bicarbonate is widely used to produce or maintain an alkaline pH in a preparation¹¹. Talc was once widely used in oral solid dosage formulations as a lubricant and diluent; however, today it is less commonly used¹¹. Titanium dioxide can occur in three distinct polymorphs: rutile, anatase and brookite³⁶ but only rutile and anatase are used in pharmaceutical formulations as a whitener. Rutile is used more frequently than anatase since most production techniques yield TiO₂ in the rutile phase^{11,36}.

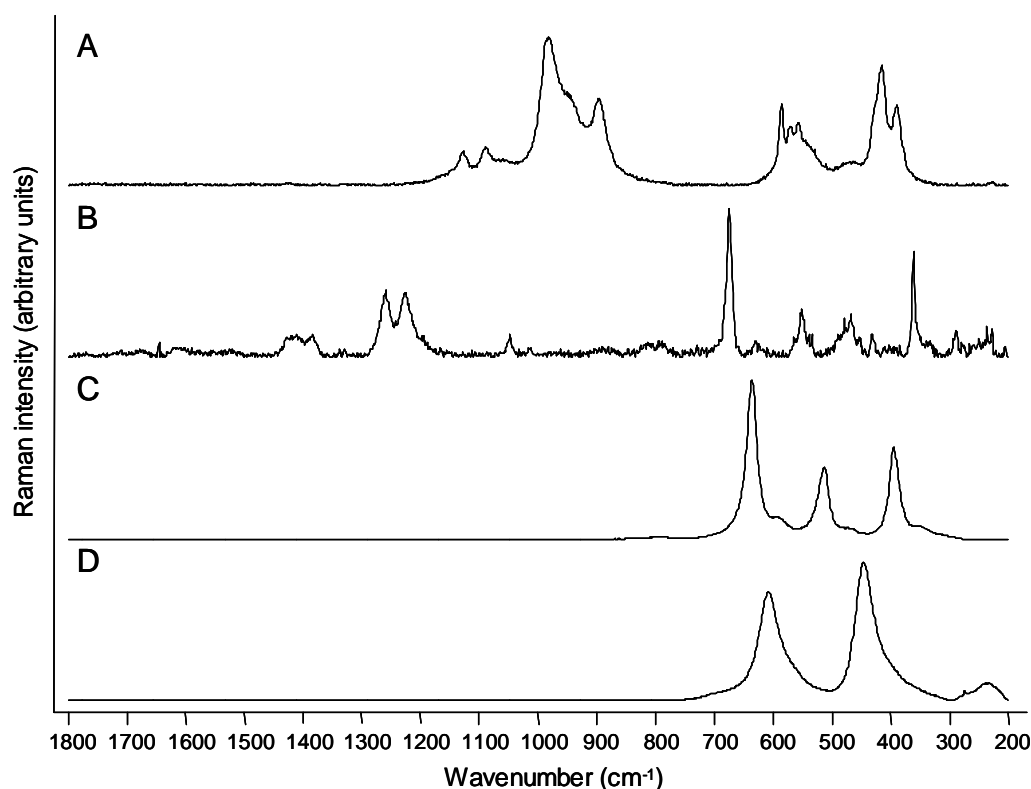


Figure 8.7 Raman spectra of inorganic substances with the Renishaw System-1000 spectrometer, A: calcium phosphate (5 acc. x 30 s), B: talc (50 acc. x 60 s), C: anatase (TiO₂, 1 acc. x 30 s) and D: rutile (TiO₂, 1 acc. x 30 s).

The Raman spectra of these inorganic substances (fig. 8.7 and 8.8) show a few strong Raman bands, which are due to the fact that these substances only have a few vibration modes. The first spectrum shown is the Raman spectrum of calcium phosphate ($\text{Ca}_3(\text{PO}_4)_2$) and has several intense Raman bands. The two Raman bands around ca. 400 cm^{-1} can be assigned to $\delta(\text{PO})$ deformations while the two bands at 896 and 983 cm^{-1} are due to the $\nu(\text{PO})$ stretching vibration³⁷. The second spectrum of talc ($3\text{ MgO} \cdot 4\text{ SiO}_2 \cdot \text{H}_2\text{O}$) in figure 8.7 has two distinguished Raman bands at 361 cm^{-1} and 675 cm^{-1} which can be assigned to the asymmetric and symmetric $\nu(\text{SiO}_4)$ stretching vibrations, respectively³⁸. The last two spectra in figure 8.7 are from two different forms of TiO_2 namely anatase (fig. 8.7C) and rutile (fig. 8.7D). Both excipients are used as a whitener in coatings of pharmaceuticals but can easily be distinguished by their Raman spectra, as has been described by Rigby et al³⁹. The Raman bands are caused by the $\delta(\text{TiO}_2)$ bending vibration (636 cm^{-1} for anatase and 446 cm^{-1} for rutile) and the symmetric $\nu(\text{TiO}_2)$ stretching vibration (513 cm^{-1} for anatase and 609 cm^{-1} for rutile)³⁹.

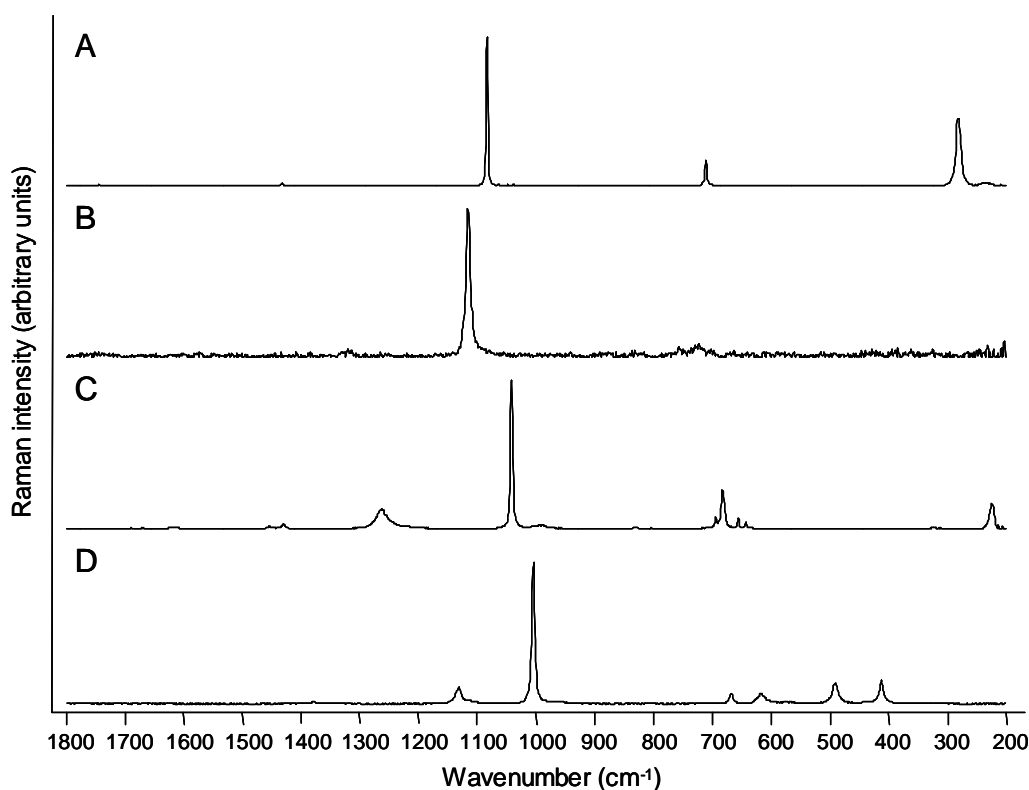


Figure 8.8 Raman spectra of inorganic substances with the Renishaw System-1000 spectrometer, A: calcium carbonate (1 acc. x 30 s), B: magnesium carbonate (3 acc. x 30 s), C: sodium bicarbonate (10 acc. x 30 s) and D: calcium sulfate (20 acc. x 30 s).

The inorganic substances, calcium carbonate (CaCO_3), magnesium carbonate (MgCO_3), sodium bicarbonate (NaHCO_3) and calcium sulfate (CaSO_4), all have one or two intense Raman band(s). The first three spectra contain carbonate or a bicarbonate group. The Raman band between 600 and 700 cm^{-1} can be assigned to the ν_4 symmetric stretch while the intense Raman band between 1000 and 1100 cm^{-1} can be assigned to the ν_1 symmetric stretch^{28,40,41}.

8.3.7 Others

Figure 8.9 presents 4 excipients, which are also commonly used in pharmaceutical formulations. Gelatine is widely used in a variety of pharmaceutical formulations, although it is most frequently used to form either hard or soft gelatine capsules. These capsules are unit-dosage forms that are filled with an active drug and are generally designed for oral administration¹¹.

Macrogol is a polyethylene glycol (PEG) which is a polymer of ethylene oxide and water and exists with different molecular weights (200 till 6000 g/mol), for this database macrogol with a molecular mass of 4000 was used. These PEGs can be used as ointment base, suppository base, suspending agent or act as an emulsion stabilizer¹¹.

Another excipient that can be used in a variety of pharmaceutical formulations is povidone (polyvinylpyrrolidone, PVP), namely as binder, solubilizer, coating agent, suspending agent, stabilizing agent or as a viscosity-increasing agent¹¹.

Sodium lauryl sulfate (also known as dodecyl sodium sulfate) is an anionic surfactant which is applied in a wide range of pharmaceutical formulations. The spectra of these four substances are presented in figure 8.9.

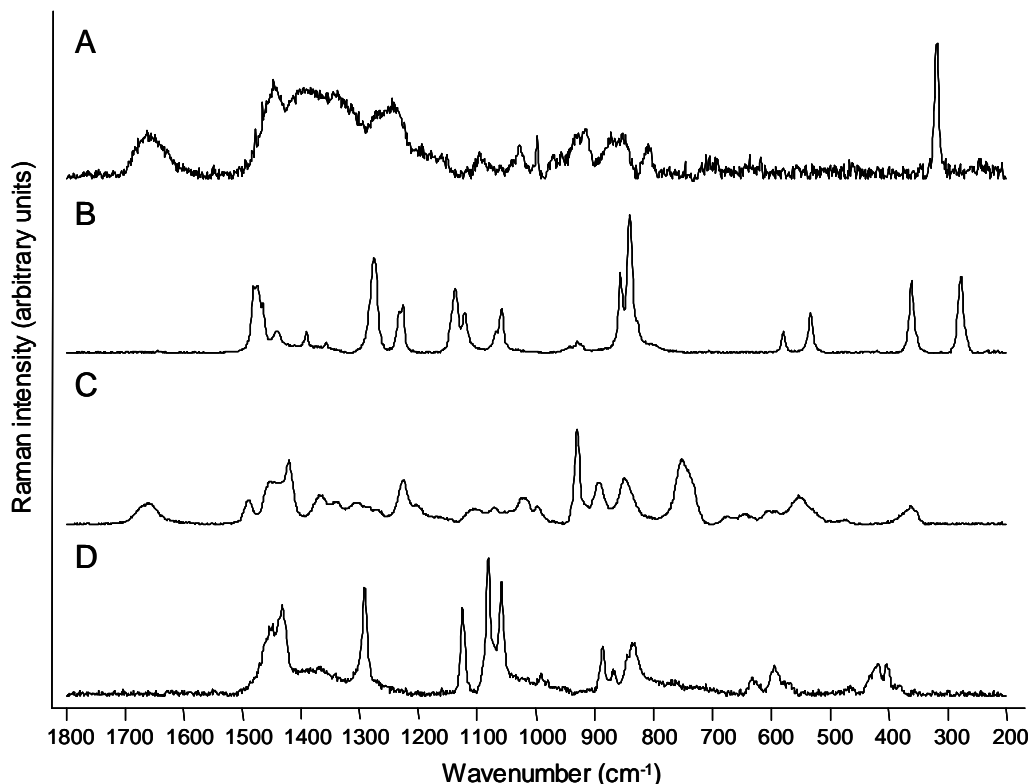


Figure 8.9 Raman spectra of other substances with the Renishaw System-1000 spectrometer, A: gelatin (40 acc. x 30 s), B: macrogel 4000 (10 acc. x 30 s), C: polyvinyl pyrrolidone (20 acc. x 30 s) and D: sodium laurilsulfate (10 acc. x 30 s).

In the spectrum of gelatine (fig. 8.9A) the Raman bands between 800 and 950 cm^{-1} can be assigned to the $\nu(\text{COC})$ stretching vibrations while the Raman bands between 1000 and 1100 cm^{-1} can be assigned to the $\delta(\text{CH}_2)$ deformations, $\nu(\text{CC})$ and $\nu(\text{CO})$ stretching vibrations. Two Raman bands at 1246 cm^{-1} and 1663 cm^{-1} can also be assigned to the amide III and the amide I bond, respectively^{24,42}.

Macrogol 4000 (fig. 8.9B) is a polyethylene glycol and this spectrum shows multiple strong Raman bands at 858 cm^{-1} , between 1050 and 1130 cm^{-1} and at 1444 cm^{-1} , which can be assigned to the symmetric $\nu(\text{COC})$ stretch, the $\nu(\text{CC})$ stretch and to $\delta(\text{CH})$ deformations, respectively³⁴. This product is a polymer and the Raman bands are rather broad²⁸. The distinct Raman band in the spectrum of polyvinyl pyrrolidone (fig. 8.9C) at ca. 1660 cm^{-1} is characteristic for the $\nu(\text{C=O})$ stretching vibrations, while the bands in the area

between 1400 and 1500 cm^{-1} can be assigned to $\nu(\text{CC})$ stretching vibrations and $\nu(\text{CN})$ in-plane vibrations. The ring vibration causes a very strong Raman band at 932 cm^{-1} with next to it two bands (850 and 892 cm^{-1}) due to the $\nu(\text{CNC})$ stretching modes¹⁴. The last excipient of this database is sodium lauryl sulfate which has intense Raman bands related to the $\nu(\text{CC})$ stretching vibration in the region between 1000 and 1150 cm^{-1} , a band at 1294 cm^{-1} related $\nu(\text{SO}_4)$ stretch and at 1433 cm^{-1} $\delta(\text{CH}_2)$ deformations²⁸.

8.4 Table with Raman bands of the 43 excipients

<i>Name</i>	<i>Raman bands (cm^{-1})</i>	<i>Acc. & Time¹</i>	<i>Fig.</i>
Dextrose	232(w), 288(w), 363(w), 396(m), 404(s), 422(w), 439(w), 539(vs), 653(w), 770(w), 841(m), 913(w), 1020(w), 1053(w), 1073(m), 1106(w), 1119(w), 1147(w), 1272(w), 1331(w), 1343(w), 1458(w)	3 x 30s	1a
Lactitol	249(m), 299(w), 327(w), 356(vs), 405(w), 426(w), 475(vs), 544(w), 614(w), 857(w), 878(m), 895(m), 929(m), 945(w), 1010(m), 1025(m), 1045(w), 1062(m), 1087(m), 1121(m), 1145(w), 1236(w), 1271(w)	5 x 120s	1b
Maltitol	239(w), 302(m), 318(w), 373(s), 397(w), 414(s), 431(vs), 474(w), 507(vs), 541(m), 574(s), 635(w), 709(w), 743(w), 784(w), 844(m), 872(s), 900(s), 910(vs), 929(m), 969(w), 986(s), 1017(m), 1039(s), 1071(s), 1097(m), 1123(s), 1147(m), 1206(w), 1251(w), 1298(w), 1332(m), 1340(m), 1365(m), 1399(w), 1433(w), 1458(m)	5 x 60s	1c
Lactose	256(w), 353(vs), 374(s), 395(m), 474(m), 551(w), 629(w), 847(m), 873(m), 912(w), 950(w), 1015(w), 1037(w), 1049(w), 1083(m), 1117(w), 1139(w), 1258(w), 1323(w), 1344(w), 1377(w)	5 x 120s	1d
Sucrose	283(w), 314(w), 363(m), 400(vs), 441(m), 473(w), 495(w), 523(m), 553(m), 582(w), 639(m), 847(s), 867(w), 908(w), 920(w), 940(w), 1011(w), 1035(w), 1102(w), 1122(w), 1160(w), 1237(w), 1259(w), 1460(w)	20 x 30s	1e
Microcrystalline cellulose	343(w), 378(s), 435(m), 457(m), 517(m), 894(w), 1093(vs), 1120(s), 1152(m), 1335(m), 1378(m), 1473(w)	10 x 30s	2a
Methylcellulose	890(m), 943(s), 1024(m), 1118(vs), 1149(s), 1265(w), 1363(s), 1450(s)	15 x 60s	2b
Carboxymethylcellulose	719(m), 804(w), 911(s), 1098(vs), 1265(m), 1325(s), 1372(s), 1408(s)	15 x 60s	2c

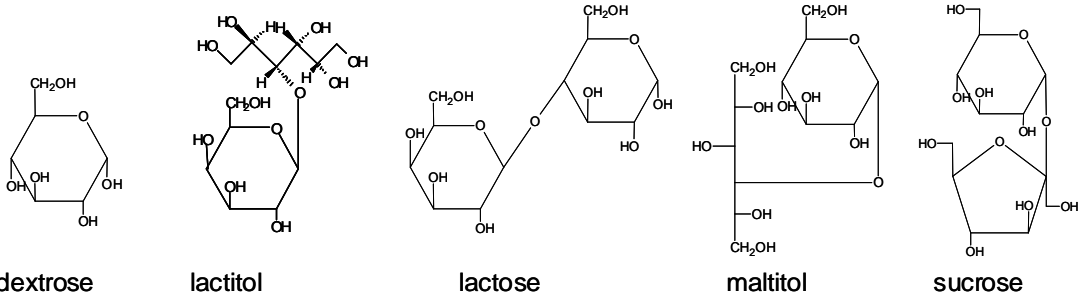
Hydroxypropyl cellulose	848(vs), 923(m), 1086(s), 1124(s), 1249(m), 1361(s), 1454(vs)	15 x 60s	2d
Hydroxypropyl methylcellulose	495(w), 637(w), 709(w), 829(m), 907(m), 944(m), 1008(m), 1119(s), 1152(m), 1208(w), 1263(w), 1366(vs), 1452(s), 1739(w)	15 x 60s	2e
Wheat starch	302(w), 359(w), 409(w), 439(w), 477(vs), 576(w), 867(w), 940(m), 1050(w), 1081(m), 1126(m), 1261(w), 1338(w), 1379(w), 1458(w)	15 x 60s	3a
Maltodextrin	319(w), 355(w), 402(w), 438(m), 477(vs), 575(w), 849(m), 938(m), 1040(m), 1079(m), 1119(m), 1259(w), 1333(m), 1381(m), 1456(w)	20 x 60s	3b
Primojel	229(w), 303(w), 355(w), 439(w), 476(vs), 574(w), 864(m), 940(m), 1053(m), 1077(m), 1122(m), 1260(w), 1339(m), 1378(m), 1456(w)	20 x 30s	3c
Tragacanth	260(w), 336(w), 368(m), 419(vs), 510(s), 561(m), 589(w), 770(w), 854(m), 913(m), 923(m), 1020(w), 1055(w), 1071(m), 1096(w), 1124(m), 1157(w), 1226(w), 1249(w), 1327(m), 1358(w), 1384(w), 1423(w), 1452(w)	30 x 30s	3d
Pectin	452(m), 487(w), 550(w), 719(w), 836(m), 876(m), 972(w), 1073(s), 1261(m), 1355(vs), 1454(m)	15 x 60s	3e
Propylene glycol	383(w), 522(m), 802(m), 838(vs), 921(w), 1045(w), 1079(w), 1457(w)	5 x 30s	4a
Erythritol	246(w), 265(w), 384(w), 487(m), 698(vs), 862(m), 874(s), 918(s), 1029(w), 1040(w), 1107(m), 1125(m), 1236(w), 1414(w), 1468(w)	5 x 120s	4b
Xylitol	238(w), 318(w), 353(vs), 424(m), 459(w), 851(s), 882(m), 913(w), 1000(w), 1056(m), 1069(m), 1089(m), 1105(m), 1276(w), 1313(w), 1330(w), 1459(m)	5 x 60s	4c
Mannitol	240(w), 284(w), 365(w), 473(m), 490(w), 515(w), 644(w), 784(w), 872(vs), 1034(m), 1114(w), 1130(w), 1228(w), 1360(w), 1456(w)	5 x 120 s	4d
Sorbitol	246(w), 263(w), 342(w), 415(w), 478(w), 499(w), 642(w), 773(w), 876(vs), 936(w), 1054(m), 1091(w), 1129(w), 1250(w), 1325(w), 1369(w), 1446(w)	5 x 60s	4e
Alginic acid	813(s), 890(m), 956(m), 1093(m), 1346(vs), 1409(vs)	15 x 60s	5a
Glycine	357(w), 500(w), 599(w), 695(w), 890(vs), 1032(w), 1322(m), 1406(w), 1436(w)	15 x 30s	5b
Magnesium stearate	888(w), 945(w), 1061(s), 1102(w), 1128(s), 1294(vs), 1437(s), 1458(m)	5 x 50s	5c
Sodium acetate	656(w), 928(vs), 1414(w)	5 x 30s	5d
Sodium benzoate	612(w), 676(w), 843(m), 1003(vs), 1028(w), 1156(w), 1180(w), 1434(w), 1601(w)	10 x 30s	5e

Arachis oil	401(w), 477(w), 722(w), 844(m), 867(m), 908(w), 968(w), 1061(m), 1079(m), 1117(w), 1261(m), 1298(m), 1436(vs), 1653(vs), 1743(w)	20 x 60s	6a
Lubritab	888(w), 1059(s), 1102(w), 1126(s), 1172(w), 1294(vs), 1415(w), 1438(m), 1461(m)	15 x 60s	6b
Dibutyl sebacate	275(w), 527(w), 804(vs), 837(vs), 883(s), 1057(m), 1130(s), 1239(m), 1280(vs), 1387(m), 1468(vs)	20 x 30s	6c
Triacetin	230(m), 425(w), 628(vs), 832(m), 858(m), 890(s), 991(w), 1013(w), 1053(w), 1098(w), 1312(w), 1366(w), 1437(w), 1736(m)	5 x 30s	6d
Eudragit E 100	234(w), 361(w), 482(w), 555(w), 601(vs), 778(w), 817(s), 878(w), 963(m), 1121(w), 1153(w), 1231(w), 1444(m), 1723(w)	20 x 30s	6e
Eudragit RL 100	362(m), 483(w), 552(w), 598(m), 715(m), 809(vs), 852(m), 962(w), 985(w), 1112(w), 1450(w), 1726(w)	20 x 30s	6f
Calcium phosphate	390(m), 416(s), 557(m), 571(m), 587(m), 896(m), 983(vs), 1090(w), 1128(w)	5 x 30s	7a
Talc	361(s), 466(w), 550(m), 675(vs), 1050(w), 1229(m), 1260(m), 1385(w), 1412(w)	50 x 60s	7b
Anatase (TiO ₂)	395(m), 513(m), 636(vs)	1 x 30s	7c
Rutile (TiO ₂)	234(w), 446(vs), 609(s)	1 x 30s	7d
Calcium carbonate	281(m), 711(w), 1084(vs)	1 x 30s	8a
Magnesium carbonate	1117(vs)	3 x 30s	8b
Sodium bicarbonate	224(w), 683(w), 1043(vs), 1264(w)	10 x 30s	8c
Calcium sulfate	1133 (w), 1005(vs)	20 x 30s	8d
Gelatin	318(vs), 809(w), 854(m), 915(m), 998(m), 1029(w), 1098(w), 1246(m), 1338(s), 1384(s), 1448(s), 1663(m)	40 x 30s	9a
Macrogol 4000	277(m), 360(m), 533(w), 579(w), 842(vs), 858(m), 1060(m), 1123(w), 1138(m), 1228(m), 1277(s), 1393(w), 1444(w), 1476(m)	10 x 30s	9b
Polyvinyl pyrrolidone	362(w), 553(m), 606(w), 645(w), 753(s), 850(m), 892(m), 932(vs), 999(w), 1022(w), 1073(w), 1109(w), 1225(m), 1272(w), 1307(w), 1340(w), 1369(m), 1423(s), 1454(m), 1490(w), 1662(w)	20 x 30s	9c
Sodium lauryl sulfate	404(w), 418(w), 595(w), 633(w), 833(m), 867(w), 887(m), 1060(s), 1082(vs), 1126(s), 1294(s), 1368(w), 1433(s), 1449(m)	10 x 30s	9d

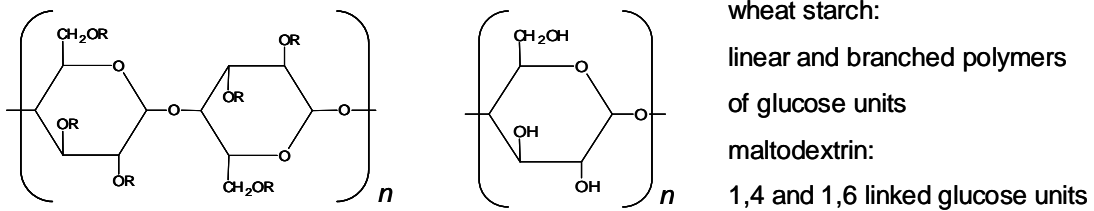
Table 8.2, Raman bands and intensities for each reference product (very weak bands are not listed). Abbreviations: w, weak; m, medium; s, strong; mw, medium weak; vs, very strong.

8.5 Chemical structures of the 43 excipients

mono- and disaccharides



polysaccharides



carboxymethylcellulose:

$R = H$ or CH_2COONa

microcrystalline cellulose:

$R = H$

methylcellulose:

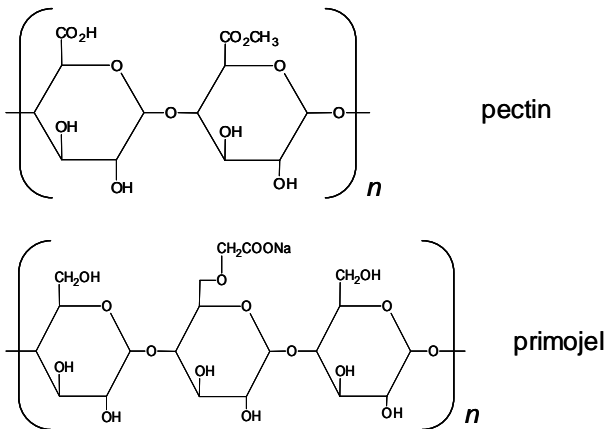
$R = H$ or CH_3

hydroxypropyl cellulose:

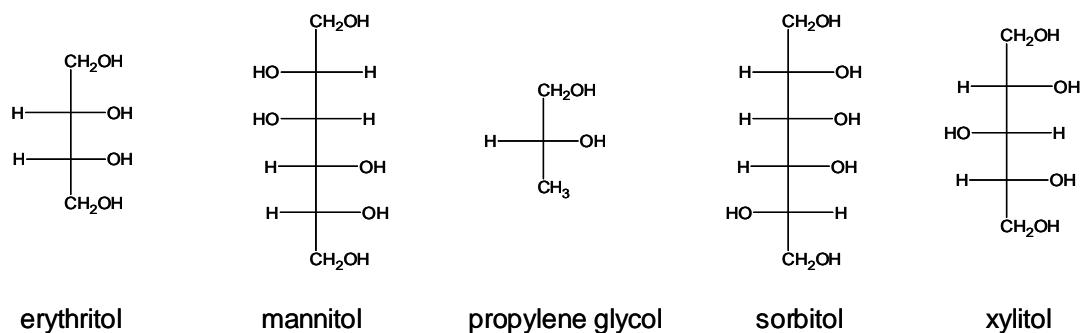
$R = H$ or $[CH_2CH(CH_3)O]_mH$

hydroxypropyl methylcellulose:

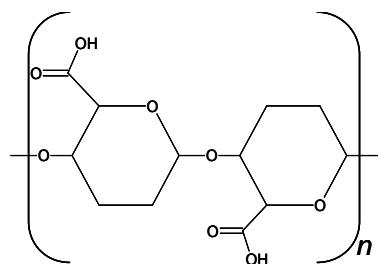
$R = H, CH_3$ or $[CH_2CH(CH_3)O]_mH$



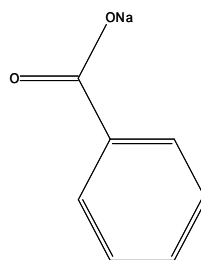
polyalcohols



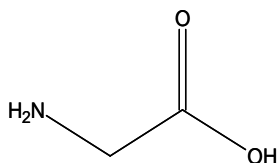
carboxylic acids and salts



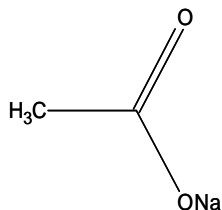
alginic acid



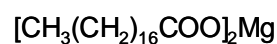
sodium benzoate



glycine

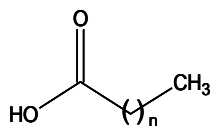


sodium acetate

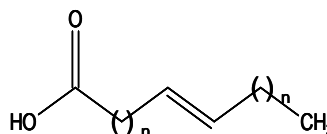


magnesium stearate

esters



n = 14: palmitic acid
n = 16: stearic acid
n = 18: arachidic acid



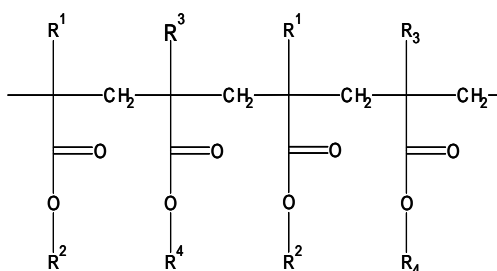
n = 7 oleic acid

arachis oil:

triglycerides with palmitic acid, oleic acid and arachidic acid

lubritab:

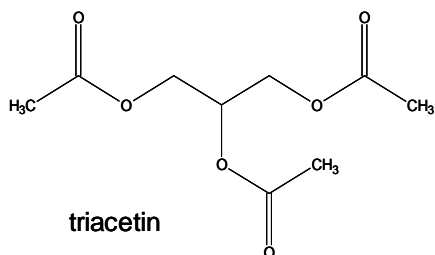
triglycerides with stearic acid and arachidic acid



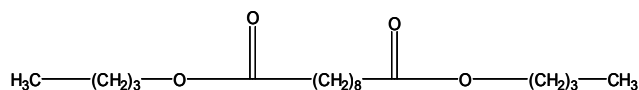
eudragit E 100:

R¹, R³ = CH₃R² = CH₂CH₂N(CH₃)₂R⁴ = CH₃, C₄H₉

eudragit RL 100:

R¹ = H, CH₃R² = CH₃, C₂H₅R³ = CH₃R⁴ = CH₂CH₂N(CH₃)₃⁺Cl⁻

triacetin

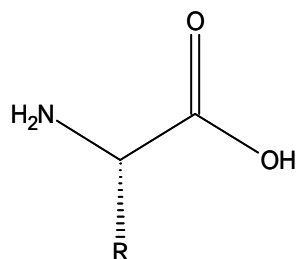


dibutylsebacate

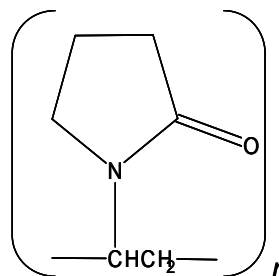
inorganic substances

talc:	$3 \text{ MgO} \cdot 4 \text{ SiO}_2 \cdot \text{H}_2\text{O}$	calcium sulphate:	CaSO_4
titanium dioxide:	TiO_2	magnesium carbonate:	MgCO_3
calcium carbonate:	CaCO_3	sodium bicarbonate:	NaHCO_3
calcium phosphate:	$\text{Ca}_3(\text{PO}_4)_2$		

others

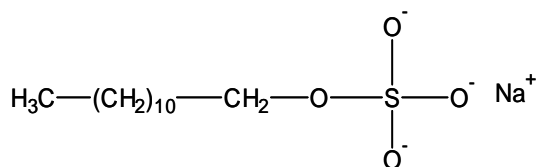


R = H glycine
R = CH₃ alanine
R = CH(CH₃)₂ leucine

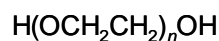


gelatin: glycine, alanine and leucine

polyvinyl pyrrolidone



sodium lauryl sulfate



macrogol 4000

8.6 Conclusion

In the field of pharmaceutical analysis, the focus is on the active ingredient and hardly any attention is paid to the excipients present. In this work, the Raman spectra of 43 commonly used excipients in pharmaceutical formulations are presented and Raman bands are identified (table 8.2). Since the excipients usually have several purposes in the pharmaceutical process, the excipients were divided based on their chemical structure into seven different groups. The recorded spectra of these excipients show clear differences and specific Raman bands and could be of help when an excipient needs to be identified. This database will also be of great help for the identification of excipients present in genuine and counterfeit drugs or for instance illicit drugs based on their Raman spectrum.

8.7 Notes on publication

This database shows the 43 most commonly used excipients present in pharmaceutical dosages. These Raman spectra can help with the detection of excipients present and lacking in counterfeit drugs as described in the three previous chapters. It has to be noted that identification of excipients should not be based on one single Raman band. Excipients often do present similar Raman bands, like for instance lactose (figure 8.1.D) and starch (figure 8.1.E) which both present a Raman band at 847 cm^{-1} . Based on this Raman band no conclusions can be formed whether lactose or starch is present in the drug. However, lactose shows a strong Raman band at 374 cm^{-1} while sucrose has a very strong Raman band at 400 cm^{-1} , which makes it possible to distinguish these two excipients. In order to make conclusions about the presence of an excipient in the drug, more Raman bands should be investigated.

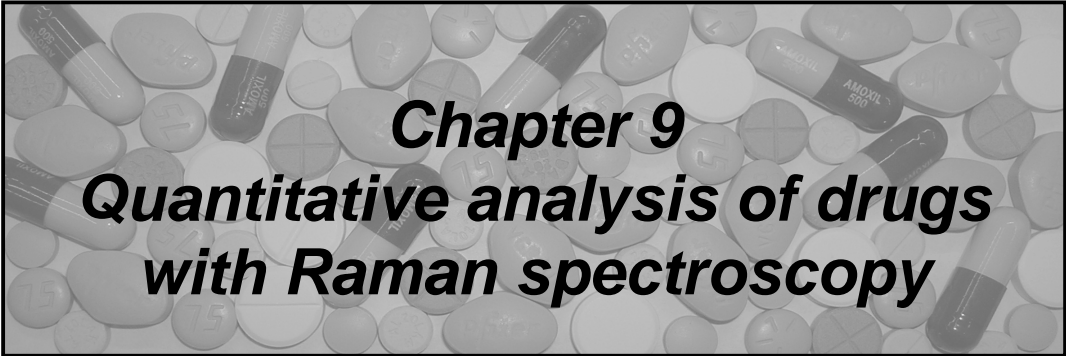
Chapter 8 and the three previous chapters are focusing on the qualitative analysis of counterfeit drugs. Since these counterfeiters are becoming more sophisticated, quantitative analyses will be necessary as well. This subject is discussed in the next chapter, chapter 9.

8.8 References

1. Fini G, *J. Raman Spectrosc.* 2004; 35(5): 335-337.
2. Skoulika SG, Georgiou CA, *Appl. Spectrosc.* 2003; 57(4): 407-412.
3. Pinzaru SC, Pavel I, Leopold N, Kiefer W, *J. Raman Spectrosc.* 2004; 35(5): 338-346.
4. Karabas I, Orkoula MG, Kontoyannis CG, *Talanta* 2007; 71(3): 1382-1386.
5. Edwards HGM, Munshi T, Anstis M, *Spectroc. Acta Pt. A-Molec. Biomolec. Spectr.* 2005; 61(7): 1453-1459.
6. Eliasson C, Matousek P, *Anal. Chem.* 2007; 79(4): 1696-1701.
7. De Beer TRM, Baeyens WRG, Ouyang J, Vervaet C, Remon JP, *Analyst* 2006; 131(10): 1137-1144.

-
8. Walker G, Bell SEJ, Vann M, Jones DS, Andrews G, *Chem. Eng. Sci.* 2007; 62(14): 3832-3838.
 9. de Veij M, Vandenabeele P, Alter Hall K, Fernandez FM, Green MD, White NJ, Dondorp AM, Newton PN, Moens L, *J. Raman Spectrosc.* 2007; 38(2): 181-187.
 10. de Veij M, Deneckere A, Vandenabeele P, de Kaste D, Moens L, *J. Pharm. Biomed. Anal.* accepted (doi:10.1016/j.jpba.2007.10.021)
 11. Rowe RC, Sheskey PJ, Owen SC, *Handbook of Pharmaceutical Excipients*. 5th edition, Royal pharmaceutical society of great Britain: London, 2005.
 12. Halttunen H, Rajakylä E, Nurmi J, Perkkalainen P, Pitkänen I, *Thermochim. Acta* 2001; 380(1): 55-65.
 13. Baldrick P, Bamford DG, *Food. Chem. Toxicol.* 1997; 35(7): 719-733.
 14. Socrates G, *Infrared and Raman characteristic group frequencies*, 3rd edition, John Wiley & Sons Ltd: London, 2001.
 15. Cerchiaro G, Sant'Ana AC, Temperini MLA, Ferreira AMD, *Carbohydr. Res.* 2005; 340(15): 2352-2359.
 16. Murphy BM, Prescott SW, Larson I, *J. Pharm. Biomed. Anal.* 2005; 38(1): 186-190.
 17. Liu L, Fishman ML, Hicks KB, *Cellulose* 2007; 14(1): 15-24.
 18. Schenzel K, Fisher S, *Cellulose* 2001; 8(1): 49-57.
 19. De Gussem K, Vandenabeele P, Verbeken A, Moens L, *Spectrochim. Acta, Part A* 2005; 61(13-14): 2896-2908.
 20. Alvarez-Lorenzo C, Lorenzo-Ferreira RA, Gómez-Amoza JL, Martínez-Pacheco R, Souto C, Concheiro A, *J. Pharm. Biomed. Anal.* 1999; 20(1-2): 373-383.
 21. Fechner PM, Wartewig S, Kiesow A, Heilmann A, Kleinebudde P, Neubert RHH, *J. Pharm. Pharmacol.* 2005; 57(6): 698-698.
 22. Eichhorn SJ, Sirichaisit J, Young RJ, *J. Mater. Sci.* 2001; 36(13): 3129-3135.
 23. Langkilde FW, Svantesson A, *J. Pharm. Biomed. Anal.* 1995; 13(4-5): 409-414.
 24. Vandenabeele P, Wehling B, Moens L, Edwards H, De Reu M, Van Hooydonk G, *Anal. Chim. Acta* 2000; 407(1-2): 261-274.

25. Edwards HGM, Falk MJ, Sibley MG, Alvarez-Benedi J, Rull F, *Spectrochim. Acta, Part A* 1998; 54(7): 903-920.
26. Roberts SNC, Williams AC, Grimsey IM, Booth SW, *J. Pharm. Biomed. Anal.* 2002; 28(6): 1135-1147.
27. Ward S, Perkins M, Zhang J, Roberts CJ, Madden CE, Luk SY, Patel N, Ebbens SJ, *Pharm. Res.* 2005; 22(7): 1195-1202.
28. Lin-Vein D, Colthup NB, Fately WG, Grasselli JG, *The handbook of Infrared and Raman Characteristic Frequencies of Organic Molecules*, Academic press: London, 1991.
29. Pyne A, Suryanarayanan R, *Pharmaceutical research*, 2001; 18(10): 1448–1454.
30. Shi Y, Wang L, *J. Phys. D Appl. Phys.* 2005; 38(19): 3741-3745.
31. Neubert R, Rettig W, Wartewig S, Wegener M, Wienhold A, *Chem. Phys. Lipids*, 1997; 89(1): 3-14.
32. Frost RL, Kloprogge JT, *J. Mol. Struct.* 2000; 526: 131-141.
33. Badr Y, Mahmoud MA, *J. Mol. Struct.* 2005; 749: 187-192.
34. Islam MT, Rodriguez-Hornedo N, Ciotti S, Ackermann C, *Pharm. Res.* 2004; 21(10): 1844-1851.
35. Beattie JR, Bell SEJ, Moss BW, *Lipids*, 2004; 39(5): 407-419.
36. Mo SD, Ching WY, *Phys. Rev. B.* 1995; 51(19): 13023-13032.
37. Mitchell PCH, Parker SF, Simkiss K, Simmons J, Taylor MG, *J. Inorg. Biochem.* 1996; 62(3): 183-197.
38. Kloprogge JT, Frost RL, Rintoul L, *Phys. Chem. Chem. Phys.* 1999; 1(10): 2559-2564.
39. Rigby SJ, Al-Obaidi AHR, Lee SK, McStay D, Robertson PKJ, *Appl. Surf. Sci.* 2006; 252(22): 7948-7952.
40. Edwards HGM, Villar SEJ, Jehlicka J, Munshi T, *Spectroc. Acta Pt. A-Molec. Biomolec. Spectr.* 2005; 61(10): 2273-2280.
41. Martinez I, Sanchez-Valle C, Daniel I, Reynard B, *Chem. Geol.* 2004; 207(1-2): 47-58.
42. Meade AD, Lyng FM, Knief P, Byrne HJ, *Anal.Bioanal.Chem.* 2007; 387(5): 1717-1728.



Chapter 9
Quantitative analysis of drugs
with Raman spectroscopy

9 Quantitative analysis of drugs with Raman spectroscopy

9.1 Introduction

The benefits of Raman spectroscopy as a fast qualitative analysis method to detect counterfeit drugs, have been described in chapters 5, 6 and 7. Since the counterfeiters are becoming increasingly sophisticated, quantitative analysis is necessary as well. Raman spectroscopy can be used for quantitative analysis, since the intensity of the vibrational bands is directly proportional to the concentration of the species (chapter 2.3)¹. Different examples of quantitative analysis with Raman spectroscopy in other research fields have been shown in chapter 3.4.5.

In general, a calibration curve is generated, using different mixtures of known composition¹. The accuracy of the calibration curve can be significantly influenced by the homogeneity of the tablets used¹. The first step in this quantitative analysis process, is to develop homogenized calibration tablets. Secondly, by rotating the tablet during analyses the precision between analyses, is decreased¹. These two subjects are discussed in paragraphs 9.3.1 and 9.3.2. and describe the steps that have to be undertaken before the start of the quantitative analysis of the counterfeit drugs.

Some of the counterfeit drugs used for the qualitative analysis (antimalarial and Viagra[®] tablets, as described in chapters 6 and 7), are used for the quantitative study. The quantitative results of the antimalarial tablets with Raman spectroscopy are compared with the results of liquid chromatography mass spectrometry (LC-MS) analyses, while the Viagra[®] tablets are compared to the results of high performance liquid chromatography with diode-array detection (HPLC-DAD) analyses.

The concentration of active ingredient in the possible counterfeits can be calculated in different ways. This concentration can be determined by using the intensity or the area of individual bands, but also with multivariate methods

like principal component regression (PCR). The advantage of these multivariate methods is that the whole spectrum is used, rather than an individual band. This chapter describes the use of calibration curves based on a single band in paragraph 9.4, while the chemometrical approaches are described in paragraph 9.5.

The counterfeit Viagra[®] tablets are analysed with Fourier-Transform (FT) Raman spectroscopy (paragraph 9.6) as well. Additionally, the Viagra[®] tablets are grinded and pressed again to see if the coating of the tablets could have a negative influence on the quantitative analysis (paragraph 9.7).

9.2 Experimental

Two dispersive Raman spectrometers (MArtA and Renishaw System-1000) and a FT-Raman spectrometer (Bruker Equinox 55) were used for the quantitative analysis and is described below.

- **MArtA:**

Details about the MArtA instrument are given in paragraph 5.2.

- **Renishaw:**

The Renishaw System-1000 instrument is described in paragraph 5.2.

- **Bruker Equinox 55S⁸:**

The Bruker Equinox 55S spectrometer with Raman module FRA 106, is a hybrid FT-IR/FT-Raman spectrometer fitted with a cooled (77K) germanium high sensitivity detector D418-T. The data transfer, collection, and processing is automated using the Bruker OPUS[™] software. The spectrum recorded ranges from -100 to 3500 cm⁻¹ with a spectral resolution of ca. 4 cm⁻¹. The laser wavelength used is the 1064 nm line of an air cooled diode pumped

neodymium yttrium aluminium garnet laser (Nd:YAG). During analyses the power of the laser is set at 35.5 % (max. power of 500 mW). Each sample is measured five times with 100 scans during each measurement.

To verify the results obtained with Raman spectroscopy, two analytical methods were used. The antimalarial tablets are analysed with LC-MS and the Viagra[®] tablets with HPLC-DAD.

- **LC - MS⁶:**

The liquid chromatography mass spectrometry (LC-MS) instrument is described in detail in paragraph 6.2.

- **HPLC - DAD⁷:**

High-performance liquid chromatography with diode-array detection (HPLC-DAD) experiments were performed on an Waters HPLC-DAD combination, Alliance 2690 separation module with a DAD detector 996¹⁴.

For the homogeneity and rotation experiments, pure paracetamol (4-acetamidophenol, Acros organics) is used. The artesunate samples were collected in Cambodia, Lao PDR (Laos), the Thai Burma border, Burma and Hong Kong⁶. Pure artesunate (Dafra Pharma) is used for the calibration tablets. The Viagra[®] tablets were donated by the National Institute for Public Health and the Environment (RIVM) in the Netherlands, including the pure active ingredient, sildenafil citrate, for the production of calibration tablets⁷.

The calibration tablets for the antimalarial and Viagra[®] analyses consist of different dosages of the active ingredient and the following excipients: magnesium stearate (Sigma-Aldrich), microcrystalline cellulose (Sigma-Aldrich), silica (Sigma-Aldrich), and corn starch (Sigma-Aldrich). The tablets were made with the use of the Parr Pellet Press (Parr Instrument Company, Moline, IL, U.S.A.) and have a diameter of 1 cm.

In order to calculate the intensity or area of the three Raman bands used, the recorded spectra are averaged and baseline-corrected to eliminate the influence of broadband fluorescence. Two computer programmes are used, ACD/Specmanager (version 9.13, Advanced Chemistry Development, Inc. Toronto, Canada) and Grams/AI(7.01) (Thermo Galactic, Waltham, MA, U.S.A.). Chemometrical calculations are executed by Matlab 6.5 (The MathWorks Inc., Natick, MA, U.S.A.) and the PLS toolbox, version 3.0 (Eigenvector Research Inc., Manson, WA, U.S.A.). The paired *t*-test, for statistical evaluation, was calculated using Excel[®].

9.3 Preparation of calibration tablets and analysis conditions

9.3.1 Homogeneity of the calibration tablets

As mentioned before, one of the major errors in quantitative analysis, is the lack of homogeneity of the tablets. Calibration tablets are made of a mixture of one or more active ingredient(s) and several excipients which had to be thoroughly mixed to make sure that the active ingredient is equally distributed throughout the entire tablet.

In total, 8 plastic tubes, with the same amount of paracetamol and three excipients (magnesium stearate, microcrystalline cellulose and corn starch), are placed in a Turbula T2F instrument. After different mixing times (5 up till 360 minutes), a plastic tube is removed and a tablet is made using the Parr Pellet Press (\varnothing 1 cm). From these 8 tablets, a 15 x 15 mapping, is made with the use of the MArtA instrument (discussed in chapter 3.4.3).

The Raman band at 855 cm^{-1} of paracetamol, which can be assigned to the symmetrical $\nu(\text{CNC})$ stretching vibration³, is chosen to calculate the average intensity and standard deviation. A Raman spectrum, retrieved during the mapping experiment of a paracetamol tablet with the MArtA instrument, is shown in figure 9.1.

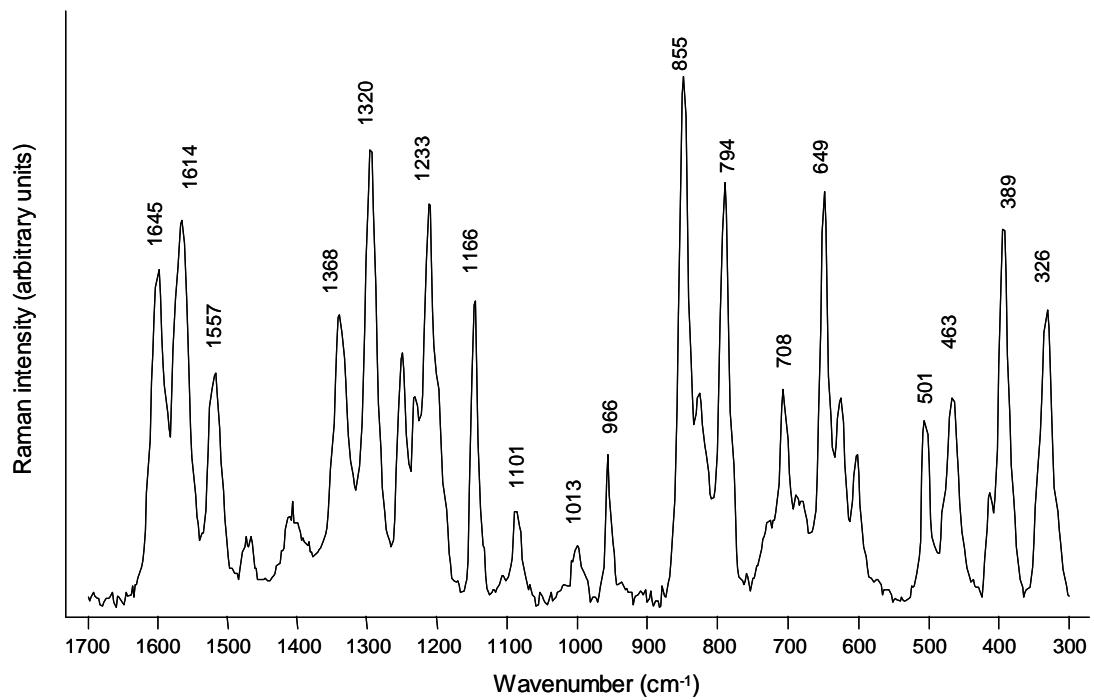


Figure 9.1 Spectrum of a paracetamol tablet analysed with the MArtA instrument (1 acc. x 3 s).

The 15x15 mapping of the paracetamol tablet, rotated for 5 minutes in the Turbula T2F instrument, consists of 225 spectra (fig. 9.2).

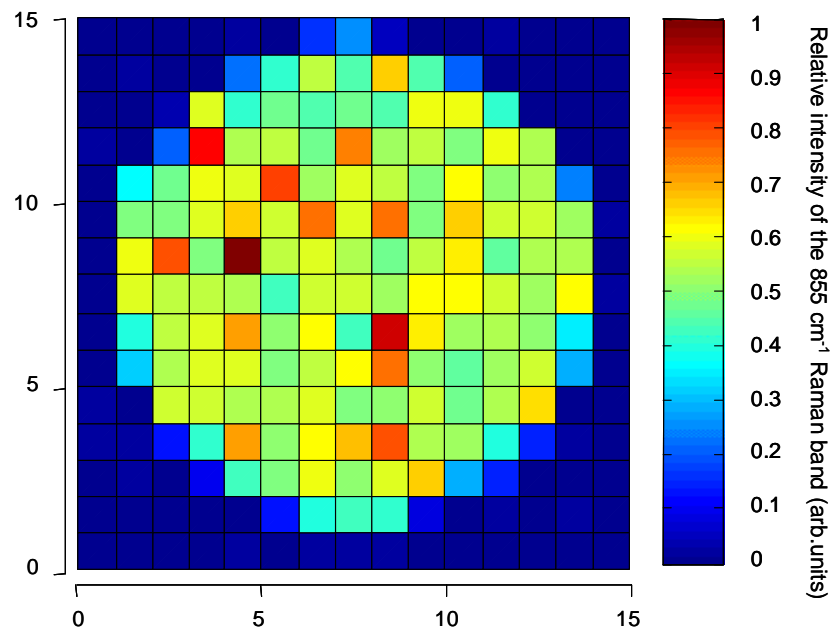


Figure 9.2 A 15x15 mapping (steps of 500 μm) of a paracetamol tablet after 5 minutes homogenization in the Turbula T2F instrument based on the Raman band at 855 cm^{-1} (MArtA, 1 acc. x 3 s).

Figure 9.2 shows that the active ingredient is not equally dispersed throughout the tablet. For the different tablets, the intensity, standard deviation and the relative standard deviation (RSD) of the Raman band at 855 cm^{-1} is calculated and shown in table 9.1 and figure 9.3.

Mixing time (min.)	Average intensity*	Standard deviation*	RSD (%)
5	0.404	0.259	64.2
30	0.353	0.201	56.9
60	0.225	0.126	56.0
90	0.663	0.119	18.0
180	0.489	0.116	23.7
240	0.629	0.113	17.9
300	0.486	0.109	22.4
360	0.505	0.108	21.3
commercial tablet	0.671	0.115	17.1

Table 9.1 Average intensity, standard deviation and RSD (%) (* arbitrary units) of Raman band of paracetamol (855 cm^{-1}) at different shaking times with the Turbula T2F instrument.

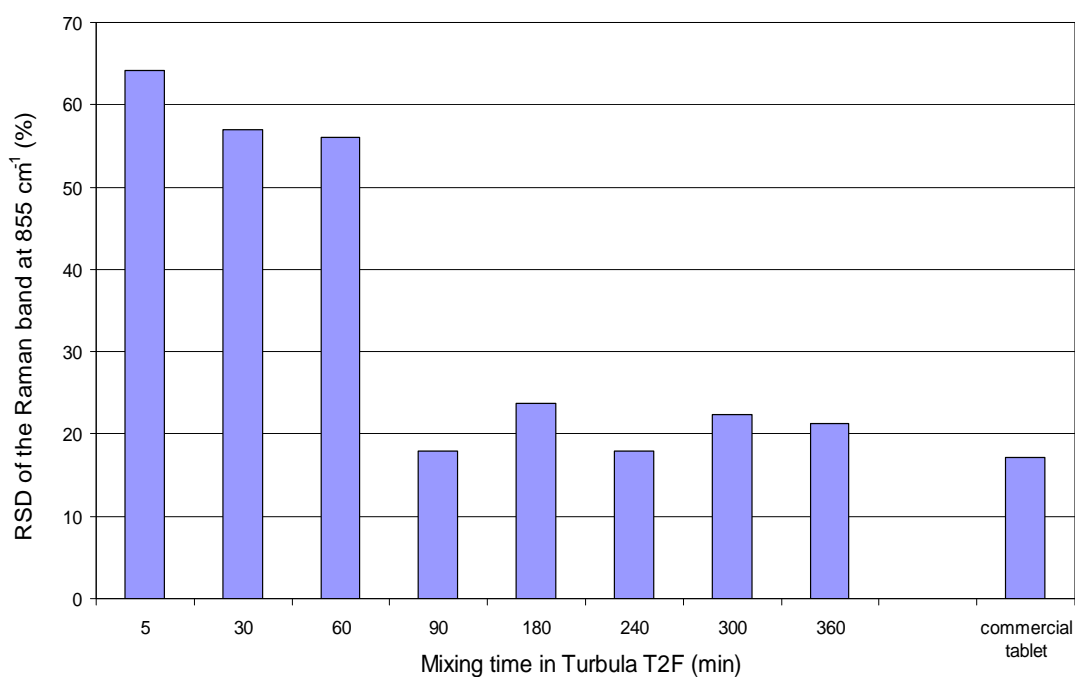


Figure 9.3 RSD of the Raman band at 855 cm^{-1} (%) in function of the mixing time in the Turbula T2F (min).

The standard deviation of the 8 tablets, as presented in table 9.1, drops significantly after 90 minutes to a range of 0.108 till 0.119. The RSD drops to a range of 17.9 to 23.7%. The standard deviation and the RSD of a commercial paracetamol tablet (ETOS, the Netherlands) is respectively 0.115 and 17.1%. This shows that 90 minutes mixing time can be used as a minimum for the production of calibration tablets. For the quantitative analysis of counterfeit drugs, the calibration tablets were shaken for 360 minutes in order to have sufficient margin to obtain homogeneous tablets.

9.3.2 Influence of the rotation of tablets during analysis

Another way to reduce the error during quantitative analysis, is the rotation of the tablet during measurement. When rotating the tablet, a larger area is measured, as shown in figure 9.4. To rotate the tablet, a small device has been developed, and can be positioned under the microscope. The speed of this motor can be varied between 12 and 82 rotations per minute.

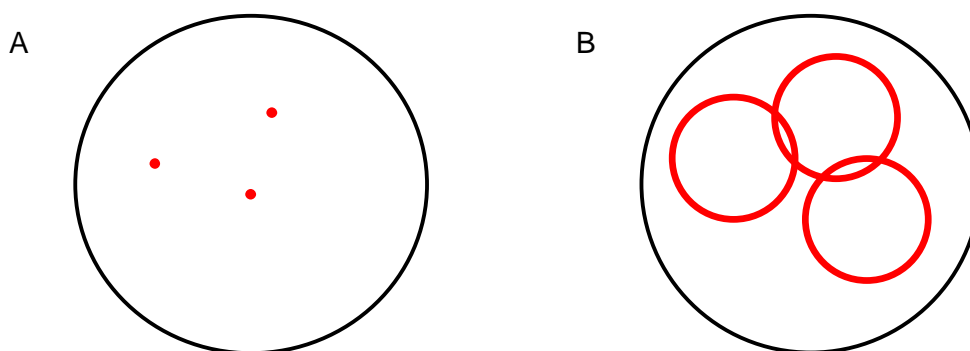


Figure 9.4 (A) represents three analyses of a tablet without rotation, while (B) represents three analyses of a tablet with rotation.

To establish the influence of rotation on the accuracy of the measurements, the paracetamol tablet used in the homogeneity study (tablet 60 min mixing time, paragraph 9.3.1) is analysed. The tablet is analysed 30 times with and without rotating. For each spectrum, the intensity is calculated and the standard deviation of the Raman band at 855 cm^{-1} is calculated (shown in fig. 9.5).

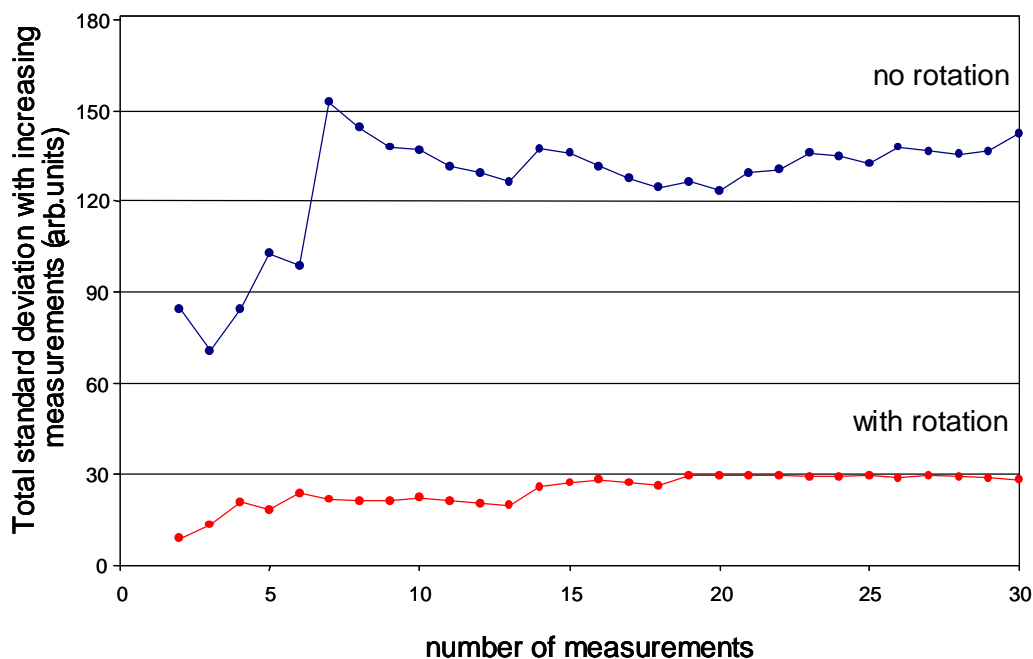


Figure 9.5 The lines represent the standard deviation between the intensities of the Raman band at 855 cm^{-1} for each measurement, with and without rotation (12 rotations per minute, Renishaw System-1000 spectrometer, 1 acc. x 3s).

The intensities of the Raman band of the analysis without rotation vary between 216 and 777 arbitrary units, while the analyses with rotation varies between 415 and 519 arbitrary units. Although the average intensity for both methods after 30 measurements is 469 arbitrary units, the standard deviation of the measurements without rotation is circa 4 times higher than with rotation. This shows that, when rotating the sample, less analyses are required and a better accuracy is obtained. For the quantitative analyses of the counterfeit drugs, discussed in this chapter, an average of 5 measurements with rotation (12 rotations per minute) are used, in order to minimize the level of error.

The quantitative analysis in this work is focussed on measuring two counterfeit drugs, namely antimalarial tablets and Viagra[®]. The quantitative analysis can be executed in two ways. The first is the use of calibration curves, which are based on the intensity or area of specific Raman bands (paragraph 9.4), whereas the second option is the use of chemometrical methods, which are based on the complete Raman spectrum (paragraph 9.5).

9.4. Quantitative analysis based on specific Raman bands

With a calibration curve, based on the intensity or area of a specific Raman band of the active ingredient, the counterfeit tablets will be analysed. This approach is used on the antimalarial tablets as well as on Viagra[®] tablets.

9.4.1 Analysis based on the intensity of three Raman bands

9.4.1.1 Antimalarial tablets

For this quantitative analysis, 11 tablets of the 50 tablets used in chapter 6 are used and the results are compared to liquid chromatography-mass spectrometry (LC-MS) results, as performed by Hall et al.⁶. The first step in this research is the production of calibration tablets. The concentration of the active ingredient, artesunate, in the 6 calibration tablets varies from 9% w/w up to 36% w/w. Since producers of the artesunate tablets from southeast Asia did not give any information about excipients used in their tablets, the following commonly used excipients were chosen: magnesium stearate (2% w/w), microcrystalline cellulose (5% w/w), silica (7% w/w) and corn starch (50 - 77% w/w). The ingredients for the calibration tablets are thoroughly mixed in the Turbula T2F instrument for 6 hours in total.

For this quantitative analysis, 3 Raman bands were selected, namely the bands at 307 cm⁻¹ and at 679 cm⁻¹ due to skeletal modes of the alkenes and the $\nu(\text{C}=\text{O})$ stretching vibration at 1757 cm⁻¹ (see chapter 6, fig. 6.1). These Raman bands are selected based on the absence of overlapping Raman bands due to excipients. The intensity of these Raman bands are used to produce three calibration curves.

With the MArtA instrument, each tablet is analysed and the intensity of the three Raman bands at 307, 679 and 1757 cm⁻¹ is determined for all 6 calibration tablets. The average intensities and standard deviations of these three Raman bands are used to establish calibration curves which are shown in figure 9.6.

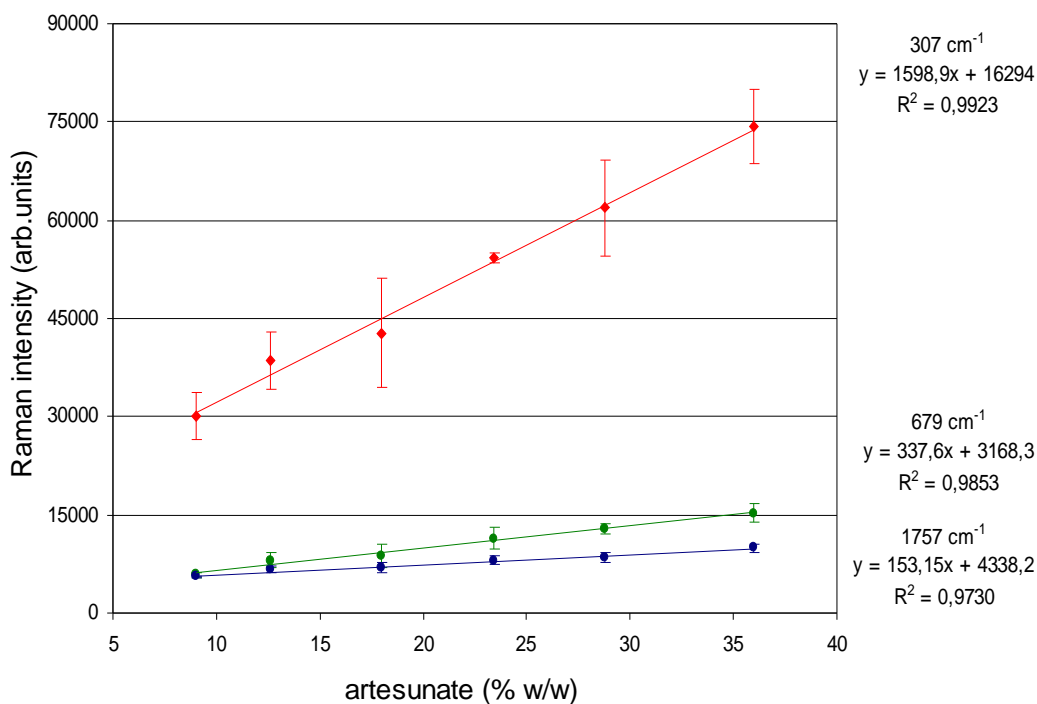


Figure 9.6 Average intensity and standard deviation in arbitrary units for 6 calibration tablets measured with the MArtA instrument (5 acc. x 120 s).

For each calibration curve the coefficient of determination (R^2) is determined which can range between 0 and 1 ($0 \leq R^2 \leq 1$)¹¹. The closer the value of R^2 is to 1, the larger is said to be the degree of linearity between the concentration and the Raman intensity¹¹. Although, the calibration curve of 307 cm^{-1} has the highest R^2 , its standard deviation is high as well.

The function of the three calibration curves are used, in combination with the intensities of the corresponding three bands for the 11 tablets from southeast Asia. Based on the intensities of these tablets, the concentration in % w/w of the active ingredient artesunate is calculated. Table 9.2 shows these results and the relative difference in % between the Raman analyses and the LC-MS results⁶.

Tablet	LC-MS (% w/w)	Calculated active ingredient with Raman spectroscopy and relative difference with the LC-MS results (%).					
		307 cm ⁻¹		679 cm ⁻¹		1757 cm ⁻¹	
		% w/w	% diff.	% w/w	% diff.	% w/w	% diff..
5	21	17	-17	14	-33	10	-52
13008	8	15	96	9	23	3	-61
13009	32	16	-48	10	-67	25	-20
13013	22	17	-25	11	-50	16	-28
12064	30	21	-30	19	-37	41	39
12065	27	22	-20	38	39	43	59
63001	21	24	12	25	19	7	-67
artesor 4	30	8	-75	29	-4	35	16
artesor 7	25	8	-68	15	-41	-8	-131
artesor 9	24	8	-68	12	-48	24	2
artesor 10	21	10	-51	30	44	14	-33
average			54		40		57

Table 9.2 Calculated amount of active ingredient (% w/w) in 11 antimalarial tablets from southeast Asia, measured with the MArtA instrument (5 acc. x 120 s) and with LC-MS with the relative difference between these two analytical techniques (%). The average of all tablets is calculated (square root of the average quadratic value).

The results in table 9.2 are determined with the use of the three calibration curves presented in figure 9.6. The difference between the two analytical methods (Raman spectroscopy and LC-MS) of these tablets is significant and ranges from 2 up to 131%. A positive difference indicates overestimation by Raman spectroscopy compared to LC-MS, while negative differences indicate an underestimation of the amount of active ingredient. Even the calibration curve with the highest R^2 , 307 cm⁻¹, shows an average difference of 54%.

In addition, a paired t-test is performed on the results ($\alpha = 0.05$) in order to see if there is a significant difference between the results based on Raman spectroscopy and LC-MS ($P < 0.05$).

The results based on the Raman band at 307 cm^{-1} showed a significant difference with the LC-MS results ($P = 0.004$), while the results based on the Raman bands at 679 and 1757 cm^{-1} , showed no significant difference ($P = 0.22$ and $P = 0.39$).

Next, Viagra[®] tablets are analysed in a similar way (paragraph 9.3.3.2). Additionally, these Viagra[®] tablets (calibration and counterfeits) are analysed using the two dispersive Raman spectrometers, namely the MArtA and Renishaw System-1000 instrument.

9.4.1.2 Viagra[®] tablets

The same quantification process used on the antimalarial tablets is also performed on the 6 Viagra[®] tablets which have been quantitatively analysed with HPLC-DAD by RIVM⁷. The Viagra[®] tablets are analysed with both the MArtA instrument and the Renishaw System-1000 spectrometer.

Original Viagra[®] tablets contain approximately 16% w/w active ingredient (sildenafil citrate). Three different doses are sold, with respectively 25, 50 and 100 mg sildenafil citrate. The ratio of active ingredient in all three dosages is therefore the same, the variation is created by increasing the weight of the tablet. The 6 possible counterfeit Viagra[®] tablets are received from RIVM and made up of the three different sizes (1 x 25, 2 x 50 mg and 3 x 100 mg)

The first step in the quantitative analysis is the preparation of calibration tablets, made with the active ingredient sildenafil citrate. The chemical structure and the Raman spectra of the active ingredient is shown in chapter 7 (fig. 7.3). The concentration of the active ingredient in the 7 calibration tablets varies from 4% w/w up to 30% w/w, were genuine Viagra[®] contains circa 16%. Based on the information of the producer, the following excipients were chosen, namely: calcium hydrogen phosphate (4% w/w), titanium dioxide (15% w/w), magnesium stearate (4% w/w) and cellulose (47 - 77% w/w).

The tablets are analysed using the following three Raman bands: the ring vibration at 818 cm^{-1} , the $\nu(\text{C}=\text{N})$ stretching vibration at 1239 cm^{-1} and the $\nu(\text{C}=\text{C})$ stretching vibration at 1580 cm^{-1} .

- **Analysis with the MArtA spectrometer:**

Each tablet (calibration and possible counterfeits) are analysed five times. The intensities and standard deviation for the three Raman bands, as indicated above, results in the following calibration curves (fig. 9.7).

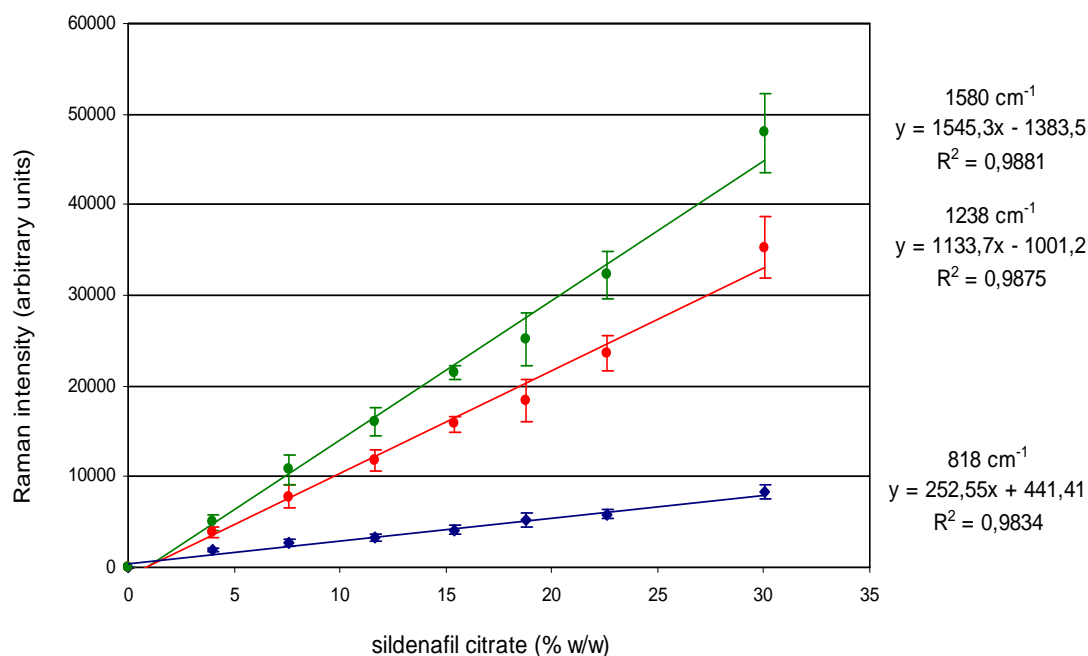


Figure 9.7 Average intensity and standard deviation in arbitrary units for 7 calibration tablets, measured with the MArtA instrument (100 acc. x 1 s).

These calibration curves are used to estimate the amount of active ingredient in the possible counterfeit Viagra[®] tablets and are compared to the results of the HPLC-DAD analyses. Results are shown in table 9.3

Tablet	HPLC - DAD (% w/w)	Calculated amount active ingredient based on Raman spectroscopy and relative difference with the HPLC-DAD results.					
		818 cm ⁻¹		1239 cm ⁻¹		1580 cm ⁻¹	
		% w/w	% diff.	% w/w	% diff.	% w/w	% diff.
1	16	20	23	21	33	21	30
2	17	24	45	30	76	29	73
3	12	15	18	18	50	18	44
4	15	20	39	22	50	21	47
5	15	20	38	24	64	23	57
6	17	22	28	26	56	26	53
average			33		54		50

Table 9.3 Calculated amount of active ingredient (% w/w) in the 6 Viagra[®] tablets with the MArtA instrument (100 acc. x 1 s) and HPLC-DAD, with the relative difference between these two analytical methods (%). The average of the differences of all 6 tablets is calculated (square root of the average quadratic value).

The average difference between the results of HPLC-DAD and Raman spectroscopy of the 6 Viagra[®] tablets ranges between 33 and 54%. The difference for the Viagra[®] tablets is a bit lower than the difference for the artesunate tablets, which ranges between 40 and 57% (paragraph 9.4.1.1).

A paired t-test ($\alpha = 0.05$) is performed to confirm the results of the analyses with the MArtA spectrometer. Based on this test there is a significant difference between the HPLC-DAD results and the results based on the three Raman bands ($P < 0.05$).

These same tablets (7 calibration and 6 possible counterfeits) are analysed with the Renishaw System-1000 spectrometer, in order to verify if the quantitative analysis with the second dispersive Raman spectrometer shows improvement in the accuracy.

The analyses, so far, are analysed with the mobile Raman spectrometer (MArtA). The Renishaw System-1000 spectrometer is a bench top spectrometer which could improve the results.

- **Analysis with the Renishaw System-1000 spectrometer:**

Similar to the analyses with the MArtA instrument, the intensities and standard deviations of the three Raman bands of the calibration tablets are used to establish calibration curves (fig. 9.8).

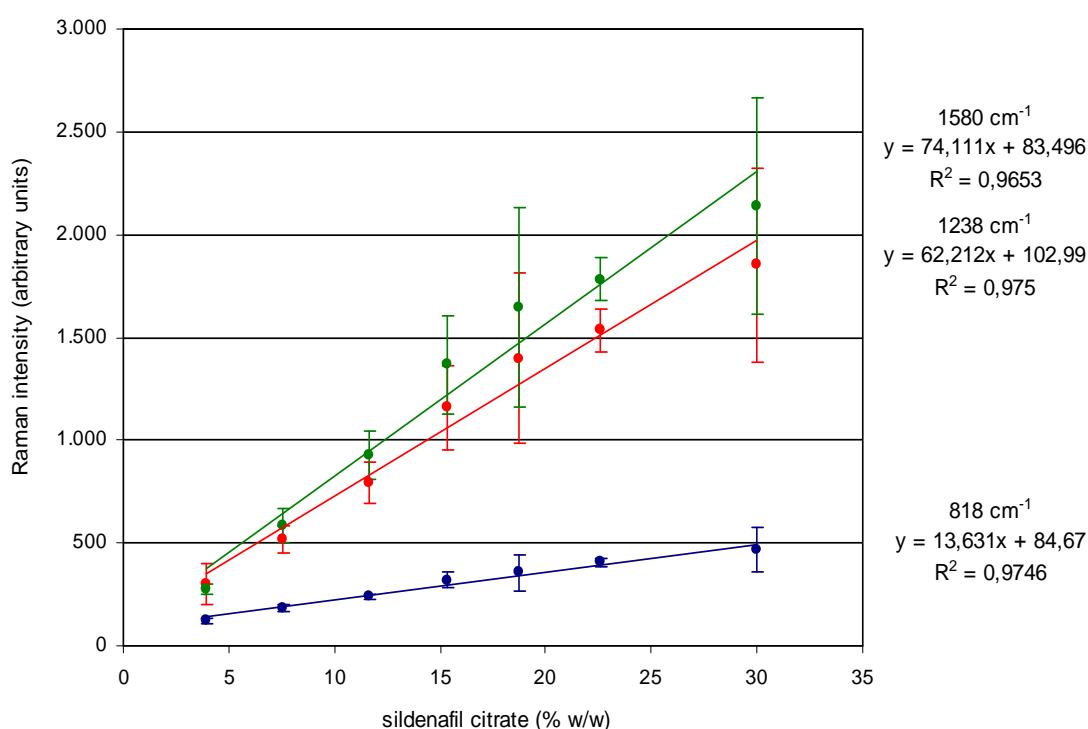


Figure 9.8 Average intensity and standard deviation in arbitrary units for 7 calibration tablets, measured with the Renishaw System-1000 spectrometer (5 acc. x 30 sec).

The intensities of the three Raman bands of the 6 Viagra[®] tablets are used to estimate the amount of active ingredient, which is compared to the HPLC-DAD analyses performed by RIVM. Results are shown in table 9.4.

Tablet	HPLC - DAD (% w/w)	Calculated amount active ingredient based on Raman spectroscopy and relative difference with the HPLC-DAD results.					
		818 cm ⁻¹		1239 cm ⁻¹		1580 cm ⁻¹	
		% w/w	% diff.	% w/w	% diff.	% w/w	% diff.
1	16	14	-13	9	-42	11	-29
2	17	27	59	15	-12	22	32
3	12	18	44	17	38	18	43
4	15	16	10	14	-3	17	15
5	15	18	26	16	10	18	23
6	17	14	-15	9	-45	13	-25
average			33		30		29

Table 9.4 Calculated amount of active ingredient (% w/w) in the 6 Viagra[®] tablets with the Renishaw System-1000 spectrometer (5 acc. x 30 s) and the HPLC-DAD analyses, with the relative difference between these two analytical methods (%). The average of all 6 tablets is calculated (square root of the average quadratic value).

The average difference between the results with the HPLC-DAD and Raman spectroscopy (Renishaw System-1000) of the 6 Viagra[®] tablets ranges between 29 and 33%, which shows an improvement compared to the results with the MArtA spectrometer (table 9.3). To confirm these results, a paired t-test ($\alpha = 0.05$) is performed. According to this test, there is no significant difference between the HPLC-DAD analyses and the analyses based on the three specific Raman bands ($P = 0.21$, $P = 0.29$ and $P = 0.49$).

The results of the quantification of the antimalarial and Viagra[®] tablets based on the intensities of three Raman bands, analysed with the MArtA instrument and the Renishaw System-1000 spectrometer, are shown below. These results represent the minimum and maximum average difference of the counterfeit tablets with Raman spectroscopy and LC-MS or HPLC-DAD, respectively.

-
- | | | |
|-------------------------------------|------------------------------|----------|
| • MArtA instrument | antimalarial tablets: | 40 – 57% |
| | Viagra [®] tablets: | 33 – 54% |
| • Renishaw System-1000 spectrometer | Viagra [®] tablets: | 29 – 33% |

It has to be noted that the minimum and maximum difference is an average of the 11 antimalarial tablets or 6 Viagra[®] tablets. The difference per tablet can vary outside of these ranges. When focussing on these results, it can be noted that the average difference for the Renishaw System-1000 spectrometer differs less between the three Raman bands compared to the MArtA instrument. This can be due to the fact that the Renishaw System-1000 is a bench top spectrometer, while the MArtA instrument is a mobile spectrometer. Therefore, in the following paragraphs, we will continue to work with the Renishaw System-1000 spectrometer.

9.4.2 Analysis based on the area of three Raman bands

In this paragraph, a calibration curve is established, based on the area of the three Raman bands rather than this intensity. The area of the Raman band is independent of broadening effects and should enhance the results compared to the results based on the intensity of a Raman band¹². The area of the three Raman bands is determined with ACD/ Specmanager (version 9.13). This approach is used on the Viagra[®] tablets analysed with Renishaw System-1000 spectrometer since these analyses yielded the best results.

The calibration curves are similar to those used for the intensity calculations (paragraph 9.4.1) except that these are based on the area of the three Raman bands at 818 cm⁻¹, 1239 cm⁻¹ and 1580 cm⁻¹(fig. 9.9). The equations of the three calibration curves are used in combination with the areas of these three bands of the 6 Viagra[®] tablets to calculate the amount of active ingredient. The amounts of active ingredient are presented in % w/w and are compared to those of the HPLC-DAD analyses (difference in %). Results are presented in table 9.5.

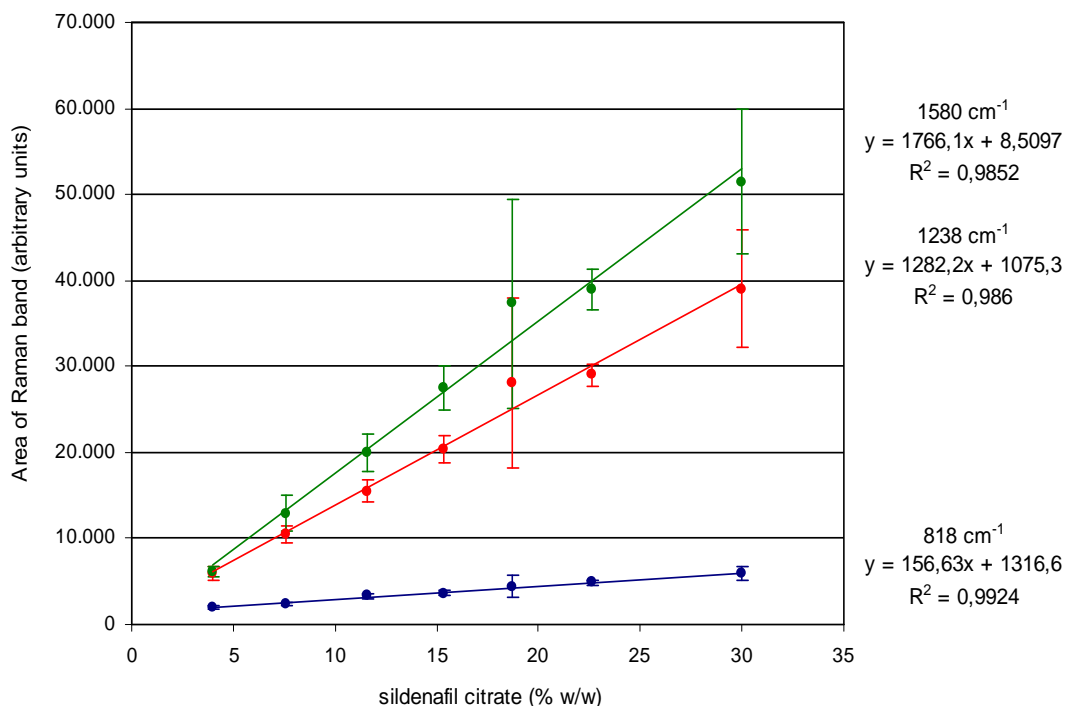


Figure 9.9 Average area and standard deviation in arbitrary units for 7 calibration tablets measured with the Renishaw System-1000 spectrometer (5 acc. x 30 s).

Tablet	HPLC - DAD (% w/w)	Calculated amount active ingredient based on Raman spectroscopy and relative difference with the HPLC-DAD results.					
		818 cm ⁻¹		1239 cm ⁻¹		1580 cm ⁻¹	
		% w/w	% diff.	% w/w	% diff.	% w/w	% diff.
1	16	17	7	10	-37	12	-26
2	17	30	77	17	-2	21	27
3	12	19	52	19	56	20	58
4	15	18	22	17	18	18	24
5	15	16	8	10	-33	13	-11
6	17	18	5	15	-13	17	-1
average			39		32		30

Table 9.5 Calculated amount of active ingredient (% w/w) in the 6 Viagra[®] tablets with the Renishaw System-1000 spectrometer (5 acc. x 30 s) and HPLC-DAD with the relative difference between these two analytical methods (%). The average of all 6 tablets is calculated (square root of the average quadratic value).

For these analyses, a paired t-test is performed as well ($\alpha = 0.05$). There is no significant difference between the analyses with Raman spectroscopy and HPLC - DAD based on the area of the three Raman bands ($P = 0.08$, $P = 0.73$ and $P = 0.38$). The average difference results of the intensity and the area are shown below.

- Intensity (paragraph 9.4.1.2): 29 – 33%
- Area: 30 – 39%

Both calculations are based on the analyses of the 6 possible counterfeit Viagra[®] tablets with the Renishaw System-1000 spectrometer. When focussing on the results shown above, it can be noted that the results based on the intensity of the Raman bands have a slightly better accuracy than the results based on the area of these Raman bands. Although, the opposite would be expected, since the band area is independent of broadening effects¹². When comparing the results with a paired t-test ($\alpha = 0.05$), no significant difference between the results based on the area and the intensity of the Raman band can be noted ($P = 0.58$, $P = 0.61$ and $P = 0.89$). The calculations presented in paragraph 9.4.1 and 9.4.2 are all based on the analyses of a single Raman band. When an excipient has a Raman band at the same position, an inaccuracy in the calculations will occur. Therefore, chemometrical methods will be used to calculate the amount of active ingredient in the Viagra[®] tablets. With these chemometrical approaches, the entire Raman spectrum is used for the calculations.

9.5 Quantitative analysis based on PCR

A commonly used chemometrical approach is PCR, which is a form of factor analysis that can be used for quantitative analysis in spectroscopy⁹. The first step in this chemometrical approach is reducing the dataset of all the Raman spectra by using principal component analysis (PCA). Secondly, a correlation is established between the PCA-scores and the concentration (see Appendix for more details). The benefit of chemometrical approaches is that the entire

Raman spectrum is considered. Therefore, this method could provide a better quantification method since it is less sensitive to interferences as, compared to the monovariate approach. The Viagra[®] tablets analysed with the Renishaw system-1000 instrument, are calculated with the use of PCR, to see if this improves the quantification process.

Calculations are performed on the raw data retrieved from the Renishaw system-1000 spectrometer. Additionally, as a pre-processing method, the 1st and 2nd derivative is taken of all spectra, with the use of the Savitsky-Golay algorithm¹⁰. By using derivatives, the contributions from the broad-featured fluorescence background are diminished. The calculations are performed with Matlab and the influence of the first 5 principal components (PCs) is investigated. With this technique the amount of active ingredient (% w/w) in the six Viagra[®] tablets and the difference (%) with the HPLC-DAD analyses are calculated. The differences (%) between the two techniques are presented in the next three tables, based on the raw data (table 9.6), 1st derivative (table 9.7), and 2nd derivative (table 9.8).

- **Analysis with raw data:**

Tablet	Difference between Raman spectroscopy and HPLC-DAD analyses in presented in %				
	1 PC	2 PCs	3 PCs	4 PCs	5 PCs
1	-77	32	-87	-91	70
2	-439	103	-380	-392	135
3	-76	23	-118	-118	-4
4	-44	24	-111	-116	51
5	-92	-8	-129	-136	72
6	-87	19	-124	-128	63
average	192	47	187	193	76

Table 9.6 Results of PCR analyses (raw data) with the use of Matlab. Difference (%) of calculated amount of active ingredient in the 6 Viagra[®] tablets between Renishaw System-1000 instrument (5 acc. x 30 s) and HPLC-DAD. The average of all 6 tablets is calculated (square root of the average quadratic value).

- **Analysis with 1st derivative of the data:**

Tablet	Difference between Raman spectroscopy and HPLC-DAD analyses in (%)				
	1 PC	2 PCs	3 PCs	4 PCs	5 PCs
1	21	34	29	19	18
2	-13	-1	-9	-21	-21
3	17	-30	-37	-53	-53
4	53	-3	-6	-6	-6
5	3	24	16	-2	-3
6	23	12	9	-1	-1
average	26	22	21	24	24

Table 9.7 Results of PCR analyses (1st derivative) with the use of Matlab. Difference of calculated amount of active ingredient in the 6 Viagra[®] tablets between Renishaw System-1000 instrument (5 acc. x 30 s) and HPLC-DAD (%). The average of all 6 tablets is calculated (square root of the average quadratic value).

- **Analysis with 2nd derivative of the data:**

Tablet	Difference between Raman spectroscopy and HPLC-DAD analyses in (%)				
	1 PC	2 PCs	3 PCs	4 PCs	5 PCs
1	24	37	34	35	26
2	-5	7	3	3	-12
3	6	-25	-32	-36	-44
4	39	1	-1	-1	-2
5	9	29	23	22	11
6	19	15	14	13	7
average	21	23	22	23	22

Table 9.8 Results of PCR analyses (2nd derivative) with the use of Matlab. Difference of calculated amount of active ingredient in the 6 Viagra[®] tablets between Renishaw System-1000 instrument (5 acc. x 30 s) and HPLC-DAD (%). The average of all 6 tablets is calculated (square root of the average quadratic value).

When focussing on the average difference results (%) of the 6 Viagra[®] tablets with the use of chemometrical approaches, it can be noted that the analyses of the raw data leads to larger errors. The results of the 1st and 2nd derivative show an improvement with an average difference varying between 21 and 26%. This can be due to the fact that the coating of the Viagra[®] tablets can cause a broad-featured fluorescence background.

Additionally, a paired t-test ($\alpha = 0.05$) is performed in order to see if there is a significant difference ($P < 0.05$) between the PCR on HPLC-DAD analyses.

Analyses based on PCR results	paired t-test ($\alpha = 0.05$)				
	1 PC	2 PCs	3 PCs	4 PCs	5 PCs
Raw data	0.07	0.06	0.01	0.01	0.00
1 st derivative	0.19	0.41	0.86	0.30	0.29
2 nd derivative	0.12	0.17	0.32	0.39	0.92

Table 9.9 Statistical evaluation (paired t-test) of the results based on PCR analyses (raw data, 1st derivative and 2nd derivative).

Based on the results of the paired t-test, there is a significant difference between the PCR results based on the raw data and the HPLC-DAD analyses ($P < 0.05$). However, this changes when using the 1st or 2nd derivative, when there is no significant difference between the two techniques ($P > 0.05$).

Results based on PCA combined with PCR are compared to the results based on the intensity of three Raman bands are shown below:

- PCR:

raw data	47 – 193%
1 st derivative	21 – 26%
2 nd derivative	21 – 23%
- Intensity (9.4.1.2):

	29 – 33%
--	----------

These results show an improvement compared to results based on a single Raman band. This can be expected, since this method incorporates the entire Raman spectrum. In order to check if the analyses can be improved, the Viagra® tablets are analysed with a FT-Raman spectrometer (Bruker Equinox 55S). Commonly, quantitative analysis of drugs is performed more often with Fourier transform (FT) Raman spectroscopy than with dispersive Raman spectroscopy.

9.6 Analysis with Fourier transform (FT) Raman Spectroscopy

For this analyses, a Bruker Equinox 55S instrument is used in combination with the intensity of three Raman bands (similar to paragraph 9.4.1.2) and PCR (similar to paragraph 9.5).

9.6.1 Analysis based on the intensity of three Raman bands

The first step in the analyses, is establishing calibration curves, based on the intensities of three Raman bands (fig. 9.10).

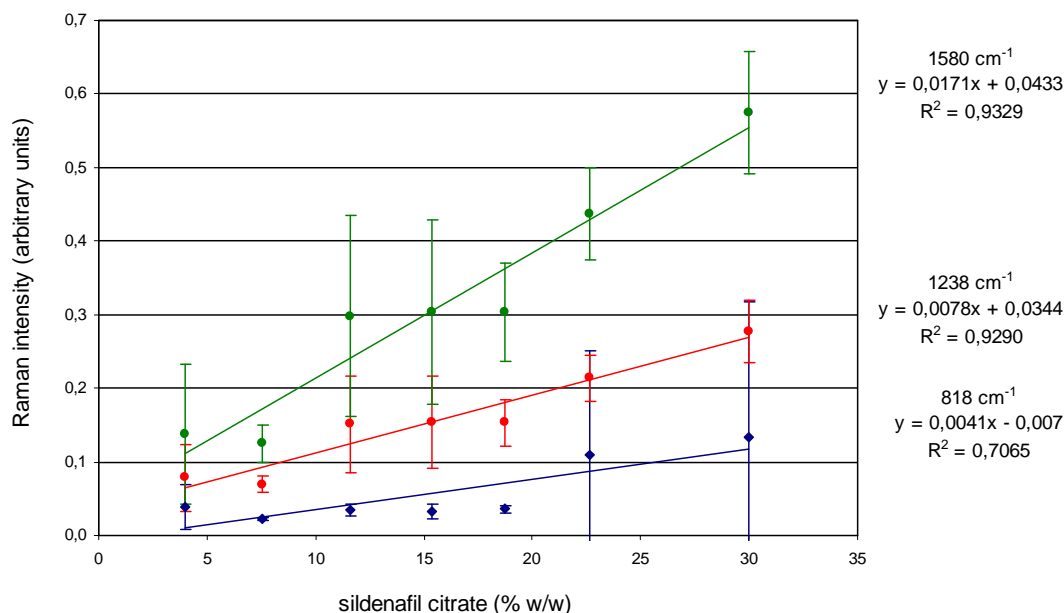


Figure 9.10 Average intensity and standard deviation in arbitrary units for 7 calibration tablets with the active ingredient sildenafil citrate analysed with the Bruker Equinox 55S spectrometer (100 scans, 178 mW).

The determination coefficients (R^2) of the calibration curves are lower, compared to those obtained with the dispersive Raman spectrometers (fig. 9.7 and 9.8). With the use of the calibration curves shown in figure 9.10, the amount of active ingredient (% w/w) in the counterfeit Viagra[®] tablets is determined. The difference between FT-Raman and the HPLC-DAD is calculated and presented in % (table 9.10).

Tablet	HPLC - DAD (% w/w)	Calculated amount active ingredient based on Raman spectroscopy and relative difference with the HPLC-DAD results.					
		818 cm ⁻¹		1239 cm ⁻¹		1580 cm ⁻¹	
		% w/w	% diff.	% w/w	% diff.	% w/w	% diff.
1	16	4	-74	1	-92	3	-82
2	17	12	-28	16	-3	17	1
3	12	13	7	18	46	17	37
4	15	7	-51	11	-25	11	-24
5	15	13	-12	22	51	21	45
6	17	8	-52	13	-21	15	-13
average			44		49		42

Table 9.10 Calculated amount of active ingredient (% w/w) in the 6 Viagra[®] tablets with the Bruker Equinox 55S spectrometer (100 scans, 178 mW) and HPLC-DAD with the relative difference between these two analytical methods (%). The average of all 6 tablets is calculated (square root of the average quadratic value).

To confirm these results, a paired t-test ($\alpha = 0.05$) is performed. The results based on the Raman band of 818 cm⁻¹ shows a significant difference ($P = 0.01$) compared to the HPLC-DAD analyses, while the two other Raman bands at 1239 and 1580 cm⁻¹ show no significant difference ($P = 0.62$ and $P = 0.65$). The results presented in table 9.10 are compared to similar analyses with the Renishaw System-1000 spectrometer.

- Bruker Equinox 55S instrument: 42 – 49%
- Renishaw system-1000 spectrometer (9.4.1.2): 29 – 33%

Although the opposite is expected, based on the literature, the difference between the results of analyses with a FT Raman spectrometer (Bruker Equinox 55S) and HPLC-DAD analyses is more significant than compared to the dispersive Raman spectrometer (Renishaw system1000).

Based on the results of the paired t-test, the Renishaw System-1000 spectrometer shows no significant difference with HPLC-DAD for all three Raman bands (paragraph 9.4.1.2) while the Bruker Equinox 55S shows no significant difference for 2 of the 3 Raman bands.

One of the reasons why the FT Raman spectrometer shows disappointing results, can be due to the fact that the tablets were difficult to position in the laser beam. With the Renishaw System-1000 spectrometer, the microscope enhances focussing of the laser beam on the sample, whereas in the case of FT-Raman spectroscopy a standard sample holder is used. Moreover, when using FT-Raman spectroscopy, the tablets could not be rotated. An alternative approach is the use of FT-Raman spectroscopy in combination with PCR.

9.6.2 Analysis based on PCR

Calculations with the use of PCR are performed analogous to the calculations described in paragraph 9.5 and are presented in table 9.11 till 9.13. Firstly, PCA is performed to reduce the data set, secondly PCR is used to establish the correlation between the Raman spectra and the concentration.

Calculations are performed with the use of Matlab and the first 5 PCs are used. Additionally, the 1st and 2nd derivative is taken of all Raman spectra, with the use of the Savitsky-Golay algorithm¹⁰ in order to eliminate the influence of the possible broad-featured fluorescence background. The amount of active ingredient (% w/w) in the six Viagra[®] tablets is calculated and the difference (%) with the HPLC-DAD analyses is established. Differences between these techniques are presented in table 9.11, 9.12, and 9.13, for the raw data, 1st derivative of this data and 2nd derivative of this data, respectively.

- **Analysis with raw data:**

Tablet	Difference between Raman spectroscopy and HPLC-DAD analyses presented in (%)				
	1 PC	2 PCs	3 PCs	4 PCs	5 PCs
1	79	74	74	74	73
2	45	5	5	4	12
3	30	-45	-46	-46	-29
4	59	59	59	59	60
5	57	7	6	6	2
6	77	26	25	25	23
average	60	44	44	44	42

Table 9.11 Results of PCR analyses (raw data) with the use of Matlab. Difference (%) of calculated amount of active ingredient in the 6 Viagra[®] tablets between Bruker Equinox 55S instrument (100 scans, 178 mW) and HPLC-DAD. The average of 6 tablets is calculated (square root of the average quadratic value).

- **Analysis with 1st derivative:**

Tablet	Difference between Raman spectroscopy and HPLC-DAD analyses presented in (%)				
	1 PC	2 PCs	3 PCs	4 PCs	5 PCs
1	98	81	66	69	78
2	40	33	27	28	32
3	95	7	-3	3	-6
4	97	55	48	53	51
5	94	-11	-24	-16	-26
6	96	15	8	12	7
average	89	43	36	38	42

Table 9.12 Results of PCR analyses (1st derivative) with the use of Matlab. Difference (%) of calculated amount of active ingredient in the 6 Viagra[®] tablets between Bruker Equinox 55S instrument (100 scans, 178 mW) and HPLC-DAD. The average of 6 tablets is calculated (square root of the average quadratic value).

- **Analysis with 2nd derivative:**

Tablet	Difference between Raman spectroscopy and HPLC-DAD analyses presented in (%)				
	1 PC	2 PCs	3 PCs	4 PCs	5 PCs
1	99	81	80	81	64
2	96	9	8	11	-17
3	96	7	7	8	-25
4	69	33	33	34	29
5	95	-11	-13	-9	-78
6	96	14	13	15	-16
average	93	37	37	37	45

Table 9.13 Results of PCR analyses (2nd derivative) with the use of Matlab. Difference (%) of calculated amount of active ingredient in the 6 Viagra[®] tablets between Bruker Equinox 55S instrument (100 scans, 178 mW) and HPLC-DAD. The average of 6 tablets is calculated (square root of the average quadratic value).

In order to see if there is a significant difference ($P < 0.05$) between the PCR results and results based on HPLC-DAD analyses, a paired t-test ($\alpha = 0.05$) is performed (table 9.14).

Analyses based on PCR results	paired t-test ($\alpha = 0.05$)				
	1 PC	2 PCs	3 PCs	4 PCs	5 PCs
Raw data	0.00	0.14	0.15	0.15	0.09
1 st derivative	0.00	0.08	0.22	0.11	0.24
2 nd derivative	0.00	0.08	0.10	0.07	0.79

Table 9.14 Statistical evaluation (paired t-test) of the results based on PCR analyses (raw data, 1st derivative and 2nd derivative).

Based on the results of the paired t-test, there is a significant difference between the two methods, only when using the first PC. For the other four PCs there is no significant difference based on the paired t-test.

A summary of the results of the chemometrical approach for this FT Raman spectrometer (Bruker Equinox 55S) and dispersive Raman spectrometer (Renishaw system-1000, paragraph 9.5) are shown below.

	<i>Bruker Equinox 55S</i>	<i>Renishaw system-1000</i>
• Intensity	42 – 49%	29 – 33%
• raw data	42 – 60%	47 – 193%
• 1 st derivative	36 – 89%	21 – 26%
• 2 nd derivative	37 – 93%	21 – 23%

The results of the PCR analyses show similar results to those based on the intensity of the three Raman bands. Additionally, a paired t-test ($\alpha = 0.05$) is performed to see if there is a significant difference ($P < 0.05$) between the results gained by the Bruker Equinox 55S spectrometer and the Renishaw System-1000 spectrometer.

The results based on the Raman band at 818 cm^{-1} between the two techniques showed a significant difference ($P = 0.006$), while the results based on the Raman bands at 1238 and 1580 cm^{-1} , showed no significant difference ($P = 0.95$ and $P = 0.43$). The results of the paired t-test on the PCR results is presented in table 9.15.

Analyses based on PCR results	paired t-test ($\alpha = 0.05$)				
	1 PC	2 PCs	3 PCs	4 PCs	5 PCs
Raw data	0.02	0.64	0.01	0.01	0.07
1 st derivative	0.00	0.20	0.29	0.05	0.11
2 nd derivative	0.00	0.34	0.26	0.19	0.84

Table 9.15 Statistical evaluation (paired t-test) of the results based on PCR analyses (raw data, 1st derivative and 2nd derivative).

Based on the results of the paired t-test, there is significant difference for the PCR results based on the first PC, similar to those results presented in table 9.14. Additionally, the results based on the raw data show a significant difference for 3 out of 5 PCs.

Although the average difference with the Bruker Equinox 55S instrument is higher than analyses with the Renishaw system-1000 spectrometer, it does show that PCR improves the quantitative analysis of counterfeit drugs compared to analyses based on the intensity of single Raman bands.

9.7 Influence of grinding and repressing of tablets

The difference between the Raman analyses and HPLD-DAD analyses might be caused by the thickness of the coating, that is used on the Viagra[®] tablets. This blue coating consist of hypromellose, lactose, triacetin, titanium dioxide and indigo carmine, which gives the tablet its distinctive colour. In order to decrease this influence, the tablets are grinded and repressed.

The six Viagra[®] tablets received from RIVM were grinded and shaken for 360 minutes in the Turbula T2F. After mixing the powders thoroughly, the tablets were repressed with the use of the Parr Pellet Press into flat round tablets with a diameter of 1 cm, similar to the calibration tablets.

These tablets were analysed with the Renishaw System-1000 spectrometer under the same conditions as described in paragraph 9.4.1.2. Firstly the calculations are performed based on the intensity of the three specific Raman bands and secondly, the calculations are performed based on PCR.

9.7.1 Analysis based on the intensity of three Raman bands

With the calibration curves, based on the intensity of three Raman bands of the active ingredient (818, 1238 and 1580 cm^{-1}), the amount of active ingredient in the 6 possible counterfeited Viagra[®] tablets is calculated.

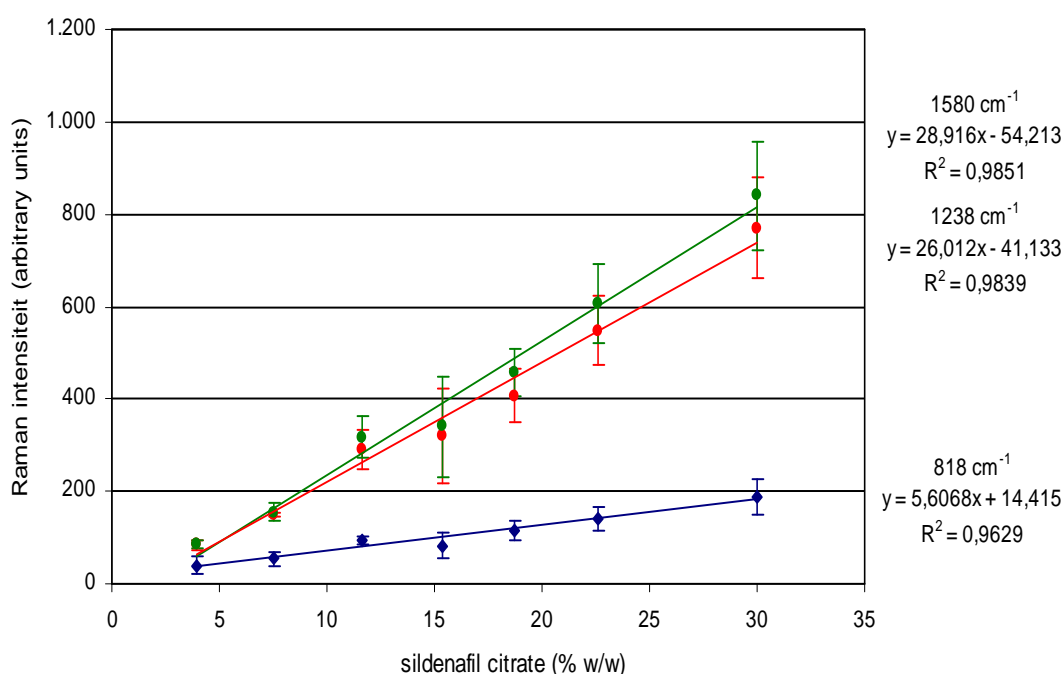


Figure 9.11 Average intensity and standard deviation in arbitrary units for 7 calibration tablets with the active ingredient sildenafil citrate analysed with the Renishaw system-1000 spectrometer (5 acc. x 30 s).

The calibration curves shown in figure 9.11 are expected to be similar to those presented in figure 9.8, since both are analysed with the Renishaw System-1000 spectrometer under the same conditions. Unfortunately, the decrease in intensity of the calibration curves shows the degradation of the Renishaw System-1000 spectrometer over the last two years. Results of the calculations using these calibration curves are presented in table 9.16.

Tablet	HPLC - DAD (% w/w)	Calculated amount active ingredient based on Raman spectroscopy and relative difference with the HPLC-DAD results.					
		818 cm ⁻¹		1239 cm ⁻¹		1580 cm ⁻¹	
		% w/w	% diff.	% w/w	% diff.	% w/w	% diff.
1	16	15	-6	13	-21	14	-16
2	17	24	46	22	33	22	32
3	12	14	14	16	28	16	29
4	15	19	31	19	31	19	30
5	15	29	97	28	93	28	91
6	17	20	21	21	21	21	21
average			47		46		44

Table 9.16 Calculated amount of active ingredient (% w/w) in the 6 Viagra[®] tablets with Raman spectroscopy (Renishaw System-1000 spectrometer, 5 acc. x 30 s) and HPLC-DAD with the relative difference between the two analytical methods (%). The average of all 6 tablets is calculated (square root of the average quadratic value).

For comparison of the methods, a paired t-test is performed ($\alpha = 0.05$). Based on the results of this t-test, there is no significant difference between the analyses with the Renishaw System-1000 spectrometer and the HPLC-DAD ($P = 0.06$, $P = 0.07$ and $P = 0.06$). It has to be noted that these results are just above the required $P > 0.05$ level.

When grinding the tablets, a decrease in difference would be expected. However, when looking at the average differences shown below, the opposite has occurred.

- Before grinding (paragraph 9.4.1.2) 29 – 33%
- After grinding 44 – 47%

Based on the results of the paired t-test, there is a significant difference ($P < 0.05$) for the results based on the intensity of the Raman band at 1239 cm^{-1} ($P = 0.03$). The other two Raman bands showed no significant difference between the results before and after grinding ($P = 0.43$ and $P = 0.22$). However, the average difference has increased after the grinding compared to results before. This suggest that the coating of the Viagra[®] tablets did not have a negative influence on the results of the quantitative analysis.

9.7.2 Analysis based on PCR

The Raman spectra used in paragraph 9.7.1 are used for PCR calculations. The difference between the results is based on comparison of the PCR calculations and the HPLC-DAD analyses. In table 9.17 till table 9.19, the average differences for the six Viagra[®] tablets for the first 5 PCs is presented. The calculations are performed on the raw data and the 1st and 2nd derivative.

- **Analysis with raw data:**

Tablet	Difference between Raman spectroscopy and HPLC-DAD analyses in (%)				
	1 PC	2 PCs	3 PCs	4 PCs	5 PCs
1	-68	43	-54	-68	-58
2	-39	-160	-81	-95	-83
3	3	-355	-48	-63	-60
4	-40	-129	-56	-79	-72
5	1	2	-107	-120	-112
6	-18	-135	-56	-66	-58
average	37	177	70	84	76

Table 9.17 Results of PCR analyses (raw data) with the use of Matlab. Difference (%) of calculated amount of active ingredient in the 6 Viagra[®] tablets between the Renishaw System-1000 spectrometer (5 acc. x 30 s) and HPLC-DAD. The average of 6 tablets is calculated (square root of the average quadratic value).

- **Analysis with 1st derivative:**

Tablet	Difference between Raman spectroscopy and HPLC-DAD analyses in (%)				
	1 PC	2 PCs	3 PCs	4 PCs	5 PCs
1	78	-60	6	8	8
2	73	-14	-33	-32	-31
3	89	-4	-20	-19	-20
4	81	-9	-33	-33	-33
5	74	-68	-88	-87	-86
6	78	-2	-29	-28	-28
average	79	38	43	42	42

Table 9.18 Results of PCR analyses (1st derivative). Difference (%) of calculated amount of active ingredient in the 6 Viagra[®] tablets between the Renishaw System-1000 spectrometer (5 acc. x 30 s) and HPLC-DAD analyses. Average of 6 tablets is calculated (square root of the average quadratic value).

- **Analysis with 2nd derivative:**

Tablet	Difference between Raman spectroscopy and HPLC-DAD analyses in (%)				
	1 PC	2 PCs	3 PCs	4 PCs	5 PCs
1	75	32	31	-52	28
2	46	-15	-17	-17	-19
3	62	-5	-5	-5	-5
4	58	-10	-11	-11	-15
5	26	-68	-70	-70	-75
6	51	-5	-8	-8	-15
average	55	32	32	37	35

Table 9.19 Results of PCR analyses (2nd derivative). Difference (%) of calculated amount of active ingredient in the 6 Viagra[®] tablets between the Renishaw System-1000 spectrometer (5 acc. x 30 s) and HPLC-DAD analyses. Average of 6 tablets is calculated (square root of the average quadratic value).

A paired t-test ($\alpha = 0.05$) is performed in order to see if there is a significant difference ($P < 0.05$) between the PCR results and results based on HPLC-DAD analyses (table 9.20).

Analyses based on PCR results	paired t-test ($\alpha = 0.05$)				
	1 PC	2 PCs	3 PCs	4 PCs	5 PCs
Raw data	0.10	0.04	0.00	0.00	0.00
1 st derivative	0.00	0.09	0.04	0.04	0.04
2 nd derivative	0.00	0.44	0.39	0.07	0.29

Table 9.20 Statistical evaluation (paired t-test) of the results based on PCR analyses (raw data, 1st derivative and 2nd derivative).

Based on the results of the paired t-test, there is a significant difference for the majority of the results, based on the analyses of the raw data and 1st derivative ($P < 0.05$). The results based on the 2nd derivative are not significantly different from the HPLC-DAD analyses since $P > 0.05$. Results based on analyses of the Viagra[®] tablets before grinding, show significant better results for the t-test (table 9.9).

Below, a short summary is presented where the results of the PCR calculations before and after grinding are compared.

	<i>Before grinding</i>	<i>After grinding</i>
• raw data	47 – 193%	37 – 177%
• 1 st derivative	21 – 26%	38 – 79%
• 2 nd derivative	21 – 23%	32 – 55%

Based on these results, it can be concluded that the coating of the Viagra[®] tablets has no negative influence on the quantitative analysis of the active ingredient in the six Viagra[®] tablets.

Moreover, the average difference after grinding has increased, compared to the results before grinding. Apparently, the fluorescence background increases after grinding, which can cause a larger error in quantification.

9.8 Conclusion

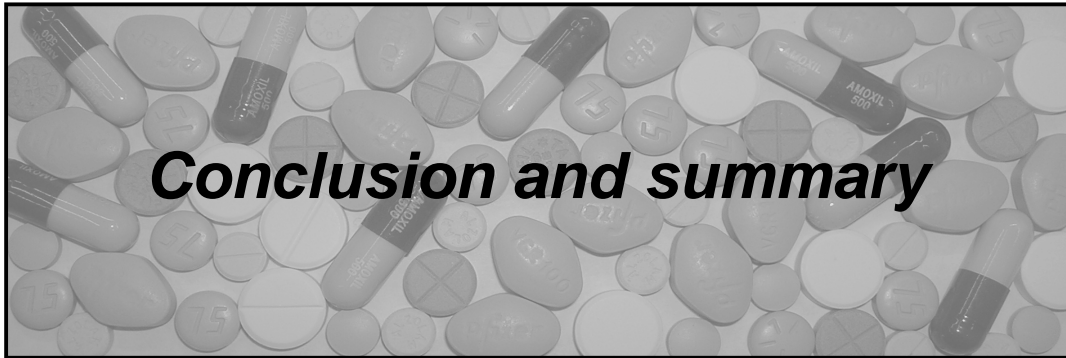
Based on the results of the quantitative analysis of counterfeit drugs some conclusions can be formulated:

- In our case, dispersive Raman spectroscopy generates better results compared to FT Raman. Additionally, the benchtop Renishaw system yields better results than the mobile MArtA spectrometer.
- Using the intensity of the three Raman bands generates better results than the use of the band areas, although the opposite would be expected since the band area is independent of broadening effects¹².
- Chemometrical approaches (PCA in combination with PCR) show better results than when based on a single Raman band. This is to be expected, since these chemometrical approaches incorporate the entire Raman spectrum.
- Grinding and repressing of the tablets show no improvement, which demonstrates that the coating of tablets has no specific influence on the quantitative analyses.

These results were confirmed with the use of a paired t-test ($\alpha = 0.05$). Similar results were obtained when analyzing circa 18 different paracetamol tablets, commercial as well as generic brands¹³. These results show that Raman spectroscopy, although an excellent method for qualitative analysis, needs improvement before being used as a quantitative analysis method for counterfeit drugs detection.

9.9 References

1. Lee DC and Webb ML , *Pharmaceutical analysis*, Oxford, Blackwell, 2003.
2. Szlagiewicz M, Marcolli C, Cianferani S, Hard AP, Vit A, Burkhard A, von Raumer M, Hofmeier UC, Zilian A, Francotte E, Schenker R, *J. Therm. Anal. Calorim.*, 1999; 57(1): 23-43.
3. Socrates G, *Infrared and Raman characteristic group frequencies: tables and charts*, 3rd ed., Wiley, Chichester, 2001.
4. Rodenas V, García MS, Sánchez-Pedreño C, Albero MI, *Talanta*, 2000; 52: 517-523.
5. Sheen CL, Dillon JF, Bateman DN, Simpson KJ, Macdonald TM, *QJ med*, 2002; 95: 609-619.
6. Hall KA, Newton PN, Green MD, Pizzanelli D, Mayxay M, Dondorp A, White NJ, Fernandez FM, *Am. J. Trop. Med. Hyg.* 2006; 75(5): 804-811.
7. Vredembregt MJ, Blok-Tip L, Hoogerbrugge R, Barends DM, de Kaste D, *J. Pharm. Biomed. Anal.* 2006; 40: 840-849.
8. Schaubroeck D, Brughmans S, Vercaemst C, Schaubroeck J, Verpoort F, *J. Mol. Catal. A-Chem.* 2006; 254 (1-2): 180-185.
9. Brereton RG, *Chemometrics, Chemometrics: data analysis for the laboratory and chemical plant*, John Wiley & Sons Ltd, Chichester, 2003.
10. Savitzky A, Golay MJE, *Anal. Chem.* 1964; 36; 8: 1627-1639.
11. Neter J, Kutner MH, Nachtsheim CJ, Wasserman W, *Applied linear statistical models*, 4th ed., Irwin, Chicago, 1996.
12. Skoog DA, West DM, Holler FJ, *Fundamentals of Analytical Chemistry*, 6th edition. Fort Worth (Tex.), Saunders college, 1992.
13. Thesis Anneleen Burggraeve, *Kwantitatieve analyse van de actieve bestanddelen in geneesmiddelen met Raman spectroscopie*, University Ghent, 2006-2007.
14. Lake OA, Slijkhuis C, Maas WF, van Vliet MEA, de Kaste D, Verdonk-Kleinjan W, RIVM report 670220001, Bilthoven, the Netherlands, 2001.



Conclusion and summary

Conclusion and summary

The amount of counterfeit drugs on the international market has increased rapidly over the last decade. Counterfeiting is an age-old practice, and is motivated mainly by the huge profits that can be made. According to the World Health Organization (WHO), a counterfeit drug is one which is deliberately and fraudulently mislabelled with respect to its identity and/or source. It can apply to both, branded and generic products. Counterfeit drugs, may include products with the correct ingredients or with the wrong ingredients, without active ingredients, with insufficient active ingredient or fake packaging.

Since counterfeiters are becoming more sophisticated, a simple visual inspection is not sufficient anymore. In literature, different analytical methods are described for the detection of counterfeit drugs. For instance, test-tube colour reactions, thin-layer chromatography (TLC), high performance liquid chromatography (HPLC), mass spectrometry (MS) and nuclear magnetic resonance (NMR). A downside of these methods is that it focuses on a specific active ingredient and gives less or no information of other substances present in the drugs. The method also requires extended sample preparation and highly trained analysts to interpret the results.

Raman spectroscopy (*chapter 2 and 3*) requires no sample preparation, the sample can be measured through glass or blister package, and above all, this technique is non-destructive. This research, focuses on the use of Raman spectroscopy for the fast detection of counterfeit drugs.

Examples of the qualitative analysis of counterfeit drugs with Raman spectroscopy are described in *chapter 5*. These counterfeit drugs are seized in Belgium and consist of erectile dysfunction drugs (Viagra[®] tablets, a gel with the active ingredient of Viagra[®] (sildenafil citrate) and tablets containing tadalafil, the same active ingredient as Cialis[®]), antibiotic (Amoxil[®]) used to treat numerous infections, and a drug to treat horses against parasites (Noromectin[®]). With the use of Raman spectroscopy, not only the content of these drugs were analysed, but the packaging and labels as well. By comparing these Raman spectra to those of the genuine products, the counterfeits could easily be detected.

This detection was based on the active ingredient, excipients present in the drug or inks used for the labels. These results, however, are only based on one or two seized examples of a specific drug.

Chapter 6 describes the qualitative analysis of 50 antimalarial tablets from southeast Asia, with the active ingredient artesunate. Based on the Raman spectra, 26 tablets contained the correct active ingredient but 24 tablets consisted of different substances. These tablets contained no detectable levels of artesunate and consisted of paracetamol (4-acetamidophenol), calcite (CaCO_3), or starch. The results are consistent with the results obtained by a colorimetric test for artesunate and by liquid chromatography mass spectrometry (LC-MS). Moreover, principal component analysis (PCA) combined with hierarchical cluster analysis (HCA) was used to establish an automated approach for the discrimination between different groups of counterfeits and genuine artesunate tablets.

Additionally, 18 possible counterfeit Viagra[®] tablets are qualitatively analysed (*chapter 7*). All the tablets contained the correct active ingredient, namely sildenafil citrate. However, when focusing on the Raman bands of excipients used in the tablets, differences could be noted. From the 18 tablets investigated, 6 are considered as genuine Viagra[®] tablets while 12 tablets are counterfeited since they contain less or other inactive compounds. Additionally, PCA combined with HCA, confirmed these findings.

Since counterfeits are detected, based on excipients present in the drugs, a database of excipients is established. For this database the Raman spectra of 43 commonly used pharmaceutical excipients are analysed and are presented in *chapter 8*.

So far, Raman spectroscopy shows to be a fast and easy detection method for the qualitative analysis of counterfeit drugs. Unfortunately, since the counterfeiters are becoming more sophisticated, quantitative analysis will be necessary as well. Since the intensity of the vibrational bands is directly proportional to the concentration of the species, Raman spectroscopy can be used for quantitative analysis.

The accuracy of the quantitative analysis can be significantly influenced by the homogeneity of the tablets used. The first step in the quantitative analysis process, described in *chapter 9*, is to develop homogenized calibration tablets. For this research, mixtures of paracetamol tablets are made, which were mixed during different times. Afterwards, tablets were pressed and a mapping was performed with the use of Raman spectroscopy. Based on the standard deviation of the intensity of the Raman band at 855 cm^{-1} , it was established that the homogeneity stabilized after 60-90 minutes of mixing. In order to minimize the error caused by inhomogeneity, the mixing time for the calibration tablets was set at 360 minutes.

Secondly, the influence of rotating the tablet during the analysis was investigated. Although the average intensity was similar for the analysis with and without rotation, the standard deviation of the measurements without rotation is circa 4 times higher. This research confirmed that the error between analyses significantly decreased by rotating the tablet. Based on these results, the tablets were rotated during quantitative analyses.

Next, *chapter 9* describes the quantitative analysis of 11 antimalarial tablets and 6 Viagra[®] tablets. Results are compared to LC-MS or HPLC combined with diode array detection (DAD) for the antimalarial tablets and Viagra[®] tablets, respectively. The quantitative analysis is either based on a single Raman band (intensity or area) or by using PCA combined with principal component regression (PCR), which integrates the entire Raman spectrum. Differences (%) are calculated between the amount of active ingredient as calculated with Raman spectroscopy and LC-MS or HPLC-DAD. Additionally, a paired t-test, with a 95% interval, is used to confirm these results.

First, quantitative analysis is performed by using the intensity of a specific Raman band. Calibration tablets are analysed and the function of the calibration curve based on the Raman bands is used to calculate the amount of active ingredient in the possible counterfeit tablets. The difference (%) between this amount and the reference method (LC-MS or HPLC-DAD) is calculated.

Based on this analysis, the difference for the antimalarial tablets ranges from 40 to 57% (MARTa spectrometer) while the difference for the Viagra[®] tablets ranges from 33 to 54% (MARTa spectrometer) and 29 to 32% (Renishaw System-1000 spectrometer). According to the paired t-test, the analysis with the MARTa spectrometer were predominantly significantly different compared to HPLC-DAD while the results with the Renishaw System-1000 spectrometer showed no significant difference (95% confidence interval). Therefore, for further quantitative research, the Renishaw System-1000 spectrometer is used. Since the area of a Raman band is independent of broadening effects, these last results are recalculated by using the area of the three Raman bands. However, using the area, instead of a decrease, the average difference with HPLC-DAD increased from 29 - 32% up to 30 - 39%. With the use of the paired t-test ($\alpha = 0.05$) no significant difference ($P > 0.05$) could be noted between the calculations based on the intensity and the area of the three Raman bands ($P = 0.58$, $P = 0.61$ and $P = 0.89$).

Chemometrical approaches (PCA combined with PCR) are used on the Raman spectra (Renishaw system-1000) of the Viagra[®] tablets. Calculations are performed using the first 5 principal components (PC), in combination with the raw data or derivatives (1st and 2nd). By using derivatives, the influence of the broad-featured fluorescence background can be minimized. The average difference for the Viagra[®] tablets ranges from 47 to 193% (raw data), 21 to 26% (1st derivative) and 21 to 23% (2nd derivative). By using derivatives, a higher accuracy is created when comparing these to the results based on the intensity of a single Raman band. In addition, a t-test shows that there is significant difference between PCR results based on the raw data and results based on HPLC-DAD analysis. No significant difference based on the paired t-test can be found between the results based on the 1st and 2nd derivative.

Commonly, quantitative analysis is performed with Fourier Transform (FT) Raman spectroscopy rather than dispersive Raman spectroscopy (MARTa and Renishaw System-1000). In order to check if the analysis can be improved, the Viagra[®] tablets are analysed with a Bruker Equinox 55S FT Raman spectrometer. However, FT-Raman spectroscopy shows less promising results than by using the Renishaw System-1000 spectrometer. This can be caused by difficulties positioning the tablets

in the laser beam, due to the standard sample holder of the Bruker Equinox 55S instrument. With the Renishaw system-1000 spectrometer, the microscope enhances focusing the laser beam on the sample. Moreover, when using the Bruker Equinox 55S spectrometer the samples could not be rotated, to cover sample inhomogeneity. Based on this quantitative analysis, the best results were achieved by using dispersive Raman spectrometry (Renishaw System-1000). Results with the use of PCA in combination with PCR showed the most promising results when used in combination with the 1st or 2nd derivative.

Finally, the presence of the blue coating of the Viagra tablets might have an influence on the quantitative analysis. The Viagra[®] tablets were grinded, thoroughly mixed and repressed and analysed (Renishaw system-1000 spectrometer). When comparing the results before and after grinding, no improvement can be detected, indicating that the coating has no negative effect on the quantitative analysis with Raman spectroscopy.

This research shows that Raman spectroscopy can be used as a fast and easy method of analysis for the qualitative detection of counterfeit drugs. A major topic of interest still remains; improving the quantitative analysis of counterfeit drugs with dispersive Raman spectroscopy. For further research, other chemometrical approaches, such as partial least squares regression (PLS-regression) can be investigated to see if the analysis can be improved. Additionally, the use of Raman spectroscopy as quantitative method of analysis should to be demonstrated on a larger number of counterfeit drugs, in order to see if our findings are consistent. This is an interesting item for further research and a real challenge to demonstrate the use of dispersive Raman spectroscopy for the detection of counterfeit drugs, qualitative as well as quantitative.



Conclusie en samenvatting

Samenvatting en besluit

De laatste jaren is de hoeveelheid vervalste geneesmiddelen op de internationale markt snel toegenomen. Vervalsingen bestaan al eeuwen en de voornaamste drijfveer zijn de enorme winsten die behaald kunnen worden. Volgens de Wereldgezondheidsorganisatie (World Health Organization, WHO) worden vervalsingen als volgt gedefinieerd: doelbewust en frauduleus verkeerd gelabelde producten met betrekking tot identiteit en/of oorsprong. Zowel merk- als generische producten kunnen worden vervalst. Er zijn verschillende soorten vervalsingen, namelijk met de correcte ingrediënten in de verkeerde verpakking, met de verkeerde ingrediënten, zonder actieve ingrediënten of met een te lage concentratie actief ingrediënt.

Aangezien vervalsers steeds beter worden in het vervalsen van geneesmiddelen, is een eenvoudige visuele inspectie van het medicijn en haar verpakking niet meer voldoende. In de literatuur worden verschillende analytische methoden beschreven voor de detectie van vervalste geneesmiddelen. Enkele voorbeelden hiervan zijn colorimetrie, dunnelaagchromatografie (TLC), hogedrukvlloeistofchromatografie (HPLC), massaspectrometrie (MS) en kernspinresonantie (NMR). Een nadeel van deze methoden is dat zij gericht zijn op een specifiek actieve ingrediënt en er weinig of geen informatie vrijkomt over andere stoffen aanwezig in het medicijn. Bovendien vergen deze methodes veel monstervoorbereiding en is er een gespecialiseerde analist nodig om de resultaten te interpreteren.

Dit onderzoek richt zich op de snelle detectie van vervalste geneesmiddelen met behulp van Raman spectroscopie. Raman spectroscopie (*hoofdstuk 2 en 3*) vereist geen monstervoorbereiding, het medicijn kan geanalyseerd worden door glas of de plastic verpakking en is bovenal niet destructief.

Hoofdstuk 5 beschrijft enkele voorbeelden van de kwalitatieve analyse van vervalste geneesmiddelen met Raman spectroscopie. Deze vervalsingen zijn onderschept in België en bestaan uit erectiepillen (Viagra[®] tabletten, een gel met het actieve ingrediënt van Viagra[®] (sildenafil citraat) en tabletten met tadalafil, hetzelfde actieve ingrediënt als Cialis[®]), antibiotica (Amoxil[®]) gebruikt voor verschillende infecties en

een medicijn gebruikt voor het bestrijden van parasieten bij paarden (Noromectine[®]). Met behulp van Raman spectroscopie is niet alleen de inhoud van deze geneesmiddelen geanalyseerd, maar eveneens de verpakking en etiketten. De Raman spectra zijn vergeleken met spectra van de originele producten en op basis hiervan konden de vervalsingen eenvoudig gedetecteerd worden. De vervalsingen zijn gedetecteerd op basis van het actieve ingrediënt of vulmiddelen gebruikt in het medicijn of op basis van de inkt gebruikt voor de labels. Deze resultaten zijn echter alleen gebaseerd op 1 à 2 stalen van een specifiek medicijn.

Hoofdstuk 6 beschrijft de kwalitatieve analyse van 50 antimalaria tabletten uit Zuidoost-Azië met het actieve ingrediënt artesunaat. Op basis van de Raman spectra, kon worden bepaald dat 26 tabletten het juiste actieve ingrediënt bevatten en dat 24 tabletten bestonden uit andere producten. Na verdere analyse bleek dat de 24 tabletten bestonden uit paracetamol (4-acetamidophenol), calcium carbonaat (CaCO₃) of zetmeel. Deze resultaten komen overeen met de resultaten van een colorimetrische test specifiek voor artesunaat en vloeistofchromatografie gekoppeld met massaspectrometrie (LC-MS). Door middel van het gebruik van principale componenten analyse (PCA) en hiërarchische clusteranalyse (HCA) konden de vervalsingen eveneens van de echte tabletten worden onderscheiden.

Voorts werden er 18 mogelijk vervalste Viagra[®] tabletten kwalitatief geanalyseerd (*hoofdstuk 7*). Op basis van de Raman spectra bleek dat alle tabletten het correcte actief ingrediënt (sildenafil citraat) bevatte. Wanneer echter werd gekeken naar Raman banden afkomstig van vulmiddelen, konden verschillen worden waargenomen. Van de 18 tabletten bleken 12 tabletten vervalst te zijn, aangezien ze minder vulmiddel of andere vulmiddelen bevatten. Deze resultaten werden bevestigd door het gebruik van PCA in combinatie met HCA.

Aangezien een deel van de vervalsingen konden worden gedetecteerd op basis van de vulmiddelen in het medicijn, is er een databank opgezet. Deze databank bevat de Raman spectra van de 43 meest gebruikte vulmiddelen en wordt beschreven in *hoofdstuk 8*.

Tot nu toe is aangetoond dat Raman spectroscopie een gemakkelijke en snelle detectiemethode is voor de kwalitatieve analyse van vervalste geneesmiddelen. Helaas worden de vervalsers steeds geraffineerder en is kwantitatieve analyse noodzakelijk geworden. Aangezien de intensiteit van de Raman banden evenredig is met de concentratie kan Raman spectroscopie gebruikt worden voor kwantitatieve analyse. De nauwkeurigheid van de kwantitatieve analyse kan worden beïnvloed door de homogeniteit van de te analyseren tabletten.

De eerste stap bij kwantitatieve analyse is het produceren van homogene calibratie tabletten (*hoofdstuk 9*). Voor deze analyses worden mengsels voor paracetamol tabletten voor een bepaalde tijd gemengd. Hierna worden de tabletten geperst en wordt er een mapping uitgevoerd van de tablet met behulp van Raman spectroscopie. Met behulp van de standaarddeviatie van de intensiteit van de Raman band (855 cm^{-1}) blijkt dat deze constant blijft na een mengtijd van circa 60 minuten. Op basis hiervan is besloten dat voor de aanmaak van de calibratie tabletten een mengtijd van 360 minuten wordt gebruikt om de homogeniteit van de tabletten zeker te stellen.

Eveneens is er gekeken naar de invloed van rotatie van het tablet tijdens de analyses. Voor dit onderzoek werd een paracetamol tablet 30 maal geanalyseerd met behulp van rotatie en zonder rotatie. Na 30 analyses bleek de gemiddelde intensiteit gelijkaardig te zijn. De standaarddeviatie van analyses zonder rotatie bleek echter ca. 4 maal hoger te liggen dan met rotatie. Op basis van deze resultaten is besloten tijdens kwantitatieve analyses de tabletten te roteren.

Vervolgens wordt in *hoofdstuk 9* de kwantitatieve analyse van 11 antimalaria tabletten en 6 Viagra[®] tabletten weergegeven. Deze resultaten werden vergeleken met LC-MS en HPLC in combinatie met diode array detectie (DAD) voor de antimalaria en Viagra[®] tabletten, respectievelijk. De kwantitatieve analyse is gebaseerd op de intensiteit of oppervlakte van een enkele Raman band of met behulp van PCA in combinatie met Principale Componenten Regressie (PCR), die gebruik maakt van het hele Raman spectrum.

Verschillen worden berekend (%) tussen de hoeveelheid actieve ingrediënt bepaald met Raman spectroscopie en LC-MS of HPLC-DAD. Om te bepalen of er significant verschil is tussen de twee methoden, wordt er een gepaarde t-toets (95% betrouwbaarheids niveau) uitgevoerd.

Als eerste wordt de kwantitatieve analyse uitgevoerd op basis van de intensiteit van een specifieke Raman band. Met behulp van calibratietabletten wordt de calibratiecurve opgesteld. De functie van deze calibratiecurve wordt gebruikt om de hoeveelheid actief ingrediënt in de mogelijke vervalste tabletten te berekenen. Het verschil in percentage wordt bepaald tussen deze hoeveelheid en de referentiemethode (LC-MS of HPLC-DAD). Gebaseerd op deze analyse varieert het verschil voor de antimalaria tabletten tussen de 40 en 57% (MArtA spectrometer) terwijl het verschil voor de Viagra[®] tabletten varieert tussen 33 en 54% (MArtA spectrometer) en tussen de 29 en 32% (Renishaw system-1000 spectrometer). Aan de hand van de gepaarde t-toets bleek dat de resultaten bepaald met de MArtA spectrometer significant verschillen met de referentie analyses terwijl de resultaten met de Renishaw system-1000 spectrometer niet significant verschillen. Voor verdere analyses werd er dus gebruik gemaakt van de Renishaw system-1000 spectrometer.

Bij kwantitatieve analyses wordt er voornamelijk gebruik gemaakt van de oppervlakte van een band in plaats van de intensiteit. Dit komt omdat de oppervlakte van een band onafhankelijk is van mogelijke verbredingseffecten. De resultaten verkregen voor de Viagra[®] tabletten met de Renishaw system-1000 spectrometer worden herbekend op basis van de oppervlakte. Uit deze resultaten blijkt echter dat het verschil niet afneemt, maar toeneemt van 29 – 32% tot 30 – 39%. De resultaten van de gepaarde t-toets ($\alpha = 0,05$) laten zien dat er geen significant verschil ($P > 0,05$) is tussen beide methoden ($P = 0,58$, $P = 0,61$ en $P = 0,89$).

Chemometrische analysemethoden (PCA in combinatie met PCR) worden gebruikt op de analyse van de Viagra[®] tabletten met de Renishaw system-1000 spectrometer. Berekeningen worden uitgevoerd met gebruik van de eerste vijf principale componenten (PC). Niet alleen de onbewerkte data, maar ook de 1^{ste} en 2^{de} afgeleide van deze data worden gebruikt.

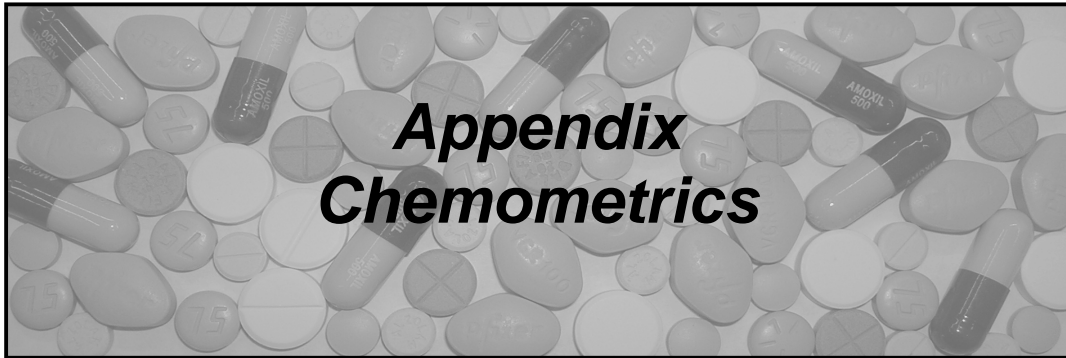
Door middel van het gebruik van deze afgeleiden van de Raman spectra, kan de invloed van de achtergrondfluorescentie worden geminimaliseerd. Het gemiddelde verschil voor de Viagra[®] tabletten varieert van 47 tot 193% (onbewerkte data), van 21 tot 26% (1^{ste} afgeleide) en van 21 tot 23% (2^{de} afgeleide). Met behulp van de afgeleiden worden er betere resultaten verkregen dan in vergelijking met analyses gebaseerd op een enkele Raman band. Met behulp van de gepaarde t-test bleek er een significant verschil te zijn tussen de HPLC-DAD resultaten en de Raman analyse op basis van de onbewerkte Raman data. Er bleek echter geen significant verschil te bestaan voor de resultaten gebaseerd op de 1^{ste} en 2^{de} afgeleide.

In het algemeen wordt kwantitatieve analyse vaak uitgevoerd met behulp van Fourier Transform (FT) Raman spectroscopie in plaats van het dispersieve Raman spectroscopie (MArtA en Renishaw system-1000). Daarom worden de Viagra[®] tabletten nogmaals geanalyseerd, nu met behulp van een Bruker Equinox 55S – FT Raman spectrometer. Desondanks resulteerden deze analyses in slechtere resultaten dan met behulp van de Renishaw system-1000 spectrometer. Dit kan veroorzaakt worden de problemen met het focuseren van de laser op de tablet, aangezien bij de Bruker Equinox 55S gebruik wordt gemaakt van een standaardhouder. Bij de Renishaw system-1000 spectrometer wordt de laser met behulp van een microscoop gefocuseerd op het staal. Eveneens kan bij de Bruker Equinox 55S het staal niet worden geroteerd tijdens de analyses.

Gebaseerd op deze kwantitatieve analyses, blijken de beste resultaten verkregen te worden met behulp van de dispersieve Raman spectrometer (Renishaw system-1000). PCA in combinatie met PCR gaf de meest belovende resultaten wanneer gecombineerd met de 1^{ste} of 2^{de} afgeleiden. Als laatste wordt de invloed van de blauwe coating van de Viagra[®] tabletten onderzocht. De tabletten worden vermalen, gemengd en opnieuw geperst. Hierna worden de tabletten opnieuw geanalyseerd met de Renishaw system-1000 spectrometer. Uit vergelijking van deze resultaten met de analyses voordat de tabletten werden vermaald, blijkt dat er geen verbetering optreedt. Dit betekent dat de coating geen negatieve effect heeft op de kwantitatieve analyse met behulp van Raman spectroscopie.

Dit onderzoek toont aan dat Raman spectroscopie gebruikt kan worden als een snelle en gemakkelijke analysemethode voor de kwalitatieve detectie van vervalste geneesmiddelen.

Een belangrijk onderwerp voor toekomstig onderzoek is de kwantitatieve analyse van de vervalsingen met behulp van dispersieve Raman spectroscopie. Voor vervolgonderzoek kunnen andere chemometrische methoden worden onderzocht, zoals bijvoorbeeld partiële kleinste kwadraten regressie (PLS). Eveneens zou het gebruik van Raman spectroscopie voor kwantitatieve analyse op een grotere hoeveelheid vervalste geneesmiddelen moeten worden onderzocht, om na te gaan of deze techniek geschikt is. Dit is een zeer interessant onderwerp voor verder onderzoek en een belangrijke uitdaging om in de toekomst Raman spectroscopie, zowel kwalitatief als kwantitatief, te kunnen toepassen voor de detectie van vervalste geneesmiddelen.



***Appendix
Chemometrics***

Appendix: Chemometrics

Chemometrics is used for many different applications in chemistry, for instance in physical chemistry (kinetics, equilibrium studies, etc.), reaction optimisation in organic chemistry, theoretical chemistry and in many areas of chromatography and spectroscopy¹.

In this appendix, different chemometrical techniques used during this research project are briefly described. These chemometrical techniques are:

1. Window functions:
 - moving average filters (MA)
 - Savitsky-Golay filters
 - derivatives (first and second)
2. Principal Component Analysis (PCA)
3. Principal Component Regression (PCR)
4. Hierarchical Cluster Analysis (HCA)

1 Window functions

Every signal contains always a certain amount of noise, which influences the quality of the signal in a negative way. This hampers the interpretation of spectroscopic data. An increase of noise can also lead to an increase in error during calibration. Therefore, an important step in using chemometrics for spectroscopic methods like Raman spectroscopy, is smoothing of a spectrum. A number of filters have been developed to decrease the amount of noise in a spectrum whilst the intensity of the signal remains. In this part, only the moving average filter as well as the Savitsky-Golay filter will be described.

An example of an easy to apply filter is the moving average (MA) filter, which comes with $2N+1$ points, with N being a positive integer. For instance, the 3 points MA filter uses an average for each point made from itself, the point before and the point after, hence, a 3 points filter¹. As can be expected, the 5 points MA filter includes 2 points before and 2 points after the re-calculated data point. This is illustrated in figure 1, where part from the Raman spectrum of a genuine artesunate tablet is shown.

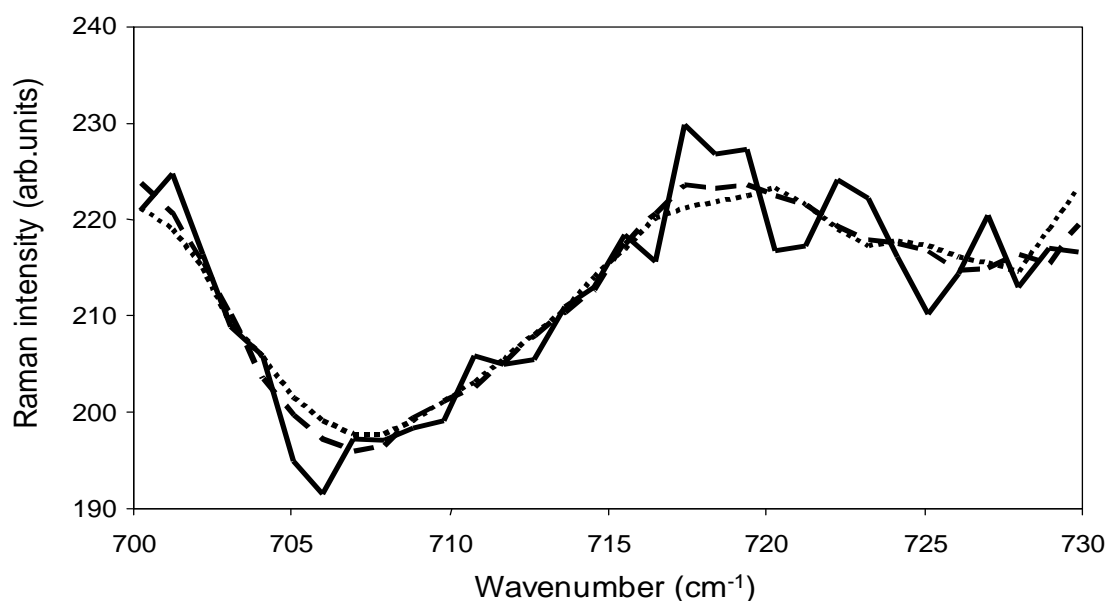


Figure 1. The solid line represents the raw data of the Raman spectrum of an artesunate tablet, the striped line is the filtering of the data with a 5 points MA filter, and the dotted line is the filtering of the data with a 7 points MA filter

When increasing the number of points in the MA filter, the influence of the noise decreases, but the signal becomes more flattened. Another disadvantage of these MA filters is that a linear approximation is used, while the bands in a Raman spectrum are best estimated by using a polynomial function¹.

Abraham Savitsky and Marcel J.E. Golay presented an alternative for the MA filters in 1964². This filter involves simple summations and is widely used in analytical chemistry, especially in chromatography³. The principal goal of the Savitsky-Golay filter is to smooth the data, to decrease the noise level, and to avoid blurring of the signal.

Each filter is characterized by a window size and an order of a polynomial (quadratic, cubic, etc.)³. The next step is to multiply each data point within the window with a specific coefficient (c_{i+j}) and then to divide it by the normalization constant, depending on the window size and order of polynomial. Here, c_i represents the coefficient of the point in the spectrum which is re-calculated with the Savitsky-Golay filter and j represents the data points below and above this data point.

The normalization constant is the sum of the Savitsky-Golay coefficients, size depending on a 5, 7 or 9 points filter. The coefficients and normalization constants for these three filters are shown in Table 1.

Window size j	5 points	7 points	9 points
- 4			- 21
- 3		- 2	14
- 2	- 3	3	39
- 1	12	6	54
0	17	7	59
1	12	6	54
2	- 3	3	39
3		- 2	14
4			- 21
normalization constant	35	21	231

Table 1. Quadratic Savitsky-Golay coefficients c_{i+j} for smoothing^{1,2,5}.

The coefficients c_{i+j} in table 1 are used to obtain the coefficients (number depending on how many points are used in the filter) which will be used to calculate the smoothed value from the raw data^{1,2,3}.

For instance, the five coefficients for a 5 points quadratic filter are:

- $c_{i-2} = c_{i+2} = - 3 / 35 = - 0.086$
- $c_{i-1} = c_{i+1} = 12 / 35 = 0.343$
- $c_i = 17 / 35 = 0.486$

These coefficients are then used to multiply them with the data; the sum is the smoothed value of the data¹:

$$X_{i,new} = - 0.086 \cdot X_{i-2} + 0.343 \cdot X_{i-1} + 0.486 \cdot X_{i,original} + 0.343 \cdot X_{i+1} - 0.086 \cdot X_{i+2}$$

where $X_{i,\text{original}}$ represents the original datapoint being re-calculated into $X_{i,\text{new}}$. X_{i-1} and X_{i-2} represents the two datapoints left from $X_{i,\text{original}}$ while X_{i+1} and X_{i+2} represents the datapoints right from $X_{i,\text{original}}$.

In figure 2, the effect of the Savitsky-Golay filter is illustrated by using the raw data of the Raman spectrum of a genuine artesunate tablet as shown in figure 1. It shows the raw data (solid line) and the effect of Savitsky-Golay filters (5 and 7 points), presented as the striped and dotted line.

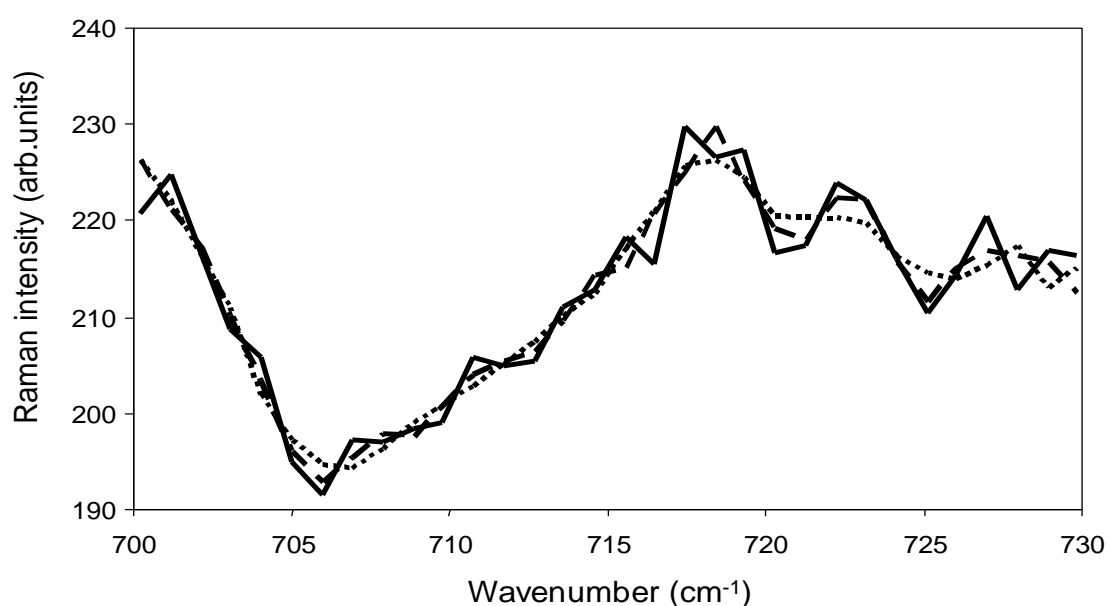


Figure 2. The solid line represents the raw data of the Raman spectrum of an artesunate tablet, the striped and dotted line represent the filtering of the data with two different quadratic Savitsky-Golay filter, namely the 5 (striped) and 7 points filters (dotted).

The moving average filter and the Savitsky-Golay filter both smooth the Raman spectrum by removing part of the noise. The downside of these filters is the decrease in intensity, which is more obvious with the MA filters than the Savitsky-Golay filters. To emphasize these differences, figure 3 shows in more detail a small part of the spectra shown in figure 1 and 2.

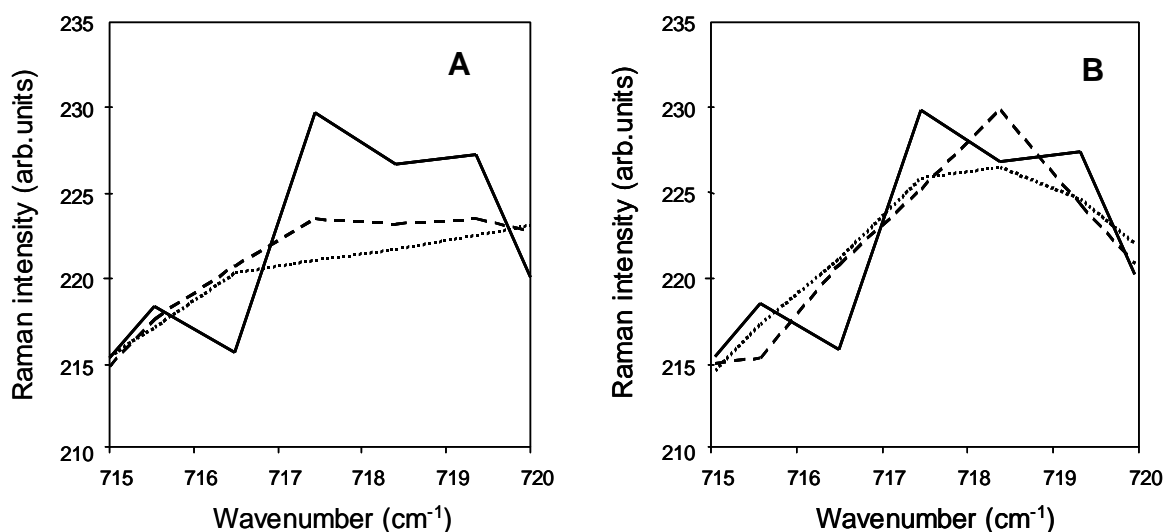


Figure 3. (A) Moving average filters (detail figure 1) and (B) Savitsky-Golay filters (detail figure 2). The red line represents the raw data of the Raman spectrum while the blue and green line represent the filtering of the data with a 5 and 7 points filters, respectively.

When focussing on the intensity of the Raman band between 717 cm^{-1} and 718 cm^{-1} it turns out that MA filters tend to broaden the bands more than the Savitsky-Golay filters. Hence, this illustrates that Savitsky-Golay filters are better suitable than moving average filters, which is logical since the Savitsky-Golay filter is based on a polynomial function.

Once the Raman spectrum has been smoothed, the maximum of a Raman band can be determined by a simple method, using derivatives, mainly first and second¹. The principle behind the method is that inflection points (maximum of a Raman band) become turning points in the derivatives. The first derivative equals zero at the centre of the peak and exhibits two turning points. The second derivative has a minimum at the centre of the peak and crosses zero at the positions of the turning points of the first derivative³. By using the first derivative, it is easy to pinpoint the exact position of the Raman band, but overlapping Raman bands are not detected. However, with the second derivative two overlapping bands can be easily separated. This can be seen in figure 4 where two closely overlapping bands are shown (A) and the first (B) and second derivative (C). The second derivative clearly indicates two bands, and fairly accurately pinpoints their positions¹.

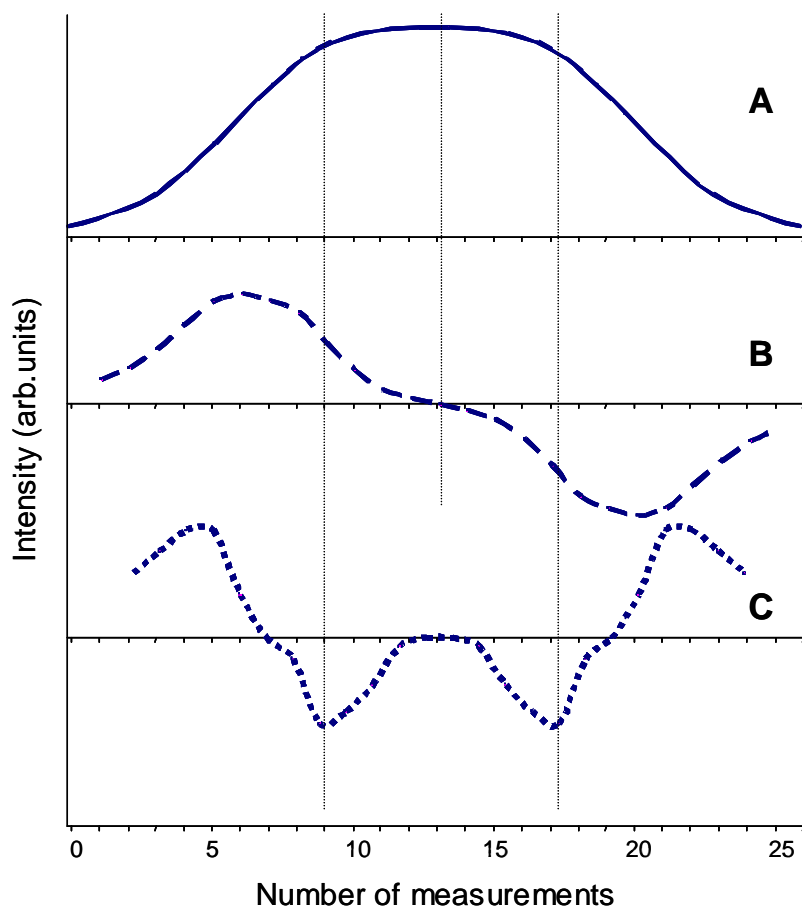


Figure 4. Two closely overlapping bands (A, solid line) together with their first (B, striped line) and second derivatives (C, dotted line)¹.

In order to use derivatives, the Raman bands have to consist of sufficient data points, so that there is sufficient information for calculating the derivatives³. A disadvantage of derivatives is that noise is amplified substantially¹.

2 Principal Component Analysis (PCA)

After applying the filters and/or derivatives, principal component analysis (PCA) can be applied. PCA is mathematical method for reducing a large dataset to a much smaller, more manageable dataset, which can be interpreted more easily¹. This is the most widespread multivariate chemometric technique used nowadays^{1,3}. It can be used when a dataset which contains a large number of variables, as for instance with spectroscopic data.

During PCA, the principal components (PC's) are calculated, which are the variables that account for the majority of the variability in the spectroscopic data³. A benefit of this method is that, even though the dataset has been reduced, a very high percentage of the information content is retained (usually more than 99,9%)³.

PCA results in an abstract mathematical transformation of the original data matrix, which takes the following form (equation 4.1)¹:

$$\mathbf{X} = \mathbf{T} \cdot \mathbf{P} + \mathbf{E} \quad (\text{eq. 4.1})$$

\mathbf{X} = original data matrix

\mathbf{T} = scores (as many rows (samples) as the original data matrix)

\mathbf{P} = loadings (as many columns (wavelengths) as the original data matrix)

\mathbf{E} = error matrix

The scheme, as presented in figure 5, visualizes this process.

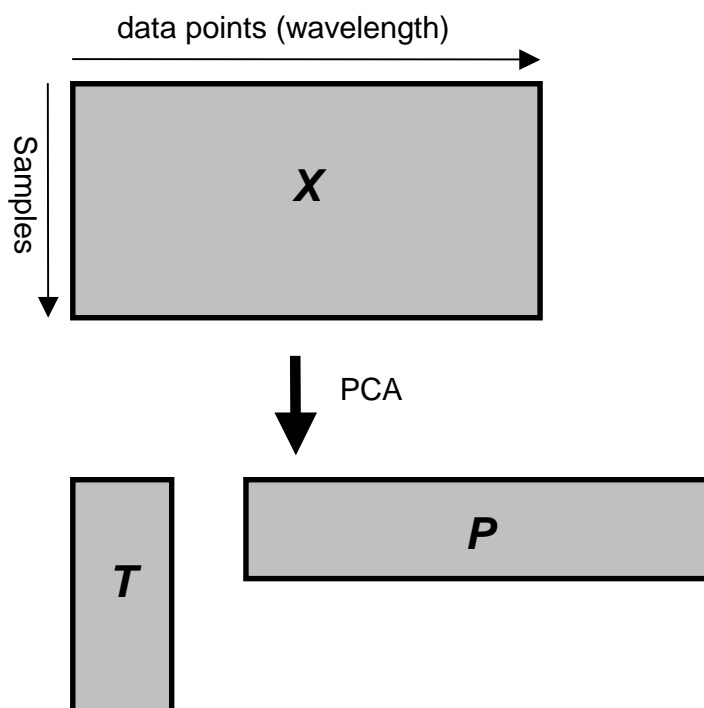


Figure 5. Principal Component Analysis (PCA)¹.

To illustrate the use of PCA, the Raman spectra of the artesunate tablets, measured from 200 till 1800 cm^{-1} , which involves about circa 1600 data points for each spectrum are used.

The averages of three spectra recorded for each tablet, have been used to construct a data matrix. This matrix consists of circa 1600 columns and 50 rows (samples). The first 10 principal components (PCs) were calculated. Table 2 shows the percentage of the variance that is captured by each PC and the cumulative percentage of the variance captured.

<i>PC Number</i>	<i>% variance captured by PC</i>	<i>% variance captured total</i>
1	94.54	94.54
2	3.20	97.74
3	1.39	99.13
4	0.44	99.57
5	0.20	99.77
6	0.09	99.86
7	0.05	99.90
8	0.02	99.93
9	0.02	99.95
10	0.01	99.96

Table 2. Information of the first 10 PCs on the data matrix of the Raman spectra of the 50 artesunate tablets from the antimalarial research project.

The first PC (94.54 % variance captured) is the direction through the data that explains the largest possible variation in the data and accounts for most of the information⁵. The second PC (3.20 % variance captured) is orthogonal to the first PC while PC 3 (1.39 % variance captured) is at right angles to the first two PCs. It shows that the first three principal components contain more than 99 % of the variance (information) that can be retrieved from the circa 1600 data points for the 50 tablets.

3. Principal Component Regression

Principal component regression (PCR) is considered as a form of factor analysis and has been very useful in spectroscopy since the 1970s and is used for quantitative analysis¹. PCR is of significant interest when analysing mixtures, for instance drugs, with Raman spectroscopy, since not all compounds in the drug are known or can even be identified. There are a few steps that need to be undertaken when performing PCR, which are shown in figure 6.

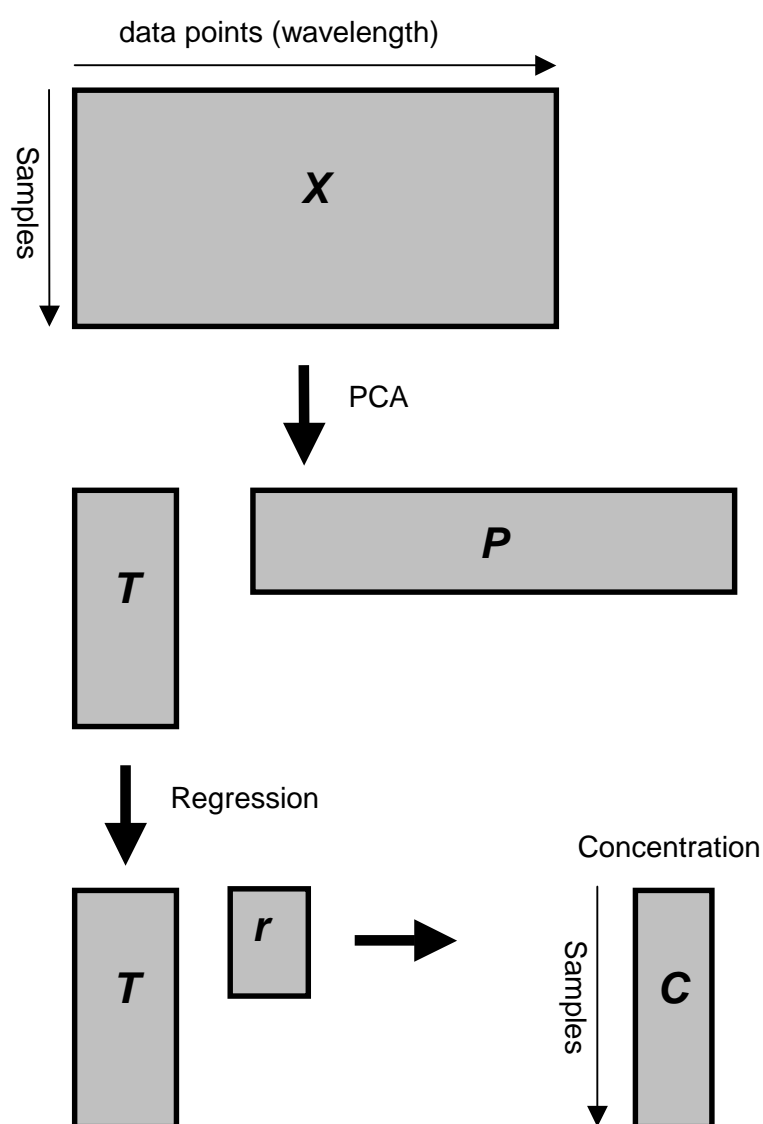


Figure 6. Principal Components Regression (PCR)¹.

The first step is to obtain a matrix with the data of all the samples, for instance a 50 x 1600 data matrix for the case of the artesunate samples. The next step is to perform PCA on the data to obtain the scores (**T**) and loadings matrices (**P**).

A crucial step is to determine how many PCs should be retained in order to perform PCR. In this step a relationship is determined between the scores (**T**) and the true concentrations (*c*) of each sample by using the equation $c = \mathbf{T} \cdot \mathbf{r}$. Where **r** stands for a column vector, whose length equals the number of PCs retained, also called a rotation or transformation vector¹.

The principles behind PCR are fairly straightforward and involve performing a PCA and subsequently regressing the components. The final step is to establish a correlation between the Raman spectrum and the concentration¹.

4 Hierarchical Cluster Analysis (HCA)

The final step in our qualitative analysis of counterfeit drugs, is hierarchical cluster analysis (HCA). In this process, the results of PCA are used. Cluster analysis can be used by chemists, to see if there is a relationship between different samples in a dataset¹.

Using a few principal components, it is possible to see if there is a similarity between different samples and draw a picture of these similarities, such as a dendrogram. In this dendrogram, the groups that are closely related, are closer to each other and the groups with less similarity are presented further from each other.

The first step in HCA is to determine the similarity between different Raman spectra³. A number of common numerical measures of similarity are available; in this appendix the correlation coefficient, Euclidian distance and Mahalanobis distance will be discussed^{1,3}.

- *Correlation coefficient*

The correlation coefficient has a value between -1 and +1. A correlation coefficient of 1 (+1 or -1) implies identical characteristics, while a value near zero makes it difficult to use a variable to predict another³. The coefficient is calculated using the equation 4.2^{1,5,6}.

$$r_{xy} = \frac{\text{COV}_{xy}}{s_x \cdot s_y} = \frac{\sum_{i=1}^l (x_i - \bar{x})(y_i - \bar{y})}{\sqrt{\sum_{i=1}^l (x_i - \bar{x})^2 \sum_{i=1}^l (y_i - \bar{y})^2}} \quad (\text{eq. 4.2})$$

r_{xy}	=	Pearson correlation coefficient
COV_{xy}	=	Covariance of the variables x and y
s_x, s_y	=	Standard deviations of x and y
x_i, y_i	=	Samples x and y
\bar{x}, \bar{y}	=	Sample means of variables x and y
l	=	Number of measurements

- *Euclidean distance*

The distance between samples k and l can be calculated using equation 4.3^{3,6}:

$$d_{kl} = \sqrt{\sum_{i=1}^l (x_{ki} - x_{li})^2} \quad (\text{eq. 4.3})$$

d_{kl}	=	Euclidean distance between k and l
l	=	Number of measurements
k, l	=	Indices for objects k and l
x_{kj}	=	j^{th} measurement on sample k

The Euclidean distance works the opposite way, compared to the correlation coefficient, since a value close to zero means a higher similarity³. Sometimes the equation is presented in matrix format (equation 4.4)^{1,6}.

$$d_{kl} = \sqrt{(x_k - x_l) \cdot (x_k - x_l)'} \quad (\text{eq. 4.4})$$

Where x_k and x_l represents the column vectors for object k and l , respectively. In this format, the objects are row vectors making it easy to implement in excel or matlab¹.

- *Mahalanobis distance*

This method is quite similar to the Euclidean distance, but it also takes into account that some variables may be correlated and so measure more or less the same properties¹. The distance between samples k and l is defined in matrix terms by equation 4.5¹:

$$d_{kl} = \sqrt{(x_k - x_l) \cdot C^{-1} \cdot (x_k - x_l)'} \quad (\text{eq 4.5})$$

where C is the variance-covariance matrix of the variables, whose elements represent the covariance between any two variables. This variance-covariance matrix is inserted as a scaling factor and that distinguishes this Mahalanobis distance from the Euclidean distance¹. The downside of this method is that it can not be easily applied to a matrix where the number of variables exceeds the number of objects, since in that case, the variance-covariance matrix can not have an inverse.

The next step in the hierarchical cluster analysis, is to link the different objects. There are numerous linkage methods, but the most commonly used one is the agglomerative clustering where the objects are connected to each other in groups^{1,3}.

The first step in this clustering protocol is to find the two most similar objects from the raw data. These will be the object with the highest correlation coefficient or smallest distance and these two objects will form a “group”³. The next step is to look at the numerical similarity values between this new group and the remaining objects, for this there are three important methods available, namely^{1,3}:

- *Nearest neighbour*

With this method, the new group is compared to the other objects. The object with the highest similarity is then linked to this new group. This method will continue until all objects are linked to each other, also called a dendrogram^{1,3}.

- *Furthest neighbour*

This method is the opposite of the nearest neighbour, and hence the lowest similarity within the group is used³.

- *Average linkage*

There are two different ways of applying the average linkage, namely unweighted or weighed, which is according to the size of each group being joined together¹.

If they are equal of size both methods are equivalent¹.

- Weighted. The distance d to a new object or cluster k is computed by calculating the average distance from the objects A and B to i . The new similarity is given by equation 4.6⁶:

$$d_{ki} = (d_{Ai} + d_{Bi})/2 \quad (\text{eq. 4.6})$$

- Unweighted. The number of objects in a cluster is used for weighting the cluster distances which is given by (eq. 4.7)⁶:

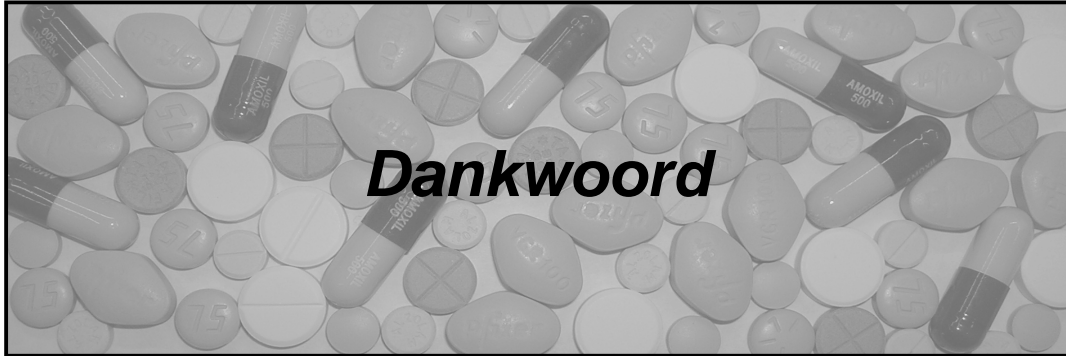
$$d_{ki} = \frac{n_A}{n}d_{Ai} + \frac{n_B}{n}d_{Bi} \quad \text{with } n = n_A + n_B \quad (\text{eq. 4.7})$$

where n_A and n_B are the numbers of object in a clusters A and B , respectively⁶.

The next steps consist of continuing with one of these linkage methods until all the data form one large group^{1,3}. At each step, the most similar pair of objects or clusters are identified, then they are combined into one new cluster until all objects have been joined¹.

References:

1. Brereton RG, Chemometrics, Chemometrics : data analysis for the laboratory and chemical plant, John Wiley & Sons Ltd, Chichester, 2003.
2. Savitsky A, Golay MEJ, *Anal.Chem.*, 1964; 36(8): 1627-1639.
3. Brereton RG, Applied chemometrics for scientist, John Wiley & Sons Ltd, Chichester, 2007.
4. Davies AMC, Fearn T, *Spectros. Europe*, 2004 ; 16(4): 20-23.
5. Massart DL, Vandeginste BGM, Buydens LMC, De Jong S, Lewi PJ, Smeyers-Verbeke J, Data handling in science and technology 20A, Handbook of Chemometrics and Qualimetrics Part A, Elsevier, Amsterdam, 1997.
6. Otto M, Chemometrics, Statistics and Computer Application in Analytical Chemistry, Wiley-VCH, Weinheim, 1999.



Dankwoord

In Augustus 2003 werd ik nog slaperig, na een zeer korte nacht, gebeld door professor Dams met de mededeling dat ik kon beginnen als assistent aan de Universiteit Gent. Mijn eerste reactie: “zou ik daar effe over na kunnen denken?” werd beantwoord door professor Dams met de vraag “maar mevrouw, hoe lang is effe?” Uiteindelijk duurde het slechts tien minuten voordat ik besloot om naar het verre België te verhuizen. Hier heb ik meer dan vier jaar met veel plezier aan mijn doctoraat gewerkt en zonder de steun, inzet en hulp van velen zou dit onderzoek nooit mogelijk zijn geweest.

Allereerst wil ik mijn promotor vice-rector prof. dr. Luc Moens, vakgroepvoorzitter prof. dr. Karel Strijkmans, ex-vakgroepvoorzitter prof. dr. em. Richard Dams en natuurlijk mijn co-promoter prof. dr. Peter Vandenabeele hartelijk bedanken om een Hollandse de kans te hebben gegeven om te kunnen doctoreren in het Gentse.

Mijn doctoraat onderzoek zou niet mogelijk zijn geweest zonder degenen die alles in het werk zetten om vervalsingen van geneesmiddelen te kunnen detecteren. Zonder hun donatie van de vervalste geneesmiddelen zou er geen onderzoek mogelijk zijn geweest. Ik wil graag de volgende mensen bedanken omdat ze in mij en dit onderzoek geloofden: Facundo Fernandez, Michael Green, Paul Newton, Nicholas White, Krystyn Hall, Dries de Kaste, Paul Meuleniëre en Roy VanCauwenbergh. eveneens gaat mijn dank uit naar professor Jean Paul Remon voor de hulp met mijn onderzoek en het leveren van vele farmaceutische producten en professor Francis Verpoort voor het ter beschikking stellen van FT-Raman voor mijn onderzoek.

Daarnaast zou ik ook mijn (ex-) collega's van het INW willen bedanken. Niet alleen voor de hulp bij mijn onderzoek en practica maar wil ook voor de nodige afleiding als het even tegen zat: Annelien, Bart, Björn, Chantal, David, Didier, Hans, Isolde, Ine, Jan, Kris, Lieve, Lucien, Maite, Marc, Pieter, Roger, Rudy, Tine en Tony. Sylvia en Joke, bedankt voor jullie hulp, het luisterend oor tijdens de fietstochtjes door gent of in het bureau, en natuurlijk de gezellig lunchpauzes.

Natuurlijk wil ik hiernaast de drie thesis studenten, Nathalie Willems, Anneleen Burggraeve en Annelien Deneckere bedanken voor hun bijdrage aan mijn onderzoek. Ik heb jullie met veel plezier begeleid.

Tijdens de afgelopen vier jaar zat ik niet alleen op het INW maar was ik ook regelmatig te vinden in de Gentse cafeetjes en restaurants. Bij deze wil ik graag Niko bedanken voor de gezellige avondjes (dansend of zittend aan de bar). Daarnaast ook een speciaal plekje voor Isabel. Zonder haar zou een Hollandse niet weten dat frieten frieten zijn en patatten patatten. Daarnaast zal ik onze squashpartijtjes en etentjes na afloop erg gaan missen.

Eveneens wil ik Pauline, Wouter, Ati, Liana en de rest van mijn vrienden in Nederland en omstreken bedanken. De feestjes, gezellige avondjes stappen, de leuke concerten en natuurlijk de legendarische festivals zorgden voor een zeer gezellige noot. Catrien, bedankt voor alle leuke tripjes en vakanties, en vooral voor de gezelligheid.

Als een van de laatste maar zeker niet de onbelangrijkste, Jasper. Bedankt voor je steun, luisterend oor, de nodige afleiding en je vermogen om me af en toe goed aan het lachen te krijgen. Helaas zijn we op dit moment verder van elkaar verwijderd en is een eenvoudig treinritje niet meer voldoende. Nog maar enkele maanden en dan zien we elkaar eindelijk een stuk vaker. Ik kijk er erg naar uit!

Als laatste wou ik mijn ouders, Nella en Wim, bedanken. Jullie hebben altijd in me geloofd en mij gestimuleerd om verder te gaan ondanks het feit dat anderen zeiden dat het te hoog gegrepen. Nella, bedankt voor alle hulp die je de laatste jaren geboden hebt. Als er problemen waren was je de eerste die me hielp, als ik ziek was kon ik altijd even lekker naar huis komen, en al die weken in het AMC week je geen moment van mijn zijde. Wim, bedankt voor alles. Al je hulp tijdens mijn doctoraat, voor het meedenken als er problemen waren, voor het nalezen van teksten, eigenlijk voor alles maar dan ook alles, hartstikke bedankt!

Marleen

